

# **Virtual Paleontology in Ancient Seas**

A three-dimensional voyage through morphology  
and kinematics of early Palaeozoic  
marine euarthropods



Dissertation zur Erlangung des Doktorgrades der Naturwissenschaften  
Dr. rer. nat.  
der Fakultät für Biologie  
der Ludwig-Maximilians-Universität München

vorgelegt von  
**M. Sc. Michel Schmidt**  
München, 2022

Für meine Mutter.



LUDWIG-  
MAXIMILIANS-  
UNIVERSITÄT  
MÜNCHEN

FAKULTÄT FÜR BIOLOGIE



Diese Dissertation wurde im Rahmen einer deutsch-chinesischen Kooperation an der Zoologischen Staatssammlung München, Staatliche Naturwissenschaftliche Sammlungen Bayerns, unter der Leitung von Prof. Dr. Roland R. Melzer angefertigt.

Erstgutachter: **Prof. Dr. Roland R. Melzer**

Zweitgutachter: **Prof. Dr. Martin Heß**

Tag der Abgabe: 27.01.2022

Tag der Verteidigung: 24.06.2022

## **Erklärung**

Diese Dissertation wurde im Sinne von §12 der Promotionsordnung von Prof. Dr. Roland R. Melzer betreut. Ich erkläre hiermit, dass die Dissertation nicht einer anderen Prüfungskommission vorgelegt wurde und dass ich mich nicht anderweitig einer Doktorprüfung unterzogen habe.

München, 25. Januar 2022

**Michel Schmidt**

## **Eidesstattliche Erklärung**

Hiermit versichere ich an Eides statt, dass die vorgelegte Dissertation von mir selbstständig und ohne unerlaubte Hilfsmittel angefertigt wurde.

München, 25. Januar 2022

**Michel Schmidt**

# Table of contents

<b>List of publications included</b>	I
<b>Declarations of contributions as a co-author</b>	II
<b>Summary</b>	III
<b>Aim and structure of the thesis</b>	IV
<b>1. Introduction</b>	1
<b>1.1 A virtual view</b>	2
<b>1.2 The Cambrian (541-485.4 mya)</b>	3
<b>1.2.1 – Life in Cambrian seas: The awakening of armors and weapons</b>	3
<i>The evanescence of the Ediacaran</i>	3
<i>The Cambrian world</i>	3
<b>1.2.2 – Fossil sites and preservation modes in the Cambrian: the historical places</b>	4
<i>Example: Burgess Shale: The arthropod treasure trove I</i>	5
<i>Example: Chengjiang: The arthropod treasure trove II</i>	5
<i>Other famous fossil sites: Many more arthropod treasure troves</i>	7
<b>1.2.3 – Chengjiang euarthropods of South China: the flowering of life</b>	8
<i>Paleoecology of the Chengjiang biota</i>	8
<i>Phylogeny of the Chengjiang euarthropods</i>	8
<b>1.3 The later worlds (485.4 – 419.2 mya)</b>	10
<b>1.3.1 – The Ordovician (485.4 – 443.8 mya)</b>	10
<i>The Ordovician world back then</i>	10
<i>The fall, the rise, and the fall of organisms</i>	10
<b>1.3.2 – The Silurian (443.8 – 419.2 mya)</b>	11
<i>The Silurian world back then</i>	11
<i>A new fauna, new predators</i>	11
<b>1.3.3 – Ordovician and Silurian eurypterid fossil sites</b>	12
<b>1.4 The eurypterids: the tale of early Paleozoic sea scorpions</b>	12
<i>Phylogeny and evolution of voracious villains and calm companions</i>	13
<i>What makes a sea scorpion?</i>	14
<i>Massive euchelicerate apex predators with spines and baskets</i>	16
<b>2. Results</b>	17
<b>Part 1: Digitally unraveling the morphology of early Cambrian Chengjiang euarthropods from China</b>	18
* <b>Chapter I:</b> “Before trilobite legs: <i>Pygmaclypeatus daziensis</i> reconsidered and the ancestral appendicular organization of Cambrian arthropods”	19
* <b>Chapter II:</b> “Intraspecific variation in the Cambrian: new observations on the morphology of the Chengjiang euarthropod <i>Sinoburius lunaris</i> ”	54
* <b>Chapter III:</b> “Exit in Cambrian arthropods and homology of arthropod limb branches”	71

<b>Part 2: Performing virtual euarthropod appendage kinematics as an integrative, conceptualized approach</b>	93
* <b>Chapter IV:</b> “Moving legs: A workflow on how to generate a flexible endopod of the 518 million-year-old Chengjiang arthropod <i>Ercaicunia multinodosa</i> using 3D- kinematics (Cambrian, China)”	94
<b>Part 3: Digitally unveiling prosomal appendage kinematics in Ordovician and Silurian sea scorpions and modern analogs</b>	105
* <b>Chapter V:</b> “Three-dimensional kinematics of euchelicerate limbs uncover functional specialization in eurypterid appendages”	106
* <b>Chapter VI:</b> “Kinematics of whip spider pedipalps: a 3D comparative morpho-functional approach”	118
* <b>Chapter VII:</b> “Spines and baskets of apex predatory sea scorpions uncover unique feeding strategies using 3D-kinematics”	132
<b>3. Discussion</b>	158
<b>3.1 The euarthropod appendage</b>	159
<b>3.1.1 – Biramous and uniramous appendages</b>	159
<b>3.1.2 – Evolutionary and developmental aspects of euarthropod appendages</b>	159
<i>Phylogenetic relationships among euarthropods</i>	159
<i>The ancestral condition</i>	160
<i>Developmental perspectives of euarthropod appendage types</i>	161
<b>3.2 Appendages in Cambrian Chengjiang euarthropods</b>	161
<b>3.2.1 – Considerations about euarthropod appendage structures</b>	161
<i>The protopodite, endites and exites</i>	161
<i>The endopodite</i>	162
<i>The exopodite</i>	163
<b>3.2.2 – Considerations about numbers and elements of appendages</b>	164
<i>Number of appendages of the body</i>	164
<i>Number of elements in the appendages</i>	165
<b>3.2.3 – Progress in virtual paleontology research of Chengjiang euarthropods</b>	165
<b>3.3 Appendages in Ordovician and Silurian sea scorpions</b>	169
<b>3.3.1 – Morphology and kinematics in eurypterid walking appendages</b>	169
<i>Eurypterus</i>	169
<i>Pentecopterus</i>	170
<b>3.3.2 – Morphology and kinematics in eurypterid grabbing appendages</b>	170
<i>Pentecopterus</i>	170
<i>Megalograptus, Mixopterus</i>	170
<b>3.3.3 - Appendage morphology and kinematics in modern analogs</b>	171
<b>3.3.4 – Progress in virtual paleontology research of eurypterid kinematics</b>	172
<b>3.4 Limitations of the studies: a critical view</b>	173
<i>Morphology of Chengjiang euarthropods</i>	173
<i>Kinematics of sea scorpion appendages</i>	174
<b>3.5. Conclusions and perspectives: the future of virtual paleontology research</b>	175
<i>Perspectives in virtual paleontology research of Chengjiang euarthropods</i>	175

<i>Perspectives in virtual paleontology research of sea scorpion morpho-functionality</i>	176
<b>Supplemental</b>	177
<b>4. Methodological approaches</b>	178
<b>4.1 The arthropod machines: application of micro-computer tomographs for understanding the morphology of euarthropods</b>	178
<b>4.2 The visualization of volumetric datasets and the reconstruction of surfaces</b>	179
<i>Drishti</i>	179
<i>Amira</i>	179
<i>Post-processing steps and data formats</i>	180
<b>4.3 The building of 3D computer models and the construction of kinematic marionettes</b>	180
<i>Blender</i>	180
<i>Maya</i>	181
<b>4.4 The study of euarthropod appendage kinematics and the application of range of motion analyses</b>	182
<i>Euarthropod kinematics</i>	182
<i>Range of motion analyses</i>	182
<i>Measurement of joint angles</i>	183
<b>4.5 Terminology</b>	183
<b>References</b>	186
<b>Acknowledgements</b>	204
<b>Curriculum Vitae</b>	205
<b>Publication history</b>	207

## List of publications included

### Publication I:

To be published in *Philosophical Transactions of the Royal Society, B: Biological Sciences* as:

**Schmidt, M.**, Hou, X.-G., Zhai, D., Mai, H., Belojević, J., Chen, X., Melzer, R. R., Ortega-Hernández, J., & Liu, Y. (in press, 2022). Before trilobite legs: *Pygmaclypeatus daziensis* reconsidered and the ancestral appendicular organization of Cambrian artiopods. *Philosophical Transactions of the Royal Society, B: Biological Sciences*, 20210030.

<https://doi.org/10.1098/rstb.2021.0030>

### Publication II:

Published in *BMC Ecology and Evolution* as:

**Schmidt, M.**, Liu, Y., Hou, X.-G., Haug, J. T., Haug, C., Mai, H., & Melzer, R. R. (2021). Intraspecific variation in the Cambrian: new observations on the morphology of the Chengjiang euarthropod *Sinoburius lunaris*. *BMC Ecology and Evolution*, 21, 127.

<https://doi.org/10.1186/s12862-021-01854-1>

### Publication III:

Published in *Nature Communications* as:

Liu, Y., Edgecombe, G. D., **Schmidt, M.**, Bond, A. D., Melzer, R. R., Zhai, D., Mai, H., Zhang, M., & Hou, X.-G. (2021). Exites in Cambrian arthropods and homology of arthropod limb branches. *Nature Communications*, 12, 4619. <https://doi.org/10.1038/s41467-021-24918-8>

### Publication IV:

Published in *Microscopy Research and Technique* as:

**Schmidt, M.**, Liu, Y., Zhai, D., Hou, X.-G., & Melzer, R. R. (2021). Moving legs: A workflow on how to generate a flexible endopod of the 518 million-year-old Chengjiang arthropod *Ercaicunia multinodeosa* using 3D-kinematics (Cambrian, China). *Microscopy Research and Technique*, 84, 695–704.

<https://doi.org/10.1002/jemt.23628>

### Publication V:

Published in *Biological Journal of the Linnean Society* as:

Bicknell, R. D. C., Melzer, R. R., & **Schmidt, M.** (2021). Three-dimensional kinematics of euchelicerate limbs uncover functional specialization in eurypterid appendages. *Biological Journal of the Linnean Society*, 135, 174–183. <https://doi.org/10.1093/biolinnean/blab108>

### Publication VI:

Published in *Integrative Zoology* as:

**Schmidt, M.**, Melzer, R. R., & Bicknell, R. D. C. (2022). Kinematics of whip spider pedipalps: a 3D comparative morpho-functional approach. *Integrative Zoology*, 17, 156–167.

<https://doi.org/10.1111/1749-4877.12591>

### Publication VII:

Published in *iScience* as:

**Schmidt, M.**, Melzer, R. R., Plotnick, R. E., Bicknell, R. D. C. (2022). Spines and baskets of apex predatory sea scorpions uncover unique feeding strategies using 3D-kinematics. *iScience*, 25, 103662.

<https://doi.org/10.1016/j.isci.2021.103662>



## Declarations of contributions as a co-author

### Publication III:

Liu, Y., Edgecombe, G. D., **Schmidt, M.**, Bond, A. D., Melzer, R. R., Zhai, D., Mai, H., Zhang, M., & Hou, X.-G. (2021). Exites in Cambrian arthropods and homology of arthropod limb branches. *Nature Communications*, *12*, 4619.

- I created the three-dimensional Blender models of the appendages of *Leancoilia illecebrosa*, *Leancoilia obesa*, *Naraoia spinosa* and *Retifacies abnormalis* (Fig. 3), provided the figure items for the appendages, contributed to interpretations and the discussion.

### Publication V:

Bicknell, R. D. C., Melzer, R. R., & **Schmidt, M.** (2021). Three-dimensional kinematics of euchelicerate limbs uncover functional specialization in eurypterid appendages. *Biological Journal of the Linnean Society*, *135*, 174–183.

- I performed the kinematic analyses of the *Limulus polyphemus* walking leg and pushing leg (Fig. 1) in Maya, created the three-dimensional Blender models of prosomal appendage IV of *Eurypterus tetragonophthalmus* (Fig. 2) as well as of prosomal appendages III and V of *Pentecopterus decoharensis* (Fig. 3). I also conducted the kinematic analyses of those three eurypterid appendages and finally measured the maximum excursion angle in each joint of all five analyzed euarthropod appendages. I provided all figure items of Figs. 1-3, contributed to interpretations and discussions, and drafted the methods part of the paper.

## Summary

Life on earth began hundreds of millions of years ago. While the early biota was dominated by prokaryotic life, during the Ediacaran period (635–541 mya), the first metazoan organism appeared. And in the succeeding Cambrian period (541–485.4 mya), nearly all other groups of animals occurred. Among them, especially the arthropods arose, with “arms and weapons”, and structures evolved for hunting and shelter.

Several famous Cambrian fossil sites worldwide are known. Among them, especially the Chengjiang biota in Yunnan Province, China, stands out. The preservation mode of the fossils of this Lagerstätte (mainly pyritized, non-biomineralized structures) allows for the application of  $\mu$ CT studies, that is, analyzing fossils with X-ray technology and three-dimensional scans to look inside the fossil slabs.

With this technique, the morphology of several unique taxa of the Chengjiang biota in the past years has been unraveled, extending the knowledge of its arthropods as well as allowing assumptions and interpretations on the paleoecology of those animals.

While the euarthropods of the Cambrian were rather small (besides some anomalocaridids), often benthic or pelagic, in the middle of the succeeding Ordovician period (485.4–443.8 mya), large, nektobenthic predators arose, the so-called eurypterids or sea scorpions. During the Silurian period (443.8–419.2 mya), they could even grow up to more than one meter. Several species were likely apex predators in those early Paleozoic seas, owing to their specialized appendages.

Thus, both groups—early Cambrian Chengjiang euarthropods and Ordovician and Silurian sea scorpions—are organisms suitable for applying virtual paleontological techniques to look for their hidden morphology and to model their complex appendage kinematics based on built 3D models.

Virtual paleontology is a research field in paleontology and paleobiology. It encompasses methods to unravel the ventral or inner structures of organisms by scanning the fossil slabs, for instance via  $\mu$ CT, and hereafter revealing their appendicular morphology via imaging techniques based on the digital output of the scans. Besides those imaging techniques, also kinematic approaches can be conducted, with 3D models built upon fossil images, being hereafter digitally equipped with hypothetical joint axes, to explore their range of motion.

This thesis represents genuine and advanced research on the morphology and functionality of early Paleozoic marine euarthropods in the field of virtual paleontology.

**Chapter I** (Schmidt et al., in press, 2022) reveals the ventral as well as the entire appendicular morphology of the enigmatic artiopodan *Pygmaclypeatus daziensis*, using the 3D visualization software Drishti. A species, priorly only known from studies which used light microscopic imaging techniques. This publication uncovers a rather uncommon mode of heteronomy, with three distinct types of appendages throughout the body. It presents the first evidence of sub-chelate endopods in all biramous appendages throughout the trunk of an early Cambrian Chengjiang euarthropod, slightly comparable to the pincer-like endopods in *Limulus polyphemus*, an extant horseshoe crab, and it draws conclusions on the paleoecology of this rare Chengjiang species.

**Chapter II** (Schmidt et al., 2021a) reinvestigates the morphology of three specimens of the previously examined artiopodan *Sinoburius lunaris* with another 3D visualization software, Amira. This publication presents 3D computer models built with Blender of each specimen of this species and hints at different morphological characters presumably owing to intraspecific variation. Furthermore, it shows up differences in the appendage number and location of the eyes as well as the number of elements in the antennae and their length and distance to the anterior margin of the head shield. This publication, thus, presents an advanced approach of taking intraspecific variation into account when considering the morphology of early Cambrian Chengjiang euarthropods, and highlights the challenges of having a greater number of specimens available for severe morphological descriptions.

**Chapter III** (Liu et al., 2021) uncovers previously unknown, additional structures of the protopodite of the biramous trunk appendages of the two euarthropod leanchoiliids *Leanchoilia illecebrosa* and *L. obesa*, as well as of two artiopodans, *Naraoia spinosa* and *Retifacies abnormalis*. Those structures, revealed with Drishti, are interpreted as exites, that is, lateral outgrowths. While in the two leanchoiliids and in *N. spinosa*, only the basal lamella is attached to the protopodite, and the remaining, overlying lamellae are attached to the basal one, in *R. abnormalis* all lamellae are attached to the protopodite. Those additional structures were unknown in any other early Cambrian Chengjiang euarthropod described before and raise questions about the homology of the branches of euarthropod appendages.

**Chapter IV** (Schmidt et al., 2021b) illustrates the complex design process of a kinematic marionette for further purposes on functional morphology, exemplified by the putative crustacean-related early Cambrian Chengjiang euarthropod *Ercaicunia multinodosa*. The morphology of this species was figured with Amira, and three endopods of the trunk appendages were surface reconstructed, and the models hereafter uploaded to Maya to demonstrate the design process and the subordination chain. Thus, this paper encompasses two topics. It combines the morphological research on early Cambrian Chengjiang euarthropods with the morpho-functional and methodological approach applied in the succeeding papers on Ordovician and Silurian Sea scorpion appendage kinematics.

**Chapter V** (Bicknell, Melzer & Schmidt, 2021) analyzes the kinematics of the prosomal appendages III and V of the Middle Ordovician megalograptid sea scorpion *Pentecopterus decoharensis*—the oldest described sea scorpion—and the Silurian eurypterid sea scorpion *Eurypterus tetragonophthalmus*. This study deals with generated 3D computer models of those appendages made in Blender, which were hereafter equipped with hypothetical joint axes in Maya, for purposes on functional morphology following instructions presented in **Chapter IV**. This study further compares the results to the kinematics in the walking and pushing leg of the extant horseshoe crab *Limulus polyphemus*, and constitutes that regarding its feeding ecology, those eurypterid appendages were better in walking than in getting food to the gnathal edges. This study is furthermore the first in this thesis to establish a comparison of extant euarthropod appendage kinematics to those examined in extinct taxa.

**Chapter VI** (Schmidt, Melzer & Bicknell, 2022) investigates the range of motion and the kinematics in the pedipalps of two extant whip spider species (Amblypygi), *Damon medius* and *Heterophrynus elaphus*, and collects data on the excursion angles in the pedipalp joints. Those euarthropods were scanned with a  $\mu$ CT, and surface reconstructions of their pedipalps were conducted in Amira. The pedipalp surface models were equipped with hypothetical joint axes, and the kinematic analyses afterwards were performed in Maya. While former analyses of whip spider pedipalp kinematics based on video capturing or dissecting live or dead animals, this *ex vivo* approach contributes to a proper understanding of the kinematic limitations of whip spider pedipalps, as those *ex vivo* excursion angles represent maximum values, which can never be achieved in *in vivo* analyses. This publication, thus, sets a new frame for interpreting the range of motion and the functional morphology of whip spider pedipalps, allows a better understanding of their strike kinematics—and yields data for a comparison to morphologically similar structures in ancient euchelicerates like sea scorpions.

**Chapter VII** (Schmidt et al., 2022), the last chapter in this thesis, explores the strike kinematics and the flexibility of the frontal most appendages in two famous Ordovician sea scorpion species: *Megalograptus ohioensis* and *Mixopterus kiaeri*. Those taxa are well known for having elongate and spinose appendages II and III, tentatively considered in earlier studies to play a major role in their foraging behavior. To test this, 3D computer models were generated in Blender and kinematically tested in Maya—to uncover that both species had their individual strategies in hunting and manipulating prey with their uniquely shaped appendages. This publication also compares the collected data on the range of motion of the sea scorpion appendages to the data of the extant whip spider species gathered in the former **Chapter VI**, concluding that in both groups the kinematics are similar, though one group being terrestrial and the other aquatic.

This thesis presents integrative and innovative approaches for the application of virtual paleontology in the research area of early Paleozoic marine euarthropods. It expands the knowledge on the Chengjiang biota and uncovers previously unknown structures. It raises awareness of the severe differences within several specimens of a species. It enlightens ecological strategies in movement and feeding behavior in sea scorpions. And it shows how useful and necessary the comparison of extinct kinematic data to extant relatives and modern analogs is.

Virtual paleontology is a challenging and sophisticated, and relatively new field of research—and its techniques in the future will unveil further unexpected morphological details and solve long-established mysteries on the behavior of early Paleozoic marine euarthropods.

## Aim and structure of the thesis

This doctoral thesis introduces recent research on morphology and ecology of early Paleozoic marine euarthropods in the field of virtual paleontology. It gives an overview of hybrid methods and covers a vast range of taxa and techniques to explore the morphological diversity in early Cambrian euarthropods and the appendage kinematics in Ordovician and Silurian eurypterids as well as modern analogs.

**Part 1** includes three publications dealing with early Cambrian Chengjiang species. It reveals new aspects of the ventral morphology of enigmatic euarthropods, shows up intraspecific variation and highlights previously unknown appendage structures. Those publications base on micro-computed tomography data of scanned Chengjiang fossils, which were three-dimensionally reconstructed with the programs Drishti and Amira. Furthermore, they contain three-dimensional models of specimens and appendages built in the software Blender.

**Part 2** includes one publication and exemplifies the method of assembling a kinematic marionette with the software Maya. This technique is illustrated by showing the Chengjiang euarthropod *Ercaicunia multinodosa* re-analyzed in Amira. Surface reconstructions of endopods are conducted to further explain how to equip those appendage surface models with artificial joints in Maya. This publication is a how-to-do approach on constructing a movable appendage, which could be used for further kinematic analyses and morpho-functional approaches.

**Part 3** includes three publications dealing with kinematic analyses of euchelicerate appendages of Ordovician and Silurian sea scorpions and modern analogs. The functional morphology of four different, extinct sea scorpion species, two

extant whip spider species and one extant horseshoe crab species are investigated regarding their feeding ecology and appendage flexibility.

While one of the three publications exclusively highlights pedipalp kinematics in whip spiders, the other two publications compare the modeled sea scorpion appendage motions to modern analogs like the horseshoe crab *Limulus polyphemus*, and the whip spiders (*Damon medius*, *Heterophrynus elaphus*) analyzed in the single publication. Part 3, thus, deals with three-dimensional models of sea scorpions built in Blender upon fossil photographs, while the models of the appendages of the three modern analogs were surface rendered with the software Mimics. All three-dimensional models were then kinematically analyzed in Maya following the introduced and published steps in Part 2.

In summary, this thesis, and the publications therein, cover several methods and techniques used in recent virtual paleontology. It encompasses a wide range of different programs like Amira, Drishti, and Mimics to visualize morphological information formerly hidden in the stones based on micro-computed tomography technique, and to perform surface reconstructions of both, suitable fossils, as well as extant euarthropods.

On the other hand, this thesis presents Blender and Maya work, used to build three-dimensional models based on photographic rather than tomographic images and to kinematically analyze three-dimensional appendage models of different euchelicerates to unravel their motion possibilities and their feeding ecology.

Eventually, this thesis tries to answer questions on the morphological innovations and previously undetected appendicular details, as well morpho-functional aspects, and ecological implications of appendage kinematics in early Paleozoic marine euarthropods and modern analogs.

# Introduction

# 1. Introduction

## 1.1 A virtual view

The analysis of fossils using computer-aided visualization methods has revolutionized how paleontologists and paleobiologists work (Cunningham et al., 2014; Garwood, Rahman & Sutton, 2010; Sutton, Rahman & Garwood, 2014; Yin & Lu, 2019).

Following Sutton, Rahman & Garwood (2014), *virtual paleontology* is the study of fossils through interactive digital visualizations. This refers to the application of a variety of ways for understanding the complex morphology of fossilized animals. Those digital visualization methods broadly can be divided into surface-based and tomographic (slice-based) approaches. While surface-based approaches contain methods like laser scanning and photogrammetry, thus digitizing the external surface of a fossil, tomographic approaches refer to the understanding of 3D structures through a series of 2D slices of the respective fossil. The latter can be subdivided into destructive tomography (e.g., serial grinding, where the fossil may be partly or completely destroyed) and non-destructive tomography. Especially, the use of non-destructive tomography, like X-ray computed tomography (CT), has yielded to a fundamentally enhanced understanding of the morphology of fossil euarthropods.

As an example, lots of Cambrian euarthropods have been analyzed using micro-computed tomography ( $\mu$ CT), a different approach of CT for smaller objects of interest (Chen X et al., 2019a; Jin et al., 2021; Liu Y et al., 2016, 2020a, b, 2021; Liu Y, Scholtz & Hou, 2015; Schmidt et al., 2021a, b; Zhai et al., 2019a, b, c, preprint, 2021; Zhang M et al., submitted; Zhang X et al., under review). This is feasible due to the pyritized euarthropod fossils of the famous Chengjiang biota from China, owing to

their unique mode of preservation and post-depositional environmental circumstances.

However, the application of  $\mu$ CT is not limited to Cambrian animals. The famous Late Ordovician (Caradoc, ca. 445 mya) Beecher's Trilobite Bed in Oneida County, New York, USA (Briggs, Bottrell & Raiswell, 1991) also contains pyritized euarthropods, especially well-preserved trilobites. Using  $\mu$ CT, Hegna, Martin & Darroch (2017) were able to uncover *in situ* trilobite eggs under the cephalon of a well-studied Upper Ordovician trilobite.

Clark et al. (2020) analyzed Early Ordovician stylophoran echinoderm arms. Sutton et al. (2002) as well as Briggs et al. (2012) unveiled the appendicular morphology of a chelicerate relative and a horseshoe crab, respectively; both fossils were from the mid-Silurian Herefordshire Lagerstätte. However, as the fossil material was not suitable for  $\mu$ CT scanning, they used serial grinding, a destructive tomography technique.

Sutton, Rahman & Garwood, (2014, p. 1) excluded the process of designing idealized virtual 3D models (for instance, in Maya or Blender) from their definition of virtual paleontology.

However, in this thesis, the term will be extended to also include biomechanical and kinematic studies on fossil euarthropods.

Analyses of kinematics and biomechanics in vertebrate fossils have been widely performed (Falkingham & Gatesy, 2014; Nyakatura et al., 2015, 2019; Rayfield, 2007; Turner, Falkingham & Gatesy, 2020).

Moreover, those techniques were applied to fossil invertebrates as well: enrollment in trilobites was modelled (Esteve et al., 2017, 2018), as well as arm waving in fossil echinoderms (Hegna, Martin & Darroch, 2017).

Furthermore, finite element analyses (FEA) were applied to a mid-Cambrian Vicissicaudate (Bicknell et al., 2018a) as well as to Cambrian trilobites (Bicknell et al., 2021).

Another morpho-functional approach, the method of computational fluid dynamics (CFD), was adapted to analyze queuing behavior in Devonian trilobites (Song et al., 2021) or even to enlighten suspension feeding in the Ediacaran biota (Gibson et al., 2019).

Only recently, the application of kinematic studies of 3D models of euarthropod appendages showed a wide variety of morpho-functionality in early Paleozoic seas (Bicknell, Melzer & Schmidt, 2021; De Vivo, Lautenschlager & Vinther, 2021; Schmidt et al., 2021b, 2022)

Virtual paleontology is an auxiliary and unique tool to uncover the morphology and function in early Paleozoic animals. And to unravel the secrets of Cambrian, Ordovician and Silurian marine euarthropods.

## 1.2 The Cambrian (541 – 485.4 mya)

### 1.2.1 – Life in Cambrian seas: The awakening of armors and weapons

Life on earth already existed probably 3400 million years ago, or even longer (Javaux, 2019). In the earliest phase, that lasted many millions of years, life was dominated by prokaryotic organisms like sulfur-metabolizing bacteria (Wacey et al., 2011) or photosynthetically active stromatolites (Allwood et al., 2006).

#### The evanescence of the Ediacaran

With the beginning of the Ediacaran period (635-541 mya; Knoll et al., 2006), the first ostensible animals appeared (McMenamin, 1996; Pehr et al., 2018; Sprigg, 1947). However, the fossil record of those animals, which were first unearthed in the Ediacaran Hills in South Australia (Knoll et al., 2004), is still challenging and some taxa still remain phylogenetic

conundrums. The biota consisted of probably sessile soft-bodied organisms, with fragile structures and without a clear cephalization (MacGabhann, 2014; Watson, 2020).

While the feather-like *Charnia* sp. (Dunn et al., 2021) may have been composed of repeated branches and grew from pre-existing branches, the leaf-like *Dickinsonia* sp. (Bobrovskiy et al., 2018) may have had an osmotrophic feeding ecology (Sperling & Vinther, 2010). The worm-like *Yilingia* sp. (Chen Z et al., 2019b) or *Ikaria* sp. (Evans et al., 2020) may have shown a burrowing lifestyle.

Eventually, this rather calm and quiet time with only smaller sized, “peaceful” animals was the last period in the late Neoproterozoic—and the last before the Cambrian.

#### The Cambrian world

The Cambrian (541-485.4 mya), the first period of the Paleozoic, is divided into four series (Terreneuvian, “Series 2”, Miaolingian, Furongian), which are further subdivided into ten stages (Fortunian, “Stage 2”, “Stage 3”, “Stage 4”, Wuliuan, Drumian, Guzhangian, Paibian, Jiangshanian and “Stage 10”). The preliminary named “Series” and “Stages” are yet to define by the International Commission on Stratigraphy. The early Cambrian world faced a break-up of the putative short-living supercontinent Pannotia (Bond, Nickeson & Kominz, 1984), resulting in smaller continents like Baltica, Laurentia and Siberia, thus being separated from Gondwana (Mckerrow, Scotese & Brasier, 1992). This massive southern continent united present-day South America, Africa, Antarctica, India and Australia. Besides the smaller continents mentioned above, also South China was separated as an isolated land mass, western to Gondwana (Cocks & Torsvik, 2013). There, three distinct sedimentary provinces were defined (Yangtze Platform, Jiangnan Belt, Southeast China Fold Belt; Zhang W, Chen & Palmer, 2003), with the Yangtze platform



yielding the famous Chengjiang biota of present-day Yunnan Province, South China.

The climate during the Cambrian period might have been warm or rather hot, with vague estimates above tropical 30°, though depending on the estimation of the  $\delta^{18}\text{O}$  values (compare Scotese et al., 2021, sections 2.4.1 and 5.2, see also Royer et al., 2004, Fig. 4A). The oxygen level might have been up to 13 Vol.-% (Bernier, 2006; Gill et al., 2011; Sperling et al., 2013; Zhang X & Cui, 2016). The sea level, in average, was rising during the Cambrian, from only 20-30 m to about 200 m above PD during the transition to the Ordovician (Haq & Shutter, 2008, Fig. 1).

Back in 1835, Adam Sedgwick coined the name Cambrian period based on the Latin name of Wales, *Cambria* (Sedgwick & Murchinson, 1835). As Robert Murchinson also assigned parts of the lower Silurian to the Cambrian period (Murchinson, 1839), Charles Lapworth erected the Ordovician period based on the interval he excluded to solve this issue (Basset, 1985; Lapworth, 1879). The beginning of the Cambrian back in time was defined as the first appearance of trilobite fossils (Walcott, 1890, Wheeler, 1947). However, the lower boundary later was shifted downwards and set as the first appearance of the trace fossil *Trichophycus pedum* (Narbonne et al., 1987).

The “Cambrian Explosion” represents the beginning of a phase of rapid diversification in animal life and biodiversity (Budd, 2008; Chen J, 2009; Erwin & Valentine, 2013; Marshall, 2006; Morris, 2000, 2003, 2006; Zhang X & Shu, 2021). Some authors amended to reassess the term “explosion” and suggested a more apt term like *Great Cambrian Biodiversification* (Beasecker et al., 2020) to avoid misinterpretations as a single event happening in a brief time scale. However, the beginning of the Cambrian, especially the beginning of “Series 2” (ca.

529 mya) denotes the rise of beweaponed organisms, the start of a severe occurrence of armored euarthropods with biomineralized hard shells like trilobites (Babcock, 2003; Blaker & Peel, 1997; Jell, 2003; Palmer, 1973) and with morphological raptorial structures and acute vision for hunting like in radiodonts (Daley & Edgecombe, 2014; De Vivo, Lautenschlager & Vinther, 2021; Hou X & Bergström, 1995; Pateron et al., 2011).

While the Ediacaran biota is thought to presumably have been osmotrophically feeding (Sperling & Vinther, 2010) or grazing on algae and bacteria (Brocks et al., 2017), fossils of the Cambrian biota show the rise of hunting behavior and the beginning of a predatory lifestyle (Nedin, 1999).

### 1.2.2 – Fossil sites and preservation modes in the Cambrian: the historical places

In 1909 and 1981, respectively, Charles Doolittle Walcott and Xiang-guang Hou found fossil specimens by chance—and their findings changed the perspective on early euarthropod life and animal evolution ever since.

While C. D. Walcott discovered the famous Burgess Shale biota, located in the Yoho National Park in the Canadian Rocky Mountains of British Columbia, Canada, X.-G. Hou unearthed fossils which later would be known as belonging to the tremendously well-preserved Chengjiang biota in Yunnan Province, South China.

Both remarkable Cambrian fossil sites were inscribed to the UNESCO World Heritage list. And both fossil sites display elusive arthropod fossils in an absolute delicate state of preservation.

Example: Burgess Shale:The arthropod treasure trove I

At the age of 44, Charles Doolittle Walcott acquired the position as the director of the United States Geological Survey in 1894. After the first fossils were excavated on Mount Steven from what is now known as the Trilobite beds, he became interested in the Rocky Mountains, and in 1907 went there for stratigraphical work. He searched for fossils from what he called the “*Ogygopsis* shale”, referring to the trilobite taxa which dominated the biota there. In 1909, he turned back to look for more fossil sites of this “*Ogygopsis* shale”—but allegedly stumbled over fossils which later would be known worldwide as *Marella splendens* Walcott, 1912, *Waptia fieldensis* Walcott, 1912 and *Naraoia compacta* Walcott, 1912 (Walcott, 1912). Those were arthropod fossils unlike all fossils hitherto known.

This treasure trove changed the view on the evolution of early marine animals and the understanding of arthropods ever since (Briggs, Erwin & Collier, 1994; Gould, 1989; Morris, 1998; Walcott, 1911; Yochelson, 1996).

The Burgess Shale (508 mya, Miaolingian) exhibits fossil-rich black shale rock units (Butterfield, 2003). The delicate preservation of the Burgess Shale taxa, the so-called Burgess Shale-type Preservation (BST), is due to distinct factors (Gaines, 2014; Gaines, Briggs & Zhao, 2008; Gaines et al., 2012). Most of the fossils are preserved as carbonaceous compressions of non-mineralized sections of the organisms, some exhibit also a silvery patina, but the fossils in general underwent a metamorphism process what is understood as greenschist facies metamorphism (Butterfield, 1990, 2003; Butterfield, Balthasar & Wilson, 2007; Hou X et al., 2017; Page et al., 2008; Powell, 2003). It is the preservation of soft-body parts, what makes the Burgess Shale biota so impressive and outstanding—

in comparison to the biomineralized fossils of prior to that time well-known trilobite fossils.

The Burgess Shale biota is thought to have inhabited different niches in an around 200 m high water column of the western edge of what is known as the Cathedral Escarpment (Morris & Whittington, 1985), and over time was buried by sediments—which have protected them from scavengers or further decay, repeatedly.

More than 172 Burgess Shale species are described, with arthropods being the dominant group (Caron & Jackson, 2008). While most arthropods had been described in the early years after the discovery in the Rocky Mountains (Walcott, 1911, 1912) and yielded to celebrated compendia about the life in the middle Cambrian Burgess Shale (Briggs, Erwin & Collier, 1994; Gould, 1989; Morris, 1998), recent studies also took virtual paleontological considerations into account (Bicknell et al., 2018a, 2021; De Vivo, Lautenschlager & Vinther, 2021; Haug C & Haug J, 2016; Haug J, Briggs & Haug C, 2012; Haug J et al., 2012).

Worldwide, more than 40 localities exhibiting BST preservation are known today (Hou X et al., 2017). And besides the Burgess Shale, another remarkable fossil site is the Chengjiang Lagerstätte in Yunnan Province, South China.

Example: Chengjiang:The arthropod treasure trove II

Back in 1984, Xian-guang Hou collected bradoriids at Maotianshan, northeast of Fuxian Lake near Chengjiang, South China. Those small bivalved arthropods were well known early Cambrian arthropods back then, and Xian-guang Hou—now Prof. em. of the Yunnan Key Laboratory of Palaeobiology in Kunming—started collecting them for his Master’s degree back in 1980. In his field diary in 1984, he noted the significant discovery of fossils apparently having soft-tissue and delicate appen-

dages preserved. This specimen—which later would be known as *Naraoia longicaudata* Zhang & Hou 1985 (now transferred to *Misszhouia longicaudata* (Chen J, Edgecombe & Ramsköld, 1997; Zhang W & Hou, 1985; Zhao T et al., 2017)—marked the discovery of the soft-bodied biota of Chengjiang (Hou X et al., 2017; Hou X & Sun, 1988). After its discovery, Prof. Hou and colleagues described dozens of new species (Hou X, 1987a, b, c; Hou X & Bergström, 1991, 1997, 1998; Hou X, Chen & Lu, 1989; Hou X, Ramsköld & Bergström, 1991; Hou X et al., 1999; see also Hou X et al., 2017), and the Chengjiang fossil site in Yunnan Province, South China (Fig. 1) ultimately would be inscribed to the UNESCO World Heritage List in 2012 (IUCN, 2012).

Fossils of the Chengjiang Lagerstätte (518 mya, Series 2, Stage 3)—also ranging as a BST Lagerstätte—are found in the Yu'an-shan Member, Chiungussu formation, and occur in the so-called *Eoredlichia-Wutingaspis* trilobite biozone (Hou X et al., 2017; Zhu, Zhang & Li, 2001).



**Figure 1.** Geographical setting of the main localities of the Chengjiang biota. After Hou et al. (2017), reprinted with permission from Wiley Blackwell.

For the environment during the deposition of the Chengjiang biota, several models have been proposed (Babcock, Zhang & Leslie, 2001; Zhang X et al., 2001).

However, Hu S (2005) speaks of the depositional environment as a *gently eastwardly sloping epeiric shelf*, being filled with sands and muds, and with that basin being influenced occasionally by storms. This is the generally favored model (Zhang X, Liu & Zhao, 2008).

The common understanding is that the biota represents a biocoenosis (*in vivo* community) rather than a taphocoenosis (dead assemblage) due to post-mortem transportation (Zhao F et al., 2009, 2012).

In general, carcasses needed to be prevented from scavengers and enzymatic decomposition by microbial activity to become fossils. A rapid burial might have prevented the carcasses from scavenging, and anoxic conditions might have hampered enzymatic and bacterial activity (Gabbott et al., 2004). Though the early Cambrian saw the so-called Cambrian substrate revolution or agronomic revolution (Bottjer, Hagadorn & Dornbos, 2000; Seilacher & Pflüger, 1994), there was less diversity and complexity of burrowing organisms compared to later periods (Orr, Benton & Briggs, 2003). Furthermore, Chengjiang soft-bodied fossils were not found next to burrows yet, which also favors sedimentary sustained anoxia conditions prohibiting bioturbation (Hou X et al., 2017).

The distinct processes of the preservation of soft tissue in the early Cambrian Chengjiang Lagerstätte is not fully understood yet and remains controversial, though a complete or semi-anoxic environment alone would not have prevented microbial and enzymatic destruction (Gabbott et al., 2004; Hou X et al., 2017).

The Chengjiang biota is around a 10 million years younger than the celebrated Burgess Shale biota, thus opening a window to earlier animal evolution.

However, the general mode of preservation in both fossil sites is similar. The animals in both Lagerstätten are mostly preserved as carbonaceous compression (Gaines et al., 2012), but the Chengjiang fossils also exhibit pyritization as a preservation mode (Gabbott et al., 2004), which makes it furthermore suitable for  $\mu$ CT research (Liu Y, Scholtz & Hou, 2015). Moreover, post-depositional aspects need to be considered. The Chengjiang Lagerstätte contains fossils, which experienced deep weathering (Gabbott et al., 2004; Hou X et al., 2017); the Burgess Shale Lagerstätte contains fossils, which faced greenschist facies metamorphism (Powell, 2003).

The best exposure sites of the Chengjiang biota are Maotianshan or Ma'anshan near the Chengjiang county, but also Ercaicun, Jianshan, or the Haikou area, near the Dianchi Lake (Hou X et al., 2017). Famous fossil species (e.g., *Ercaicunia* sp., *Jianshaniania* sp.) were named after those locations as well. Besides the Chengjiang biota, there are several other Cambrian biotas in China, like the biota of the Kaili formation (Zhao Y et al., 1999), the Qingjiang biota (Fu et al., 2019) or the Guanshan biota (Hu S et al., 2013).

However, among all those, the preservation of the Chengjiang fossils is the most sophisticated and extensive – and further allows in-depth  $\mu$ CT research.

#### Other famous fossil sites:

##### Many more arthropod treasure troves

Besides those two famous and celebrated fossil sites with all their further locations, some more might be briefly mentioned, like the Sirius Passet, the Emu Bay Shale and the Orsten biota.

The Sirius Passet in Peary Land, North Greenland (520–535 mya; Babcock, 2005) was discovered in J. P. Koch Fjord in 1984 with early Cambrian fossils being preserved in dark

colored black slates (Peel & Ineson, 2011). This fossil site contains about 50 species; it does not show a BST preservation either, but rather exhibits silification owing to benthic cyanobacterial mats (Strang et al., 2016).

The Emu Bay Shale (515 mya) is a Cambrian fossil deposit in Kangaroo Island, South Australia. The biota is preserved as carbonaceous compressions, having some associated iron pyrite and calcium phosphate (Gehling et al., 2011; Paterson et al., 2015). The Emu Bay Shale contains similar famous taxa (*Anomalocaris* sp., *Isoxys* sp.) like present in the Burgess Shale or the Chengjiang Lagerstätte, with arthropods being the most dominant group as well.

Fossils from the Orsten-type were first discovered in 1979 in Sweden (Müller, 1979). They range among the most interesting and special Cambrian fossils, owing to their preservation mode (Haug J et al., 2010; Müller & Waloszek, 1985; Schoenemann, 2012; Waloszek et al., 2014) and mostly date back to mid-Cambrian to the Furongian (Maas et al., 2006). Those fossils represent small (ca. 2 mm) animal carcasses preserved mostly three-dimensionally as phosphate replacements in organic-rich nodular limestone (Müller, 1985; Waloszek, 2003a, b), and are also known to other fossil sites worldwide (Waloszek et al., 1993; Waloszek, Repetski & Müller, 1994; Waloszek & Szaniawski, 1991).

All those famous fossil sites exhibit remarkable eumetazoan fossils, which are delicately preserved—but the Chengjiang Lagerstätte contains fossil euarthropods suitable to apply virtual paleontology techniques to unravel their ventral and appendicular secrets.

### 1.2.3 – Chengjiang euarthropods of South China: the flowering of life

#### *Paleoecology of the Chengjiang biota*

Since its discovery in 1984 (Hou X & Sun, 1988) and all the detailed descriptions of the morphology of those early organisms, the Chengjiang biota got more and more worldwide courtesy. The paleoecology of this ecosystem has already been portrayed (Vannier, 2007, 2009). Present-day studies cannot recapitulate the original faunal composition, as species got different potential to fossilize, and furthermore might have been transported through currents. However, there is common agreement on that the vast majority of the Chengjiang biota represents a single marine community, once inhabiting the ancient South China paleocontinent during the early Cambrian (Hou X et al., 2017; Zhao F et al., 2009, 2014). More than one-third of this biota is represented by euarthropods, followed by poriferans and priapulids (Hou X et al., 2017, Fig. 6.1). Nearly all niches were formed, from the infaunal priapulids and—less abundant in the fossil record—sipunculids, to swimming or floating cnidarians and ctenophores, and among euarthropods, leancholiids, bradoriids or fuxianhuiids.

Nektobenthic nektaspidids crawled above the sea floor, as well as vagile epibenthic lobopodians. Vannier (2007) estimated that more than 90% of the Chengjiang species lived as epibenthos.

The average body size was rather small, with the biggest arthropods being the putative Cambrian apex predators, the pelagic anomalocaridids like *Anomalocaris saron* Hou, Bergström & Ahlberg, 1995 reaching about 1 m (Hou X et al., 1999). Its Burgess Shale counterpart, *Anomalocaris canadensis* Whiteaves, 1892 (Daley & Edgecombe, 2014), reached similar sizes.

#### *Phylogeny of the Chengjiang euarthropods*

Among the around 300 formally described Chengjiang species (Hou X et al., 2017), more than 80 are considered to belong to the stem group Euarthropoda Lankester, 1904. Euarthropods (Aria, preprint, 2021; Ortega-Hernández, 2016) are designated as having a segmented body, an exoskeleton, specialized head appendages and jointed paired appendages in the body (Aria et al., 2020). Extant crown-group euarthropods comprise Chelicerata Heymons, 1901 and Mandibulata Snodgrass, 1938. Though there were some debates about the relationships within the euarthropod stem lineage (Budd, 2002; Edgecombe & Legg, 2014; Ortega-Hernández, 2016), the common agreement according to Ortega-Hernández (2016) is on a division into extinct lower and upper stem group euarthropods.

The lower stem group Euarthropoda comprises early lobopodians like *Hallucigenia fortis* Hou & Bergström, 1995 or *Microdictyon sinicum* Chen, Hou & Lu, 1989 (Ramsköld & Chen, 1998), but also radiodonts like *Amplectobelua symbrachiata* Hou, Bergström & Ahlberg, 1995 (Hou X et al., 1999).

The upper stem group comprises famous taxa like *Isoxys auritus* (Jiang, 1982) (Hou X et al., 1999; Zhang C et al., preprint, 2021) and other bivalved euarthropods like *Kunmingella douvillei* (Mansuy, 1912) or *Kunyangella cheni* Huo, 1965 (Duan et al., 2014, Zhai et al., 2019c), furthermore fuxianhuiids like *Fuxianhuia protensa* Hou, 1987 (Ma et al. 2012) or *Chengjiangocaris longiformis* Hou & Bergström, 1991 (Yang et al., 2013).

Megacheirans are either considered as upper stem group euarthropods (Edgecombe & Legg, 2014; Legg et al., 2012; Legg, Sutton & Edgecombe, 2013) or as part of the Chelicerata in the crown group Euarthropoda (Chen J, Waloszek & Maas, 2004; Cotton & Braddy, 2003; Dunlop, 2006; Haug J, Briggs & Haug C, 2012; Haug J et al., 2012; Liu Y et al., 2014; Liu Y, Hou & Bergström, 2007).

This taxon comprises species like *Jianfengia multisegmentalis* Hou, 1987 (Haug J et al., 2012; Hou X et al., 1999, Zhang X et al., under review, 2022), *Fortiforceps foliosa* Hou & Bergström, 1997 (Dunlop, 2006; Haug J et al., 2012; Hou X et al., 1999) or the Burgess Shale *Yohoia tenuis* Walcott, 1912 (Haug J et al., 2012). Furthermore, the famous Leanchoiliidae are part of the megacheiran clade with the well-studied *Leanchoilia* sp. (Lan et al., 2021; Liu Y, Hou & Bergström, 2007; Liu Y et al., 2014, 2016, 2021; Haug J, Briggs & Haug C, 2012) and *Alalcomenaeus* sp. (Lan et al., 2021; Tanaka et al., 2013).

Besides chelicerates and mandibulates, the crown group euarthropods consists of the extinct Artiopoda Hou and Bergström, 1997, the latter containing trilobites and non-trilobite artiopodans (Daley et al., 2018, Fig. 3; Ortega-Hernández, Legg & Braddy, 2013; Paterson et al., 2010).

Non-trilobite artiopodans comprise many Chengjiang species; they are morphologically similar to trilobites in having, for instance, dorso-ventrally flattened bodies. Famous non-trilobite artiopodans, like the well-known *Acanthomeridion serratum* Hou X et al., 1989, *Cindarella eucalla* Chen et al., 1996; *Kuamaia lata* Hou, 1987, *Saperion glumaceum* Hou et al., 1991, *Skioldia aldna* Hou & Bergström, 1997 or *Squamacula clypeata* Hou & Bergström, 1997, to name just a few, had already been described and investigated using traditional methods like camera lucida drawings (Bergström & Hou, 1998; Chen J et al., 1996; Chen J & Zhou, 1997; Edgecombe & Ramsköld, 1999; Hou X, 1987b; Hou & Bergström, 1997; Hou X, Chen & Lu, 1989; Hou X et al., 1999, 2017; Hou X, Ramsköld & Bergström, 1991; Legg, Sutton & Edgecombe, 2013; Paterson, García-Bellido, & Edgecombe, 2012; Ramsköld et al., 1996, 1997; Zhang X et al., 2004; Zhao F et al., 2013).

However, since the beginning of the application of virtual paleontology techniques to extinct euarthropods using  $\mu$ CT (Liu Y, Scholtz & Hou, 2015), the ventral and appendicular morphology of Chengjiang species has been unraveled as well (Chen X et al., 2019a; Jin et al., 2021; Liu Y et al., 2016, 2020a, b, 2021; Liu Y, Scholtz & Hou, 2015; Schmidt et al., 2021a, b; Zhai et al., 2019a, b, c, preprint, 2021; Zhang M et al., submitted; Zhang X et al., under review).

In this thesis, publications unveiling the ventral morphology of *Pygmaclypeatus daziensis* Zhang, Han & Shu, 2000 (Schmidt et al., in press, 2022, **Chapter I**) and highlighting intra-specific variation in *Sinoburius lunaris* Hou et al., 1991 (Schmidt et al., 2021a, **Chapter II**) will be portrayed and discussed.

Furthermore, new appendicular details on *Leanchoilia illecebrosa* (Hou, 1987), *Leanchoilia obesa* He et al., 2017, *Naraoia spinosa* Zhang & Hou, 1985 and *Retifacies abnormalis* Hou et al., 1989 will be enlightened (Liu Y et al., 2021, **Chapter III**), and a technique to explore appendage kinematics in extinct euarthropod animals (Schmidt et al., 2021b, **Chapter IV**) will be exemplified by *Ercaicunia multinodosa* Luo & Hu (in Luo et al., 1999).

## 1.3 The later worlds (485.4 – 419.2 mya)

### 1.3.1 – The Ordovician (485.4 – 443.8 mya)

The Ordovician is the second period in the Paleozoic era and predated the Cambrian. It was erected in 1879 by Lapworth as an attempt to accommodate the difference between Adam Sedgwick (who defined the Cambrian) and Roderick Murchinson (who defined the Silurian), as both considered the same strata belonging to their erected system, respectively (Basset, 1985; Lapworth, 1879; Murchinson, 1839; Sedgwick & Murchinson, 1835).

It is divided into three series (Early, Middle, Late Ordovician), which are further subdivided into seven stages (e.g., the Darriwilian, 467.3–458.4 mya). However, besides this formal international system of the ICS, there are several regional subdivisions.

#### The Ordovician world back then

During the Ordovician period, the southern great continent Gondwana still covered the southern part of the hemisphere, surrounded by smaller dispersed land masses like Siberia, Baltica and Laurentia.

Especially, the last two exhibited famous euarthropod biota, now unearthed for example in the Winneshiek Lagerstätte in Iowa (e.g., Lamsdell et al., 2015), USA, back then Laurentia. The micro-continent Avalonia, which at the end of the Ordovician would collide with Baltica, rifting away from Gondwana since the beginning of the Ordovician (Torsvik & Cocks, 2004). The Ordovician saw the highest sea level of the Paleozoic. In average, the sea level was between 100–200 m above PD, thus higher than during the Cambrian, and got its peak (225 m above PD) during the Late Ordovician (Sandbian, early Katian, see Haq & Shutter, 2008, Fig. 1). The overall temperature saw a decrease after the

(sub)tropical conditions in the Cambrian and ended in end-Ordovician glaciation events (Royer et al., 2004, Fig. 4A; Scotese et al., 2021). The oxygen level was about 13,5 Vol.-% (Stigall, 2017).

#### The fall, the rise, and the fall of organisms

The Ordovician period lasted for 41.6 million years, hence shorter than the previous Cambrian period (which lasted 55.6 million years; ICS, 2021).

The Cambrian period ended around 485.4 million years ago with a mass extinction known as Cambrian-Ordovician extinction event. Theories of the cause of this event differ (e.g., Kravchinsky, 2012), but range from flood basalt events to glaciation. The biota experienced a major decline, with almost all typical Cambrian arthropod taxa found in the Burgess Shale or the Chengjiang Lagerstätte diminished (though there were some successors, for instance the radiodont *Schinderhannes bartelsi* Kühl, Briggs & Rust, 2009, which was found in the Hunsrück Slate in Devonian strata, Kühl, Briggs & Rust, 2009). Trilobites survived the Cambrian; however, they experienced a decline as well, with some groups like the redlichiid trilobites went extinct even during the mid-Cambrian. This taxon also comprised famous Chengjiang trilobites like *Eoredlichia intermedia* (Lu, 1940) or *Yunnanocephalus yunnanensis* (Mansuy, 1912). Furthermore, some brachiopod and conodont groups vanished.

However, the Ordovician period is also known for another event, the so-called GOBE (Great Ordovician Biodiversity Event, Sepkoski & Sheehan, 1983). Servais & Harper (2018) defined it as “(...) the sum of the diversity trends of all individual fossil groups showing rapid increases, diachronously, during different intervals and across different regions.” (Servais & Harper, 2018, p. 151).

The Ordovician experienced a vast incline in organismal diversity, which has hereafter never

been so high. As the Cambrian set the beginning of the so-called phyla—the higher ranks sharing the gross morphology in terms of their morphological ground pattern—the Ordovician faced an incline in lower-level taxa (Servais et al., 2009, 2010). Many new groups appeared (e.g., tabulate and rugose corals, also bryozoans) or diversified (articulate brachiopods, spiny species of trilobites).

While the Cambrian nektonic niche primarily was inhabited by Cambrian radiodont apex predators (Daley & Edgecombe, 2014; De Vivo, Lautenschlager & Vinther, 2021), the Ordovician nektonic niche was dominated by large cephalopods like the endocerids (Barskov et al., 2008; Moore, Teichert & Robinson, 1953). Those gigantic nautiloid cephalopods might have grown up to 6 m and possibly played a major role at the top of the pelagic food chain (Teichert & Kummel, 1960). Though there were also some thoughts about a suspension feeding lifestyle (Mironenko, 2018), they might have presumably fed on smaller pelagic prey – but due to their sheer size, maybe also on another but benthic apex predator group: eurypterids.

The Ordovician period ended 443.8 mya ago with the first of the “big five” mass extinction events in the timeline, and the second most important after the end-Permian mass extinction, when it comes to the reduction of biota (Brenchley & Nevall, 1984; Harper, Hammerlund & Rasmussen, 2014). During this mass extinction (likely a series of events rather than a single event), many groups of brachiopods, bryozoans, conodonts and graptolites vanished, and within the trilobites, the agnostids and the ptychopariids.

Eventually, this multi-causal series of biomes (Palmer, 1973, 1984), gave rise to the following period: the Silurian.

### 1.3.2 – The Silurian (443.8 – 419.2 mya)

The Silurian period lasted only 24.6 million years. It was the shortest period of the Paleozoic and the successor of the Ordovician. It was erected in by Roderick Murchinson in 1835 (Murchinson, 1839; Sedgwick & Murchinson, 1835) and comprises four epochs (Llandovery, Wenlock, Ludlow, Přídolí), further subdivided into seven stages (ICS, 2021).

#### *The Silurian world back then*

After the collision of the smaller landmasses of Avalonia and Baltica at the end of the Ordovician, this new micro-continent collided with the landmass of Laurentia, and during the mid-Silurian formed the new bigger continent Laurussia, or Euamerica. Meanwhile, the biggest continent, Gondwana, drifted towards the equator (Seton et al., 2012; Torsvik & Cocks, 2004). The oxygen level reached about 14 Vol.-%, and the temperature during the Silurian was increasing after the decline in the end-Ordovician (Royer et al., 2004, Fig. 4A). The sea level was about 180-190 m above PD (Haq & Shutter, 2008, Fig. 2), thus still high, also owing to the melting ice caps after the glaciation events late in the Ordovician.

#### *A new fauna, new predators*

After the major decline of the biota due to the end-Ordovician extinction events, the faunal composition at the beginning of the Silurian was rather poor.

However, the Silurian marks the beginning of fossil discoveries of the earliest vascular land plants (Lang & Cookson, 1935) – though microbial life might have inhabited terrestrial areas millions of years before (McMahon et al., 2021), while there were also some considerations about an early eukaryotic land-living



Ediacaran biota (see Retallack, 2012; Runnegar, 2021; but also, Xiao & Knauth, 2013).

Life in the seas now faced a radiation of jawless and jawed pelagic fish-like groups, for example, acanthodians, chondrichthyids, early osteichthyids and placoderms.

As the water column now was inhabited by probably fast swimming prey, there was a major radiation in also fast swimming predators – for example the pterygotid sea scorpions (Jaekel, 1914; Kjellesvig-Waering, 1964; McCoy et al., 2015; Waterston, 1964). This group arose during the Llandovery epoch (ca. 443.8 mya) and bore massive and huge taxa like *Acutiramus* sp. (Laub, Tollerton & Berkof, 2010) or the Devonian *Jaekelopterus* sp. (Braddy, Poschmann & Tetlie, 2008). With their elongate and probably pincer-like chelicerae, they were likely the euarthropod apex-predators of the Silurian – together with their mixopterid sea scorpion companions, bearing elongate and spiny frontal most appendages derived from walking legs and modified for hunting (Clarke & Ruedemann, 1912; Ruedemann, 1921; Schmidt et al., 2022; Størmer, 1934).

### 1.3.3 – Ordovician and Silurian eurypterid fossil sites

Famous eurypterid fossil sites and formations in the Ordovician are for example the Winneshiek Lagerstätte, Iowa, USA, (Lamsdell et al., 2015), or the Elkhorn formation, Ohio, USA (Caster & Kjellesvig-Waering, 1964), which contain megalograptids, among others. Well known Silurian formations are the Viita Formation, Saaremaa, Estonia, containing *Eurypterus* sp. fossil material (Holm, 1898), or the Downtonian sandstone at Rudstangen, Ringerike, Norway, where mixopterid fossils were found (Størmer, 1934).

## 1.4 – The eurypterids: the tale of early Paleozoic sea scorpions

Sea scorpions (Eurypterida Burmeister, 1843) were early Paleozoic aquatic euchelicerates (Bicknell, Smith & Poschmann, 2020; Lamsdell & Selden, 2017). They roamed the seas and rivers for more than 200 million years (Ordovician, 467 mya – Permian, 254 mya; ICS, 2021).

The first ever to describe a eurypterid was Samuel L. Mitchill in 1818, who erroneously misidentified it as a catfish (Tetlie & Rábano, 2007). Later, in 1825, James E. De Kay recognized this fossil as an euarthropod (De Kay, 1825; Kjellesvig-Waering, 1958) and named it *Eurypterus remipes* De Kay, 1825 deriving from Ancient Greek εὐρύς (eurús = “wide”) and πτερόν (pteron= “wing”). This was a reference to the paddle shaped 6<sup>th</sup> prosomal appendage, which would later be the main character to distinguish between the two subgroups of the Eurypterida.

However, back then De Kay did not recognize *E. remipes* as a sea scorpion at all.

He thought it represents a branchiopod taxon.

In 1843, it was Burmeister, who ultimately erected the group Eurypterida (Burmeister, 1843), which comprises all species now considered as sea scorpions.

Though he grouped them together with trilobites, he was the first to discern their unique nature.

*Phylogeny and evolution of voracious villains and calm companions*

The taxon Eurypterida is comprised of two major groups: the Eurypterina Burmeister, 1843 and the Stylonurina Diener, 1924 (Fig. 2). Those two taxa clearly represent monophyletic groups (see Braddy, Poschmann & Tetlie, 2008; Lamsdell, Braddy & Tetlie, 2010; Tetlie & Cuggy, 2007; Tetlie & Poschmann 2008).

Eurypterine eurypterids shared a common morphological feature which enabled them to form a wide variety of niches: they developed their last pair of appendages to a powerful set of swimming legs (Tetlie & Cuggy, 2007).

Stylonurine eurypterids, however, retained their posterior prosomal appendages for walking (Lamsdell, Braddy & Tetlie, 2010; Tollerton, 1989).

The oldest known and described eurypterine eurypterid is *Pentecopterus decorahensis* Lamsdell et al., 2015, a marine megalograptid species dating back to the Middle Ordovician (Darrivillian, 467.3 mya, Lamsdell et al., 2015).

The youngest stylonurid taxon described, *?Woodwardopterus freemanorum* Poschmann & Rozefelds, 2021, occurred during the Late Permian (Changhsingian, ca. 252 mya), presumably in freshwater habitats (Poschmann & Rozefelds, 2021).

With more than 200 described species (Tetlie, 2007), the Eurypterida exhibited the highest species diversity among Paleozoic euechelicerates (Dunlop, Penny & Jaekel, 2020; Dunlop et al., 2008). While the earliest sea scorpion taxa inhabited the seas, later species occurred in brackish or freshwater environments (Hallam & Wignall, 1997; Lamsdell et al., 2020) solely, or were partly inhabiting terrestrial areas (Lamsdell et al., 2020; Whyte, 2005).

After the Devonian biotic crisis, the overall diversity declined (Lamsdell et al., 2015; Lamsdell & Selden, 2017), and towards the Permian, most marine groups went extinct, and only freshwater or brackish water taxa survived.

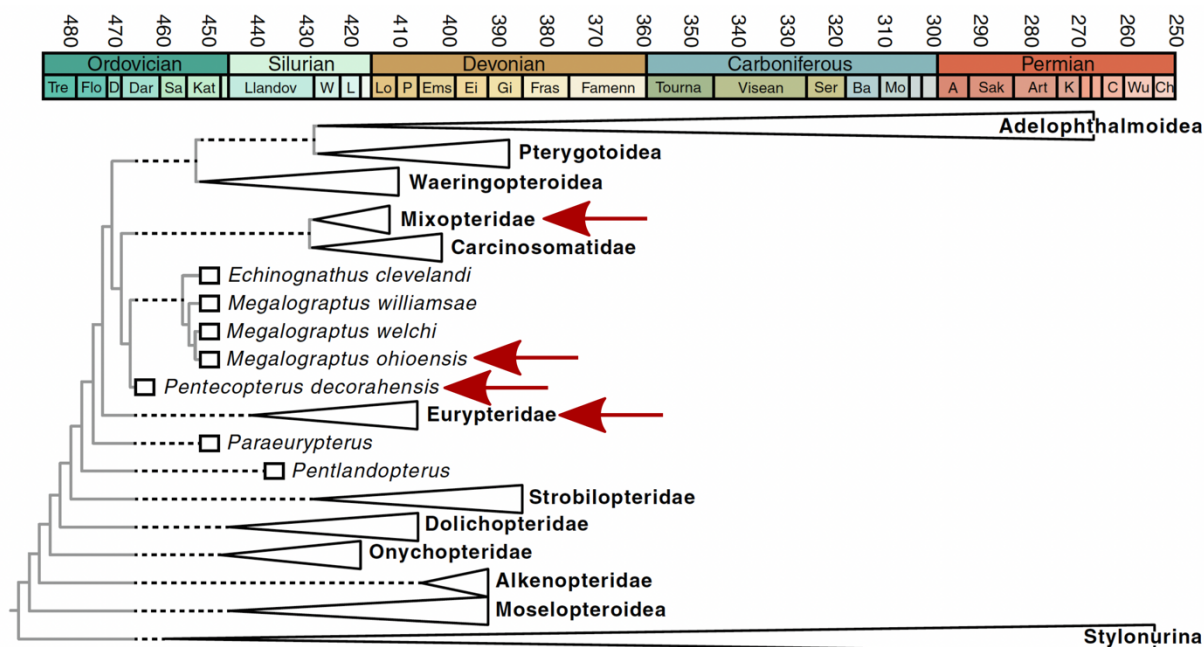


**Figure 2.** Phylogenetic tree of the major eurypterid groups (triangles) and single taxa (squares). Arrows mark groups and select species treated in this thesis. Modified after Lamsdell et al. (2015).

Before the Eurypterida ultimately vanished at the end of the Paleozoic, only the Styronurina, and among eurypterine eurypterids, only the Adelophthalmoidea Tollerton, 1989 persisted (Lamsdell et al., 2020; Poschmann & Rozeffels, 2021, Tetlie & Poschmann, 2008).

The Eurypteridae Burmeister, 1843 comprise the two genera *Erieopterus* Kjellesvig-Waering, 1958 and *Eurypterus* De Kay, 1825, which lived during the Silurian and the Devonian period (Lamsdell & Selden, 2017; Tetlie, 2007). With more than 90% of all known eurypterid fossil specimens, *Eurypterus* is the most abundant genus in the fossil record of sea scorpions (Tetlie, 2007).

Moreover, *Eurypterus* (for example *E. tetragonophthalmus* Fischer, 1839) is not only a taxon with a long research history (Burmeister, 1843; De Kay, 1825; Fischer, 1839; Holm, 1898; Nieszkowski, 1858; Woodward, 1865). Together with *Pentecopterus*, it ranges among the species with the most detailed morphological descriptions owing to explicitly preserved fossil material (*P. decoharensis* material is from the Winneshiek Lagerstätte, Iowa, USA, Liu H et al., 2009; *E. tetragonophthalmus* material is from the Viita Formation, Silurian, Wenlock, Homerian, in Saaremaa, Estonia, see Holm, 1898).

*Pentecopterus* resolves as a basal member of the group Megalograptidae Caster & Kjellesvig-Waering, 1955, which furthermore comprises *Megalograptus* Miller, 1874 and *Echinognathus* Walcott, 1882. One of the famous morphological features of those taxa is the development of spinous and elongate frontal most appendages. This is also present in members of the group Mixopteridae Caster & Kjellesvig-Waering, 1955, both belonging to the Carcinomatoidea Størmer, 1934 (Caster & Kjellesvig-Waering, 1955, 1964; Clarke & Ruedemann, 1912; Ritchie, 1968; Ruedemann, 1921; Størmer, 1934).

### What makes a sea scorpion?

Though eurypterid morphology varies greatly among all the different groups, there is a general morphological pattern, which should be exemplified by the famous and well-studied *Eurypterus tetragonophthalmus* (Fig. 3).

Being a member of the Chelicerata s. str. (sensu Maas et al., 2004), sea scorpions were generally divided into a prosoma and an opisthosoma.

Despite the deceptive name and their broader morphological resemblance (especially mixopterid taxa, Ruedemann, 1921; Størmer, 1934), they were not closely related to scorpions, hence their morphology was just owing to homoplasy.

The prosoma bore six pairs of uniramous appendages, which, for instance, in the Eurypteridae increased in size from anterior to posterior, and in the Eurypterina in general ended in a paddle-shaped 6<sup>th</sup> prosomal appendage that aided in swimming (Plotnick, 1985). In stylonurids, the appendages also increased from anterior to posterior, but this group showed no specialized appendages, and no swimming leg-modifications of the posterior most appendage (Størmer, 1955).

However, in some carcinosomatoids, appendages decreased in size from anterior to posterior (not taking the chelicerae into consideration), or showed other length patterns (Lamsdell et al., 2015; Tollerton, 1989).

While the swimming leg, appendage 6, only showed smaller morphological variation (for example, see Fig. 14 in Lamsdell, Gunderson & Meyer, 2019; also, Tetlie & Cuggy, 2007; Plotnick, 1985), especially appendages 2 and 3 were of a remarkable different shape in some groups like mixopterids and megalograptids (Caster & Kjellesvig-Waering, 1955, 1964; Ruedemann, 1921; Størmer, 1934).

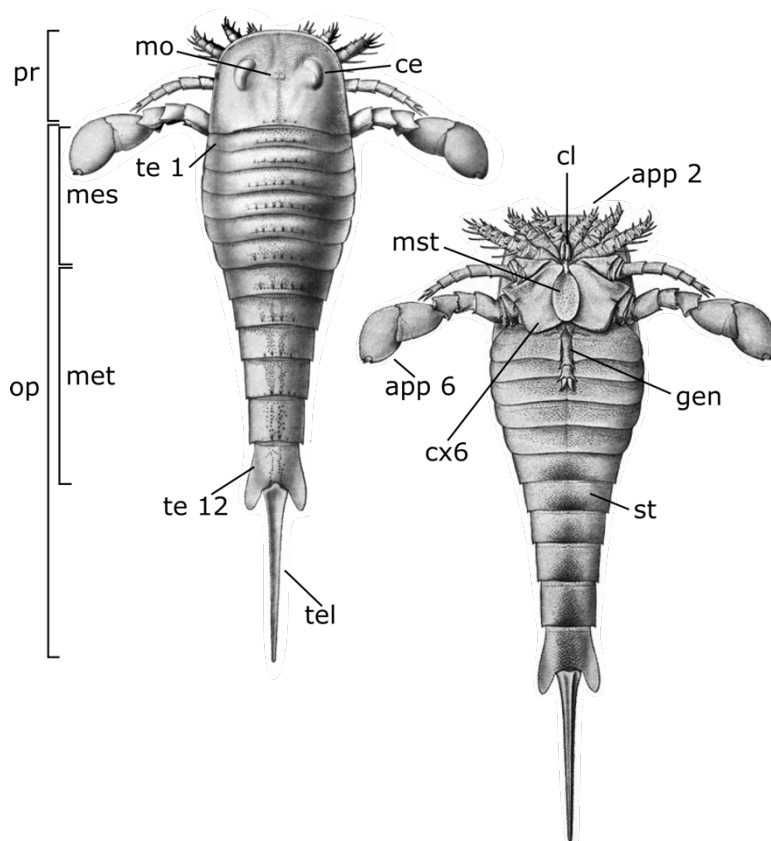


**Figure 3.** General body parts of a sea scorpion, exemplified by *Eurypterus tetragonophthalmus*. Abbreviations: app 2, 6: appendages 2, 6. ce: compound eyes. cl: chelicerae. cx6: coxae of appendage pair 6. gen: genital appendage. mes: mesosoma. met: metasoma. mo: median ocelli. mst: metastoma. op: opisthosoma. pr: prosoma. st: sternites. te1, 12: tergites 1, 12. tel: telson. Modified after Holm (1898).

Otherwise, the Pterygotoidea Clarke & Ruedemann, 1912 possessed really elongate chelicerae, a morphological adaptation unlike in any other sea scorpion (Braddy, Poschmann & Tetlie, 2008; Clarke & Ruedemann, 1912; Jaekel, 1914; Lamsdell & Legg, 2010; Waterston, 1964).

Besides the appendages, the prosoma furthermore possessed two lateral compound eyes and two median ocelli. The visual system among eurypterids might have been well developed, making them highly agile aquatic predators (McCoy et al., 2015; Poschmann, Schoenemann & McCoy, 2016; Schoenemann et al., 2019).

The opisthosoma was comprised of the mesosoma (tergites 1-6), the metasoma (tergites 7-12) and the telson (Tollerton, 1989). Whether or not the opisthosoma showed a high degree of flexibility was already up for discussion (see argumentation in Persons & Acorn, 2017, as well as the reaction of Lamsdell, Marshall & Briggs, 2018—and the reaction to this of Persons, 2018).

Indeed, when considering the scorpionoid telson of mixopterids, one could suggest that those eurypterids may have used it as a weapon or for defense (see Hanken & Størmer, 1975, p. 267, Fig. 9D; also Ruedemann, 1921, Plate 1, Fig. 5; Størmer, 1934, p. 114).

However, there is no proof in the fossil record.

Looking from ventral, eurypterids gave sight to the chelicerae and the proximal parts of the appendages 5-6. While the coxae of the anterior appendages were involved in feeding (Haug C, 2020), the impressive coxae of appendage 6, surrounding a plate-like structure known as the metastoma (Dunlop & Selden, 1998; Holm, 1898; Tollerton, 1989), mainly aided in swimming.

The first two mesosomal segments (the first two segments of the opisthosoma or the 7<sup>th</sup> and 8<sup>th</sup> segment in total) were fused together to form the so-called genital operculum, from which a specialized genital appendage protruded. (Braddy & Dunlop, 1997; Tollerton, 1989).

The mesosoma itself possessed structures known as “Kiemenplatten”, serving respiration (Lamsdell et al., 2020; Manning & Dunlop, 1995; Selden, 1985); the metasoma bore sternites.

Massive euchelicerate  
apex predators with spines and baskets

Size varied strongly among eurypterids. Basal taxa (e.g., Moselopteridae Lamsdell, Braddy & Tetlie, 2010; see Poschmann & Tetlie, 2004) encompassed rather small species, while Eurypteridae like *Eurypterus* sp. showed a variation of 13–60 cm. The biggest eurypterids ever described were pterygotids like *Jaekelopterus* Waterston, 1964 (Jaekel, 1914; McCoy et al., 2015). They could grow up to 2 m or even more and were likely the pelagic apex predators in the Silurian seas (Lamsdell & Braddy, 2009). After all, they were most likely the biggest aquatic euarthropods ever to live (the biggest terrestrial one might be *Arthropleura*, see Davies et al., 2021).

Megalograptids like the famous *Megalograptus ohioensis* Caster & Kjellesvig-Waering 1955, and since Lamsdell et al. (2015), the remarkable *Pentecopterus decoharensis*, could reach more than 1 m of body length (Lamsdell et al., 2015; Caster & Kjellesvig-Waering, 1955, 1964). Likewise, mixopterids, as for instance *Mixopterus kiaeri* Størmer, 1934, could grow up to similar sizes (Størmer, 1934). However, besides their sheer size, they ranged doubtlessly among the morphologically most diverse and disparate eurypterids, with spiny and elongate frontal most appendages, presumably to catch prey.

However, this specific question on the functional morphology has never been tested before. Though there were some severe studies on eurypterid appendage kinematics in the past (Briggs, Dalingwater & Selden, 1991; Plotnick, 1985; Plotnick & Baumiller, 1988; Selden,

1981, 1984), only recently advanced 3D kinematic approaches were applied to eurypterid appendages.

In this thesis, publications are presented dealing with advanced appendage kinematics in *Eurypterus tetragonophthalmus* and *Pentecopterus decoharensis* (Bicknell, Melzer & Schmidt, 2021, **Chapter V**), as well as *Megalograptus ohioensis* and *Mixopterus kiaeri* (Schmidt et al., 2022, **Chapter VII**). A focus here lies on the comparison to modern analogs, to get a more fundamental understanding of how those appendages could have functioned. While *E. tetragonophthalmus*' and *P. decoharensis*' appendages are compared to modern *Limulus polyphemus* (Linnaeus, 1758) walking and pushing leg, the megalograptid and mixopterid species' frontal most appendages are compared to extant whip spider pedipalps.

Eventually, those pedipalp kinematics of the whip spiders *Damon medius* (Herbst, in Lichtenstein & Herbst, 1797) and *Heterophrynus elaphus* Pocock, 1903 are further analyzed in a separate publication (Schmidt, Melzer & Bicknell, 2022, **Chapter VI**) in this thesis.

# Results

# Part 1

## Digitally unraveling the morphology of early Cambrian Chengjiang euarthropods from China

# Chapter I

## “Before trilobite legs: *Pygmaclypeatus daziensis* reconsidered and the ancestral appendicular organization of Cambrian artiopods”

### Preface

The Cambrian Stage 3 Chengjiang biota in South China is one of the most influential Konservat-Lagerstätten worldwide thanks to the fossilization of diverse non-biomineralizing organisms through pyritization. Despite their contributions to understanding the evolution of early animals, several Chengjiang species remain poorly known owing to their scarcity and/or incomplete preservation. Here, we use micro-computed tomography to reveal in detail the ventral appendage organization of the enigmatic non-trilobite artiopod *Pygmaclypeatus daziensis*—one of the rarest euarthropods in Chengjiang—and explore its functional ecology and broader evolutionary significance. *Pygmaclypeatus daziensis* possesses a set of uniramous antennae and 14 pairs of post-antennal biramous appendages, the latter of which show an unexpectedly high degree of heteronomy based on the localized differentiation of the protopodite, endopodite and exopodite along the antero-posterior body axis. The small body size (less than 2 cm), presence of delicate spinose endites, and well-developed exopodites with multiple paddle-shaped lamellae on the appendages of *P. daziensis* indicate a nekto-benthic mode of life, and a scavenging/detritus feeding strategy. *Pygmaclypeatus daziensis* shows that appendage heteronomy is phylogenetically widespread within Artiopoda—the megadiverse clade that includes trilobites and their relatives with non-biomineralizing exoskeletons—and suggests that a single exopodite lobe with paddle-like lamellae is ancestral for this clade.

This publication shows Drishti renderings based on micro-computed tomography data of four specimens, as well as 3D Blender models of a ventrally never explored early Cambrian Chengjiang euarthropod.

received: 19 April 2021

revised: 11 June 2021

accepted: 11 July 2021

to be published: 07 February 2022

**included as unpublished manuscript**

Accepted for publication in *Philosophical Transactions of the Royal Society B: Biological Sciences* as: Schmidt, M.; Hou, X.-G.; Zhai, D.; Mai, H.; Belojević, J.; Chen, X.; Melzer, R. R.; Ortega-Hernández, J.; Liu, Y. (in press, 2022). Before trilobite legs: *Pygmaclypeatus daziensis* reconsidered and the ancestral appendicular organization of Cambrian artiopods. *Philosophical Transactions of the Royal Society, B: Biological Sciences*, 20210030.



## Before trilobite legs: *Pygmaclypeatus daziensis* reconsidered and the ancestral appendicular organization of Cambrian artiopods

Michel Schmidt<sup>1,3,4</sup>, Xianguang Hou<sup>1,2</sup>, Dayou Zhai<sup>1,2</sup>, Huijuan Mai<sup>1,2</sup>, Jelena Belojević<sup>3</sup>, Xiaohan Chen<sup>1,2</sup>, Roland R. Melzer<sup>1,3,4,5,\*</sup>, Javier Ortega-Hernández<sup>6,\*</sup>, Yu Liu<sup>1,2,\*</sup>

<sup>1</sup>MEC International Joint Laboratory for Palaeobiology and Palaeoenvironment, Yunnan University, 2 North Cuihu Road, Kunming 650091, People's Republic of China

<sup>2</sup>Yunnan Key Laboratory for Palaeobiology, Institute of Palaeontology, Yunnan University, North Cuihu Road 2, Kunming 650091, People's Republic of China

<sup>3</sup>Bavarian State Collection of Zoology, Bavarian Natural History Collections, Münchhausenstr. 21, 81247 Munich, Germany

<sup>4</sup>Department Biology II, Ludwig-Maximilians-Universität Munich, 82152 Planegg-Martinsried, Germany

<sup>5</sup>GeoBio-Center, Ludwig-Maximilians-Universität Munich, Luisenstr. 37, 80333 Munich, Germany

<sup>6</sup>Museum of Comparative Zoology and Department of Organismic and Evolutionary Biology, Harvard University, 26 Oxford Street, 791 Cambridge, MA 02138, USA.

\*Corresponding authors: melzer@snsb.de; jortegahernandez@fas.harvard.edu; yu.liu@ynu.edu.cn

### Summary

The Cambrian Stage 3 Chengjiang biota in South China is one of the most influential Konservat-Lagerstätten worldwide thanks to the fossilization of diverse non-biomineralizing organisms through pyritization. Despite their contributions to understanding the evolution of early animals, several Chengjiang species remain poorly known owing to their scarcity and/or incomplete preservation. Here, we use micro-computed tomography to reveal in detail the ventral appendage organization of the enigmatic non-trilobite artiopod *Pygmaclypeatus daziensis*—one of the rarest euarthropods in Chengjiang—and explore its functional ecology and broader evolutionary significance. *Pygmaclypeatus daziensis* possesses a set of uniramous antennae and 14 pairs of post-antennal biramous appendages, the latter of which show an unexpectedly high degree of heteronomy based on the localized differentiation of the protopodite, endopodite and exopodite along the antero-posterior body axis. The small body size (less than 2 cm), presence of delicate spinose endites, and well-developed exopodites with multiple paddle-shaped lamellae on the appendages of *P. daziensis* indicate a nekto-benthic mode of life, and a scavenging/detritus feeding strategy. *Pygmaclypeatus daziensis* shows that appendage heteronomy is phylogenetically widespread within Artiopoda—the megadiverse clade that includes trilobites and their relatives with non-biomineralizing exoskeletons—and suggests that a single exopodite lobe with paddle-like lamellae is ancestral for this clade.

**Keywords:** Cambrian, Chengjiang, heteronomy, computed tomography, exceptional preservation

## Introduction

The artiopods compose a megadiverse clade of crown-group euarthropods with a distinctively flattened dorsal exoskeleton and are among the dominant epibenthic animals in lower Paleozoic marine deposits [1–4]. Trilobites are by far the most ubiquitous members of Artiopoda thanks to the higher preservation potential granted by their calcitic dorsal exoskeleton [5], but the group also contains a significant diversity of non-biomineralizing taxa that are primarily known from Cambrian Konservat-Lagerstätten around the world, particularly from localities in South China [e.g., 6], North America [e.g., 7], North Greenland [e.g., 8, 9] and South Australia [e.g. 10, 11]. Although these “soft-bodied” non-trilobite artiopods are moderately disparate in terms of the dorsal exoskeletal morphology, their appendicular organization has been traditionally regarded as a largely homonomous series of biramous gnathobasic limbs consisting of multi-segmented endopodites, and lamellate or broad flap-like exopodites [1, 6, 12, 13]. Thus, most non-trilobite artiopods are usually considered as epibenthic deposit feeders or generalized scavengers/predators based on their conservative limb construction [e.g., 6, 14], with only rare cases of clear anatomical adaptations for more specialized dietary preferences such as durophagy [15–17].

The application of micro-computed tomography (micro-CT) to study pyritized macrofossils from the Cambrian (Stage 3) Chengjiang biota in South China can inform the ventral three-dimensional organization of fossil euarthropods in greater detail than would be possible under conventional imaging techniques [e.g., 18–21]. Recent studies of the

appendicular organization in the xandarellid *Sinoburius lunaris* [22] and the nektaspid *Naraoia spinosa* [23] demonstrate a higher degree of morphological differentiation in artiopods than previously appreciated [e.g., 1, 6, 7, 24], including the regionalization of the biramous appendages along the antero-posterior body axis, as well as functional changes in feeding strategy during ontogeny. Although these examples demonstrate the cryptic complexity of the appendages in two of the main lineages of Trilobitomorpha [25], namely the group that includes all those forms more closely related to trilobites than to vicissicaudates (xenopods, cheloniellids aglaspidids; see [3]), the organization of early branching members of Artiopoda remains enigmatic owing to the scarcity of fossil taxa with well-preserved and clearly exposed limbs.

In this study, we describe the appendicular organization of the rare and enigmatic non-trilobite artiopod *Pygmaclypeatus daziensis* [26] and explore its ecological and evolutionary implications. More than 20 years after its original description, the morphology, ecology, and affinities of *P. daziensis* remain problematic [27, 28]. Type material from Chengjiang hints at the preservation of appendages (Fig. 1a), but fine morphological details concealed within the rock matrix are inaccessible through conventional photography and preparation methods. The early branching phylogenetic position of *P. daziensis* within the artiopod tree [10, 30] makes it directly significant for reconstructing the ancestral appendage organization and functional morphology of this major clade of Paleozoic euarthropods.

## Material and methods

### *Material*

The studied material includes four specimens (YKLP 11427, 11428, 13928, and 13929a) of *Pygmaclypeatus daziensis* collected from the Yu'an-shan Member of the Chiungchussu Formation, Dazi section of Haikou in Yunnan Province, South China. All specimens are deposited at the Yunnan Key Laboratory for Palaeobiology at Yunnan University, Kunming. All specimens are preserved in dorsal view, and are replicated in pyrite and/or iron oxides as typically observed in fossil euarthropods from the Chengjiang Lagerstätte [31, 32].

### *Fossil imaging*

Light photography was performed with either a Canon EOS 5DSR camera (DS126611) with an MP-E 65mm macro photo lens or a Keyence VHX-5000 digital microscope. Except for YKLP 13929, scans of all the other specimens were performed using an Xradia 520 Versa (Carl Zeiss X-ray Microscopy, Pleasanton, USA) either at the Yunnan Key Laboratory for Palaeobiology (YKLP 11428) or at the Institute of Geology and Geophysics, Chinese Academy of Sciences (YKLP 11427, 13928). YKLP 13929 was scanned using a Phoenix Nanotom (GE Sensing & Inspection Technologies) cone-beam CT scanner located at the Bavarian State Collection of Zoology, Munich. Scanning parameters are: YKLP 11427 (Fig. 1b-g): Beam

strength: 60kV/5W, Filter: no, Resolution: 8.79 $\mu$ m, Number of TIFF images: 2030; YKLP 11428 (Fig. 2): Beam strength: 50kV/4W, Filter: no, Resolution: 8.74 $\mu$ m, Number of TIFF images: 1937; YKLP 13928 (Extended Data Figure 1c, d): Beam strength: 60kV/5W, Filter: no, Resolution: 8.79 $\mu$ m, Number of TIFF images: 2030; YKLP 13929 (Extended Data Figure 1a, b): Beam strength: 130kV/14W, Filter: no, Resolution: 17.5 $\mu$ m, Number of TIFF images: 2397. Volume and surface renderings for YKLP 11428, and YKLP 11429 were produced in Drishti 2.4 [29]. Three-dimensional morphological reconstructions were created in Blender 2.9 [33].

### *Phylogenetic analysis*

The character matrix used for the phylogenetic analysis consists of 65 taxa and 92 characters. We employed an updated version of the dataset used by Chen et al. [22], including new morphological characters and updates to previous codings (Supplementary Information). Parsimony analyses were performed with TNT v.1.5 [34] under New Technology Search, using Driven Search and Sectorial Search, Ratchet, Drift, and Tree fusing options activated with standard settings. The analysis was set to find the minimum tree length 100 times and to collapse trees after each search. All characters were treated as unordered. Analyses were performed under equal and implied weights.

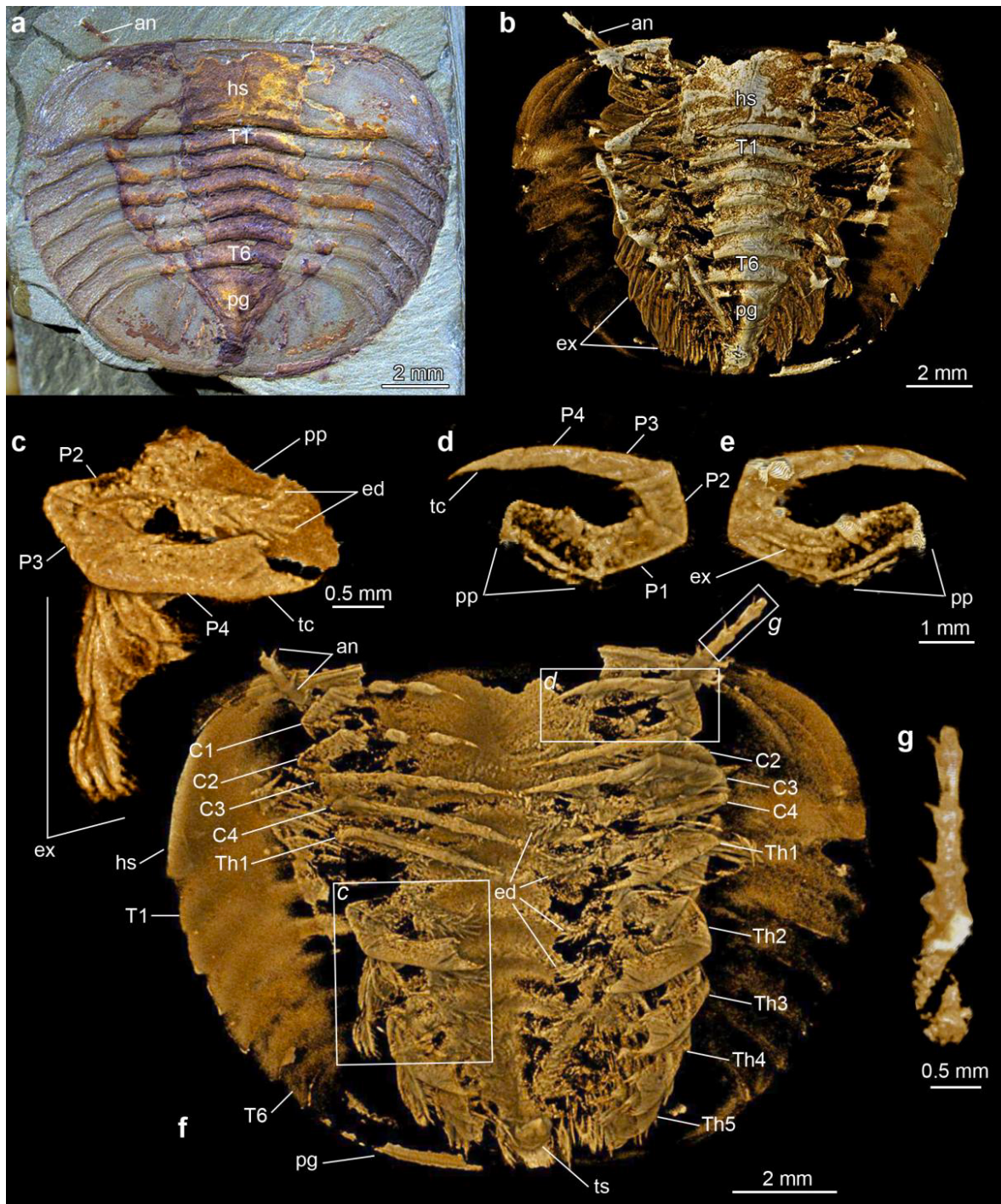


**Figure 1.** *Pygmaclypeatus daziensis* from the Cambrian (Stage 3) Chengjiang biota of South China. **a.** Specimen YKLP 11427, photographed under light microscopy. **b.** Dorsal view of three-dimensional computer model based on X-ray tomographic data rendered in Drishti [29]. **c.** Isolated three-dimensional model of second thoracic appendage in ventral view. **d.** Isolated three-dimensional model of first post-antennal cephalic appendage in ventral view. **e.** Isolated three-dimensional model of first post-antennal cephalic appendage in dorsal view, showing attachment site of elongate stenopodous exopodite. **f.** Ventral view of three-dimensional computer model based on X-ray tomographic data, exceptionally preserved appendage morphology. **g.** Isolated three-dimensional model of left antenna, showing segmental boundaries and accessory spines. Abbreviations: an, antenna;  $Cn$ , cephalic post-antennal appendage pair number; ed, enditic spine bristles; ex, exopodite; hs, head shield;  $Pn$ , podomere number; pg, pygidium; pp, protopodite; tc, terminal claw;  $Tn$ , tergite number;  $Thn$ , thoracic appendage pair number; ts, tailspine.

## Results

### *Systematic Paleontology*

Euarthropoda Lankester, 1904 [35]

Artiopoda Hou and Bergström, 1997 [6]

*Pygmaclypeatus* Zhang, Han, and Shu, 2000 [26]

*Emended diagnosis:* Small artiopod with dorso-ventrally flattened exoskeleton, broader than long. Dorsal exoskeleton with poorly defined axial region without clearly developed axial furrows. Cephalon short, covering widely conterminant hypostome, uniramous antennae, and four appendage pairs. Trunk consists of six freely articulating tergites, each covering a single appendage pair. Pygidium nearly isopygous, covering four appendage pairs, and short multiarticulated tailspine. All post-antennal appendages biramous, consisting of protopodite, endopodite with five podomeres, and exopodite. Biramous appendage construction variable throughout the body; anterior three pairs of cephalic limbs lacking protopodal gnathobases and with reduced stenopodous exopodite, whereas all remaining posterior pairs have delicate spinose endites on protopodite, and well-developed exopodite lobe bearing thick paddle-shaped lamellae. Modified from Zhang et al. [26].

*Remarks:* *Pygmaclypeatus* is among the rarest fossil taxa in the Chengjiang biota, with an estimated total of around 10 specimens available to date [28]. Since its original description [26], only one study has made further contributions to the morphology and preservation of *Pygmaclypeatus*, namely the recognition of a short multiarticulated tailspine [27]. The phylogenetic position of *Pygmaclypeatus* within Artiopoda has also received little attention, although most studies concur in close affinities with the similarly enigmatic *Retifacies* based on the presence of a pygidium with a multiarticulated

tailspine [6, 10, 11], and *Squamacula* from Chengjiang based on their overall shield-like shape and body proportions [36]. Our new morphological data allows us to produce a more accurate diagnosis for *Pygmaclypeatus* in the context of Artiopoda.

*Pygmaclypeatus daziensis* Zhang, Han and Shu, 2000

2000 Zhang, Han and Shu, p. 980, Fig. 1 [26]

2004 Xu, p. 331, Plate 1, Figs 4 and 5 [27]

2017 Hou et al., p. 197, Fig. 20.28 [28]

### *Diagnosis:*

As for genus.

*Description:* All known individuals are preserved in a dorsoventrally flattened position. Completely articulated specimens have a broad dorsal exoskeleton that is slightly wider than long, reaching up to 14 mm in length (sagittal), and a maximum width (transverse) of up to 17.5 mm measured at the level of the anterior trunk (Fig. 1). The dorsal exoskeleton has a shield-like rounded outline, with the anterior end of the body being easily distinguished by featuring a straight margin. The body consists of a cephalon, a trunk with six freely articulating tergites, and a pygidial shield associated with a multisegmented tailspine (Figs 1-3). The cephalon constitutes approximately 25% of the total body length (sag.). The cephalic outline is sub-rectangular with a straight anterior margin, rounded antero-lateral edges that develop into posterior-facing acute genal angles, and a posterior margin that is gently reflexed adaxially (Fig. 1a). The dorsal surface of the cephalon is mostly featureless, without dorsal ecdysial sutures, and lacks evidence of eyes or other ocular-derived structures (*contra* [27]). Although the main body axis is demarcated by a difference in

coloration relative to the lateral areas of the cephalon, there is no indication of an elevated axial region or furrows. Previous studies have interpreted the presence of a rostral plate or anterior sclerite in the type material of *Pygmaclypeatus daziensis* (e.g., [10, 26, 37, 38]). Close examination of our material, including micro-CT data, does not demonstrate the presence of a discrete anterior sclerite. Instead, the anterior margin of the head shield frequently features a transverse narrow band that appears to be a compaction artifact produced by the direct contact between the head shield and the ventral hypostome (Fig. 2d). We find no evidence of an anterior sclerite in *P. daziensis*.

The ventral side of the cephalon includes a hypostome, a pair of uniramous antennae, and four pairs of post-antennal biramous appendages (Fig. 1d, f; 2a, d). The hypostome is conterminant, directly attached to the anterior margin of the cephalon. The hypostome transversely covers ca. 33% of the width of the cephalon, and extends posteriorly to ca. 50% of the length of the cephalon, completely covering the proximal bases of two post-antennal appendages. Morphologically, the hypostome has a rounded posterior margin, including a small median notch that most likely indicates the position of the posterior-facing mouth as typically located in arthropods [39]. The edges of the hypostome are strengthened by convex crescent-shaped ridges that meet adaxially, defining the median notch, conveying a bi-lobed appearance. The antennae are antero-laterally oriented and attach ventrally in the cephalon close to the antero-lateral edges of the hypostome (Fig. 1f; 2d). The proximal portions of the antennae are well preserved in YKLP 11427 (Fig. 1b, f), consisting of at least four articles. The antennae appear to have a sub-cylindrical cross-section, and gently taper in width distally. The articles telescope into each other, with each featuring a pair of short spines located on their anterior margin and facing adaxially relative to the main body axis. The full extent of the antennae is unknown owing to their fragmentary preservation.

The first four post-antennal biramous appendages become progressively larger towards the posterior end of the cephalon and include two morphological variants. The first three post-antennal appendages consist of a sub-rectangular protopodite attached to an endopodite with five podomeres, and a reduced stenopodous exopodite (Fig. 1d, e; 2b). The exopodites lack a clear indication of segmental boundaries, but it is unclear if this results from a preservation artifact or accurately reflects the original morphology. The endopodites are preserved in a strongly curved orientation facing towards the main body axis, and taper to an acute terminal claw. The podomeres are laterally compressed. In these limbs, there is little evidence of well-developed endites or any other processes on the protopodite or the endopodites in either of the examined specimens (Fig. 1d, e, f), suggesting that this absence is legitimate rather than taphonomic.

The only exception is the presence of a short ventral spine on the anterior margin of the second endopodite podomere (Fig. 1d, 3e). The cephalic endopodites are prominent in size, and are the only appendages that extend beyond the exoskeleton margins (Fig. 2a). The exopodite is attached dorsally to the protopodite (Fig. 1d, 3e), and consists of a slender rod-shaped branch less than half the length of each corresponding endopodite. The fourth post-antennal biramous appendage pair has a similar –albeit more robust –overall endopodite organization but differs substantially in the morphology of other components. The protopodite bears gnathobases along the ventral margin consisting of two or three densely populated rows of delicate spinose endites (Fig. 1f).

The exopodite is fully developed, consisting of a sub-triangular proximal base attached to the protopodite, and which bears up to six thick paddle-shaped lamellae (Fig. 2c). Each of the paddle-shaped lamellae shows a preferential preservation along the edges, suggesting that this region had strengthened cuticle relative to

the interior face of the paddle. Within each exopodite, only the most distal paddle-shaped lamella bears a series of short marginal setae (Fig. 2c); the fact that this pattern is observed in several appendage pairs argues that this organization is not the result of a preservation artifact, and instead suggests that it is a legitimate biological feature. The variable orientation in the preservation of the paddle-shaped lamellae, as seen from dorsal view, indicates that these structures were freely articulated and allowed some degree of motion through pivoting relative to the exopodite lobe (Fig. 2a, d).

The trunk of *Pygmaclypeatus daziensis* consists of six freely articulating tergites that overlap widely with each other (Fig. 1a, b). The trunk makes up approximately 50% of the total body length (sag.). All trunk tergites are much wider (trans.) than long (sag.) and share the same overall morphology. The axial region of the trunk suggests a weak elevation, which is also indicated by the anteriorly reflexed posterior margin of the tergites. The tergites have a sub-rectangular outline adaxially with straight margins, but become progressively curved posteriorly and abaxially, terminating in acute pleural angles. The first trunk tergite is approximately the same width (trans.) as the head shield, whereas the subsequent tergites gently taper in width towards the posterior end, conveying a rounded body outline (Fig. 1a, b). Each trunk tergite is associated with a single pair of biramous appendages on the ventral side.

The trunk limbs are morphologically similar to the fourth post-antennal appendage pair, including the presence of a protopodite with delicate spinose ventral endites, endopodites with five podomeres, and exopodites with a triangular base that supports paddle-shaped lamellae with marginal setae (Fig. 1c). However, the trunk appendages differ in some details. The trunk endopodites are more robust and the podomeres are laterally compressed. Most significantly, the

distal most part of the endopodite, consisting of second to last podomere and the terminal claw, is modified into a strong sub-chelate termination (Fig. 1c). The terminal claw is broad and sub-triangular, and features a wide area of articulation with the neighboring podomere that suggests a function as a moveable finger with a finely serrated inner edge, whereas the pre-terminal podomere is enlarged distally forming a robust thumb-like projection (fixed finger). Lastly, the larger size of the trunk exopodites can accommodate up to nine thick lamellae. A dorsal view of the articulated trunk appendage series shows that the ventral limbs are entirely concealed within the margins of the exoskeleton (Fig. 1a, b), which explains the difficulty of resolving these structures without the aid of micro-CT imaging.

The pygidium of *Pygmaclypeatus daziensis* consists of an unsegmented shield covering the posterior segments and has a gently rounded posterior margin (Fig. 1a, b). The pygidium corresponds to approximately 25% of the total body length (sag.), but is narrower (trans.) than the cephalon and the anterior portion of the trunk. The weakly defined axial region of the cephalon and trunk continues into the pygidium, but ends at approximately the middle portion of the posterior shield with a rounded sub-triangular termination. The ventral side of the pygidium shows the presence of at least four pairs of biramous appendages; these indicate that *P. daziensis* has ca. 14 pairs of post-antennal appendage pairs (Fig. 1f; 2a, d). The morphology of the biramous appendages under the pygidium is identical to that of those in the trunk region, although the limbs become progressively smaller posteriorly and closer towards the midline. The posterior end of the body bears a short multi-articulated tailspine tucked underneath the body in YKLP 11427 (Fig. 1f), which corroborates the most recent revision of *P. daziensis* [27].

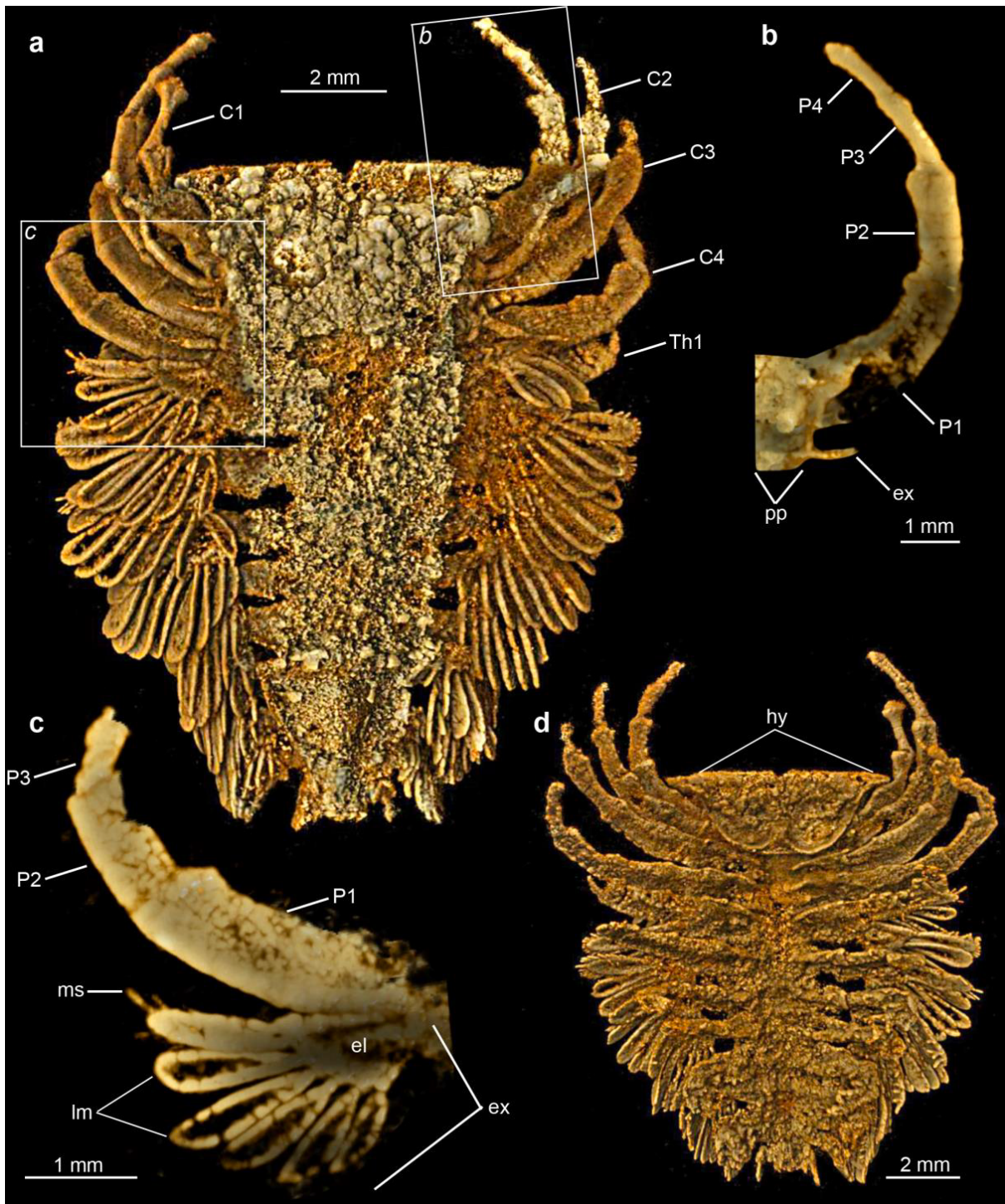


**Figure 2.** *Pygmaclypeatus daziensis* from the Cambrian (Stage 3) Chengjiang biota of South China. **a.** Specimen YKLP 11428, dorsal view of three-dimensional computer model based on X-ray tomographic data rendered in Drishti [32]; dorsal exoskeleton tergites removed to illustrate the appendage organization. **b.** Isolated three-dimensional model of first post-antennal cephalic appendage in dorsal view, showing attachment site of elongate stenopodous exopodite. **c.** Isolated three-dimensional model of first thoracic appendage in dorsal view, showing morphology and attachment site of well-developed exopodite with paddle-shaped lamellae; note that marginal setae are only present on the distal most lamella. **d.** Ventral view of three-dimensional computer model based on X-ray tomographic data, showing well-preserved hypostome. Abbreviations: *Cn*, cephalic post-antennal appendage pair number; *el*, exopodite lobe; *ex*, exopodite; *hy*, hypostome; *lm*, paddle-shaped lamellae; *ms* marginal setae; *Pn*, podomere number; *pp*, protopodite; *Thn*, thoracic appendage pair number.



## Discussion

### *Appendicular heteronomy in Pygmaclypeatus*

The use of micro-CT in pyritized Chengjiang fossils reveals the overall appendage morphology of *Pygmaclypeatus daziensis* in substantial detail (Figs 1-3), made all the more striking by the fact that the known ventral organization of this taxon until now consisted of faint impressions of the hypostome and fragmentary antennae [26–28]. The appendages of *P. daziensis* combine a unique suite of ancestral and derived characters within the broader context of Artiopoda, and significantly, demonstrate a higher degree of appendage heteronomy than any other representative of this clade described to date.

Flagelliform antennae are widespread among artiopods, present in both trilobites (e.g., [13, 40]) and their non-biomineralized relatives (e.g., [6, 23, 37]); the Chengjiang xandarellid *Sinoburius lunaris* represents the only known case to date where the antennae are highly reduced and non-flagelliform [22]. Paired spines on the uniramous antennae are also expressed in several non-biomineralizing artiopods such as *Retifacies*, *Kuamaia* and *Emeraldella* (e.g., [6, 37, 41]), and even trilobites, as in *Hongshiyanspis* [13]. Although the antennae of *P. daziensis* fall within the known diversity observed in artiopods, this is not the case for the post-antennal appendages.

The organization of the first to third post-antennal biramous appendage pairs of *P. daziensis* is uncommon in the absence of well-developed spinose endites along the ventral edge, typical in most artiopods, with the exception of short spines associated with the anterior podomere margins in the endopodite (Fig. 1d, e; 2b). Intriguingly, this organization parallels that of the prosomal endopodites in the extant horseshoe crab (Xiphosura) *Limulus polyphemus*

[42], in terms of both the number of podomeres and the presence of sparse short spines on their anterior edge. The occurrence of highly reduced stenopodous exopodites associated with the first to third post-antennal biramous appendages is also notable, as this precise morphology is unknown from most other artiopods. Comparable structures among Cambrian representatives include the flagelliform cephalic exopodites of *S. lunaris* [22] and *Sanctacaris uncata* [43], although these differ in being longer and multiarticulated, and the so-called proximo-lateral process found on the protopodite of *Sidneyia inexpectans* [2, 17, 44]. Significantly, the latter comparison invites further parallels with the “flabellum” of *L. polyphemus*, a small lobe-like structure found on the protopodite of the sixth prosomal limb pair that has been interpreted as either a vestigial exopodite [45] or possibly an exite [46, 47].

The fourth pair of biramous appendages in *P. daziensis* has a more conventional organization based on the presence of prominent endites on the protopodite and a well-developed exopodite, but their precise morphology also has some uncommon features. The protopodite endites of *P. daziensis* are delicate and spinose, similar to those recently described in the protopodite of adult *Naraoia spinosa* from Chengjiang [23], and those of the anterior walking legs of *Limulus polyphemus* [15, 17]. However, the detailed morphology of the exopodite differs drastically from the elongate lobed organization observed in most artiopods, in which the exopodite typically consists of a rod-like shaft (e.g., *Misszhouia longicaudata*, *Naraoia compacta*, *Xandarella spectaculum*), or is differentiated into a slender proximal and large tear-shaped distal lobe (e.g., *Naraoia spinosa*, *Olenoides serratus*, *Saperion glumaceum*) (see fig. 4 in [3]).

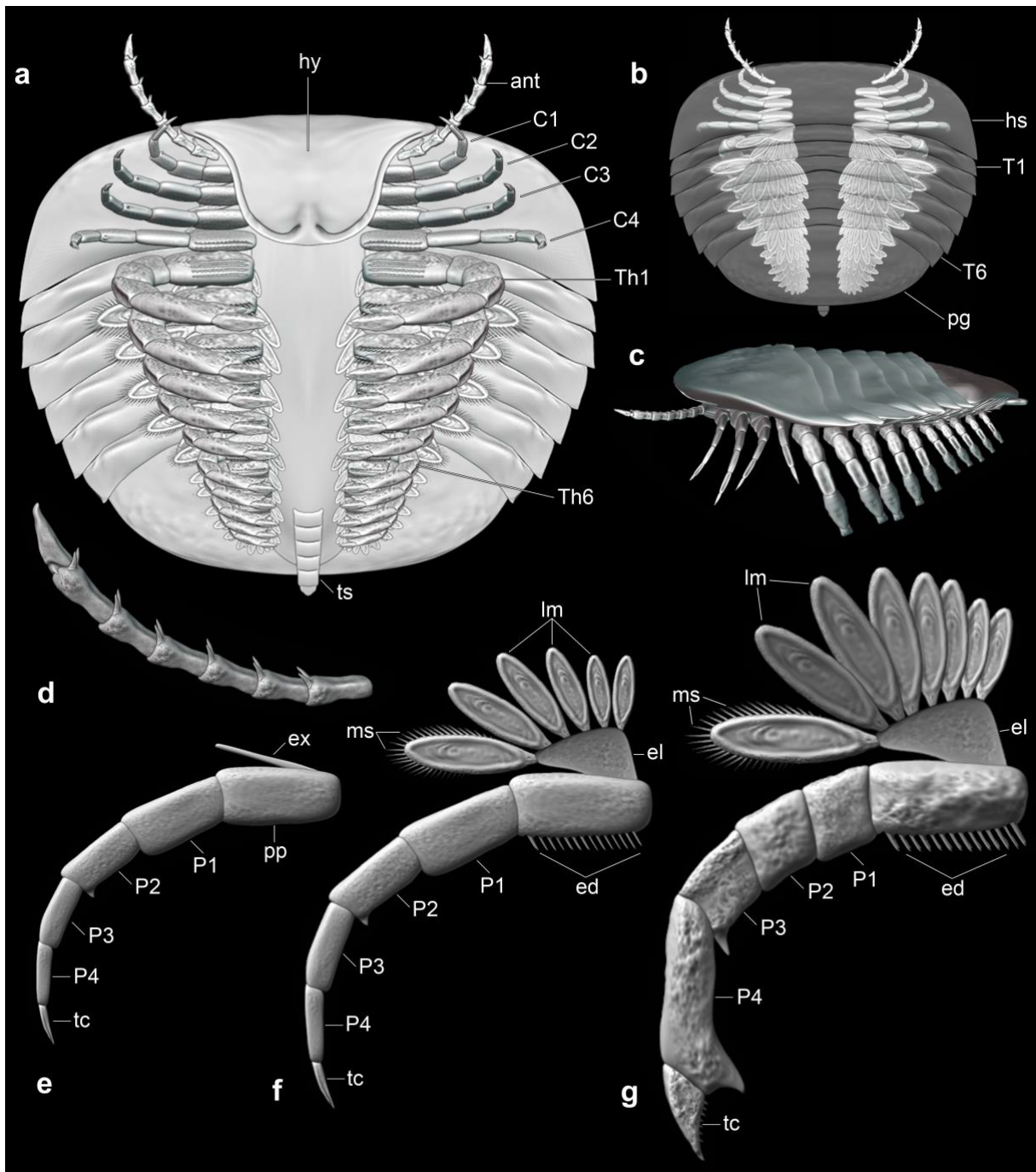


**Figure 3. Three-dimensional morphological reconstruction of *Pygmaclypeatus daziensis*.** **a.** Ventral view. **b.** Dorsal view, with transparent dorsal exoskeleton to show organization of appendages. **c.** Lateral view showing habits of ventral appendages. **d.** Antennae. **e.** Morphology of first to third post-antennal cephalic appendage pairs. **f.** Morphology of fourth post-antennal cephalic appendage pair. **g.** Morphology of thoracic and pygidial appendage pairs. Abbreviations: ant, antennae; *C<sub>n</sub>*, cephalic post-antennal appendage pair number; ed, enditic spine bristles; el, exopodite lobe; ex, exopodite; hs, headshield; hy, hypostome; Im, paddle-shaped lamellae; ms, marginal setae; pg, pygidium; *P<sub>n</sub>*, podomere number; pp, protopodite; tc, terminal claw; *T<sub>n</sub>*, tergite number; *Th<sub>n</sub>*, thoracic appendage pair number; ts, tailspine.

The fully developed exopodite of *P. daziensis* most closely resembles that of *Retifacies abnormalis* in the presence of a single robust lobe attached to the protopodite, and which bears thick paddle-shaped lamellae with short marginal setae [6]. Key differences between the exopodite in these taxa include the shape of the lobe—subtriangular in *P. daziensis* versus semiovalate in *R. abnormalis*, the presence of only up to nine lamellae in *P. daziensis* (compared with over a dozen in *R. abnormalis*), and the fact that *R. abnormalis* paddle-shaped lamellae are more elongate and more tightly imbricated.

A comparable exopodite organization has also been recently confirmed in *Naraoia compacta* from the Burgess Shale [48], and tentatively suggested for *Emeraldella brocki* [37] and *Kuamaia lata* [6]. Although *N. compacta* also features paddle-shaped lamellae with short marginal spines, it differs from *P. daziensis* and *R. abnormalis* in that the exopodite morphology consists of an elongate shaft, rather than a single robust lobe (Fig. 2c). The fifth to fourteenth post-antennal biramous appendages of *P. daziensis* share a similar overall morphology to that of the fourth pair, excluding their progressively smaller size posteriorly, but differ substantially in the morphology of the distal endopodite.

The differentiation of a modified terminal claw and pre-terminal endopodite podomere into a robust moveable finger and fixed thumb, respectively, is not known in any other artiopod, nor the biramous appendages of any Cambrian euarthropod more broadly, as the endopodite termination usually consists of a single terminal claw that may carry smaller accessory spines that form a small functional foot (e.g., [2, 13, 37]).

In this context, the sub-chelate endopodites of the trunk appendages are morphologically more comparable with the walking legs in *Limulus polyphemus* [42], even if the terminal regions of the endopodites in *P. daziensis* are not fully developed into chelae as in horseshoe crabs. Subchelate limbs are also known from more phylogenetically distant euarthropods, such as pycnogonids and crustaceans [45], and are particularly well developed among burrowing representatives [49].

The presence of four morphologically distinct sets of appendages in *Pygmaclypeatus daziensis* (i.e. antennae, first to third post-antennal, fourth post-antennal, and fifth to fourteenth post-antennal) reflects some of the highest degrees of limb heteronomy expressed in any artiopod described to date. Although artiopods have been traditionally regarded as having largely homonomous series of biramous post-antennal appendages [6, 12, 13, 50], recent investigations record a growing number of cases of limb differentiation along the body. For example, the trilobite *Redlichia rex* from the Stage 4 Emu Bay Shale shows differences between the proportions of the anterior and posterior exopodites, even if their respective endopodites are morphologically similar [51]. Limb heteronomy is more frequent among non-trilobite artiopods.

The Miaolingian vicissicaudate *Emeraldella* features long antenniform antennae, one set of seemingly uniramous post-antennal appendages, biramous trunk limbs with some variability in terms of the relative length of the distal endopodite podomeres, and a pair of caudal flaps that likely represent modified exopodites [37, 52]. *Sidneyia inexpectans* from the Wulian Burgess Shale also shows some differences between the (possibly uniramous) anterior and posterior post-antennal biramous trunk appendages [2], which might be linked with its durophagous feeding preferences [15–17, 53].

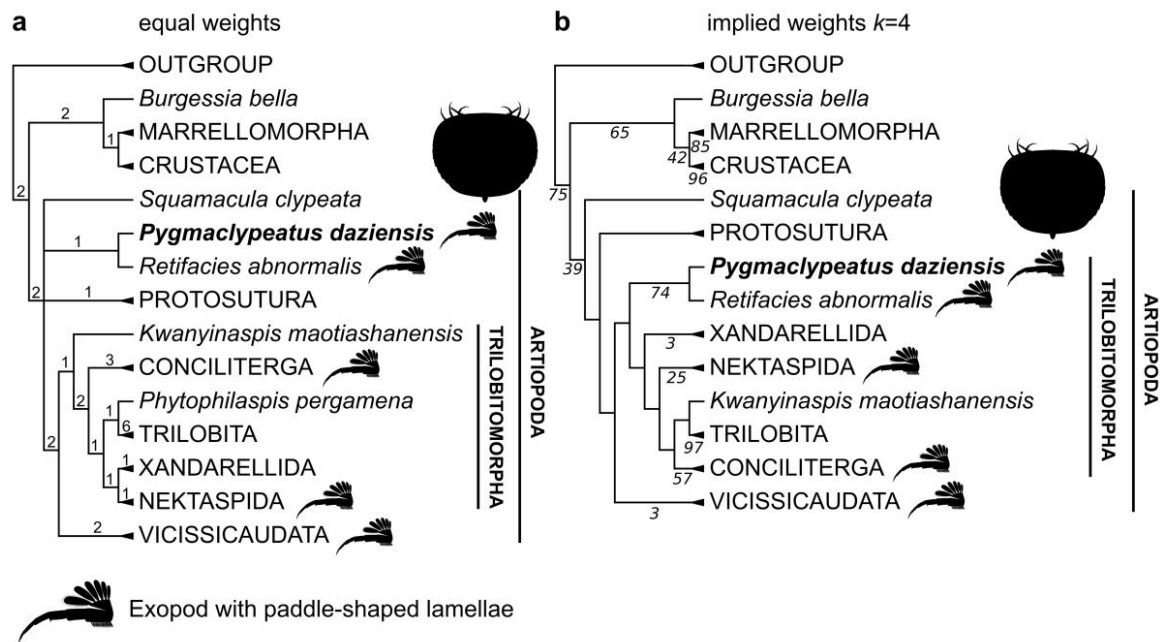


**Figure 4. Results of parsimony-based phylogenetic analyses and morphological reconstruction.** **a.** Strict consensus of four most parsimonious trees (265 steps; CI=0.419; RI=0.74) under equal weights; Bremer support values above nodes. **b.** Strict consensus of two most parsimonious trees (CI= 0.41; RI=0.73) under implied weights ( $k=4$ ); nodal support expressed as symmetric resampling after 100 repetitions. For character codings, see Extended Data Tables 1 and 2. Note the widespread occurrence of exopodites with paddle-shaped lamellae among trilobitomorpha (see text for discussion). **c.** Morphological reconstruction of *Pygmaclypeatus daziensis*. Artwork by Holly Sullivan (<https://www.sulscientific.com/>).

However, the most notable cases of limb differentiation in Cambrian artiopods are found in the trilobitomorpha *Sinoburius lunaris* [22] and *Naraoia spinosa* [23] from Chengjiang, both of which have been recently redescribed based on micro-CT imaging. In addition to greatly reduced antennae, *S. lunaris* shows a striking differentiation in exopodite structure along the body: the first two pairs of post-antennal appendages have elongated stenopodous exopodites, whereas the remaining limb pairs have a more conventional exopodite shaft with lamellae. *Sinoburius lunaris* also has well-developed ridge-like endites on the trunk protopodites, whereas these are absent from the cephalic region [22].

*Naraoia spinosa* also shows differentiation between the protopodite morphology in the cephalic and trunk regions, expressed as long spinose endites versus short blunt endites respectively, as well as more pronounced changes during ontogeny that suggest a shift from plankton/detritus feeding to scavenging [23]. *Pygmaclypeatus daziensis* reflects possibly the highest degree of appendage heteronomy and functional specialization within Artiopoda described to date, given that differentiation is expressed in all components of the biramous limbs (i.e. protopodite, endopodite, exopodite), as well as between the cephalic and trunk regions (Fig. 3).

#### *Functional morphology and paleoecology*

The new data on the ventral organization of *Pygmaclypeatus daziensis* prompt a reconsideration of its mode of life and paleoecology. Whereas earlier studies suggested an epibenthic habitus based only on the dorsoventrally flattened exoskeleton, the presence of well-developed paddle-like lamellae on the trunk exopodites suggests a considerable swimming prowess. Similar to *Naraoia compacta* [48], the exopodites would have likely produced effective propulsion during the power-stroke of

a typical metachronal wave, and allowed for low drag during the recovery phase owing to the pivot-like articulation of the individual paddles relative to the exopodite lobe. Taken together, the imbrication of the trunk exopodites coupled with the small overall body size (less than 2 cm) suggest that *P. daziensis* would have been able to swim in the water column periodically, in line with an active nektobenthic mode of life.

Based on recent studies supporting a gill-like function for the trilobite exopodite [54], the well-developed exopodites of *P. daziensis* may have effectively conveyed a large surface area for gas exchange thanks to the presence of more than 200 individual paddle-shaped lamellae (Figs 2, 3). The functional morphology of the protopodite and endopodites further informs the feeding habits of *P. daziensis*. The presence of delicate spinose endites on the protopodite of most biramous appendages suggests a diet consisting of soft-food items and organic-rich particles, compatible with scavenging / detritus feeding. The morphology of the endites rules out a durophagous diet, as shell crushing requires robust molariform gnathobases on transversely elongate protopodites, as seen in *Sidneyia inexpectans*, *Redlichia rex* and *Limulus polyphemus* [17].

The absence of endites on the ventral side of the endopodites suggests that food processing mainly took place proximally within the trunk protopodites that form a food groove leading to the posteriorly directed mouth opening underneath the hypostome (Fig. 2d), whereas the cephalic endopodites would be better suited for object manipulation in front of the body. The distal portion of all the endopodites would have been primarily used for locomotion. In particular, the strong ventral curvature of the legs, coupled with the presence of subchelate terminations on the trunk region consisting of the fixed thumb and the moveable finger appear to be well suited for a more specialized grabbing/anchoring function on hard substrates, and possibly burrowing behavior, as observed in extant

forms such as amphipods [54–56]. The similarities between *P. daziensis* and *L. polyphemus* (see previous section) suggest that these organisms shared a broadly comparable mode of life, the only important exception being that the lack of robust gnathobases in the former argues against effective durophagy as observed in *L. polyphemus* [17, 53], and instead favors a diet based on soft food items and/or decaying organic matter.

#### *Implications for artiopod evolution*

The detailed three-dimensional appendage organization of *Pygmaclypeatus daziensis* contributes towards a better understanding of the paleobiology of this taxon (Fig. 3) and has direct implications for reconstructing the evolutionary history of Artiopoda. The results of our phylogenetic analyses consistently resolve *P. daziensis* as the sister-taxon to *Retifacies abnormalis*, supported by the organization of the exopodite (single lobe with paddle-shaped lamellae with marginal setae), and the presence of both a pygidium and a multiarticulated tailspine; these results concur with earlier analyses that also support a close relationship between these two taxa [10, 11, 30]. Implied weights ( $k=4$ ) support the position of *P. daziensis* + *R. abnormalis* as the earliest branching clade within trilobitomorpha (Fig. 4b), although its precise placement relative to the former is unresolved under equal weights (Fig. 4a).

Despite the difference in these topologies, both analyses support an early-branching position within Artiopoda, which allows reconstructing the ancestral organization for these euarthropods.

The morphology of *P. daziensis* and *R. abnormalis* includes some characters that are widespread – and possibly ancestral – for trilobitomorpha, such as the conterminant hypostome and the presence of a pygidium. The presence of a multi-articulated tailspine appears to be unique to these two taxa within trilobitomorpha, even though this character is known from more distantly related Cambrian forms such as *Molaria spinifera* [58]; the latter case is most likely a result of homoplasy.

A potentially significant new insight consists of the clarification of the detailed exopodite structure in *P. daziensis* and *R. abnormalis*, and its bearing for understanding the evolution of this structure among trilobitomorpha. The exopodite of *P. daziensis* and *R. abnormalis* is unique as it consists of a single lobe with paddle-shaped lamellae, whereas the exopodite of most other trilobitomorpha is differentiated into a proximal lobe with lamellae and a distal lobe with short setae. As highlighted in recent work [48], and further demonstrated in the present study, the repeated occurrence of paddle-shaped lamellae in artiopods could argue in favor of an ancestral organization of the exopodites that has not been fully appreciated owing to the delicate nature of these structures, and the bias caused by compaction during burial.

We explored this hypothesis through the optimization of paddle-shaped lamellae (Char. 15, state 2; see Supplementary Information) using the character mapping function in TNT [34, 58]. Under equal weights (Fig. 4a), the ancestral organization of the exopodite lamellae for Artiopoda remains uncertain in all four most parsimonious trees recovered owing to topology conflict resulting in a polytomy at the base of this clade. By contrast, the two most parsimonious trees recovered under implied weights ( $k=4$ ) support the paddle-shaped lamellae as ancestral for Artiopoda, in line with our hypothesis (Fig. 4b). A more definitive test for this hypothesis will require further investigations on the detailed appendage morphology of several early branching artiopods (e.g. *Squamacula*, Protosutura; see [57]), trilobitomorpha (e.g. Nektaspida, Xandarellida, Conciliterga; see [1, 6, 7]) and vicissicaudates (e.g., Xenopoda, Cheloniellida, Aglaspida; see [3, 60]).

The presence of only five endopodite podomeres (including the terminal claw) in *P. daziensis* is remarkable in the context of Artiopoda, as most of these organisms feature the typical seven-segmented endopodite that is considered as ancestral for crown-group Euarthropoda in a broad sense [45, 47].

Evidence for endopodites with fewer than seven podomeres in artiopods is rare. Possible cases include the reduced endopodites on the anteriormost biramous limbs of *Sinoburius lunaris* [22] and *Emeraldella* [37, 52] based on their small size compared with trunk appendages, but in both cases, the proximal portions of the endopodites are not well known. *P. daziensis* represents the only Cambrian artiopod for which all the post-antennal biramous appendages have a five-segmented endopod, as even its sister taxon *Retifacies abnormalis* shows more conventional limbs [6]. The Devonian cheloniellid *Cheloniellon calmani* [61] is the only other known artiopod with consistently five-segmented endopodites throughout the body confirmed to date, although their structure is much closer to a generalized walking leg when compared with *P. daziensis*.

Beyond Artiopoda, the five-segmented endopodite is widespread among mandibulates, and in particular crustaceans, whereas the seven-segmented endopodite is common among chelicerates [45, 47]. Although the number of endopodite podomeres carries little phylogenetic information by itself, the biramous appendage construction of *P. daziensis* can be confidently interpreted as a derived trait among artiopods, with rare instances of convergence, as observed in the phylogenetically and biostratigraphically distant *C. calmani* [61].

Another significant implication of this study is that it challenges the traditional notion that trilobitomorpha, and more broadly artiopods, are characterized by largely homonomous post-antennal appendage pairs [1, 6, 13, 62]. Instead, *Pygmaclypeatus daziensis* reveals that some of the earliest branching representatives of this clade already demonstrate substantial limb differentiation (Fig. 4). Although *P. daziensis* is the latest example, it is by far not the only one, as variable degrees of post-antennal appendage specialization have been described in the literature (see discussion above). Most of the main artiopod clades include at least one representative for which there is substantial

evidence of limb differentiation, including also Nektaspida (e.g., *Naraoia spinosa* [23]), Xandarellida (e.g., *Sinoburius lunaris* [22]), Trilobita (e.g., *Redlichia rex* [51]), and Vicissicaudata (e.g., *Emeraldella* [37, 52], *Sidneyia inexpectans* [2]). It is notable that these taxa are among the most complete and recently re-described representatives of their respective groups, which suggests that antero-posterior limb differentiation might be more widespread within Artiopoda than it is currently considered. Other clades, such as Conciliterga, include taxa that have not been revised in at least the last decade, or that contain forms mostly known from the dorsal exoskeleton without complete appendage series. In this context, it appears likely that the archetypical homonomous appendage series of trilobites could represent a phylogenetically derived trait, rather than an ancestral one as commonly considered historically (e.g., [13, 45, 50, 62]).

Further morphological investigations on the appendage structure of Artiopoda that provide more comparable information between species are required, but the increased availability of new data on Chengjiang euarthropods through micro-CT imaging offers great promise for testing this hypothesis.

## Acknowledgements

This study was supported by the NSFC grant (41861134032), DFG grant (Me-2683/10-1), Natural Science Foundation of Yunnan Province grants (2015HA021, 2018FA025, 2018IA073 and 2019DG050), and the Harvard China Fund.

## Author contributions

M.S., R.R.M., J.O.-H. and Y.L. designed the research. X.H., R.R.M., J.O.-H., and Y.L. secured

the funding. X.H. and D.Z. collected all the material. R.R.M. and H.M. scanned YKLP 13929 and YKLP 11428, respectively). X.C. documented all the specimens with light photography. M.S. and Y.L. processed the tomographic models. M.S. rendered the 3D models. J.O.-H. performed the phylogenetic analysis. J.B. helped with the supplementary figure. M.S., J.O.-H. and R.R.M. wrote the paper with input from all the other coauthors. All authors participated in the interpretation of the material and the discussions.



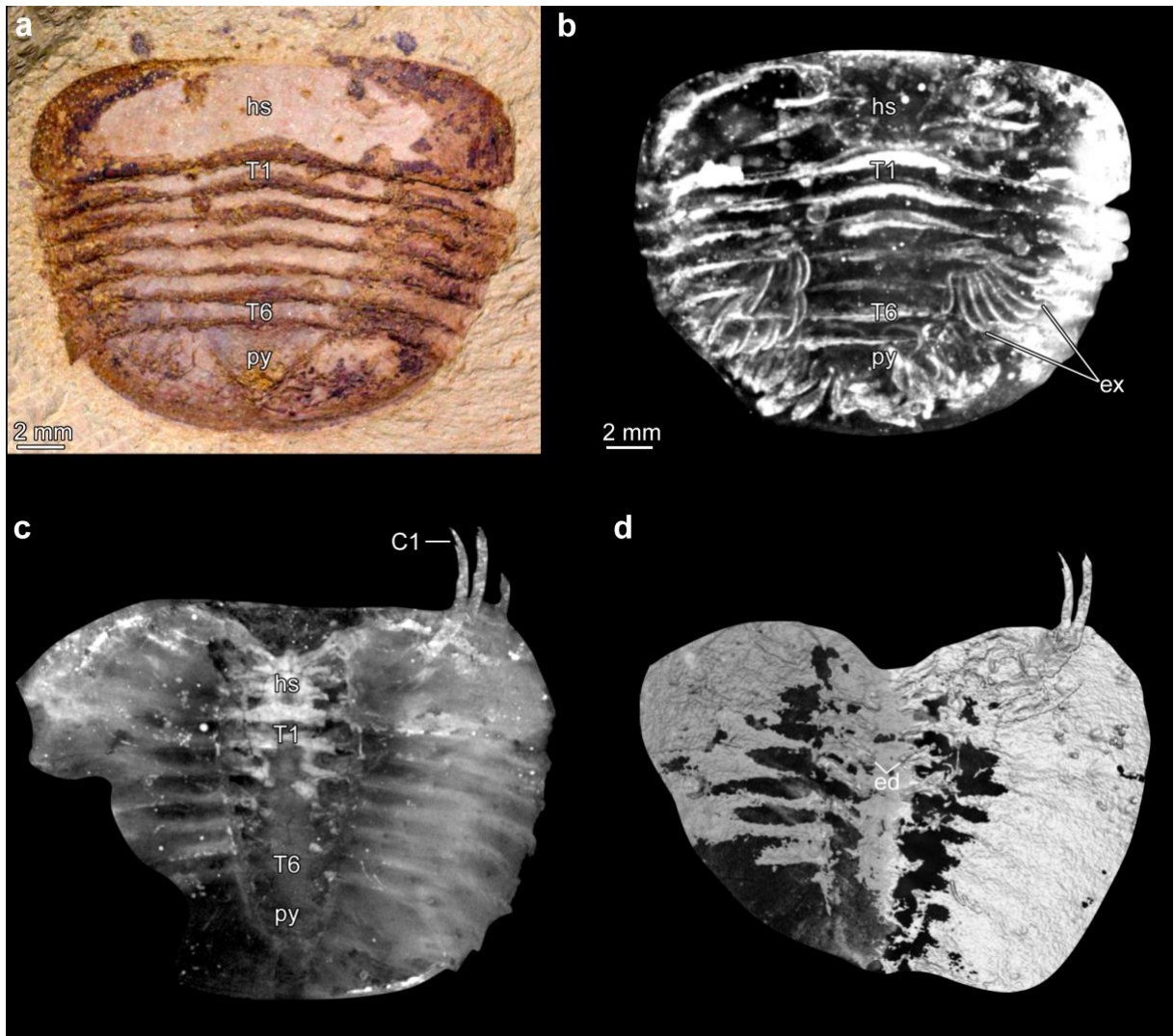
## References

1. **Edgecombe, G. D., & Ramsköld, L. (1999).** Relationships of Cambrian Arachnata and the systematic position of Trilobita. *Journal of Paleontology*, 73(2), 263–287.
2. **Stein, M. (2013).** Cephalic and appendage morphology of the Cambrian arthropod *Sidneyia inexpectans*. *Zoologischer Anzeiger-A Journal of Comparative Zoology*, 253(2), 164–178.
3. **Ortega-Hernández, J., Legg, D. A., & Braddy, S. J. (2013).** The phylogeny of aglaspidid arthropods and the internal relationships within Artiopoda. *Cladistics*, 29(1), 15–45.
4. **Bond, A. D., & Edgecombe, G. D. (2021).** Phylogenetic response of naraoiid arthropods to early–middle Cambrian environmental change. *Palaeontology*, 64(1), 161–177.
5. **Wilmot, N. V. (1990).** Primary and diagenetic microstructures in trilobite exoskeletons. *Historical Biology*, 4(1), 51–65.
6. **Hou, X. G., & Bergström, J. (1997).** Arthropods of the Lower Cambrian Chengjiang fauna, Southwest China. *Fossils Strata*, 45, 1–116.
7. **Mayers, B., Aria, C., & Caron, J. B. (2019).** Three new naraoiid species from the Burgess Shale, with a morphometric and phylogenetic reinvestigation of Naraoiidae. *Palaeontology*, 62(1), 19–50.
8. **Budd, G. E. (2011).** *Campanamuta mantonae* gen. et. sp. nov., an exceptionally preserved arthropod from the Sirius Passet Fauna (Buen Formation, lower Cambrian, North Greenland). *Journal of Systematic Palaeontology*, 9(2), 217–260.
9. **Stein, M., Budd, G. E., Peel, J. S., & Harper, D. A. (2013).** *Arthroaspis* n. gen., a common element of the Sirius Passet Lagerstätte (Cambrian, North Greenland), sheds light on trilobite ancestry. *BMC Evolutionary Biology*, 13(1), 1–34.
10. **Paterson, J. R., Edgecombe, G. D., García-Bellido, D. C., Jago, J. B., & Gehling, J. G. (2010).** Nektaspid arthropods from the lower Cambrian Emu Bay Shale Lagerstätte, South Australia, with a reassessment of lamellipedian relationships. *Palaeontology*, 53(2), 377–402.
11. **Paterson, J. R., García-Bellido, D. C., & Edgecombe, G. D. (2012).** New artiopodan arthropods from the early Cambrian Emu Bay Shale Konservat-Lagerstätte of South Australia. *Journal of Paleontology*, 86(2), 340–357.
12. **Wills, M. A., Briggs, D. E. G., & Fortey, R. A. (1998).** Evolutionary correlates of arthropod tagmosis: scrambled legs. In Fortey, R. A., & Link, R. H. T. (eds) *Arthropod relationships* (pp. 57–65). Springer, Dordrecht.
13. **Zeng, H., Zhao, F., Yin, Z., & Zhu, M. (2017).** Appendages of an early Cambrian metadoxidid trilobite from Yunnan, SW China support mandibulate affinities of trilobites and artiopods. *Geological Magazine*, 154(6), 1306–1328.
14. **Vannier, J., & Chen, J. Y. (2002).** Digestive system and feeding mode in Cambrian naraoiid arthropods. *Lethaia*, 35(2), 107–120.
15. **Zacai, A., Vannier, J., & Lerosey-Aubril, R. (2016).** Reconstructing the diet of a 505-million-year-old arthropod: *Sidneyia inexpectans* from the Burgess Shale fauna. *Arthropod Structure & Development*, 45(2), 200–220.
16. **Bicknell, R. D. C., Paterson, J. R., Caron, J. B., & Skovsted, C. B. (2018).** The gnathobasic spine microstructure of recent and Silurian chelicerates and the Cambrian artiopodan *Sidneyia*: functional and evolutionary implications. *Arthropod Structure & Development*, 47(1), 12–24.
17. **Bicknell, R. D. C., Holmes, J. D., Edgecombe, G. D., Losso, S. R., Ortega-Hernández, J., Wroe, S., & Paterson, J. R. (2021).** Biomechanical analyses of Cambrian euarthropod limbs reveal their effectiveness in mastication and durophagy. *Proceedings of the Royal Society B*, 288(1943), 20202075.

18. **Zhai, D., Ortega-Hernández, J., Wolfe, J. M., Hou, X.-G., Cao, C., & Liu, Y. (2019).** Three-dimensionally preserved appendages in an early Cambrian stem-group pancrustacean. *Current Biology*, 29(1), 171–177.
19. **Zhai, D., Williams, M., Siveter, D. J., Harvey, T. H., Sansom, R. S., Gabbott, S. E., Siveter, D. J., Ma, X., Zhou, R., Liu, Y., & Hou, X.-G. (2019).** Variation in appendages in early Cambrian bradoriids reveals a wide range of body plans in stem-euarthropods. *Communications biology*, 2(1), 1–6.
20. **Liu, Y., Ortega-Hernández, J., Chen, H., Mai, H., Zhai, D., & Hou, X.-G. (2020).** Computed tomography sheds new light on the affinities of the enigmatic euarthropod *Jianshania furcatus* from the early Cambrian Chengjiang biota. *BMC Evolutionary Biology*, 20, 62.
21. **Liu, Y., Ortega-Hernández, J., Zhai, D., & Hou, X.-G. (2020).** A reduced labrum in a Cambrian great-appendage Euarthropod. *Current Biology*, 30(15), 3057–3061.
22. **Chen, X., Ortega-Hernández, J., Wolfe, J. M., Zhai, D., Hou, X., Chen, A., Mai, H., & Liu, Y. (2019).** The appendicular morphology of *Sinoburium lunaris* and the evolution of the artiopodan clade Xandarellida (Euarthropoda, early Cambrian) from South China. *BMC evolutionary biology*, 19(1), 1–20.
23. **Zhai, D., Edgecombe, G. D., Bond, A. D., Mai, H., Hou, X.-G., & Liu, Y. (2019).** Fine-scale appendage structure of the Cambrian trilobitomorph *Naraoia spinosa* and its ontogenetic and ecological implications. *Proceedings of the Royal Society, B*, 286(1916), 20192371.
24. **Zhang, X. L., Shu, D. G., & Erwin, D. H. (2007).** Cambrian naraoiids (Arthropoda): morphology, ontogeny, systematics, and evolutionary relationships. *Journal of Paleontology* 81(sp68), 1–52.
25. **Størmer, L. (1944).** On the relationships and phylogeny of fossil and recent Arachnomorpha. *Skrifter Utgitt av Det Norske Videnskaps-Akademi i Oslo. I. Matematisk-Naturvitenskapelig Klasse, 1944*, 158 pp.
26. **Zhang, X., Han, J., & Shu, D. (2000).** A new arthropod *Pygmaclupeatus daziensis* from the early Cambrian Chengjiang Lagerstätte, South China. *Journal of Paleontology*, 74(5), 979–983.
27. **Xu, G. H. (2004).** New specimens of rare arthropods from the early Cambrian Chengjiang fauna, Yunnan, China. *Acta Palaeontologica Sinica*, 43(3), 325–331.
28. **Hou, X. G., Siveter, D. J., Siveter, D. J., Aldridge, R. J., Pei-Yun, C., Gabbott, S. E., Xiao-Ya, M., Purnell, M. A., & Williams, M. (2017).** *The Cambrian fossils of Chengjiang, China: The flowering of early animal life*. John Wiley & Sons.
29. **Limaye, A. (2012).** Drishti: a volume exploration and presentation tool", Proc. SPIE 8506, Developments in X-Ray Tomography VIII, 85060X. International Society for Optics and Photonics.
30. **Legg, D. A., Sutton, M. D., & Edgecombe, G. D. (2013).** Arthropod fossil data increase congruence of morphological and molecular phylogenies. *Nature communications*, 4(1), 1–7.
31. **Gabbott, S.E., Hou, X.-G., Norry, M. J., & Siveter, D. J. (2004).** Preservation of Early Cambrian animals of the Chengjiang biota. *Geology*, 32(10), 901–904.
32. **Zhu, M., Babcock, L. E., & Steiner, M. (2005).** Fossilization modes in the Chengjiang Lagerstätte (Cambrian of China): testing the roles of organic preservation and diagenetic alteration in exceptional preservation. *Palaeogeography, Palaeoclimatology, Palaeoecology*, 220(1-2), 31–46.
33. **Garwood, R., & Dunlop, J. (2014).** The walking dead: Blender as a tool for paleontologists with a case study on extinct arachnids. *Journal of Paleontology* 88(4): 735–746.
34. **Goloboff, P.A., & Catalano, S. A. (2016).** TNT version 1.5, including a full implementation of phylogenetic morphometrics. *Cladistics*, 32(3), 221–238.

35. **Lankester, E. R. (1904).** The structure and classification of Arthropoda. *Quarterly Journal of Microscopical Sciences*, 47, 523–582.
36. **Zhang, X., Han, J., Zhang, Z., Liu, H., & Shu, D. (2004).** Redescription of the Chengjiang arthropod *Squamacula clypeata* Hou and Bergström, from the Lower Cambrian, south-west China. *Palaeontology*, 47(3), 605–617.
37. **Stein, M.; Selden, P.A. (2012).** A restudy of the Burgess Shale (Cambrian) arthropod *Emeraldella brocki* and reassessment of its affinities. *Journal of Systematic Palaeontology* 10(2): 361–383.
38. **Ortega-Hernández, J. (2015).** Homology of head sclerites in Burgess Shale euarthropods. *Current Biology* 25(12): 1625–1631.
39. **Ortega-Hernández, J., Janssen, R., & Budd, G. E. (2017).** Origin and evolution of the panarthropod head—a palaeobiological and developmental perspective. *Arthropod structure & development*, 46(3), 354–379.
40. **Zeng, H., Zhao, F., Niu, K., Zhu, M., & Huang, D. (2020).** An early Cambrian euarthropod with radiodont-like raptorial appendages. *Nature*, 588(7836), 101–105.
41. **Whittington, H. B. (1980).** Exoskeleton, moult stage, appendage morphology, and habits of the Middle Cambrian trilobite *Olenoides serratus*. *Palaeontology*, 23, 171–204.
42. **Haug, C., & Rötzer, M. A. (2018).** The ontogeny of *Limulus polyphemus* (Xiphosura s. str., Euchelicerata) revised: looking “under the skin”. *Development genes and evolution*, 228(1), 49–61.
43. **Legg, D. A. (2014).** *Sanctacaris uncata*: the oldest chelicerate (Arthropoda). *Naturwissenschaften*, 101(12), 1065–1073.
44. **Bruton, D. L. (1981).** The arthropod *Sidneyia inexpectans*, Middle Cambrian, Burgess Shale, British Columbia. *Philosophical Transactions of the Royal Society of London. B, Biological Sciences*, 295(1079), 619–653.
45. **Boxshall, G. A. (2004).** The evolution of arthropod limbs. *Biological Reviews*, 79(2), 253–300.
46. **Wolff, C.; Scholtz, G. (2008).** The clonal composition of biramous and uniramous arthropod limbs. *Proceedings of the Royal Society B: Biological Sciences*, 275(1638), 1023–1028.
47. **Bruce, H. S. (2021).** How to align arthropod legs. *bioRxiv*. (<https://doi.org/10.1101/2021.01.20.427514>)
48. **Haug, C., & Haug, J. T. (2016).** New insights into the appendage morphology of the Cambrian trilobite-like arthropod *Naraoia compacta*. *Bulletin of Geosciences*, 91(2), 221–227.
49. **Faulkes, Z. (2013).** Morphological adaptations for digging and burrowing. *Functional morphology and diversity*, 1, 276–295.
50. **Whittington, H. B., & Almond, J. E. (1987).** Appendages and habits of the Upper Ordovician trilobite *Triarthrus eatoni*. *Philosophical Transactions of the Royal Society of London. B, Biological Sciences*, 317(1182), 1–46.
51. **Holmes, J. D., Paterson, J. R., & García-Bellido, D. C. (2020).** The trilobite *Redlichia* from the lower Cambrian Emu Bay Shale Konservat-Lagerstätte of South Australia: systematics, ontogeny and soft-part anatomy. *Journal of Systematic Palaeontology*, 18(4), 295–334.
52. **Lerosey-Aubril, R., & Ortega-Hernández, J. (2019).** Appendicular anatomy of the artiopod *Emeraldella brutoni* from the middle Cambrian (Drumian) of western Utah. *PeerJ* 7, p.e7945.
53. **Bicknell, R. D. C., Ledogar, J. A., Wroe, S., Gutzler, B. C., Watson III, W. H., & Paterson, J. R. (2018).** Computational biomechanical analyses demonstrate similar shell-crushing abilities in modern and ancient arthropods. *Proceedings of the Royal Society, B*, 285(1889), p.20181935.
54. **Vader, W. (1983).** Prehensile pereopods in gammaridean Amphipoda. *Sarsia*, 68(2), 139–148.

55. **Holmquist, J. G. (1982).** The functional morphology of gnathopods: importance in grooming, and variation with regard to habitat, in talitroidean amphipods. *Journal of Crustacean Biology*, 2(2), 159–179.
56. **Bousfield, E. L. (1965).** Haustoriidae of New England (Crustacea: Amphipoda). *Proceedings of the United States National Museum*, 117(3512), 159–240.
57. **Whittington, H. B. (1981).** Rare arthropods from the Burgess Shale, Middle Cambrian, British Columbia. *Philosophical Transactions of the Royal Society of London, B, Biological Sciences*, 292(1060), 329–357.
58. **Goloboff, P. A., Farris, J. S., & Nixon, K. C. (2008).** TNT, a free program for phylogenetic analysis. *Cladistics*, 24(5), 774–786.
59. **Hou, J. B., Hughes, N.C., & Hopkins, M. J. (2021).** The trilobite upper limb branch is a well-developed gill. *Science Advances*, 7(14), p.eabe7377.
60. **Lerosey-Aubril, R., Zhu, X., & Ortega-Hernández, J. (2017).** The Vicissicaudata revisited—insights from a new aglaspidid arthropod with caudal appendages from the Furongian of China. *Scientific Reports*, 7(1), 1–18.
61. **Stürmer, W., & Bergström, J. (1978).** The arthropod *Cheloniellon* from the Devonian Hunsrück shale. *Paläontologische Zeitschrift*, 52(1), 57–81.
62. **Hughes, N. C. (2007).** The evolution of trilobite body patterning. *Annual Review of Earth and Planetary Sciences*, 35(1), 401–434.



**Extended Data Figure 1. Additional specimens of *Pygmaclypeatus daziensis*.** **a.** Specimen YKLP 13929, photographed under light microscopy. **b.** Dorsal view of three-dimensional computer model. **c.** Specimen YKLP 13928, volume rendering. **d.** Isosurface model showing ventral endites. Abbreviations: *Cn*, cephalic post-antennal appendage pair number; *ed*, endites; *ex*, exopodite; *Tn*, tergite number.

**Extended Data Table 1. Phenotypic characters of *Pygmaclipeatus daziensis*.**

## Array characters

01. nature of first appendage: raptorial appendage (0); antennae (1).
02. number of podomeres on raptorial limb: four (0); three (1); two (2).
03. raptorial appendages with flagellum: absent (0); present (1).
04. length of distal spines on podomeres: absent or shorter than podomere (0); subequal to length of podomeres (1); longer than entire podomere series (2).
05. number of post-ocular head segments: none (0); one (1); two (2); three (3); four (4); five (5); six (6); seven (7).
06. nature of second appendage pair: biramous walking leg or antennae (0); uniramous walking leg (1).
07. nature of third appendage pair: biramous walking leg (0); uniramous walking leg (1).
08. appendages under cephalo-thoracic articulation: absent (0); present (1).
09. trunk endopods: absent or reduced (0); present (1).
10. trunk exopod structure (UPDATED): simple oval flap (0); exopod differentiated into proximal and distal lobes, the proximal lobe bearing lamellar setae, the distal lobe bearing short setae (1); numerous podomeres, each bearing a single seta (2); undivided lobe with lamellae (3); book gills (4).
11. proximal exopod lobe: flattened lobe (0); slender shaft (1).
12. distal exopod lobe: small to moderate sized flap (0); large, teardrop shaped lobe with long attachment (1).
13. exopod with articulations: absent (0); present (1).
14. imbricate exopod lamellae: absent (0); present (1).
15. lamellae structure (UPDATED): thick, flat lamellae (0); delicate, comb-like lamellae (1); paddle-shaped lamellae with marginal setae (2).
16. non-overlapping marginal setae on distal lobe: absent (0); small setae (1); long spines or filaments (2).
17. gnathobasic limbs: absent (0); present (1).
18. lateral eyes: absent (0); present (1).
19. nature of lateral eyes: stalked (0); sessile (1).
20. ventral eyes in front of head: absent (0); present (1).
21. calcified eyes: absent (0); present (1).
22. dorsal exoskeletal bulge: absent (0); present (1).
23. eye slits: absent (0); present (1).
24. dorsal median eyes: absent (0); present (1).
25. free head shield: absent (0); present (1).
26. bivalved carapace: absent (0); present (1).
27. cephalic doublure: absent (0); present (1).
28. cephalon notched: absent (0); present (1).
29. hypostome: median extension of the doublure, with no suture (0); natant, sclerite not in contact with doublure (1); with narrow overlap with pre-hypostomal sclerite (2); narrow attachment to doublure at hypostomal suture (3); absent (4).
30. anterior sclerite: absent (0); present (1).
31. ecdysial sutures: absent (0); present (1).
32. position of ecdysial sutures: marginal (0); dorsal (1).
33. elevated marginal rim: absent (0); present (1).
34. marginal rim ornamented: absent (0); present (1).
35. differentiated glabellar region: absent (0); present (1).
36. head shield outline: genal spines (0); acute genal angles (1); rounded genal angles (2); lateral spine-like extensions of the carapace (3).
37. posterior cephalic band: absent (0); present (1).
38. pleural cephalic furrows: absent (0); present (1).

39. cuticle sculpture: absent (0); present (1).
40. mineralized cuticle: absent (0); present (1); State 2 (2).
41. expanded lateral pleurae: absent (0); present (1).
42. free thoracic tergites: absent (0); present (1).
43. decoupling of tergites and limb pairs: absent (0); present (1).
44. tergite articulations: tergites non-overlapping (0); extensive overlap of tergites (1); edge to edge pleural articulations (2).
45. dorsal trunk effacement: trunk with defined (separate or fused) tergite boundaries (0); trunk tergite boundaries effaced laterally (1); trunk tergite boundaries completely effaced (2).
46. cephalic articulation fused: absent (0); present (1).
47. head shield extends over anterior tergites: overlap absent or identical to overlap between thoracic segments (0); head shield covers first thoracic tergite only (1); head shield covers multiple anterior trunk tergites (2).
48. articulation with reduced tergite: absent (0); present (1).
49. trunk narrowed anteriorly: absent (0); present (1).
50. trunk tergites reflexed anteriorly: absent, boundaries transverse or reflexed posterolaterally (0); present (1).
51. joints between posterior tergites functional: absent (0); present (1).
52. posterior tergite with single axial spine: absent (0); present (1).
53. radial pleurae: absent (0); present (1).
54. raised axial region: absent or weakly defined (0); present and well defined (1).
55. anterior tergal processes: absent (0); present (1).
56. tuberculation of posterior tergite margin: absent (0); present (1).
57. axial spines or nodes: absent (0); present (1).
58. length of postabdomen: one segment (0); two segments (1); three segments (2); five segments (3).
59. postabdomen without walking legs: absent (0); present (1).
60. postabdomen as differentiated tergites: absent (0); present - tergite free (e.g. some aglaspidids, cheloniellids, *Emeraldella*, *Sidneyia*) (1); present - preterminal tergite fused with telson (most aglaspidids) (2).
61. posterior tergites strongly curved: absent (0); present (1).
62. pygidium: absent (0); present (1).
63. position of anus: terminal, within telson (0); at base of telson (1).
64. pygidium with median keel: absent (0); present (1).
65. pygidium with broad median spine: absent (0); present (1).
66. pygidium with lateral spines: absent (0); present (1).
67. tailspine: absent (0); present (1).
68. tailspine shape: spinose (0); paddle shaped (1); cap-like (2).
69. length of tailspine: shorter than half the length of the trunk (0); longer than half the length of the trunk (1).
70. marginal spines on tailspine: absent (0); present (1).
71. tailspine with medial cleft or keel: absent (0); present (1).
72. paddle with projections: absent (0); present (1).
73. ventral sclerite covering anal region: absent (0); present (e.g. aglaspidids, *Sidneyia*) (1).
74. paired modified appendages: absent (0); present (1).
75. nature of preterminal appendages: uropods (0); furca (1).
76. reduced carapace: absent (0); present (1).
77. width of doublure: narrow to moderately wide (0); wide (1); covers entire ventral side of cephalon (2).
78. length of thorax relative to pygidium: longer than pygidium (0); shorter than pygidium (1).
79. articulating half rings: absent (0); present (1).
80. axial furrows on trunk: absent (0); present (1).
81. postventral plate medial attachment: narrow attachment by central portion (0); wide longitudinal attachment (1).

82. dorsal eyes confined to anterior half: absent (e.g. Trilobita) (0); present (e.g. Aglaspidida) (1).
83. dorsal eye abutting glabella anteriorly: absent (e.g. Trilobita) (0); present (e.g. Aglaspidida) (1).
84. dorsal eyes merge anteriorly into cephalon: absent (e.g. Trilobita) (0); present and eyes are separate (e.g. *Glypharthrus*) (1); present and eyes are medially fused (e.g. *Cyclopites*) (2).
85. nature of anal sclerite: anal plate (e.g. *Sidneyia*) (0); postventral plate (e.g. Aglaspidida) (1).
86. nature of differentiated preterminal tergite: tergite with reduced pleurae (e.g. *Weinbergina*) (0); cylindrical tergite without pleurae (e.g. Aglaspidida, Cheloniellida, *Emeraldella*) (1).
87. pleural tips on posterior end with elongate spines: absent (0); present (1).
88. antennal scale: absent (0); present (1).
89. head shield with lateral notches: absent (0); present (1).
90. tailspine with multiple articulations (NEW): absent (0); present (1).
91. shape of undivided exopod lobe with lamellae (NEW): broad lobe (e.g. *Retifacies*, *Pygmaclypeatus*) (0); slender shaft (e.g. *Naraoia compacta*) (1).
92. head/trunk exopods heteronomous (NEW): absent, exopods with same morphology in head and trunk (0); present, exopods with different morphology in head and trunk (1).



**Extended Data Table 2. Character matrix for phylogenetic analyses.** Coded only for use in TNT. Species names not in Italics.

Fortiforceps_foliosa (OUTGROUP)	0	2	0	1	4	0	0	0	0	0	0
1	0	-	-	-	0	-	1	0	1	0	1
0	0	0	0	0	-	0	0	4	0	0	-
0	-	0	2	0	0	0	0	1	1	0	1
0	0	0	0	0	0	0	0	0	0	0	0
0	-	0	0	0	0	1	-	-	-	1	0
0	0	0	0	0	0	-	0	?	-	0	0
-	-	-	-	-	-	0	0	0	0	-	0
Aglaspella_granulifera	?	?	?	?	?	?	?	?	?	?	?
?	?	?	?	?	?	?	1	1	-	0	-
0	0	0	-	1	0	?	0	0	-	1	0
1	1	0	1	1	1	1	1	?	1	0	0
0	0	0	0	0	0	0	0	1	0	0	1
1	2	1	0	?	-	-	-	1	0	1	0
0	-	1	0	-	0	0	-	0	0	0	1
1	1	1	1	0	?	0	0	?	?		
Aglaspis_spinifer	?	?	?	?	?	4	?	?	1	1	?
?	?	?	?	?	?	?	1	1	-	0	-
0	0	0	-	1	0	0	0	0	-	1	1
1	0	1	1	1	1	1	1	0	1	0	0
0	0	0	0	0	0	0	0	1	1	0	1
1	2	1	0	?	-	-	-	1	0	1	0
0	-	1	0	-	0	0	-	0	0	0	1
1	1	1	1	1	?	0	0	?	?		
Alalcomenaeus_cambricus	0	1	1	2	4	0	0	0	0	0	1
0	-	-	-	0	-	2	1	1	0	1	0
0	0	0	0	-	0	0	4	0	0	-	0
-	0	1	0	0	0	0	1	1	0	1	0
0	0	0	0	0	0	0	0	0	0	0	0
-	0	0	0	0	1	-	-	-	1	1	0
1	0	0	0	0	-	0	-	-	0	0	-
-	-	-	-	-	0	0	0	0	-	0	
Australaglaspis_stonyensis	?	?	?	?	?	?	?	?	?	?	1
?	?	?	?	?	?	?	?	1	1	-	0
-	0	0	0	-	?	0	0	0	0	-	1
0	1	1	0	?	0	1	1	1	?	1	0
0	0	0	0	0	0	0	0	0	?	0	?
1	1	?	1	0	?	-	-	-	1	0	1
0	1	-	1	0	-	0	?	-	0	0	1
1	1	?	1	?	0	?	0	0	?	?	
Beckwithia_typa	?	?	?	?	?	?	?	?	?	?	?
?	?	?	?	?	?	?	1	1	-	0	-
0	0	0	-	1	0	?	0	0	-	1	1
1	0	0	0	1	1	1	1	?	1	0	0
0	0	0	0	0	?	0	0	0	0	1	?
?	?	1	0	?	-	-	-	1	0	1	1
0	-	?	0	-	0	0	-	0	0	?	1
1	1	?	?	0	?	0	0	?	?		
Brachyaglaspis_singularis	?	?	?	?	?	?	?	?	?	?	?
?	?	?	?	?	?	?	?	0	-	-	-

	-	-	0	0	-	?	0	?	0	0	-	1
	0	0	2	0	0	?	1	1	1	?	1	0
	0	?	?	0	0	0	0	0	1	?	0	0
	?	1	?	1	0	?	-	-	-	1	0	0
	0	1	-	1	?	?	0	?	-	?	0	1
	-	-	-	1	?	0	?	0	0	?	?	
Buenaspis	?	?	?	?	?	?	?	?	?	?	?	?
	?	?	?	?	?	?	?	?	?	?	0	0
	0	0	-	1	0	?	0	0	-	0	-	0
	2	0	0	0	0	1	1	?	1	0	0	0
	0	1	0	0	0	0	0	0	0	0	-	0
	-	0	1	1	?	0	0	0	-	-	-	-
	-	0	0	-	0	0	0	1	0	-	-	-
	-	-	-	0	?	0	-	?	?			
Burgessia_bella1	-	-	0	0	0	4	0	0	0	1	0	-
	-	-	0	-	0	0	0	-	-	-	-	-
	0	0	-	1	0	4	0	0	-	0	-	0
	2	0	0	0	0	0	1	0	0	0	0	2
	0	0	0	0	0	0	0	0	0	0	-	0
	0	0	0	1	-	-	-	1	0	1	0	0
	-	0	0	-	0	-	-	0	0	-	-	-
	-	-	-	-	0	0	0	-	0			
Cheloniellon_calmani	1	-	-	-	0	5	1	1	1	0	1	1
	?	1	1	?	?	1	1	1	1	-	0	-
	0	0	0	-	1	0	1	0	0	-	0	-
	0	2	0	0	1	0	1	1	0	1	0	0
	0	0	0	1	0	0	1	1	0	0	0	0
	1	1	1	0	?	-	-	-	1	2	0	0
	0	-	0	1	1	1	0	-	0	1	-	0
	-	-	-	1	0	0	0	0	-	-		
Chlupacaris_dubia	?	?	?	?	?	?	?	?	?	?	?	?
	?	?	?	?	?	?	?	1	1	-	?	-
	0	0	0	-	1	0	1	0	0	-	1	?
	?	2	?	0	?	1	1	1	?	?	?	0
	?	?	0	0	0	0	0	0	?	0	0	?
	1	?	?	0	?	-	-	-	1	0	0	0
	0	-	1	0	-	0	0	-	0	0	1	0
	?	?	1	?	?	?	0	0	?	?		
Chraspedops	?	?	?	?	?	?	?	?	?	?	?	?
	?	?	?	?	?	?	1	1	-	0	-	0
	0	0	-	0	0	?	0	0	-	1	0	1
	1	0	1	1	1	1	1	?	1	0	0	0
	0	0	0	0	0	0	0	?	0	0	?	?
	?	1	0	?	-	-	-	1	0	1	0	1
	-	?	0	-	0	-	-	0	0	?	1	1
	1	?	?	0	?	0	0	?	?			
Cindarella_eucalla	1	-	-	-	0	5	0	0	0	0	1	1
	0	0	1	1	1	1	0	1	0	1	0	0
	0	0	0	-	1	0	1	0	0	-	0	-
	0	1	0	0	0	0	1	1	1	1	0	0
	2	1	0	0	0	1	0	0	0	0	0	-
	0	0	1	1	1	0	0	0	0	-	-	-
	-	-	0	0	-	0	0	0	0	0	-	-
	-	-	-	-	0	0	1	-	-	0		

Cycloptes_vulgaris	?	?	?	?	?	?	?	?	?	?	?	?
?	?	?	?	?	?	?	1	1	-	0	-	-
0	0	0	-	?	0	?	0	0	-	1	0	0
1	2	0	0	0	1	1	1	?	1	0	0	0
0	0	0	0	0	0	0	0	1	0	0	0	1
1	2	1	0	?	-	-	-	1	0	1	0	0
0	-	1	0	-	0	?	-	0	0	0	?	1
1	2	1	1	0	?	0	0	?	?	?	?	?
Duslia_insignis	1	?	?	?	?	?	?	?	?	?	?	?
?	?	?	?	?	?	?	?	?	?	?	0	0
0	0	-	?	0	?	0	0	-	0	-	-	1
2	0	0	0	0	1	1	?	1	0	0	0	0
0	0	1	0	0	1	1	0	0	0	0	0	1
1	1	0	?	-	-	-	1	2	0	0	0	0
-	0	1	1	0	?	-	0	1	-	-	-	-
-	-	1	0	?	0	0	?	?	?	?	?	?
Emeraldella_brocki	1	-	-	0	4	1	0	0	0	1	1	1
0	1	1	1	2	1	1	0	-	-	-	-	-
-	0	0	-	1	0	0	0	0	-	0	-	-
0	1	0	0	0	0	1	1	0	1	0	0	0
0	0	0	0	0	0	0	0	0	0	0	0	0
1	1	1	0	1	-	-	-	1	0	1	0	0
0	-	0	1	0	0	0	-	0	0	-	-	-
-	-	-	1	0	0	0	0	-	0	-	-	-
Eoredlichia_intermedia	1	-	-	0	4	0	0	1	1	1	1	1
0	0	0	1	0	1	1	1	1	-	1	-	-
0	0	0	-	1	0	3	0	1	1	1	1	0
1	0	0	0	0	2	1	1	0	2	0	0	0
0	0	0	0	0	1	0	1	0	0	0	0	-
0	-	1	1	1	0	0	0	0	-	-	-	-
-	-	0	0	-	0	0	0	1	1	-	-	0
0	0	-	-	0	0	0	-	-	0	-	-	-
Eozetetes_gemelli	1	-	-	?	?	?	?	?	?	?	?	?
?	?	?	?	?	?	?	1	?	0	?	?	?
0	0	0	-	1	0	0	0	0	-	1	0	0
1	1	0	0	0	0	1	1	?	1	0	0	0
0	0	0	0	0	0	0	1	0	0	1	?	?
?	?	1	0	?	-	-	-	1	0	1	0	0
1	-	0	?	?	0	0	-	0	0	-	-	1
?	?	-	?	0	?	0	0	?	?	?	?	?
Flobertia_kochi	?	?	?	?	?	?	?	?	?	1	?	?
?	?	?	?	?	?	1	1	-	0	-	-	0
0	0	-	1	0	0	0	0	-	1	0	?	?
2	0	0	1	1	1	1	?	1	0	0	0	0
0	0	?	0	0	0	0	1	0	0	?	?	?
?	?	0	?	?	?	?	?	?	?	?	?	?
?	?	0	?	0	0	?	0	0	?	1	?	?
?	?	?	0	?	0	?	?	?	?	?	?	?
Glypharthrus_magnoculus	?	?	?	?	?	?	?	?	?	?	?	?
?	?	?	?	?	?	?	?	1	1	-	-	0
-	0	0	0	-	0	0	?	0	0	-	-	1
?	1	1	?	1	1	1	1	1	?	1	0	0
0	0	0	0	0	0	0	0	1	?	?	?	0
?	?	1	?	0	?	-	-	-	1	0	0	1

	0	0	-	?	?	?	0	-	-	0	0	?
	1	1	1	?	1	0	?	0	0	?	?	?
Glypharthritis simplex	?	?	?	?	?	?	?	?	?	?	?	?
	?	?	?	?	?	?	?	1	1	-	0	-
	0	0	0	-	0	0	?	0	0	-	1	0
	1	0	1	1	1	1	1	1	?	1	0	0
	0	0	0	0	0	0	0	0	1	1	0	2
	1	2	1	0	?	-	-	-	1	0	1	0
	0	-	1	0	-	0	-	-	0	0	1	1
	1	1	1	1	0	?	0	0	?	?	?	?
Glypharthritis thomasi	?	?	?	?	?	?	?	?	?	?	?	?
	?	?	?	?	?	?	?	1	1	-	0	-
	0	0	0	-	0	0	?	0	0	-	1	0
	1	1	?	1	?	1	1	1	?	1	0	0
	0	0	0	0	0	0	0	1	?	0	0	?
	?	2	1	0	?	-	-	-	1	0	1	0
	0	-	?	?	?	0	-	-	0	0	?	0
	1	1	?	1	0	?	0	0	?	?	?	?
Glypharthritis trispinicaudatus	?	?	?	?	?	?	?	?	?	?	?	?
	?	?	?	?	?	?	?	?	1	1	-	0
	-	0	0	0	-	?	0	?	0	0	-	1
	?	1	1	?	?	1	1	1	1	?	1	0
	0	0	0	0	0	0	0	0	1	?	?	0
	0	1	1	1	0	?	-	-	-	1	0	?
	0	0	-	?	1	0	0	?	-	0	0	?
Gogglops	1	1	1	?	1	0	?	0	0	?	?	?
	?	?	?	?	?	?	?	?	?	?	?	?
	?	?	?	?	?	?	1	1	-	0	0	0
	0	0	-	1	0	?	0	0	-	1	0	1
	0	0	1	1	2	1	1	?	2	0	0	?
	?	?	0	0	?	0	1	1	0	?	?	?
	?	1	0	?	-	-	-	1	0	0	0	0
	-	?	0	-	0	0	-	1	0	?	1	1
	1	?	?	0	?	0	0	?	?	?	?	?
Haikoucaris	0	1	0	1	4	0	0	0	0	1	0	-
	-	-	0	-	2	0	1	0	1	0	0	0
	0	0	-	0	0	4	0	0	-	0	-	0
	1	0	0	0	0	1	1	0	1	0	0	0
	0	0	0	0	0	0	0	0	0	0	-	0
	0	0	0	1	-	-	-	1	0	0	1	0
	-	0	0	-	0	0	-	0	0	-	-	-
	-	-	-	0	0	0	0	-	0	-	-	-
Helmetia expansa	?	?	?	?	?	?	4	?	?	?	?	?
	?	?	?	?	?	?	?	1	0	0	0	1
	0	0	0	-	1	1	2	1	0	-	0	-
	0	1	0	0	0	0	1	1	0	2	0	0
	0	0	0	1	1	0	0	0	0	0	0	-
	?	-	0	1	1	0	1	1	0	-	-	-
	-	-	0	0	-	0	0	0	?	0	-	-
	-	-	-	-	0	?	0	-	?	?	?	?
Kodymirus vagans	1	-	-	-	0	4	1	?	?	?	1	{0,1}
	?	?	?	?	?	1	1	1	1	-	0	-
	0	0	0	-	1	0	0	0	0	-	0	-
	1	1	0	0	1	0	1	1	?	1	0	0

	0	0	0	0	0	0	0	0	0	0	1	-
	?	2	1	0	?	-	-	-	1	0	1	0
	0	-	0	0	-	0	0	-	0	0	-	1
	1	0	-	1	0	0	0	-	-	-	-	-
Kuamaia_lata	1	-	-	0	?	0	0	?	1	1	1	0
	1	1	1	2	0	1	1	0	0	0	1	0
	0	0	-	1	1	2	1	0	-	0	-	0
	1	0	0	0	0	1	1	0	2	0	0	0
	0	0	1	1	0	0	1	0	0	0	-	0
	-	0	1	1	0	1	1	0	-	-	-	-
	-	0	0	-	0	0	0	?	0	-	-	-
	-	-	-	0	?	0	-	-	0	-	-	-
Kwanyinaspis_maotianshanensis?	?	?	?	?	?	?	?	?	0	0	?	1
	1	0	1	0	1	0	1	1	1	0	0	0
	1	0	0	0	-	1	0	0	0	0	-	1
	0	1	1	0	0	0	0	1	1	0	2	0
	0	0	0	0	1	0	0	0	0	0	0	0
	?	?	0	1	0	?	-	-	-	1	0	0
	0	0	-	?	0	-	0	0	-	?	0	?
	-	-	-	?	-	0	?	0	0	-	0	-
Leancoilia_superlata	0	1	1	2	4	0	0	0	0	0	1	0
	-	-	-	0	-	2	1	1	0	?	0	0
	0	0	0	-	0	0	?	0	0	-	0	-
	0	1	0	0	0	0	1	1	0	1	0	0
	0	0	0	0	0	0	0	0	0	0	0	-
	0	0	1	0	1	-	-	-	1	0	0	1
	0	-	0	0	-	0	-	-	0	0	-	-
	-	-	-	-	0	0	0	0	-	0	-	-
Liwia_convexa	1	-	-	0	?	0	0	?	1	1	1	?
	?	?	1	?	?	?	?	?	?	?	?	?
	0	0	-	?	0	?	0	0	-	0	-	0
	1	0	0	0	0	1	1	0	1	0	0	1
	0	1	0	0	0	0	0	0	0	0	-	?
	-	0	1	1	1	0	1	0	-	-	-	-
	-	0	0	-	0	?	1	0	0	-	-	-
	-	-	-	0	?	0	-	-	0	-	-	-
Marrella_splendens	1	-	-	0	2	1	-	-	0	1	1	2
	-	-	-	0	-	-	0	0	-	-	-	-
	-	0	0	-	0	0	?	0	0	-	0	-
	0	3	0	0	0	0	0	1	0	0	0	0
	2	0	0	0	0	0	-	0	0	0	0	-
	0	0	0	0	?	-	-	-	1	2	0	0
	0	-	0	0	-	0	-	-	0	0	-	-
	-	-	-	-	-	0	0	0	-	-	-	-
Martinsonia_elongata	1	-	-	0	5	0	0	0	0	0	1	2
	-	-	-	0	-	-	1	0	-	-	-	-
	-	0	0	0	0	0	4	0	0	-	0	-
	0	1	0	0	0	0	0	1	0	0	0	0
	2	0	0	0	0	0	0	0	0	0	0	3
	1	0	0	0	0	-	-	-	0	-	-	-
	-	-	0	0	-	0	-	-	0	0	-	-
	-	-	-	-	-	0	0	-	-	0	-	-
Mimetaster_hexagonalis		1	-	-	0	3	1	1	1	0	1	1
	2	-	-	-	0	-	-	0	1	0	0	0

	0	0	0	0	-	0	0	1	0	0	-	0
	-	0	3	0	0	0	0	0	1	0	0	0
	0	2	0	0	0	0	0	-	0	0	0	0
	-	0	0	0	0	?	-	-	-	1	2	0
	0	0	-	0	0	-	0	-	-	0	0	-
	-	-	-	-	-	-	0	0	0	-	-	-
Misszhouia_longicaudata			1	-	-	0	5	0	0	0	1	1
	1	1	0	1	1	1	1	1	1	0	0	0
	0	0	0	0	-	1	0	1	1	0	-	0
	-	0	2	0	0	0	0	1	0	0	-	2
	0	0	0	1	0	0	0	0	0	0	0	0
	-	0	-	-	1	1	0	0	0	0	-	-
	-	-	-	0	0	-	0	0	?	0	0	-
	-	-	-	-	-	-	1	0	-	-	0	-
Naraoia_compacta			1	-	-	0	{4,5}	0	0	1	1	3
	1	0	1	1	2	1	1	1	0	0	0	0
	0	0	0	-	1	0	1	0	0	-	0	-
	0	2	0	0	0	0	1	0	0	-	2	0
	0	0	1	0	0	0	0	0	0	0	0	-
	0	-	-	1	1	0	0	0	0	-	-	-
	-	-	0	0	-	0	0	?	0	0	-	-
	-	-	-	-	-	0	0	-	1	0	-	-
Naraoia_spinosa			1	-	-	0	5	0	0	1	1	1
	0	1	0	1	1	1	1	1	0	0	0	0
	0	0	0	-	1	0	1	0	0	-	0	-
	0	0	0	0	0	0	1	0	0	-	2	0
	0	0	1	0	0	0	0	0	0	0	0	-
	0	-	-	1	1	0	0	1	0	-	-	-
	-	-	0	0	-	0	0	?	0	0	-	-
	-	-	-	-	-	0	0	-	-	0	-	-
Nebalia_bipes			1	-	-	0	5	0	0	1	2	-
	-	-	0	-	-	1	1	0	1	0	0	0
	0	1	1	0	0	4	0	0	-	0	-	0
	1	0	0	0	0	0	1	0	0	0	0	2
	0	0	0	0	0	0	0	0	0	0	2	1
	0	0	0	0	-	-	-	0	-	-	-	-
	-	0	0	-	0	-	-	0	0	-	-	-
	-	-	-	-	0	0	-	-	0	-	-	-
Neostrabops			?	?	?	?	?	?	?	?	?	?
	?	?	?	?	?	?	1	1	-	0	-	0
	0	0	-	?	0	?	0	0	-	0	-	0
	2	0	0	0	0	1	1	?	1	0	0	0
	0	0	1	0	0	0	0	0	0	0	?	0
	?	1	0	?	?	?	?	?	?	?	?	?
	?	?	?	?	1	?	-	0	0	?	0	-
	0	?	?	0	?	0	?	?	?			
Olenoides_serratus			1	-	-	0	4	0	0	1	1	1
	0	0	1	1	0	1	1	1	1	-	1	-
	0	0	0	-	1	0	3	0	1	1	1	0
	1	0	0	0	1	2	1	1	0	2	0	0
	0	0	0	0	0	0	0	1	0	0	0	-
	0	-	0	1	1	0	0	1	0	-	-	-
	-	-	0	0	-	0	0	-	1	1	-	0
	0	0	-	-	0	0	0	-	-	0	-	-

Phytophilaspis_pergamena	?	?	?	?	5	?	?	?	?	?	?
?	?	?	?	?	?	?	?	?	?	?	?
1	1	0	0	-	0	0	1	0	0	-	0
-	1	1	0	0	1	1	1	0	?	?	1
0	?	1	0	0	0	0	0	1	0	0	0
-	0	-	0	1	?	0	0	0	0	-	-
-	-	-	?	0	-	0	-	1	0	1	-
0	0	0	?	-	-	?	0	-	?	?	
Quasimodaspis_brentsae	?	?	?	?	?	?	?	?	?	?	?
?	?	?	?	?	?	?	?	1	1	-	0
-	0	0	0	-	1	0	?	0	0	-	1
0	1	1	0	0	0	1	1	1	?	1	0
0	0	0	0	0	0	0	0	1	?	0	0
?	?	?	1	0	?	-	-	-	1	0	0
0	0	-	?	0	-	0	0	-	?	0	?
1	1	1	?	?	0	?	0	0	?	?	
Rebachiella_kinnekkullensis	1	-	-	0	5	0	0	0	0	0	1
2	-	-	-	0	-	-	1	1	0	1	0
0	0	0	1	1	0	0	4	0	0	-	0
-	0	1	0	0	0	0	0	1	0	0	0
0	2	0	0	0	0	0	0	0	0	0	0
2	1	0	0	0	0	-	-	-	0	-	-
-	-	-	0	0	-	0	-	-	0	0	-
-	-	-	-	-	-	0	0	-	-	0	
Retifacies_abnormalis	1	-	-	0	4	0	0	?	?	1	3
-	-	-	1	2	-	1	?	?	?	0	0
0	0	0	-	1	0	0	0	0	-	0	-
0	0	0	0	0	0	1	1	0	1	0	0
0	0	0	0	0	0	0	0	0	0	0	-
0	-	1	1	1	0	0	1	1	0	1	0
0	-	0	0	-	0	0	0	0	0	-	-
-	-	-	-	0	0	0	1	0	?		
Pygmaclypeatus_daziensis	1	-	-	0	4	0	0	0	0	0	1
3	-	-	-	1	2	-	1	0	-	-	-
0	0	0	0	-	1	0	0	0	0	-	0
-	0	1	0	0	0	0	1	1	0	1	0
0	0	0	0	0	0	0	0	0	0	0	0
-	0	-	1	1	?	0	0	0	1	0	0
0	0	-	0	0	-	0	0	0	0	0	-
-	-	-	-	-	-	0	0	1	0	1	
Saperion	1	-	-	0	?	0	?	?	1	1	0
1	1	1	0	0	0	1	0	0	0	1	0
0	0	-	1	1	2	1	0	-	0	-	0
-	0	0	0	0	1	0	0	2	1	1	-
-	0	0	1	0	0	0	0	0	0	-	0
-	-	1	1	0	0	0	0	-	-	-	-
-	0	0	-	0	0	?	0	0	-	-	-
-	-	-	-	?	0	-	-	0			
Sidneyia_inexpectans	1	-	-	0	1	1	-	0	1	1	1
0	1	-	1	0	1	1	1	0	0	0	0
0	0	0	-	1	0	0	0	0	-	0	-
0	1	0	0	0	0	1	1	0	1	0	0
0	0	0	0	0	0	0	0	0	0	0	2
1	1	1	0	1	-	-	-	1	1	0	0

	0	0	1	1	0	0	2	-	0	0	-	-
	-	-	0	1	0	0	1	0	-	-	-	-
Sinoburius_lunaris	1	-	-	-	0	5	0	0	0	0	1	1
	1	0	1	1	1	1	1	1	0	0	0	1
	0	0	0	-	1	0	1	0	0	-	0	-
	0	0	0	0	0	0	1	1	1	1	0	0
	2	1	0	0	0	0	0	1	0	0	0	-
	0	-	0	1	?	0	1	1	0	-	-	-
	-	-	0	0	-	0	0	0	0	0	-	0
	-	0	-	-	0	1	0	-	-	1	-	-
Skioldia	1	-	-	-	0	?	0	0	?	1	1	?
	?	?	1	0	?	?	1	0	0	0	1	0
	0	0	-	1	1	2	1	0	-	0	-	0
	-	0	0	0	0	1	0	?	2	1	1	-
	-	0	0	1	0	0	0	0	0	0	-	0
	-	-	1	1	0	0	0	0	-	-	-	-
	-	0	0	-	0	0	?	0	0	-	-	-
	-	-	-	-	?	0	-	-	0	-	-	-
Soomaspis	?	?	?	?	?	?	?	?	?	?	?	?
	?	?	?	?	?	?	?	?	?	?	?	0
	0	0	-	1	0	?	0	0	-	0	-	0
	2	0	0	0	0	1	1	?	1	0	0	1
	0	1	0	0	0	0	0	0	0	0	-	0
	-	0	1	1	1	0	0	0	-	-	-	-
	-	0	0	-	0	1	1	1	0	-	-	-
	-	-	-	0	?	0	-	?	?	-	-	-
Squamacula_clypeata	1	-	-	-	0	1	0	-	0	1	0	0
	-	-	-	0	-	1	1	0	-	-	-	-
	-	0	0	-	1	0	0	0	0	-	0	-
	0	1	0	0	0	0	1	1	0	1	0	0
	0	0	0	0	0	0	0	0	0	0	0	-
	0	-	1	1	1	0	0	0	0	-	-	-
	-	-	0	0	-	0	2	0	0	0	-	-
	-	-	-	-	0	0	0	-	-	-	-	-
Tariccoia	?	?	?	?	?	?	?	?	?	?	?	?
	?	?	?	?	?	?	?	?	?	?	?	0
	0	0	-	1	0	?	0	0	-	0	-	0
	2	0	0	0	0	1	1	?	1	0	0	1
	0	1	0	0	0	0	0	0	0	0	-	0
	-	0	1	1	1	0	0	0	-	-	-	-
	-	0	0	-	0	1	1	0	0	-	-	-
	-	-	-	0	?	0	-	?	?	-	-	-
Tegopelte_gigas	1	-	-	-	0	?	0	0	?	1	?	?
	?	?	?	?	?	?	0	1	0	0	?	?
	0	0	0	-	1	1	2	1	0	-	0	-
	0	-	0	0	0	0	1	0	?	2	1	1
	-	-	0	0	?	0	0	0	0	0	0	-
	0	-	-	1	1	0	0	0	0	-	-	-
	-	-	0	0	-	0	0	?	0	0	-	-
	-	-	-	-	-	?	0	-	?	?	-	-
Tremaglaspis_unite	?	?	?	?	?	?	?	?	?	?	?	?
	?	?	?	?	?	?	?	0	-	-	-	-
	-	0	0	-	0	0	1	0	0	-	0	-
	0	2	0	0	0	1	1	1	?	1	0	0



	0	0	0	0	0	0	0	1	?	0	0	2
	1	?	0	0	?	-	-	-	1	0	0	0
	0	-	1	0	-	0	-	-	0	0	1	-
	-	-	1	?	0	?	0	0	?	?	?	?
Tremaglaspis_vanroyi	?	?	?	?	?	?	?	?	?	?	?	?
	?	?	?	?	?	?	?	0	-	-	-	-
	-	0	0	-	0	0	?	0	0	-	1	0
	0	2	0	0	1	1	1	1	?	1	0	0
	1	1	1	0	0	0	0	1	?	0	0	?
	?	?	1	0	?	-	-	-	1	0	0	0
	1	-	?	?	?	0	-	-	0	0	?	-
	-	-	?	?	0	?	0	0	?	?	?	?
Triopus_draboviensis_Morocco	?	?	?	?	?	?	?	?	?	?	?	?
	?	?	?	?	?	?	?	?	?	?	?	0
	0	0	0	0	-	?	0	?	0	0	-	0
	-	1	2	0	0	0	0	1	1	?	1	0
	0	0	0	0	1	0	0	1	1	0	0	0
	0	1	1	1	0	?	-	-	-	1	2	0
	0	0	-	0	?	?	1	?	-	0	1	-
	-	-	-	-	1	0	?	0	0	?	?	?
Uarthrus_instabilis	?	?	?	?	?	?	?	?	?	?	?	?
	?	?	?	?	?	?	?	1	1	-	0	0
	0	0	0	-	1	0	?	0	0	-	?	?
	?	1	0	0	1	1	1	1	?	1	0	0
	0	0	0	0	0	0	0	0	?	0	0	1
	1	?	1	0	?	-	-	-	1	0	1	0
	0	-	1	0	-	0	0	-	0	0	0	1
	?	1	1	?	0	?	0	0	?	?		
Xandarella_spectaculum			1	-	-	0	7	0	0	0	0	1
	1	1	0	1	1	1	1	1	1	0	0	0
	1	1	0	0	-	1	0	1	0	0	-	0
	-	0	1	0	0	0	0	1	1	1	1	0
	0	2	1	0	0	0	0	0	0	0	0	0
	-	0	-	1	1	1	0	1	1	0	-	-
	-	-	-	0	0	-	0	0	0	0	0	-
	0	-	0	-	-	0	0	0	-	-	0	-
Acanthomeridion_anacanthus	?	?	?	?	?	?	?	?	?	?	?	?
	?	?	?	?	?	?	?	?	0	-	-	-
	-	0	0	0	-	1	0	?	0	1	1	0
	-	0	1	0	0	0	0	1	1	?	1	0
	0	0	0	0	0	0	0	0	1	0	0	0
	-	0	-	1	0	?	-	-	-	1	0	0
	0	0	-	?	0	-	0	0	-	0	0	-
	-	-	-	-	-	0	?	0	0	?	?	?
Acanthomeridion_serratum	?	?	?	?	?	?	?	?	?	?	?	?
	?	?	?	?	?	?	?	?	0	-	-	-
	-	0	0	0	-	1	0	?	0	1	1	0
	-	0	1	0	0	0	0	1	1	?	1	0
	0	0	0	0	0	0	0	0	1	0	0	0
	-	0	-	1	0	?	-	-	-	1	0	0
	0	0	-	?	0	-	0	0	-	0	0	-
	-	-	-	-	-	1	?	0	0	?	?	?
Australimicola_spriggi	1	-	-	0	?	?	?	?	?	?	?	?
	?	?	?	?	?	?	?	0	-	-	-	-

0	0	0	-	1	0	2	1	0	-	0	-
0	1	0	0	0	0	1	1	?	1	0	0
0	0	0	1	0	0	0	1	0	0	0	-
0	-	1	0	?	-	-	-	1	0	0	1
0	-	?	0	-	0	0	-	0	0	-	-
-	-	-	-	0	0	0	0	?	?	-	-
Zhiwenia_coronata	1	-	-	0	4	?	?	?	?	1	?
0	?	?	1	?	?	?	1	0	1	0	0
0	0	0	-	1	0	0	0	0	-	0	-
0	2	0	0	0	0	1	1	?	1	0	0
0	1	0	1	0	0	0	1	0	0	0	-
0	-	1	0	?	-	-	-	1	0	0	1
0	-	?	0	-	0	0	-	0	0	-	-
-	-	-	-	0	0	1	0	?	?	-	-
Luohuilinella_rarus	?	?	?	?	?	?	?	?	?	?	?
?	?	?	?	?	?	?	1	?	?	0	0
0	0	0	-	?	0	?	0	0	-	0	-
0	1	0	0	0	0	1	1	?	1	0	0
2	1	0	0	0	0	0	1	0	0	0	-
?	-	1	?	?	?	?	?	?	?	?	?
?	?	?	?	?	0	?	0	0	0	-	-
-	-	-	-	0	?	1	?	?	?	-	-
Luohuilinella_deletres	1	-	-	0	4	0	0	0	0	1	1
?	0	?	1	1	1	?	1	0	0	0	0
0	0	0	-	1	0	1	0	0	-	0	-
0	1	0	0	0	0	1	1	?	1	0	0
2	1	0	0	0	0	0	1	0	0	0	-
0	-	1	1	?	0	1	0	0	-	-	-
-	-	?	0	-	0	0	0	0	0	-	-
-	-	-	-	0	0	1	-	-	0	-	-
Haifengella_corona	?	?	?	?	?	?	?	?	?	?	?
?	?	?	?	?	?	?	1	0	0	0	1
0	0	0	-	?	1	2	1	0	-	0	-
0	0	0	0	0	0	1	1	?	2	0	0
0	0	0	0	0	0	0	0	0	0	0	-
0	-	0	1	?	0	1	1	0	-	-	-
-	-	?	0	-	0	?	0	0	0	-	-
-	-	-	-	1	?	0	-	?	?	-	-

# Chapter II

## “Intraspecific variation in the Cambrian: new observations on the morphology of the Chengjiang euarthropod *Sinoburius lunaris*”

### Preface

The Chengjiang biota from southwest China (518-million-years old, early Cambrian) has yielded nearly 300 species, of which more than 80 species represent early chelicerates, crustaceans and relatives. The application of  $\mu$ CT-techniques combined with 3D software (e.g., Drishti), has been shown to be a powerful tool in revealing and analyzing 3D features of the Chengjiang euarthropods. In order to address several open questions that remained from previous studies on the morphology of the xandarellid euarthropod *Sinoburius lunaris*, we reinvestigated the  $\mu$ CT data with Amira to obtain a different approach of visualization and to generate new volume-rendered models. Furthermore, we used Blender to design 3D models showing aspects of intraspecific variation. New findings are: (1) antennulae consist of additional proximal articles that have not been detected before; (2) compared to other appendages, the second post-antennular appendage has a unique shape, and its endopod is comprised of only five articles (instead of seven); (3) the pygidium bears four pairs of appendages which are observed in all specimens. On the other hand, differences between specimens also have been detected. These include the presence/absence of diplotergites resulting in different numbers of post-antennular appendages and tergites and different distances between the tip of the hypostome and the anterior margin of the head shield. Those new observations reveal intraspecific variation among Chengjiang euarthropods not observed before and encourage considerations about possible sexual dimorphic pairs or ontogenetic stages. *Sinoburius lunaris* is a variable species with respect to its morphological characters, cautioning that taxon-specific variabilities need to be considered when exploring new species.

This publication presents morphological reconsiderations on previously published information of the Chengjiang euarthropod *Sinoburius lunaris*. It shows new and unpublished Amira volume renderings and highlights intraspecific morphological variation by showing 3D Blender models for each of the three analyzed specimens.

received: 27 March 2021

revised: 04 May 2021

accepted: 23 May 2021

published: 21 June 2022

### Open Access

Published in *BMC Ecology and Evolution* as:

Schmidt, M., Liu, Y., Hou, X.-G., Haug, J. T., Haug, C., Mai, H., & Melzer, R. R. (2021). Intraspecific variation in the Cambrian: New observations on the morphology of the Chengjiang euarthropod *Sinoburius lunaris*. *BMC Ecology and Evolution*, 21, 127.

# Chapter III

## “Exites in Cambrian arthropods and homology of arthropod limb branches”

### Preface

The last common ancestor of all living arthropods had biramous postantennal appendages, with an endopodite and exopodite branching off the limb base. Morphological evidence for homology of these rami between crustaceans and chelicerates has, however, been challenged by data from clonal composition and from knockout of leg patterning genes. Cambrian arthropod fossils have been cited as providing support for competing hypotheses about biramy but have shed little light on additional lateral outgrowths, known as exites. Here we draw on microtomographic imaging of the Cambrian great-appendage arthropod *Leancoilia* to reveal a previously undetected exite at the base of most appendages, composed of overlapping lamellae. A morphologically similar, and we infer homologous, exite is documented in the same position in members of the trilobite-allied Artiopoda. This early Cambrian exite morphology supplements an emerging picture from gene expression that exites may have a deeper origin in arthropod phylogeny than has been appreciated.

This publication shows previously undetected appendage structures we refer to as exites in two *Leancoilia* species as well as in *Naraoia spinosa* and *Retifacies abnormalis*. We used micro-computed tomography to unravel the morphology of those structures in Drishti and created 3D Blender models of the isolated appendages of the species for a more comprehensive understanding of their structure.

received: 01 April 2021  
revised: 07 May 2021  
accepted: 14 July 2021  
published: 30 July 2022

### Open Access

Published in *Nature Communications* as:

Liu, Y., Edgecombe, G. D., Schmidt, M., Bond, A. D., Melzer, R. R., Zhai, D., Mai, H., Zhang, M., & Hou, X.-G. (2021). Exites in Cambrian arthropods and homology of arthropod limb branches. *Nature Communications*, 12, 4619.

## Part 2

**Performing virtual euarthropod  
appendage kinematics as an  
integrative, conceptualized approach**

# Chapter IV

## “Moving legs: A workflow on how to generate a flexible endopod of the 518 million-year-old Chengjiang arthropod *Ercaicunia multinodosa* using 3D-kinematics (Cambrian, China)”

### Preface

Understanding the functional morphology and mobility of appendages of fossil animals is important for exploring ecological traits such as feeding and locomotion. Previous work on fossils from the 518 million-year-old Chengjiang biota of China was based mainly on two-dimensional information captured from the surface of the specimens. Only recently,  $\mu$ CT techniques started to reveal almost the entire, though flattened and compressed, three-dimensionally preserved morphologies of the arthropods from Chengjiang. This allows more accurate work on reconstructing the possible movement of certain structures such as the appendages. Here, we present a workflow on how to reconstruct the mobility of a limb of the early Chengjiang arthropod *Ercaicunia multinodosa* from the famous Chinese fossil site. Based on  $\mu$ CT scans of the fossil, we rendered surface models of the 13th–15th right endopods using the 3D visualization and 3D-rendering software Amira. The 3D objects then were postprocessed (Collapse Hierarchy, Unify Normals) in SAP 3D Visual Enterprise Author before being imported into the 3D animation program Autodesk Maya 2020. Using the add-on tool X\_ROMM in Maya, we illustrate step-by-step on how to make the articles of the limbs swing-in toward each other. Eventually, we propose several possible limb movements of *E. multinodosa*, which helps to understand how this early arthropod could have moved its endopods.

This publication presents the novel approach of constructing a flexible appendage by equipping elements with artificial joints. We used Amira to re-analyze the early Cambrian Chengjiang euarthropod *Ercaicunia multinodosa*, surface rendered endopodites and hereafter showed step-by-step how to get an endopodite model flexible using Maya.

received: 18 May 2020  
revised: 07 October 2020  
accepted: 08 October 2020  
published: 06 November 2020

### Open Access

Published in *Microscopy Research and Technique* as:

Schmidt, M., Liu, Y., Zhai, D., Hou, X.-G., & Melzer, R. R. (2021). Moving legs: A workflow on how to generate a flexible endopod of the 518 million-year-old Chengjiang arthropod *Ercaicunia multinodosa* using 3D-kinematics (Cambrian, China). *Microscopy Research and Technique*, 84, 695–704.

## Part 3

### **Digitally unveiling prosomal appendage kinematics in Ordovician and Silurian sea scorpions and modern analogs**

# Chapter V

## “Three-dimensional kinematics of euchelicerate limbs uncover functional specialization in eurypterid appendages”

### Preface

Sea scorpions (Euchelicerata: Eurypterida) explored extreme limits of the aquatic euchelicerate body plan, such that the group contains the largest known marine euarthropods. Inferences on eurypterid life modes, in particular walking and eating, are commonly made by comparing the group with horseshoe crabs (Euchelicerata: Xiphosura). However, no models have been presented to test these hypotheses. Here, we reconstruct prosomal appendages of two exceptionally well-preserved eurypterids, *Eurypterus tetragonophthalmus* and *Pentecopterus decorahensis*, and model the flexure and extension of these appendages kinematically in three dimensions (3D). We compare these models with 3D kinematic models of *Limulus polyphemus* prosomal appendages. This comparison highlights that the examined eurypterid prosomal appendages could not have moved prey items effectively to the gnathal edges and would therefore not have emulated the motion of an *L. polyphemus* walking leg. It seems that these eurypterid appendages were used primarily to walk or grab prey, and other appendages would have moved prey for mastication. Such 3D kinematic modeling highlights how eurypterid appendage morphologies placed substantial limits on their function, suggesting a high degree of specialization, especially when compared with horseshoe crabs. Such three-dimensional kinematic modeling of these extinct groups therefore presents an innovative approach to understanding the position of these animals within their respective paleoecosystems.

This publication deals with two different sea scorpion species, the Ordovician *Pentecopterus decorahensis* and the Silurian *Eurypterus tetragonophthalmus*. We created 3D Blender models of several appendages related to walking, conducted kinematic analyses in Maya and compared the range of motion to extant *Limulus polyphemus* walking and pushing leg models surface rendered in Mimics.

received: 19 April 2021

revised: 06 July 2021

accepted: 07 July 2021

published: 14 November 2021

**Reprint allowed to incorporate in the thesis.**

(Current version was sent by the journal earlier at a time, where it was not assigned to an issue.)

Published in *Biological Journal of the Linnean Society* as:

Bicknell, R. D. C., Melzer, R. R., & Schmidt, M. (2021). Three-dimensional kinematics of euchelicerate limbs uncover functional specialization in eurypterid appendages.

*Biological Journal of the Linnean Society*, 135, 174–183.



Annotation:

The Supporting Information of this paper–Bicknell, Melzer & Schmidt (2021)–that is, three-dimensional interactive PDF's and construction files, are not considered in this thesis owing to the data size, but can be downloaded at <https://datadryad.org/stash/dataset/doi:10.5061/dryad.6m905qfzv>.

# Three-dimensional kinematics of euchelicerate limbs uncover functional specialization in eurypterid appendages

RUSSELL D. C. BICKNELL<sup>1,\*</sup>, ROLAND R. MELZER<sup>2,3,4</sup> and MICHEL SCHMIDT<sup>2,3</sup>

<sup>1</sup>Palaeoscience Research Centre, School of Environmental and Rural Science, University of New England, Armidale, NSW 2351, Australia

<sup>2</sup>Bavarian State Collection of Zoology, Bavarian Natural History Collections, Munich, Germany

<sup>3</sup>Department Biology II, Ludwig-Maximilians-Universität München, Munich, Germany

<sup>4</sup>GeoBio-Center, Ludwig-Maximilians-Universität München, Munich, Germany

Received 19 April 2021; revised 6 July 2021; accepted for publication 7 July 2021

Sea scorpions (Euchelicerata: Eurypterida) explored extreme limits of the aquatic euchelicerate body plan, such that the group contains the largest known marine euarthropods. Inferences on eurypterid life modes, in particular walking and eating, are commonly made by comparing the group with horseshoe crabs (Euchelicerata: Xiphosura). However, no models have been presented to test these hypotheses. Here, we reconstruct prosomal appendages of two exceptionally well-preserved eurypterids, *Eurypterus tetragonophthalmus* and *Pentecopterus decorahensis*, and model the flexure and extension of these appendages kinematically in three dimensions (3D). We compare these models with 3D kinematic models of *Limulus polyphemus* prosomal appendages. This comparison highlights that the examined eurypterid prosomal appendages could not have moved prey items effectively to the gnathal edges and would therefore not have emulated the motion of an *L. polyphemus* walking leg. It seems that these eurypterid appendages were used primarily to walk or grab prey, and other appendages would have moved prey for mastication. Such 3D kinematic modelling highlights how eurypterid appendage morphologies placed substantial limits on their function, suggesting a high degree of specialization, especially when compared with horseshoe crabs. Such three-dimensional kinematic modelling of these extinct groups therefore presents an innovative approach to understanding the position of these animals within their respective palaeoecosystems.

ADDITIONAL KEYWORDS: *Eurypterus tetragonophthalmus* – functional morphology – *Limulus polyphemus* – *Pentecopterus decorahensis* – three-dimensional kinematic analyses.

## INTRODUCTION

Biomechanical and kinematic examination of fossil groups has recently experienced an explosion of research. In particular, three-dimensional (3D) biomechanical analyses have massively extended our knowledge on mechanical limitations of fossil groups (Rayfield, 2007; Bright, 2014). Comparatively, 3D kinematic research has highlighted aspects of organismal motion. A key example of this is the application of kinematics in vertebrate palaeontology to explore how trace fossils were produced (Falkingham & Gatesy, 2014; Nyakatura *et al.*, 2019; Turner *et al.*,

2020). In arthropod palaeontology, 3D kinematics has been used recently to explore trilobite enrollment (Esteve *et al.*, 2017, 2018) and appendage motion in non-trilobite arthropods (Schmidt *et al.*, 2021). This last approach presents a novel avenue for understanding appendage flexure of other fossil arthropod groups. Such applications are especially useful when modern analogues can be suggested.

Sea scorpions (eurypterids) are a diverse group of extinct, primarily marine euchelicerates from the Palaeozoic (Lamsdell & Selden, 2017; Bicknell *et al.*, 2020; Dunlop *et al.*, 2020). Eurypterids were subject to innovative kinematic research during the 1980s (Selden, 1984; Plotnick, 1985; Plotnick & Baumiller, 1988; Briggs *et al.*, 1991). However, little modelling has been presented recently. This is striking, because sea

\*Corresponding author. E-mail: [rdcbicknell@gmail.com](mailto:rdcbicknell@gmail.com)

scorpions are bracketed phylogenetically by two extant clades that can be used to test functional hypotheses, namely horseshoe crabs (Xiphosura) and Arachnida (Legg *et al.*, 2013; Brandt & McCoy, 2014; Selden *et al.*, 2015). Indeed, aspects of eurypterid ecology are commonly compared with extant xiphosurans, in particular *Limulus polyphemus* (Linnaeus, 1758) (Andrews *et al.*, 1974; Dalingwater, 1975, 1985; Selden, 1981; Anderson *et al.*, 2014; McCoy *et al.*, 2015; Bicknell *et al.*, 2018c). It has been suggested that eurypterids walked and moved prey to the gnathal edge of prosomal appendages for mastication, analogous to horseshoe crabs (Selden, 1981; McCoy *et al.*, 2015). Select eurypterid prosomal appendages should therefore have a similar degree of flexure to horseshoe crab appendages. To test this hypothesis, we present the first 3D kinematic models of *L. polyphemus* walking and pushing legs and compare these with reconstructions of prosomal appendages from two disparate eurypterids. We consider the eurypterine *Eurypterus tetragonophthalmus* Fischer, 1839 from the Viita Formation (Silurian: Wenlock, Homerian), Saaremaa, Estonia and the oldest known sea scorpion, the megalograptid *Pentecopterus decorahensis* Lamsdell *et al.*, 2015 from the Winneshiek Lagerstätte of the Winneshiek Shale (Middle Ordovician, Darriwilian), IA, USA. These species represent examples of exceptionally well-preserved eurypterids with amazing appendage data that permit accurate 3D reconstructions.

## MATERIAL AND METHODS

### RECONSTRUCTION OF *L. POLYPHEMUS* APPENDAGES

Two *L. polyphemus* specimens, accessioned into the New England Natural History Arthropod collection (NENH-AR) at the University of New England (UNE), were used for the kinematic models: an anterior walking leg (prosomal appendage II; NENH-AR0002) and a pushing leg (prosomal appendage VI; NENH-AR0003). Both specimens were scanned using micro-computed tomography (micro-CT). The specimens were scanned in a GE-Phoenix V|tome|xs micro-CT scanner with 240 kV 'Direct' tube at UNE using optimized X-ray tube settings (Supplementary Data, Table S1). Data were captured using the acquisition software DATOS v.2.2.1 (phoenix, Wunstorf, Germany) and reconstruction software RTM v.2.2.1. Scans were imported into MIMICS v.23.0 (Materialise, Leuven, Belgium). Distinct appendage sections (podomeres) were separated using the 'Segmenting' tool, and any internal material (muscles, tendons, etc.) was removed with the 'Segmenting' tool. Segmented podomeres were exported as .STL files from MIMICS and imported

into GEOMAGIC STUDIO (3D Systems, Cary, NC, USA). Exoskeletal components were smoothed in GEOMAGIC STUDIO. Smoothed .STL files were exported as an .OBJ file for kinematic analyses in MAYA 2020 (Autodesk, San Rafael, CA, USA). Subsequently, .STL files were exported from MAYA (see 'Construction of kinematic marionettes') to generate 3D PDFs using TERTA4D (Adobe Systems) (Supporting Information, Figs S1–4; Data S1 and S2; Bicknell *et al.*, 2021b).

### RECONSTRUCTION OF EURYPTERID APPENDAGES

Reconstructions of the *E. tetragonophthalmus* (prosomal appendage IV) and *P. decorahensis* (prosomal appendages III and V) were rendered in 3D in BLENDER (v.2.91) (Garwood & Dunlop, 2014). The meshes were refined with the 'sculpting' tool. Reconstructions were exported as an .OBJ file for kinematic analyses in MAYA. Subsequently, .STL files were exported from MAYA (see 'Construction of kinematic marionettes') to generate 3D PDFs using TERTA4D (Supporting Information, Figs S5–10; Data S3–6 found at Bicknell *et al.*, 2021b).

Reconstructions were informed by examining fossils, high-resolution published images of appendages, proposed reconstructions and, where possible, identifying specimens that demonstrate different preservation orientations (Holm, 1898; Selden, 1981; Lamsdell *et al.*, 2015; Haug, 2020). The scale of podomeres relative to each other was also determined from fossils. Appendage 'inflation' was based on *L. polyphemus* appendages. This inflation would not impact the modelling, because overall morphology primarily influences the kinematic motion. The eurypterid material from the Viita Formation and the Winneshiek Lagerstätte is exceptionally preserved and represents two rare situations where original eurypterid cuticle is preserved (Selden, 1981; Lamsdell *et al.*, 2015; Bicknell *et al.*, 2018c; Haug, 2020). These specimens have also been successfully removed from their rock matrix. As such, they could be scanned with a micro-CT. However, specimens showing a complete array of undamaged podomeres are rare. Furthermore, owing to flattened preservation, the scans would need to be retro-deformed, introducing additional uncertainty. As such, following Bicknell *et al.* (2018b, 2021a) and Esteve *et al.* (2017, 2018), we present 3D reconstructions.

### CONSTRUCTION OF KINEMATIC MARIONETTES

Eurypterid and *L. polyphemus* appendage models were imported as .OBJ files into MAYA to perform kinematic movements (Schmidt *et al.*, 2020, 2021). Artificial joints were assigned to podomere articulations to allow for rotation using the 'X\_ROOM'

tool (Brainerd *et al.*, 2010; Gatesy *et al.*, 2010). Bicondylar joints (joints with two articulation points) were modelled because they are common in arthropods (Boxshall, 2004, 2013). These hypothetical joint axes were modelled as long cylinders; the most basic mathematical representation of joints. Given that rotation points always occur about the centre of an object, radii and cylinder size were designed entirely for graphical purposes. After all joints were equipped with joint axes, we used 'srjoints' to deflect podomeres in conjunction with adjacent podomeres following Schmidt *et al.* (2021: section 2.4.1, fig. 3). Each 'srjoint' was assigned to a joint axis with the 'point constrain' and 'orient constrain' functions. Subsequently, each 'srjoint' adopted the respective translation and rotation coordinates of the assigned axis. Then a subordination process parenting each distal podomere with its respective proximal 'srjoint' was performed (compare Schmidt *et al.*, 2020: fig. 2, step 23). This resulted in a kinematic marionette, in which distal podomeres followed the movement of deflected proximal podomeres. Selden (1981: figs 20, 21) illustrated several presumably monocondylar joints (joints with one articulation point) in *E. tetragonophthalmus*. As such, we developed two models for this appendage: one showing our interpretation of the organism and the other following the hypothesis of Selden (1981). Furthermore, for all models, the arthrodistal membranes and muscles were not considered. These would have restricted movement, and our aim was to consider podomere morphology, thus showing the maximum flexibility.

#### MEASUREMENT OF JOINT ANGLES

Joint angles were measured following Schmidt *et al.* (2021: fig. 4, section 2.4.2). The kinematic marionette of each appendage model was split into its respective joints and saved as separate MAYA files (Supporting Information, Data S1–3, S5 and S6). The original 'srjoint' from the kinematic marionette was deleted. Subsequently, both proximal and distal podomeres of each joint were parented to the joint axis. This pair was then orientated along the *y*-axis in the coordinate system. After unparenting all components, a new 'srjoint' was created. The 'rotate' tool was then used to deflect podomeres with each other and calculate the amount of rotation (in degrees) (Supporting Information, Table S2).

## RESULTS

*Limulus polyphemus* prosomal appendages show varying degrees of rotation (Ward, 1969). The walking leg (Fig. 1A–F; NENH-AR0002) can rotate the trochanter and patella to bring the tibiotarsus

and dactylopodite to the coxal region (Fig. 1C, D). This position emulates feeding. Trochanteral spines present limits on rotation and therefore how far the tibiotarsus and dactylopodite can move towards the coxal region. Furthermore, the walking leg can splay out laterally beyond the coxal edges, and the femur sits within a notch in the coxa during splay. The pushing leg (Fig. 1G–M; NENH-AR0003) has less rotation at the coxal–trochanter articulation compared with the walking leg. However, it extends more laterally. The splay of the pushing leg processes reflects the action *L. polyphemus* uses to propel the body forwards (Bicknell *et al.*, 2018a).

Two models of *E. tetragonophthalmus* are presented: our proposed interpretation of the appendage and the model presented by Selden (1981), modelled off Manton (1977). Our model reconstructs the walking leg with the coxa and podomeres 2–8 in the same plane (Fig. 2A–F, N; Supporting Information, Figs S5, S6). Kinematic modelling of this reconstruction shows that this appendage was probably unable to rotate distal podomeres to the coxal region (Fig. 2D–F). Furthermore, the appendage splay would have been limited and unable to kink, comparable to *L. polyphemus* walking legs (compare Fig. 1E, F with Fig. 2A–C). In contrast, Selden (1981; figs 20, 21) suggested a different podomere orientation and the presence of monocondylar joints (Supporting Information, Figs S7, S8). There are four key differences between our model and the hypothesis of Selden (1981): (1) podomere 2 is rotated ~45° relative to the coxal *y*-axis; (2) podomere 3 has a vertical joint axis that permits a horizontal movement along the podomere 2–3 joint; (3) podomeres 3–7 have monocondylic joints, limiting motion; and (4) the podomere 7–8 joint has a horizontal joint axis, enabling podomere 8 to swing sagittally (compare Fig. 2A–F, N with Fig. 2G–M, O). This model would not allow distal podomeres to rotate to the coxal row and would severely limit the appendage splay. Furthermore, given the arrangement of rotation points and podomere orientation, the leg could not be used in effective walking.

The modelled *P. decorahensis* prosomal appendages represent two appendage morphologies known from the taxon (Lamsdell *et al.*, 2015) (Fig. 3; Supporting Information, Figs S9, S10). Both prosomal appendages could have extended out to complete horizontality, suggesting that the appendages could extend beyond the prosomal shield. The appendages also have a similar degree of maximum flexure. However, the stout and interlocked morphology of podomeres 2–4 in prosomal appendage V limited rotation between these podomeres (compare Fig. 3A, B with Fig. 3C, D). Furthermore, podomere 2 of prosomal appendage V is rotated such that more distal podomeres fall in a different plane from the coxa (Supporting Information, Fig. S10).

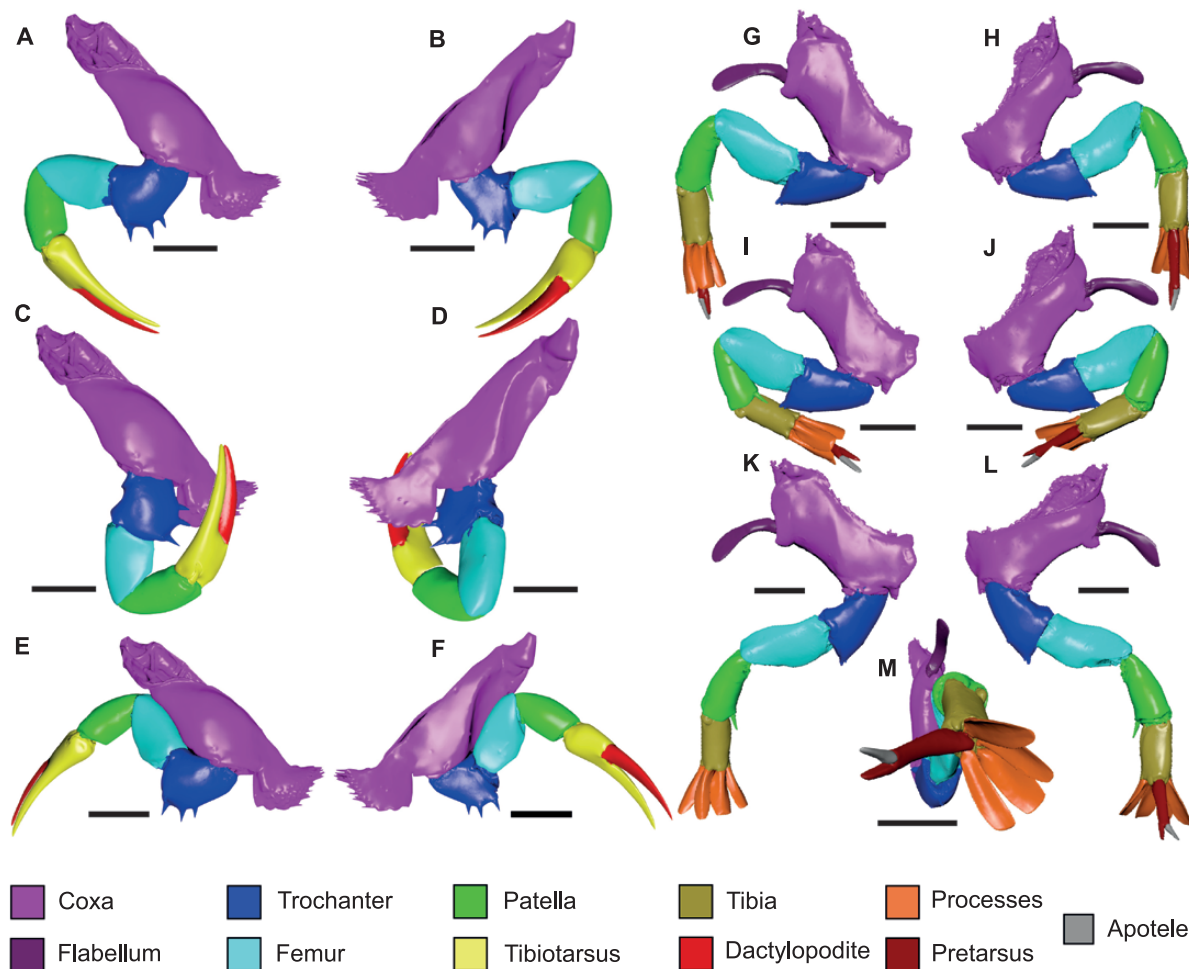


**Figure 1.** Three-dimensional kinematic models of *Limulus polyphemus* appendages. A–F, models of the walking leg (prosomal appendage II, NENH-AR0002; [Supporting Information, Figs S1, S2](#)). A, B, walking leg model in an unflexed, neutral position. C, D, walking leg model showing maximum rotation and position of distal appendage sections at the gnathal edge. E, F, walking leg model showing maximum extension; note that the femoral section fits within a divot in the coxa. G–M, models of the pushing leg (prosomal appendage VI, NENH-AR0003; [Supporting Information, Figs S3, S4](#)). G, H, pushing leg model in an unflexed, neutral position. I, J, pushing leg model in a position of maximum rotation. K, L, pushing leg model in a position of maximum extension. M, processes of the pushing leg, completely splayed. A, C, E, G, I, K, anterior view. B, D, F, H, J, L, posterior view. A–F were reflected to show appendage sections opposing each other. Scale bars: 15 mm in A–F; 20 mm in G–M.

Two groups, namely xiphosurans and eurypterids, are uncovered by considering the joint angles for the modelled appendages ([Fig. 4](#); [Supporting Information, Table S2](#)). Overall, *L. polyphemus* appendages have a notably higher range of motion than the eurypterid appendages. However, the most distal podomeres of the eurypterids have a larger range of motion than distal *L. polyphemus* appendage sections.

## DISCUSSION

Comparing the modelled eurypterid and xiphosuran appendages, there are marked differences in the

amount of motion observed ([Fig. 4](#)). In particular, the eurypterid appendages show limited ability to move distal podomeres to the gnathal edge, whereas the prosomal appendages of horseshoe crabs can complete this action effectively. This likely reflects the stout morphology of eurypterid podomeres and the limited range of motion associated with it. The eurypterid appendages modelled here would therefore have been used primarily in grabbing (*P. decorahensis* prosomal appendage III) and, potentially, walking (*P. decorahensis* prosomal appendage V; *E. tetragonophthalmus* prosomal appendage IV; [Selden, 1981](#); [Lamsdell et al., 2015](#)). Other prosomal appendages, potentially more anterior sets, would have

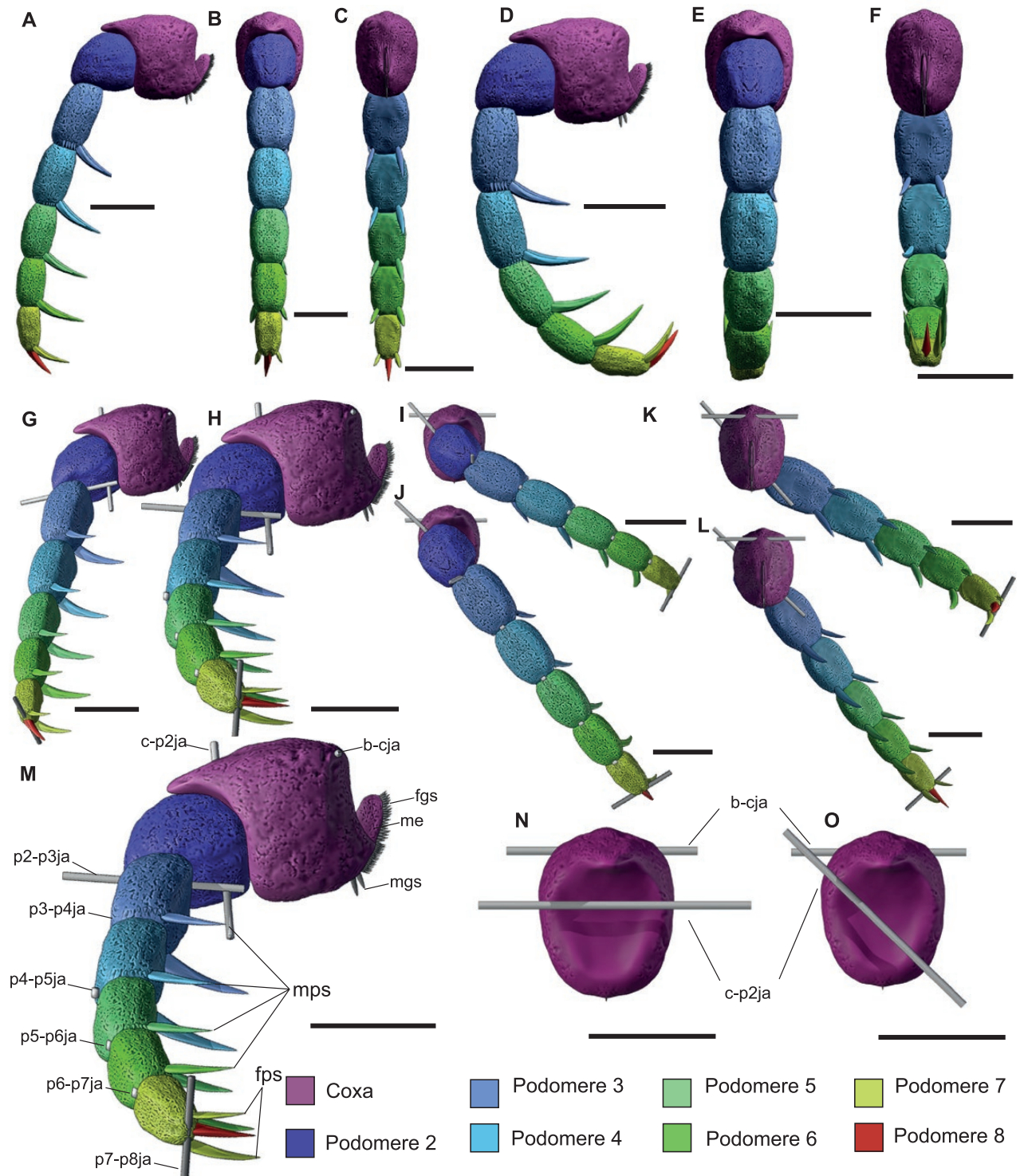


**Figure 2.** Three-dimensional kinematic models of *Eurypterus tetragonophthalmus* prosomal appendage IV. A–F, models of the prosomal appendage IV following our interpretation of the animal (Supporting Information, Figs S5, S6). A–C, prosomal appendage IV showing maximum extension. A, lateral view. B, posterior view. C, sagittal view. D–F, prosomal appendage IV showing maximum rotation. D, lateral view. E, posterior view. F, sagittal view. G–L, models of the prosomal appendage IV following Selden (1981: figs 20, 21) (Supporting Information, Figs S7, S8). G, J, L, prosomal appendage IV showing maximum extension. G, lateral view. J, posterior view. L, sagittal view. H, I, K, prosomal appendage IV showing maximum rotation. H,

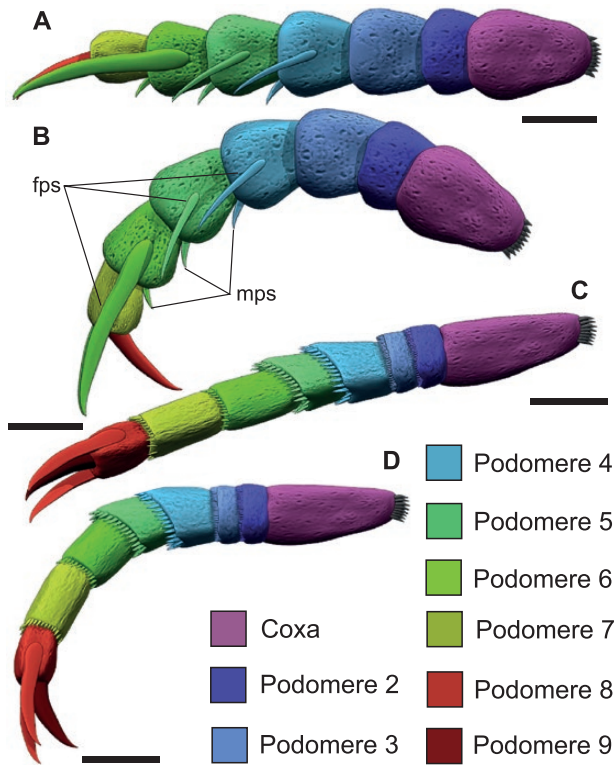


**Figure 3.** Three-dimensional kinematic models of *Pentacopterus decorahensis* prosomal appendages. A, B, models of the prosomal appendage III (Supporting Information, Fig. S9). A, dorsal view showing maximum extension. B, dorsal view showing maximum rotation. C, D, prosomal appendage V (Supporting Information, Fig. S10). C, D, lateral view showing maximum extension. D, lateral view showing maximum rotation. Scale bars: 20 mm in A, B; 10 mm in C, D. Scales are based on specimens in Lamsdell *et al.* (2015). Abbreviations: fps, fixed podomere spines; mps, moveable podomere spines.

moved prey to the gnathal edge. This situation hints at the possibility that eurypterid appendages were more specialized than those of xiphosurans. Although the modelled appendages had a limited ability to move prey to the gnathal edge, gnathobases on the coxal sections would still have been used in mastication (Barbour, 1914; Bicknell *et al.*, 2018c).

Moveable spines in eurypterid prosomal appendages reflect development of spinous endites detached from the arthrodial membrane that are occasionally socketed within appendage sections (Selden, 1981). They are, presumably, analogous to the socketed spines of xiphosuran prosomal appendages; consider trochanteral spines of the *L. polyphemus* walking legs and the hypertrophied patellar spine on the *L. polyphemus* pushing legs. However, an explanation for which prosomal appendage spines are moveable in comparison to those that are fixed is somewhat ambiguous, especially in the considered species (Selden, 1981; Lamsdell *et al.*, 2015). As such, we did not model the motion of spines in the present study. However, moveable spines, which were probably moved with small tendons, might have imposed further limits on podomere flexion. The motion of such spinous structures could therefore have played a role in constraining appendage rotation further.

Arachnids provide another analogue for examining aspects of sea scorpion function. Scorpions, in particular, might make a useful comparison, because the eurypterid *Bauplan* is morphologically comparable to that of scorpions (Dunlop & Selden, 1998; Schoenemann *et al.*, 2019). However, eurypterids were almost exclusively aquatic organisms (Lamsdell *et al.*, 2020), whereas modern scorpions are exclusively terrestrial (Wendruff *et al.*, 2020). Entirely different selection pressures acting on the two groups resulted in modifications to appendages and life modes. This makes scorpions poor analogues for exploring the motion of eurypterid appendages (Manton, 1977). However, the limits of eurypterid mesosomal and metastomal flexure could be modelled effectively by considering scorpions.

The application of the innovative 3D kinematic method used here has presented unique insight into the limits on the motion of sea scorpion appendages. It opens up the possibility for further areas of examination, including the functional morphology of eurypterid swimming legs, appendage flexibility in stylonurid eurypterids, and even exploration of metastomal and mesosomal tergal motion and testing of hypotheses on extreme eurypterid opisthosomal flexibility (Persons

lateral view. I, posterior view. J, sagittal view. M, labelled model explaining all joint axes. N, O, posterior view of coxa with podomere 2 removed showing differences in joint axis directions between our proposed model and that of Selden (1981). N, joint orientations proposed here. O, joint orientations proposed by Selden (1981). G–O, grey cylinders illustrate the direction of rotation. Grey cylinders were not included in A–F because all joint axes are perpendicular to the appendage longitudinal axis. Scale bars: 5 mm. Scale bars are based on specimens in Selden (1981). Abbreviations: b-cja, body-coxal joint axis; c-p2ja, coxa-podomere 2 joint axis; fgs, fixed gnathobasic spines; fps, fixed podomere spines; me, moveable endite; mgs, movable gnathobasic spines; mps, moveable podomere spines; p2-p3ja, podomere 2–3 joint axis; p3-p4ja, podomere 3–4 joint axis; p4-p5ja, podomere 4–5 joint axis; p5-p6ja, podomere 5–6 joint axis; p6-p7ja, podomere 6–7 joint axis; p7-p8ja, podomere 7–8 joint axis.

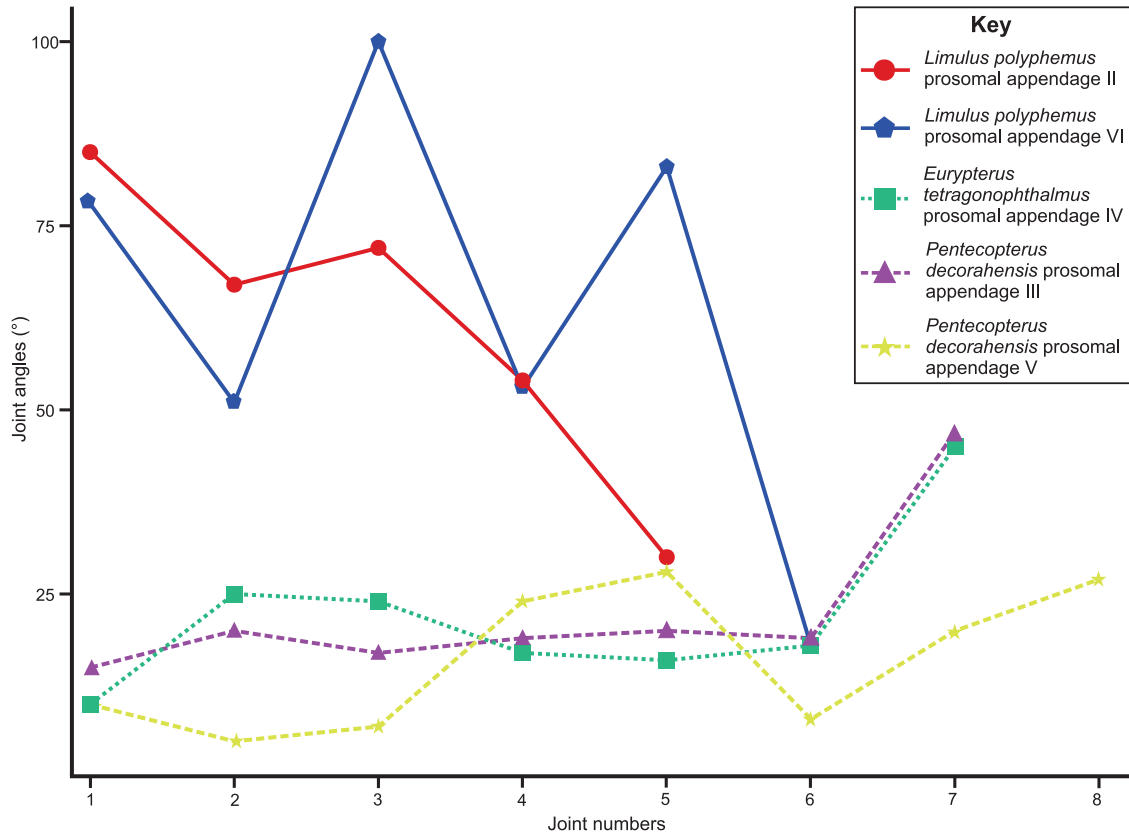


**Figure 4.** Joint angles, showing the degree of motion between maximally stretched and maximally rotated conditions for the kinematic models examined. Note the Selden *Eurypterus tetragonophthalmus* model is not presented.

& Acorn, 2017; Lamsdell *et al.*, 2018). Ultimately, by comparing precise kinematic models of eurypterid appendages with extant euchelicerates, the functional morphological restrictions experienced by eurypterids can be understood, allowing us to more completely understand the titans of the Palaeozoic oceans.

#### ACKNOWLEDGEMENTS

We thank Odd Erik Tetlie, Paul Selden, and Roy Plotnick for useful discussions regarding this work. We thank the Jorge Esteve, Loren Babcock, and an anonymous referee for their comments that improved the direction and use of the text. R.D.C.B., R.R.M. and M.S. conceived the study. R.D.C.B. and M.S. collected and analysed the data. R.D.C.B. scanned and surface rendered the *L. polyphemus* specimen. M.S. constructed the 3D eurypterid models and performed the kinematic modelling. R.D.C.B. and M.S. interpreted the results, with input from the other authors, and constructed the figures. All authors wrote, discussed, edited and approved the manuscript. We declare we have no competing interests. This research was supported by funding from

a UNE Postdoctoral Research Fellowship (to R.D.C.B.), an Australian Research Council grant (DP200102005), and a Deutsche Forschungsgemeinschaft Award (no. Me-2683/10-1, to M.S.).

#### DATA AVAILABILITY

The data from this work are available at the Dryad Digital Repository (Bicknell *et al.*, 2021b).

#### REFERENCES

- Anderson RP, McCoy VE, McNamara ME, Briggs DEG. 2014. What big eyes you have: the ecological role of giant pterygotid eurypterids. *Biology Letters* 10: 20140412.
- Andrews HE, Brower JC, Gould SJ, Reymont RA. 1974. Growth and variation in *Eurypterus remipes* DeKay. *Bulletin of the Geological Institution of the University of Uppsala* 4: 81–114.
- Barbour EH. 1914. Eurypterid beds of Nebraska with notice of a new species, *Eurypterus nebraskaensis*. *Nebraska Geological Survey* 4: 193–203.



- Bicknell RDC, Holmes JD, Edgecombe GD, Losso SR, Ortega-Hernández J, Wroe S, Paterson JR. 2021a.** Biomechanical analyses of Cambrian euarthropod limbs reveal their effectiveness in mastication and durophagy. *Proceedings of the Royal Society B: Biological Sciences* **288**: 20202075.
- Bicknell RDC, Klinkhamer AJ, Flavel RJ, Wroe S, Paterson JR. 2018a.** A 3D anatomical atlas of appendage musculature in the chelicerate arthropod *Limulus polyphemus*. *PLoS One* **13**: e0191400.
- Bicknell RDC, Ledogar JA, Wroe S, Gutzler BC, Watson WH III, Paterson JR. 2018b.** Computational biomechanical analyses demonstrate similar shell-crushing abilities in modern and ancient arthropods. *Proceedings of the Royal Society B: Biological Sciences* **285**: 20181935.
- Bicknell RDC, Melzer RR, Schmidt M. 2021b.** Supplemental data for “Three-dimensional kinematics of euchelicerate limbs uncover functional specialisation in eurypterid appendages”. *Dryad, Dataset*. doi:10.5061/dryad.6m905qfzv.
- Bicknell RDC, Paterson JR, Caron JB, Skovsted CB. 2018c.** The gnathobasic spine microstructure of recent and Silurian chelicerates and the Cambrian artiopodan *Sidneyia*: Functional and evolutionary implications. *Arthropod Structure & Development* **47**: 12–24.
- Bicknell RDC, Smith PM, Poschmann M. 2020.** Re-evaluating evidence of Australian eurypterids. *Gondwana Research* **86**: 164–181.
- Boxshall G. 2013.** Arthropod limbs and their development. In: Minelli A, Boxshall G, Fusco G, eds. *Arthropod biology and evolution*. Berlin: Springer, 241–267.
- Boxshall GA. 2004.** The evolution of arthropod limbs. *Biological Reviews* **79**: 253–300.
- Brainerd EL, Baier DB, Gatesy SM, Hedrick TL, Metzger KA, Gilbert SL, Crisco JJ. 2010.** X-ray reconstruction of moving morphology (XROMM): precision, accuracy and applications in comparative biomechanics research. *Journal of Experimental Zoology Part A: Ecological Genetics and Physiology* **313**: 262–279.
- Brandt DS, McCoy VE. 2014.** Modern analogs for the study of eurypterid paleobiology. In: Hembree DI, Platt BF, Smith JJ, eds. *Experimental approaches to understanding fossil organisms*. Dordrecht: Springer, 73–88.
- Briggs DEG, Dalingwater JE, Selden PA. 1991.** Biomechanics of locomotion in fossil arthropods. In: Rayner JMV, Wootton RJ, eds. *Biomechanics in evolution*. Cambridge: Cambridge University Press, 37–56.
- Bright JA. 2014.** A review of paleontological finite element models and their validity. *Journal of Paleontology* **88**: 760–769.
- Dalingwater JE. 1975.** Further observations on eurypterid cuticles. *Fossils and Strata* **4**: 271–279.
- Dalingwater JE. 1985.** Biomechanical approaches to eurypterid cuticles and chelicerate exoskeletons. *Transactions of the Royal Society of Edinburgh: Earth Sciences* **76**: 359–364.
- Dunlop JA, Penney D, Jekel D. 2020.** A summary list of fossil spiders and their relatives. *World Spider Catalog, version 20.5*. Bern: Natural History Museum Bern. doi:10.24436/2
- Dunlop JA, Selden PA. 1998.** The early history and phylogeny of the chelicerates. In: Fortey RA, Thomas RH, eds. *Arthropod relationships*. Dordrecht: Springer. 221–235.
- Esteve J, Gutiérrez-Marco JC, Rubio P, Rábano I. 2018.** Evolution of trilobite enrolment during the Great Ordovician Biodiversification Event: insights from kinematic modelling. *Lethaia* **51**: 207–217.
- Esteve J, Rubio P, Zamora S, Rahman IA. 2017.** Modelling enrolment in Cambrian trilobites. *Palaeontology* **60**: 423–432.
- Falkingham PL, Gatesy SM. 2014.** The birth of a dinosaur footprint: subsurface 3D motion reconstruction and discrete element simulation reveal track ontogeny. *Proceedings of the National Academy of Sciences of the United States of America* **111**: 18279–18284.
- Garwood RJ, Dunlop J. 2014.** Three-dimensional reconstruction and the phylogeny of extinct chelicerate orders. *PeerJ* **2**: e641.
- Gatesy SM, Baier DB, Jenkins FA, Dial KP. 2010.** Scientific rotoscoping: a morphology-based method of 3-D motion analysis and visualization. *Journal of Experimental Zoology Part A: Ecological Genetics and Physiology* **313**: 244–261.
- Haug C. 2020.** The evolution of feeding within Euchelicerata: data from the fossil groups Eurypterida and Trigonotarbida illustrate possible evolutionary pathways. *PeerJ* **8**: e9696.
- Holm G. 1898.** Über die Organisation des *Eurypterus fisheri* Eichw. *Memoires de l'Academie Imperiale des Sciences de St. Petersbourg* **8**: 1–57.
- Lamsdell JC, Briggs DE, Liu HP, Witzke BJ, McKay RM. 2015.** The oldest described eurypterid: a giant Middle Ordovician (Darriwilian) megalograptid from the Winneshiek Lagerstätte of Iowa. *BMC Evolutionary Biology* **15**: 169.
- Lamsdell JC, Marshall DJ, Briggs DEG. 2018.** Hit and miss: a comment on Persons and Acorn, “A sea scorpion’s strike: new evidence of extreme lateral flexibility in the opisthosoma of eurypterids”. *The American Naturalist* **191**: 352–354.
- Lamsdell JC, McCoy VE, Perron-Feller OA, Hopkins MJ. 2020.** Air breathing in an exceptionally preserved 340-million-year-old sea scorpion. *Current Biology* **30**: 4316–4321.e4312.
- Lamsdell JC, Selden PA. 2017.** From success to persistence: identifying an evolutionary regime shift in the diverse Paleozoic aquatic arthropod group Eurypterida, driven by the Devonian biotic crisis. *Evolution* **71**: 95–110.
- Legg DA, Sutton MD, Edgecombe GD. 2013.** Arthropod fossil data increase congruence of morphological and molecular phylogenies. *Nature Communications* **4**: 2485.
- Manton SM. 1977.** *The Arthropoda: habits, functional morphology and evolution*. Oxford: Oxford University Press.
- McCoy VE, Lamsdell JC, Poschmann M, Anderson RP, Briggs DEG. 2015.** All the better to see you with: eyes and claws reveal the evolution of divergent ecological roles in giant pterygotid eurypterids. *Biology Letters* **11**: 20150564.
- Nyakatura JA, Melo K, Horvat T, Karakasiliotis K, Allen VR, Andikfar A, Andrada E, Arnold P, Lauströer J, Hutchinson JR, Fischer MS, Ijspeert AJ. 2019.** Reverse-engineering the locomotion of a stem amniote. *Nature* **565**: 351–355.

- Persons WS 4<sup>th</sup>, Acorn J. 2017.** A sea scorpion's strike: new evidence of extreme lateral flexibility in the opisthosoma of eurypterids. *The American Naturalist* **190**: 152–156.
- Plotnick RE. 1985.** Lift based mechanisms for swimming in eurypterids and portunid crabs. *Transactions of the Royal Society of Edinburgh: Earth Sciences* **76**: 325–337.
- Plotnick RE, Baumiller TK. 1988.** The pterygotid telson as a biological rudder. *Lethaia* **21**: 13–27.
- Rayfield EJ. 2007.** Finite element analysis and understanding the biomechanics and evolution of living and fossil organisms. *Annual Reviews in Earth and Planetary Sciences* **35**: 541–576.
- Schmidt M, Hazerli D, Richter S. 2020.** Kinematics and morphology: a comparison of 3D-patterns in the fifth pereopod of swimming and non-swimming crab species (Malacostraca, Decapoda, Brachyura). *Journal of Morphology* **281**: 1547–1566.
- Schmidt M, Liu Y, Zhai D, Hou X, Melzer RR. 2021.** Moving legs: a workflow on how to generate a flexible endopod of the 518 million-year-old Chengjiang arthropod *Ercaicunia multinodosa* using 3D-kinematics (Cambrian, China). *Microscopy Research & Technique* **84**: 695–704.
- Schoenemann B, Poschmann M, Clarkson ENK. 2019.** Insights into the 400 million-year-old eyes of giant sea scorpions (Eurypterida) suggest the structure of Palaeozoic compound eyes. *Scientific Reports* **9**: 17797.
- Selden PA. 1981.** Functional morphology of the prosoma of *Baltoeurypterus tetragonophthalmus* (Fischer) (Chelicerata: Eurypterida). *Transactions of the Royal Society of Edinburgh: Earth Sciences* **72**: 9–48.
- Selden PA. 1984.** Autecology of Silurian eurypterids. *Special Papers in Palaeontology* **32**: 39–54.
- Selden PA, Lamsdell JC, Qi L. 2015.** An unusual euchelicerate linking horseshoe crabs and eurypterids, from the Lower Devonian (Lochkovian) of Yunnan, China. *Zoologica Scripta* **44**: 645–652.
- Turner ML, Falkingham PL, Gatesy SM. 2020.** It's in the loop: shared sub-surface foot kinematics in birds and other dinosaurs shed light on a new dimension of fossil track diversity. *Biology Letters* **16**: 20200309.
- Ward DV. 1969.** Leg extension in *Limulus*. *The Biological Bulletin* **136**: 288–300.
- Wendruff AJ, Babcock LE, Wirkner CS, Kluessendorf J, Mikulic DG. 2020.** A Silurian ancestral scorpion with fossilised internal anatomy illustrating a pathway to arachnid terrestrialisation. *Scientific Reports* **10**: 14.

## SUPPORTING INFORMATION

Supporting Information may be found at [Bicknell et al. \(2021b\)](#):

**Figure S1.** Three-dimensional (3D) interactive model of *Limulus polyphemus* prosomal appendage II, NENH-AR0002, as modelled from micro-computed tomography scanning and 3D kinematic modelling: rotated position.

**Figure S2.** Three-dimensional (3D) interactive model of *Limulus polyphemus* prosomal appendage II, NENH-AR0002, as modelled from micro-computed tomography scanning and 3D kinematic modelling: stretched position.

**Figure S3.** Three-dimensional (3D) interactive model of *Limulus polyphemus* prosomal appendage VI, NENH-AR0003, as modelled from micro-computed tomography scanning and 3D kinematic modelling: rotated position.

**Figure S4.** Three-dimensional (3D) interactive model of *Limulus polyphemus* prosomal appendage VI, NENH-AR0003, as modelled from micro-computed tomography scanning and 3D kinematic modelling: stretched position.

**Figure S5.** Three-dimensional (3D) interactive model of *Eurypterus tetragonophthalmus* prosomal appendage IV, as modelled in BLENDER and 3D kinematic modelling: rotated position.

**Figure S6.** Three-dimensional (3D) interactive model of *Eurypterus tetragonophthalmus* prosomal appendage IV, as modelled in BLENDER and 3D kinematic modelling: stretched position.

**Figure S7.** Three-dimensional (3D) interactive model of *Eurypterus tetragonophthalmus* prosomal appendage IV, as modelled in BLENDER and 3D kinematic modelling following [Selden \(1981\)](#): rotated position.

**Figure S8.** Three-dimensional (3D) interactive model of *Eurypterus tetragonophthalmus* prosomal appendage IV, as modelled in BLENDER and 3D kinematic modelling following [Selden \(1981\)](#): stretched position.

**Figure S9.** Three-dimensional interactive model of *Pentecopterus decorahensis* prosomal appendage III, as modelled in BLENDER: neutral position.

**Figure S10.** Three-dimensional interactive model of *Pentecopterus decorahensis* prosomal appendage V, as modelled in BLENDER: neutral position.

**Data S1.** STL and MAYA files associated with the *Limulus polyphemus* prosomal appendage II models.

**Data S2.** STL and MAYA files associated with the *Limulus polyphemus* prosomal appendage VI models.

**Data S3.** STL and MAYA files associated with the *Eurypterus tetragonophthalmus* prosomal appendage IV models as proposed here.

**Data S4.** STL files associated with the *Eurypterus tetragonophthalmus* prosomal appendage IV models as proposed by Selden (1981).

**Data S5.** STL and Maya files associated with the *Pentecopterus decorahensis* prosomal appendage III models.

**Data S6.** STL and Maya files associated with the *Pentecopterus decorahensis* prosomal appendage V models.

**Table S1.** Micro-computed tomography scanning conditions for examined *Limulus polyphemus* appendages.

**Table S2.** Joint angles for analysed models. Data are depicted in Figure 4.

# Chapter VI

## “Kinematics of whip spider pedipalps: a 3D comparative morpho-functional approach”

### Preface

Amblypygi are tropical and subtropical ambush predators that use elongated, raptorial pedipalps for different activities. Although pedipalp use in predation and courtship has been explored in videography in vivo analyses, kinematic ex vivo examination of these appendages has not been conducted. Here, we rectify this lack of data by using micro-CT scans to 3D-kinematically model the appendage morphology and the range of motion (ROM) of the joints for *Damon medius* and *Heterophrynus elaphus*. We illustrate the successful application of this technique to terrestrial euarthropods in determining the maximum ROM values for each pedipalp joint. We also note that, in life, these values would be lower due to motion restricting structures like tendons, arthroal membranes, and muscles. We further compare our maximum values obtained here with data from video-based motion analyses. The ROM of each joint shows the greatest flexibility in the femur-tibia joint (140–150°), the lowest in the basitarsus-claw joint (35–40°). ROM in the tibia-basitarsus joint is markedly distinct (*D. medius*: 44°; *H. elaphus*: 105°). This disparity reflects how *H. elaphus* uses the joint in the capture basket, while *D. medius* uses the femur-tibia joint to form the capture basket. We further illustrate notable vertical motion of the *H. elaphus* pedipalp compared to *D. medius*. This difference reflects the retro-ventral trochanter apophysis of *H. elaphus*. Our study opens the possibility to further whip spider kinematic understanding. Examination of other taxa using this approach will result in a more comprehensive understanding of the ecological significance and ethological implications of this unique arachnid group.

This publication deals with extant euchelicerates and highlights appendage kinematics in whip spider pedipalps. It generates novel data on morpho-functionality using Mimics to obtain surface models of the micro-computed tomography scanned specimens and Maya to perform range of motion analyses.

received: 08 May 2021  
revised: 18 July 2021  
accepted: 19 August 2021  
published: 16 September 2021

### Open Access

Published in *Integrative Zoology* as:

Schmidt, M., Melzer, R. R., & Bicknell, R. D. C. (2022). Kinematics of whip spider pedipalps: a 3D comparative morpho-functional approach. *Integrative Zoology*, 17, 156–167.

Annotation:

The Supporting Information of this paper–Schmidt, Melzer & Bicknell (2022)–that is, three-dimensional interactive PDF's, are not considered in this thesis owing to the data size, but can be downloaded at <https://onlinelibrary.wiley.com/doi/10.1111/1749-4877.12591>.

# Chapter VII

## “Spines and baskets of apex predatory sea scorpions uncover unique feeding strategies using 3D kinematics”

### Preface

Megalograptidae and Mixopteridae with elongate, spinose prosomal appendages are unique early Paleozoic sea scorpions (Eurypterida). These features were presumably used for hunting, an untested hypothesis. Here, we present 3D model-based kinematic range of motion (ROM) analyses of *Megalograptus ohioensis* and *Mixopterus kiaeri* and compare these to modern analogs. This comparison confirms that the eurypterid appendages were likely raptorial, used in grabbing and holding prey for consumption. The *Megalograptus ohioensis* model illustrates notable Appendage III flexibility, indicating hypertrophied spines on Appendage III may have held prey, while Appendage II likely ripped immobilized prey. *Mixopterus kiaeri*, conversely, constructed a capture basket with Appendage III, and impaled prey with Appendage II elongated spines. Thus, megalograptid and mixopterid frontal most appendages constructed a double basket system prior to moving dismembered prey to the chelicerae. Such 3D kinematic modeling presents a more complete understanding of these peculiar euchelicerates and highlights their possible position within past ecosystems.

This publication presents advanced data on the functional morphology of the frontal most appendages of two unique eurypterid taxa. We designed 3D Blender models of head and Appendages II and III, conducted the range of motion analyses of the appendages in Maya and compared it to the former obtained whip spider specimen range of motion data.

received: 24 October 2021  
revised: 05 November 2021  
accepted: 16 December 2021  
published: 21 January 2022

### Open Access

Published in *iScience* as:

Schmidt, M., Melzer, R. R., Plotnick, R. R., & Bicknell, R. D. C. (2022). Spines and baskets of apex predatory sea scorpions uncover unique feeding strategies using 3D-kinematics. *iScience*, 25, 103662.

# Discussion

### 3. Discussion

#### 3.1 The euarthropod appendage

##### 3.1.1 – Biramous and uniramous appendages

The morphology of euarthropod appendages, their evolutionary origin and the modifications among the euarthropod groups have been widely discussed over the last years (Boxshall, 2004, 2013; Bruce, preprint, 2021; Bruce & Patel, 2020; Jockusch, 2017; Liu Y et al., 2021; Minelli, 2003).

In general, there are two types of major euarthropod appendage constructions known: a biramous and a uniramous appendage. Biramy refers to an inner branch (the endopodite) and an outer branch (the exopodite) of an appendage, both arising from the same base section (protopodite, or basipodite). Uniramous appendages, however, do only possess one branch (telopodite, also often referred to as endopodite), which originates from the protopodite (Boxshall, 2004, 2013). However, two Silurian euarthropods are described, where the exopodite may rather originate from the body wall instead of the protopodite (Briggs et al., 2012; Sutton et al., 2002). This, though, is ambiguous, as it would represent the only two extinct species ever to bear such a distinct set-up.

It might be also owing to methodological circumstances, as those fossils were examined using serial grinding as an invasive technique. And the visualization of the volumes in SPIERS as well as the graphical output was less informative compared to  $\mu$ CT-generated data.

Despite those three major appendage elements, there are several other structures like exites or endites –depending on their orientation towards the midline of the body (Boxshall, 2004; Hansen, 1925). Euarthropod groups bearing post-

antennal biramous appendages always share a pair of uniramous first appendages (Boxshall, 2004, 2013), which are referred to as antennae—though there are several terms for several groups. There exists bi-, tri- or even multi-flagellate first appendages in several Cambrian megacheirans and extant malacostracans (Boxshall, 2013). However, there are no true biramous first appendages (despite a small myriapod group, see Boxshall, 2004, Fig. 2g).

##### 3.1.2 – Evolutionary and developmental aspects of euarthropod appendages

###### *Phylogenetic relationships among euarthropods*

The question of whether uniramous or biramous euarthropod appendages represent the ancestral state in euarthropods, is not easy to answer—and might be regarded when reviewing the current understanding of the phylogenetic relationships among euarthropods.

The common agreement on euarthropod phylogeny (Giribet & Edgecombe, 2012; Legg, Sutton & Edgecombe, 2013; Regier et al., 2010), is a sister group relationship of chelicerates and mandibulates, with mandibulates containing myriapods, crustaceans and hexapods, while the latter two together forming the so-called “Pancrustacea” or Tetraconata (Richter, 2002; see also Melzer et al., 1997; Melzer, Michalke & Smola, 2000).

The term “Pancrustacea” was suggested by Zrzavý & Štys (1997), but Tetraconata (Dohle, 2001; Richter, 2002) is more used and less ambiguous (see Richter, 2002, p. 224).

However, for the Tetraconata, molecular phylogenetic studies resolved Remipedia Yager, 1981 being rather related to hexapods (Fanenbruck, Harzsch & Wägele, 2004).

This would make the “crustacea” a paraphyletic group among the Arthropoda (Fahrbach, 2004; Regier et al., 2010; Rota-Stabelli et al., 2011).



Trilobites cluster with several non-trilobite taxa within the Artiopoda, a group being regarded as crown-group euarthropods (Legg, Sutton & Edgecombe, 2013; Ortega-Hernández, 2016). The relationships among mandibulates were once thought to resolve crustacea as a single clade and sister group to myriapods and hexapods – both together forming the so-called Atelocerata (Heymons, 1901). This group shared several morphological features (like tracheae as breathing structures) but did not resolve by molecular phylogenetic studies as a valid taxon (Friedrich & Tautz, 1995; Telford & Thomas, 1995), thus, those air-breathing structures might have evolved independently (see Bruce, preprint, 2021). Tetraconata is now widely accepted (e.g., Giribet & Edgecombe, 2012; Koenemann et al., 2009; Legg, Sutton & Edgecombe, 2013; Mallatt, Garey & Shultz, 2004; Regier et al., 2010), though some studies also favored the Atelocerata (e.g., Bitsch & Bitsch, 2004).

Despite those relationships, which all ground on the mandibulates being a monophylum containing myriapods, hexapods and crustaceans, there was also the idea of chelicerates being a sister group to myriapods. This Myriochelata or Paradoxopoda concept (Pisani et al., 2004), however, was not supported by molecular phylogenetic studies (e.g., Friedrich & Tautz, 1995; Sombke et al., 2012).

Taking the sea spiders (pygogonids) into account, which generally are thought to cluster among chelicerates, there was also the suggestion of making the pygogonids a sister taxon to all other arthropods, which were summarized then as Cormogonida (Legg, Sutton & Edgecombe, 2013).

Eventually, back in time, Tiegs & Manton (1958) even proposed a polyphyly of Arthropoda, with a group called “Uniramia” (see Manton, 1973, 1977, and Wägele, 1993, on its rejection).

### The ancestral condition

Biramy in post-antennal appendages is thought to have been the ancestral condition (Bergström & Hou, 2005; Boxshall, 2004); a plesiomorphic character for crustaceans and euarthropods. Thus, uniramous appendages might have evolved several times independently (Budd, 2002; Waloszek & Müller, 1997). In the fossil record of the earliest known euarthropod fossils from the Cambrian, there is no euarthropod known and described bearing uniramous appendages (Hou X et al., 2017).

The first well developed and clearly distinguishable uniramous appendages found in the fossil record are the appendages of xiphosurans, eurypterids and chasmataspidids, which were all aquatic chelicerates. And the earliest eurypterid fossils were found in Middle Ordovician strata (Lamsdell et al., 2015).

In extant and extinct euarthropods, uniramous appendages occur in myriapods, various insects and chelicerates. Biramous appendages in extant euarthropods are present in some crustacean groups, while in the past times most extinct chelicerates, trilobites and early crustacean relatives (like *Ercaicuna*, Schmidt et al., 2021b, **Chapter IV**; Zhai et al., 2019b) bore biramous appendages.

The general difference between uniramy and biramy is the presence of an exopodite in biramous appendages, which—occurring in primarily aquatic arthropods—aids and aided in respiration, osmoregulation, and motion (Haug C & Haug J, 2016; Hou J, Hughes & Hopkins, 2021; Schmidt et al., in press, 2022, **Chapter I**; Suzuki & Bergström, 2008). As both, trilobite relatives and crustacean relatives bear and bore biramous post-antennal appendages, the origin of biramy might root deep within the earliest crown-group euarthropods (Boxshall, 2004; Waloszek & Müller, 1997).

### Developmental perspectives of euarthropod appendage types

Uniramous appendages in some euarthropod groups were once considered to have evolved via a loss of the exopodite, the outer branch, while the inner branch, the endopodite, remained (e.g., Hansen, 1925; Olesen, Richter & Scholtz, 2001). There were also considerations of the endopodite emerging from the main axis of the appendage, while the other structures (exites, endites) emerge from additional branches (Borradaile, 1926; Snodgrass, 1958; Thiele, 1905). However, Wolff & Scholtz (2008) showed for a malacostracan eucrustacean via cell lineage studies that endopodite and exopodite of a biramous appendage develop by a split of the main axis, instead of developing from several axes. And that a uniramous appendage otherwise develops by not splitting of this main proximo-distal axis.

## 3.2 Appendages in Cambrian Chengjiang euarthropods

Among the non-trilobite arthropods, the species *Pygmaclypeatus daziensis* (Schmidt et al., in press, 2022, **Chapter I**), *Sinoburius lunaris* (Schmidt et al., 2021a, **Chapter II**), *Naraoia spinosa* and *Retifacies abnormalis* (Liu Y et al., 2021, **Chapter III**) were analyzed in this thesis. Furthermore, the two leaichoiliids *Leanchoilia illecebrosa* and *L. obesa* (Liu Y et al., 2021, **Chapter III**), as well as the crustacean-related euarthropod *Ercaicunia multinodosa* (Schmidt et al., 2021b, **Chapter IV**) were considered. Among all, the patterns of appendage structures, as well as the number of elements and appendages will be viewed and discussed.

### 3.2.1 – Considerations about euarthropod appendage structures

#### The protopodite, endites and exites

The basal most structure of an euarthropod appendage is the proto- or basipodite. From this part, each branch emerges alongside its proximo-distal axis. For euarthropods having biramous post-antennal appendages, it is easy to distinguish, being the structure where the branches emerge. However, for uniramous appendages, it is not that clear. Besides those two rami, also endites and exites emerge from the protopodite.

The biggest difference between the latter two and the two main rami are muscles. While endopodites and exopodites—known as developing by a split of the main axes, Wolff & Scholtz, 2008—do possess muscles, all additional structures like endites, exites (and among those, also epipodites), lack those.

Endites are ventrally protruding structures of the protopodite and are found in all Cambrian Chengjiang euarthropods analyzed in this thesis.

*Pygmaclypeatus daziensis* showed several rows of pointed and spinose endites (Schmidt et al., in press, 2022, Figs. 1c, 3f, g, **Chapter I**) in all trunk appendages as well as in the fourth post-antennal biramous head appendage (which is thought of as a transitory appendage sharing several morphological characters of the head and the trunk appendages).

*Sinoburius lunaris*, however, showed rather ridge-like crescentic endites (Chen X et al., 2019, Figs. 2, 3b, 7; Schmidt et al., 2021a, Fig. 2, **Chapter II**). And while in *Naraoia spinosa* and *Retifacies abnormalis*, the protopodal endites were also pointed and dense, in *Leanchoilia illecebrosa* and *L. obesa*, endites were organized in only two to three rows and were less curved (Liu Y et al., 2021, Fig. 3, **Chapter III**).

For the crustacean-related *Ercaicunia multinodosa*, the presence of endites is less clear in the fossils (Schmidt et al., 2021b, Fig. 4f, **Chapter IV**; Zhai et al., 2019b, Figs. 1E, 2F, G). However, Zhai et al. (2019b, p. 174) spoke of rather rounded endites. Interestingly, this species is the only one among all which bore another structure, so-called epipodites.

Those structures are referred to as exites in general, owing to the site of their emergence, and occur in many extant and extinct crustaceans (Boxshall, 2004). Together with the presumed presence of mandibles in *E. multinodosa*, Zhai et al. (2019b) considered it belonging to the crown-group crustaceans.

Exites are defined as structures protruding dorsally from the protopodite (Boxshall, 2004, 2013). Prior to the findings of Liu Y et al. (2021), **Chapter III**, those structures were unknown (or undescribed) in any early Cambrian Chengjiang euarthropod.

The authors could show for *L. illecebrosa* and *L. obesa*, that those exites occur as up to four lobe-like lamellae, with the biggest lamella being attached directly to the protopodite, and the three smaller lamellae emerging from the biggest lamella (Liu Y et al., 2021, Fig. 3a, **Chapter III**). While in *N. spinosa* all elongate lamellae are rather equal, with two also emerging from the main lamella (Liu Y et al., 2021, Fig. 3b, **Chapter III**), in *R. abnormalis* all exite lamellae are of different length, and all are attached to the protopodite (Liu Y et al., 2021, Fig. 3c, Suppl. Fig. 9, **Chapter III**). For the remaining analyzed species (*Pygmaclypeatus daziensis*, *Sinoburius lunaris* and *Ercaicunia multinodosa*), in-depth  $\mu$ CT studies could not uncover exites like those in the former species (Chen X et al., 2019; Schmidt et al., 2021a, b, in press, 2022, **Chapter I, II, IV**; Zhai et al., 2019b). However, in *E. multinodosa* the detected epipodites would count as such.

And even in the earlier study of *Naraoia spinosa* (Zhai et al., 2019a), the exites found by Liu Y et al. (2021), **Chapter III** were not detected.

While endites in the Chengjiang arthropods may have served functions as gnathobasic structures throughout the species, the functions of exites remain a conundrum. Nevertheless, the findings in Liu Y et al. (2021), **Chapter III** could imply that exites have a deeper origin in euarthropod phylogeny than assumed before. The four analyzed taxa are artiopodans (*N. spinosa*, *R. abnormalis*) and megacheirans (*L. illecebrosa*, *L. obesa*), with the latter group possibly being polyphyletic. Both, artiopodans as well as megacheirans had been assigned various times repeatedly to different related groups—for example, artiopods being either mandibulates (Boudreaux, 1979; Scholtz, Staude & Dunlop, 2019; Zeng H et al., 2017) or chelicerates (Aria, 2020; Legg, Sutton & Edgecombe, 2013), and megacheirans, if monophyletic, being either stem-group euarthropods (Budd, 2002; Legg, Sutton & Edgecombe, 2013) or stem-group chelicerates (Chen J, Waloszek & Maas, 2004; Cotton & Braddy, 2003; Liu Y et al., 2020b; Zeng H et al., 2020).

### The endopodite

The endopodite is defined as the inner branch of a post-antennal biramous appendage. In taxa with uniramous appendages, the term telopodite is widely accepted (Boxshall, 2004, 2013). Endopodites in early Cambrian Chengjiang euarthropods show a high degree of variability. For *Pygmaclypeatus daziensis*, Schmidt et al. (in press, 2022, Figs. 1c, d, 3e–g), **Chapter I** showed up two different endopodite types: a walking leg-like type in the head appendages, and a sub-chelate-like type in the trunk and pygidium appendages. This heteronomy of appendages is not present in the other analyzed species.

*Sinoburius lunaris* turned out to have a rather conservative set of cylindrical endopodites throughout the body, though Schmidt et al. (2021a), **Chapter II**, found a different endopodite morphology of endopodite 2 among the head appendages of at least one specimen

(YRCP 0011, Schmidt et al., 2021a, Fig. 2j–l, **Chapter II**). Furthermore, this species showed a reduction of the first endopodite of the post-antennal head appendages (Schmidt et al., 2021a, Fig. 2c, k, **Chapter III**). A common observation is that the total size of endopodites (actually, the entire post-antennal biramous appendages) decreases from anterior to posterior.

For *Naraoia spinosa*, Zhai et al. (2019a), **Chapter III**, showed in a former study the presence of cylindrical endopodites tapering in size, with pointed endopodal spines present at elements two to five (Liu Y et al., 2021, Fig. 3b; Zhai et al., 2019a, Fig. 3, **Chapter III**). This is also observable in *Retifacies abnormalis* (Liu Y et al., 2021, Fig. 3c, **Chapter III**; Zhang M et al., submitted) and the analyzed leancoiliids (Liu Y et al., 2021, Fig. 3a, **Chapter III**).

In *Ercaicunia multinodosa*, though, the endopodite morphology was rather simple (Schmidt et al., 2021b, Fig. 4, **Chapter IV**; Zhai et al., 2019b, Figs. 2f, g, 3).

The endopodites, thus, were structures primarily modified for walking. However, in taxa like *Pygmaclypeatus daziensis*, they may have served other functions like digging or grabbing, at least the sub-chelate endopodites throughout the body, while the function of the reduced first endopodite pair in *S. lunaris* still remains unclear.

### The exopodite

The exopodite is defined as the outer branch of a post-antennal biramous appendage. (Boxshall, 2004, 2013). It is in general a rather flat and broad structure, which might have served functions for respiration and osmoregulation, at least assumed for trilobites (Hou J, Hughes & Hopkins, 2021). Among non-trilobite arthropods, there is greater variability in exopodite shape and structure.

In *Pygmaclypeatus daziensis*, two types of exopodites were found: rather short, reduced and stenopodous exopodites in the first three

post-antennal biramous head appendages (Schmidt et al., in press, 2022, Figs. 1d, e, 2b, 3e, **Chapter I**) and an exopodite lobe with thick paddle-shaped lamellae in the fourth head appendage and the remaining appendages (Schmidt et al., in press, 2022, Figs. 2c, 3f, g, **Chapter I**). Like Haug C & Haug J (2016) also suggested for the Cambrian Burgess Shale species *Naraoia compacta*, those structures could have aided in swimming as well. While a similar exopodite shape with a basal lobe and several lamellae was given in the investigated leancoiliids and *N. spinosa* (Liu Y et al., 2021, Fig. 3a, b, **Chapter III**), the exopodite in *Retifacies abnormalis* differed. This species possessed a broad lobe with up to 16 single lamellae organized in a fan-like structure (Liu Y et al., 2021, Fig. 3c, **Chapter III**).

Nevertheless, the greatest morphological variation in exopodite shape may be present in *Sinoburinus lunaris*. Chen X et al. (2019) already showed that the first two exopodites of the post-antennal biramous head appendages are multi-articulated elongate structures protruding even beyond the head shield (Chen X et al., 2019, Figs. 1, 2, 6, 7; see also Schmidt et al., 2021a, Fig. 2c, k, **Chapter II**). This is among the most specialized exopodite in terms of morphology uncovered for early Cambrian Chengjiang euarthropods yet. Furthermore, also the remaining exopodites throughout the body of *S. lunaris* differed in being composed of a tri-partite shaft with short lamellae attached to the penultimate and ultimate shaft element (Chen X et al., 2019, Figs. 5b, 7c; Schmidt et al. 2021a, Figs. 2d, e, 3, **Chapter II**).

In *Ercaicunia multinodosa*, the severe morphology of the exopodite, however, is unclear but might have been a tri-partite shaft with lamellae attached to the last two exopodite elements as well (Zhai et al., 2019b, Figs. 2f, g, 3c).

### 3.2.2 – Considerations about numbers and elements of appendages

The elements, an euarthropod appendage is composed of, are often labeled as podomeres. However, this term is ambiguous, as it rather refers to malacostracan (crustacean) appendages (see Schmidt et al. 2021a, p. 12, **Chapter II**). Thus, other terms like elements or articles are less ambiguous but also precise and more appropriate.

Whichever term might be applied in the literature throughout the early Cambrian Chengjiang arthropod studies, there is high variability in both, the number of appendages in the species (and specimens) as well as the number of elements per appendage, and even throughout the body regarding several tagmata.

#### Number of appendages of the body

Trilobites in general have a rather conservative set of appendages with up to seven elements per appendage and lots of appendages throughout the body, though the number varied owing to the anamorphic development of those arthropods (e. g., Zeng F et al., 2017).

Non-trilobite artiopodans, however, are less uniform, and show great specialization. However, despite the exception of segmental mismatch in some specimens or species (Chen X et al., 2019; Schmidt et al., 2021a, **Chapter II**), each body or trunk segment was regarded to possess only one pair of appendages.

*Pygmaclypeatus daziensis* was first described by Zhang X, Han & Shu (2000) based on light microscopic imaging solely. Xu (2004) added details on an multi-articulated tailspine. However, the advanced imaging techniques in Schmidt et al. (in press, 2022), **Chapter I**, could uncover the appendicular morphology for the first time—and could reveal unique post-antennal biramous appendages, modified in a way unlike any others. The study uncovered 14 post-

antennal biramous appendages in total, four in the head, six in the trunk—related to all six tergites—as well as four in the pygidium.

*Sinoburius lunaris* once was thought to possess 17 post-antennal biramous appendages throughout the body, with four in the head, nine in the body and three (or four) in the pygidium. Schmidt et al. (2021a), **Chapter II**, though, were able to hint on possible preservation biases or intraspecific variation within this species, pointing out for *S. lunaris* the same set and arrangement of appendages only for specimen YKLP 11407. For the latter two specimens analyzed (YRCP 0011 and Hf-z-10-45), the total biramous appendage number was rather 16, with four head-, eight trunk- as well as four pygidium appendages (Schmidt et al., 2021a, Fig. 2, **Chapter II**).

This restudy, thus, showed a different approach and highlighted several aspects like possible ontogenetic or intraspecific differences among specimens of the same species, also regarding the number of their tergites.

The appendicular morphology of *Naraoia spinosa* and *Retifacies abnormalis* was already considered. Zhai et al. (2019b) could uncover up to 20 total biramous appendages in *N. spinosa*, of which up to six might belong to the head. Zhang M et al. (submitted) pointed out up to 23 total post-antennal biramous appendages for *R. abnormalis*, that is, four in the head, 14 in the trunk, and five in the pygidium.

Leancoiliids, in general, possessed around 11 trunk segments, each carrying one pair of post-antennal biramous appendages, while the number of post-SGA biramous head appendages differed between two to four (García-Bellido & Collins, 2007; Haug J, Briggs & Haug C, 2012; Liu, Hou & Bergström, 2007; Liu Y et al., 2020b, 2021, **Chapter III**), making up in total around 15 post-SGA biramous appendages.

Eventually, for *Ercaicunia multinodosa*, Zhai et al. (2019b) uncovered 16 “post-antennal” biramous trunk appendages, together with what

they believed to represent antennae, antennulae, mandibles and maxillulae in the head.

Thus, in the four analyzed arthropod taxa in this thesis, as well in *E. multinodosa*, total biramous post-antennal appendage number uncovered lies between 14 and 23, while in leanchoiliids it is about 15. This contributes to the understanding of the morphology of those arthropods. In classical studies (Hou X & Bergström, 1997; Hou X et al., 2017), the counted number of appendages was always depending on the preservation quality of the fossils.

And most dorso-ventrally flattened organisms were preserved only in dorsal aspect, sometimes not allowing any information on the exact appendage number.

#### Number of elements in the appendages

The number of elements per appendage was not very high in the investigated species. It varied between five in the endopodites of the post-antennal biramous head appendages of *Pygmaclypeatus daziensis* (Schmidt et al., in press, 2022, Fig. 3e, **Chapter I**) and nine in the two leanchoiliids (Liu Y et al., 2021, Fig. 3a, **Chapter III**). However, the major issue when counting elements of appendages, is, whether to take the terminal claw into account or not. Bruce (preprint, 2021) counted the terminal claw of extant arthropods as a distinct appendage element, not an additional structure.

This, however, is ambiguous, as true podomeres (in malacostracan crustaceans, for example), that is, true distinct appendage elements, are defined by having musculature, allowing those podomeres to fulfil a movement of a distal podomere more or less independent from the movement of the adjacent proximal one. This might not be given when considering that claws are simple cuticular structures without any musculature, like present in the tiny claws of extant arachnids, which are not to count as telopodite elements (e. g., Foelix, 2010, Fig. 2.17).

Nevertheless, this also depends on the size of the elements, and in the vast majority of early Cambrian Chengjiang euarthropods, the cylindrical endopodite tapers in size distally, ending in a terminal claw as an ultimate appendage element which is not that different in size compared to the former pen-ultimate one.

According to Boxshall (2004, 2013), the ancestral number of elements in post-antennal biramous appendages is seven. Indeed, this number is present in most arthropods. However, there are also groups described from the Chengjiang Lagerstätte which possessed another set of endopodal elements. In *Xiaocaris luoi* Liu Yet al., 2020 for example, endopodites are comprised of up to 15 elements with bulb-like ventral parts. And in fuxianhuids like *Chengjiangocaris kunmingensis* Yang et al., 2013 or *Alacaris mirabilis* Yang et al., 2018, endopodal elements might have been up to 20 or more (Yang et al., 2013, 2018).

Eventually, this raises the question of the ancestral number of endopodal elements in arthropods, which is still to discuss.

### **3.2.3 – Progress in virtual paleontology research of Chengjiang euarthropods**

Several studies showed the powerful application of  $\mu$ CT research in combination with Drishti to reveal the ventral morphology of early Cambrian Chengjiang euarthropods (Tabl. 1). Until several years ago, when Liu Y, Scholtz & Hou (2015) introduced this technique to the Chengjiang biota to enlighten the appendicular morphology of *Xandarella spectaculum* Hou et al., 1991, analyses of early Cambrian Chengjiang euarthropods were based on traditional techniques, like light microscopic imaging or camera lucida drawings. The introduction of  $\mu$ CT owing to the exceptional mode of preservation of this biota (Gabbott et al., 2004) opened a window to a world that was hidden in the slabs for millions of years.

Up to now, around 19 euarthropod species were described or re-described using virtual paleontological techniques. Many of them were only known from single specimens, (e.g., *Pygmaclypeatus daziensis*), while other species are known from hundreds of specimens (e.g., *Leancoilia illecebrosa*).

Besides the taxa analyzed in this thesis, also the naraoiid *Misszhouia longicaudata* (Zhang & Hou, 1985) (Zhao T et al., 2017) and the canadaspidiid *Pectocaris spatiosa* Hou, 1999 (Jin et al., 2021) were investigated. Furthermore,  $\mu$ CT techniques uncovered appendicular aspects of the fuxianhuides *Jianshania furcatus* Luo & Hu, 1999 (and the former mentioned *Xiaocaris luoi*, Liu Y et al., 2020a) as well as of *Fuxianhuia protensa* Hou, 1987 (Aria, Zhao & Zhu, 2021).

Zhai et al. (2019c) unveiled the magnificent specialization of appendages in the bradoriids *Kunmingella douvillei* (Mansuy, 1912), *Indiana* sp. and *Kunyangella cheni* Huo, 1965.

Eventually, the waptiid arthropod *Chuandianella ovata* (Lee, 1975) (Zhai et al., preprint, 2021a), the “bivalved” arthropod *Isoxys auritus* (Jiang, 1982) (Zhai et al., preprint, 2021b) as well as the megacheiran *Jianfengia multisegmentalis* Hou, 1987 (Zhang X et al., under review) were unmasked using those advanced imaging techniques.

The Chengjiang Lagerstätte in Yunnan Province, South China, is still a treasure trove. And among its more than 300 described species, there are many more secrets hidden in the stones, waiting to be unearthed.

**Table 1.** Comparative overview of  $\mu$ CT and classical studies of all priorly analyzed euarthropods from the Chengjiang biota, Yunnan Province, South China. Asteriks represent publications included in this thesis.

taxon	$\mu$ CT studies	classical studies
<i>Chuandianella ovata</i> (Lee, 1975)	Zhai et al. (preprint, 2021a)	Chen J & Zhou (1997) Lee (1975) Liu H & Shu (2004, 2008) Hou X & Bergström (1991, 1997) Hou X et al. (1999, 2009, 2017)
<i>Ercaicunia multinodosa</i> Luo & Hu, 1999	Schmidt et al. (2021b)* Zhai et al. (2019b)	Luo et al. (1999)
<i>Fuxianhuia protensa</i> Hou, 1987	Aria, Zhao & Zhu (2021)	Hou X (1987b)
<i>Isoxys auritus</i> (Jiang, 1982)	Zhai et al. (preprint, 2021b)	Fu et al. (2014) Hou X et al. (1999, 2017) Jiang (1982) Shu, Zhang & Geyer (1995)
<i>Jianfengia multisegmentalis</i> Hou, 1987	Zhang X et al. (under review)	Chen J, Waloszek & Maas (2004) Chen J & Zhou (1997) Hou X (1987a) Hou X et al. (1999, 2017)
<i>Jianshaniania furcatus</i> Luo & Hu, 1999	Liu Y et al. (2020a)	Chen L et al. (2002) Hou X et al. (2017) Luo et al. (1999)
<i>Kunmingella douvillei</i> (Mansuy, 1912)	Zhai et al. (2019c)	Duan et al. 2014 Huo (1965) Hou X et al. (1996, 1999, 2002, 2010, 2017) Mansuy (1912) Shu et al. (1999)
<i>Kunyangella cheni</i> Huo, 1965 & <i>Indiana</i> sp.	Zhai et al. (2019c)	Huo (1965) Hou X et al. (2002b, 2010, 2017)
<i>Leancoilia illecebrosa</i> (Hou, 1987)	Liu Y et al. (2016) Liu Y et al. (2020b) Liu Y et al. (2021)*	Liu Y et al. (2014) Liu Y, Hou & Bergström (2007) Haug J, Briggs & Haug C (2012) Hou X (1987a) Hou X & Bergström (1997) Hou X et al. (1999, 2017)
<i>Leancoilia obesa</i> He et al., 2017	Liu Y et al. (2021)*	He et al. (2017)
<i>Misszhouia longicaudata</i> (Zhang & Hou, 1985)	Zhao T et al. (2017)	Bergström, Hou & Hålenius (2007) Chen J, Edgecombe & Ramsköld (1997) Edgecombe & Ramsköld (1999) Hou X & Bergström (1997) Hou X et al. (2017) Vannier & Chen (2002) Zhang W & Hou (1985) Zhang X, Shu & Erwin (2007)



<i>Naraoia spinosa</i> Zhang & Hou, 1985	Liu Y et al. (2021)* Zhai et al. (2019a)	Bergström, Hou & Hålenius (2007) Chen J, Edgecombe & Ramsköld (1997) Chen J & Zhou (1997) Hou X & Bergström (1997) Hou X et al. (1999, 2017) Vannier & Chen (2002) Zhang W & Hou (1985) Zhang X, Shu & Erwin (2007)
<i>Pectocaris spatiosa</i> Hou, 1999	Jin et al. (2021)	Hou (1999) Hou X et al. (1999, 2017) Hou X & Sun (1988)
<i>Pygmaclypeatus daziensis</i> Zhang, Han & Shu, 2000	Schmidt et al. (in press, 2022)*	Hou X et al. (2017) Xu (2004) Zhang X, Han & Shu (2000)
<i>Retifacies abnormalis</i> Hou et al., 1989	Liu Y et al. (2021)* Zhang M et al. (submitted)	Chen J et al. (1996) Chen J & Zhu (1997) Edgecombe & Ramsköld (1999) Hou & Bergström (1997) Hou X, Chen & Lu (1989) Hou X et al. (1999, 2017)
<i>Sinoburius lunaris</i> Hou et al., 1991	Chen X et al. (2019a) Schmidt et al. (2021a)*	Chen J et al. (1996) Chen J & Zhou (1997) Edgecombe & Ramsköld (1999) Hou X & Bergström (1997) Hou X et al. (1991, 1999, 2017) Ramsköld et al. (1997)
<i>Xandarella spectaculum</i> Hou et al., 1991	Liu Y et al. (2015)	Bergström & Hou (1998) Chen J & Zhou (1997) Edgecombe & Ramsköld (1999) Hou X & Bergström (1997) Hou X et al. (1991, 1999, 2017) Ramsköld et al. (1997)
<i>Xiaocaris luoi</i> Liu et al., 2020	Liu Y et al. (2020a)	-

### 3.3 Appendages in Ordovician and Silurian sea scorpions

Being early euchelicerates, the prosomal appendages of sea scorpion always were uniramous. Sea scorpions showed a great range of morphological adaptations throughout the Paleozoic. While the clade of stylonurine eurypterids retained their last pair of appendages as walking legs, eurypterine eurypterids developed them as powerful swimming legs. However, despite this last pair of appendages, also the anterior ones underwent morphological and thus functional specialization in various species (Tollerton, 1989).

Among the four analyzed sea scorpion taxa, appendicular morphology and adaptations will be reviewed and discussed. Furthermore, the kinematic and functional specialization of the appendages will be enlightened, and the comparison of modern analogs illustrated.

Tollerton (1989) in his revision of the morphological characters of the Eurypterida introduced distinct terms for several types (spiniferous, non-spiniferous and swimming leg types) of eurypterid appendages. Based on Størmer (1974, pp. 363–364), he extended the terminological range to 11 spiniferous leg types, nine non-spiniferous leg types and eight swimming leg types.

Out of the four eurypterids analyzed in this thesis, only *Eurypterus tetragonophthalmus* is categorized as belonging to a non-spiniferous leg type, while the other three share spiniferous legs.

#### 3.3.1 – Morphology and kinematics in eurypterid walking appendages

##### *Eurypterus*

*Eurypterus* is the most detailed studied eurypterid. The appendicular morphology of the species of this genus, which were among the first eurypterids thoroughly studied, are known

in detail from lots of specimens from Silurian fossil sites (Braddy & Dunlop, 1997; De Kay, 1825; Diener, 1924; Fischer, 1839; Holm, 1898). Its appendages are classified as the non-spiniferous *Eurypterus* leg type (Tollerton, 1989, p. 647, Fig. 9.6).

The third walking leg (appendage IV) of *E. tetragonophthalmus* was composed of a coxa with distinct gnathobasic teeth, six elements and a terminal claw (Bicknell, Melzer & Schmidt, 2021, Fig. 2; Selden, 1981, Fig. 6, **Chapter V**). While Selden (1981) also proposed this number of elements for appendage III, in appendage II he considered one less—and in appendage V one more. Bicknell, Melzer & Schmidt (2021, Fig. 2A-F), **Chapter V**, considered a different approach of the orientation of the joint axes in *E. tetragonophthalmus*' prosomal appendage IV than what Selden (1981) proposed and modeled both variants as a comparison. While Selden (1981) suggested an inclination of the coxa-element 1-joint-axis, Bicknell, Melzer & Schmidt (2021), **Chapter V**, rather favored a model where the coxa-element 1-joint-axis lies in one plane with the preceding body-coxa-joint-axis (see Bicknell, Melzer & Schmidt, 2021, Fig. 2N, O, **Chapter V**, for a direct comparison of the joint axis orientation). Also, Selden (1981) mentioned monocondylar joints for all succeeding joints after the element 1-element 2-joint, whereas Bicknell, Melzer & Schmidt (2021), **Chapter V**, proposed a bicondylar state for all joints. This reinterpretation of the joint axes orientations and joint types has a great impact on the functional morphology of the walking legs of *E. tetragonophthalmus*. In the version of Selden (1981), the appendages were oriented forward under the body, while in the re-study of Bicknell, Melzer & Schmidt (2021), **Chapter V**, they were oriented ventrally. The latter variant would have enabled this species to better use those “walking legs” for a severe forward motion – especially, as the kinematic study showed that both variants did not allow great flexibility in terms of getting prey items close to the gnathobases.

*Pentecopterus*

*Pentecopterus decoharensis* occurs as the earliest eurypterine sea scorpion in the fossil record, dating back to the Middle Ordovician (Lamsdell et al., 2015). For this species, Bicknell, Melzer & Schmidt (2021, Fig. 3C, D), **Chapter V**, investigated the prosomal appendage V.

This appendage consisted of a coxa with gnathobasic edges and eight succeeding elements. Again, it depends on the viewer, whether the terminal claw might be counted as a single element. This appendage might be regarded as a non-spiniferous leg, as it lacks spines except the pair on the penultimate element. This, among others, is a morphological character that all megalograptid sea scorpions shared. The authors could show that owing to the interlocking morphology of elements 2-4 the rotation of this leg was limited; furthermore, element 2 was slightly rotated towards the coxa (Bicknell, Melzer & Schmidt, 2021, Fig. 3C, D, **Chapter V**). Overall, the kinematic construction of this appendage—the shortest among all appendages of *P. decoharensis*—allowed this species to extend this appendage beyond the prosomal shield. However, whether this appendage aided in walking, might be up for debate.

### 3.3.2 – Morphology and kinematics in eurypterid *grabbing* appendages

*Pentecopterus*

Bicknell, Melzer & Schmidt (2021, Fig. 3A, B), **Chapter V**, also considered the appendage III in *Pentecopterus decoharensis* for morphological and kinematic examinations. This appendage is the most elongated one among all (Lamsdell et al., 2015, Fig. 20A, D). Regarding several other morphological characters, it was considered as a member of the Megalograptidae, the same group containing *Megalograptus* sp. and *Mixopterus* sp. Appendage III in *P. decoharensis* was composed of a coxa and six succeeding elements (plus the terminal claw),

thus one element less compared to the prosomal appendage V of *P. decoharensis*. The spinosity together with the kinematically obtained data on the flexibility made this appendage most likely engaged in foraging, grabbing and keeping prey, rather than aiding in walking.

Eventually, the mode of abduction and adduction of the elongate frontal most appendages of megalograptids and mixopterids should be further analyzed in Schmidt et al. (2022, **Chapter VII**).

*Megalograptus, Mixopterus*

Appendages II and III in *Megalograptus* sp. and *Mixopterus* sp. range among the most complex and modified eurypterid appendages. Both genera exhibited species with a unique set of raptorial and ferocious, elongate appendages oriented forward. In *Me. ohioensis*, appendage II was composed of seven dorsoventrally flattened elements decreasing in size with lots of spines on its interior side. Appendage III consisted of eight elements, with element 4 bearing two elongate hypertrophied spines (Schmidt et al., 2022, Suppl. Fig. S1, S2, **Chapter VII**). In *Mi. kiaeri*, appendage II was composed of six elements, with the last three having elongate spines, while appendage III consisted of seven elements in total, similar to appendage III in *Me. ohioensis*, but less spinose, and without those elongate hypertrophied spines on element 4 (Schmidt et al., 2022, Suppl. Fig. S3, S4, **Chapter VII**). It needs to be mentioned that for kinematic purposes, the authors counted the ultimate spine as no independent appendage element, but rather being just a spine belonging to the preceding element.

Hence, the total count of elements of appendages II and III in both species is one less than what their original descriptions in 1934 and 1964 proposed.

Though the complex morphology of *Me. ohioensis* (Caster & Kjellesvig-Waering, 1964) and *Mi. kiaeri* (Størmer, 1934) was already described in detail, prior to Schmidt et al. (2022),

**Chapter VII**, no kinematic approach was considered to enlighten the feeding ecology of those two species.

The authors proposed a foraging strategy for both taxa. *Megalograptus ohioensis* was considered as using its appendages III as a capture basket to keep prey, while its scissor-like functioning appendages II ripped and tore prey for consumption (Schmidt et al., 2022, Fig. 4, **Chapter VII**). *Mixopterus kiaeri* was considered to also form a capture basket with its appendages III (though less spinose). However, the appendage II morphology allowed the authors to anticipate that prey was impaled with the elongate spines on the last three elements. Furthermore, the study could prove that the kinematic construction of the appendage II in *Mi. kiaeri* enabled this species to get prey items very close to the chelicerae under the prosomal shield (Schmidt et al., 2022, Fig. 5; **Chapter VII**). The frontal most appendages (that is, appendages II and III) in *Pentecopecterus*, *Megalograptus* and *Mixopterus* likely evolved to serve in feeding rather than in walking and may have played a major role in their entire foraging ecology. Nevertheless, some authors also considered sexual selection as a driving factor for the development of massive frontal most appendages, hinting at their reproductive biology (Caster and Kjellesvig-Waering, 1964, p. 335; Hanken & Størmer, 1975, Fig. 10).

Altogether, the authors provided an advanced understanding of the kinematics of prosomal appendages in eurypterids. They could demonstrate how the appendages might have been moved, applying the kinematic approach presented in Schmidt et al. (2021b, **Chapter IV**). Prior studies could only conjecture about the morpho-functionality in sea scorpion appendages, but never provided fundamental data to prove.

Nevertheless, a serious understanding of the movement capabilities in extinct euarthropods may be best accomplished by taking comparisons—to extant related groups.

### 3.3.3 – Appendage morphology and kinematics in modern analogs

In the kinematic approaches in this thesis, three extant comparisons were considered: the aquatic xiphosuran *Limulus polyphemus*, as well as the two terrestrial whip spiders (Amblypygi) *Damon medius* and *Heterophrynus elaphus*. All three represent comprehensible comparisons among euchelicerates, as sea scorpions are bracketed phylogenetically between horseshoe crabs and arachnids (Brand & McCoy, 2014; Legg, Sutton & Edgecombe, 2013; Selden, Lamsdell & Qi, 2015).

Moreover, recent studies hinted at possible similarities in the feeding ecology of horseshoe crabs and sea scorpions, considering the usage of the gnathobasic edges of their prosomal appendages for mastication (Anderson et al., 2014; Andrews et al., 1974; Bicknell et al., 2018b; Dalingwater, 1975, 1985; McCoy et al., 2015; Selden, 1981).

Bicknell, Melzer & Schmidt (2021, **Chapter V**) also obtained data on the kinematics of a walking leg in *L. polyphemus* and found that in a xiphosuran the walking leg likely better completed the action of getting food to the gnathal edge, than a *Eurypterus* was able to (Bicknell, Melzer & Schmidt, 2021, Fig. 1C, D, **Chapter V**). Thus, eurypterid appendages—even regarding their morpho-functionality—were more specialized than those of xiphosurans.

Given the broader morphological resemblance, also scorpions might be considered as modern analogs. However, their terrestrial lifestyle and the adaptations of their walking legs rather make them a poor extant group for comparative analysis of prosomal appendage kinematics.

They could be used as modern analogs when addressing questions on opisthosomal flexibility, for example. Past studies, though, resolved this as a rather problematic field of research (see argument between Lamsdell, Marshall & Briggs, 2018; Persons, 2018; Persons & Acorn, 2017).

The best extant group to conduct kinematic analyses of the forwardly oriented frontal most appendages are by far whip spiders. Amblypygids possess spinose elongate frontal most appendages: their pedipalps. Among all extant euchelicerates, those raptorial appendages make them the best modern analog for addressing questions on the kinematic capabilities of elongate spinose and forwardly oriented appendages.

Schmidt, Melzer & Bicknell (2022), **Chapter VI**, analyzed pedipalp kinematics in *Damon medius* and *Heterophrynus elaphus*, members of the two families Phrynichidae Simon, 1892 and Phrynidae Blanchard, 1852. Their *ex vivo* kinematic approach added new data on the range of motion of each pedipalp joint, that is the maximum excursion angle. Prior to this, research on arachnids was based rather on *in vivo* analyses like video capturing to explore strike kinematics and angle values (McLean, Garwood & Brassey, 2020; Santer & Hebets, 2009; Seiter et al., 2019), or on *in vivo* measurements of dissected or live animals (Ellis, 1944; Manton, 1977; Petrunkevitch, 1909; Shultz, 1989; Wolff et al., 2016). Thus, the kinematically obtained data of Schmidt, Melzer & Bicknell (2022), **Chapter VI**, contributed to a broader understanding of the physical basics and capabilities of whip spider pedipalp usage, which in later approaches could be compared to *in vivo* obtained data.

Schmidt et al., (2022), **Chapter VII**, used the data calculated by Schmidt, Melzer & Bicknell (2022), **Chapter VI**, on the range of motion of the joints to compare them to the data obtained in the megalograptid and mixopterid frontal most appendages. They were able to show that the excursion angles in both, the eurypterids and the whip spiders were highest in joint 3 (that is, the element 3-element 4 joint in eurypterids and the femur-tibia joint in amblypygids, Schmidt et al., 2022, Suppl. Figs. 6, 7, **Chapter VII**).

However, whip spider pedipalps in this precise joint (which combines the longest elements of the entire pedipalps) obtained an excursion angle twice as high as in the respective joint in eurypterids.

### 3.3.4 – Progress in virtual paleontology research of eurypterid kinematics

Thoughts of how ancient sea scorpions might have moved, have a long history (Briggs, Dalingwater & Selden, 1991; Plotnick, 1985; Plotnick & Baumiller, 1988; Selden, 1981, 1984). Those early studies focused on mathematical and hypothetical considerations of the biomechanics of eurypterid motion and appendage flexure and yielded also acrylic glass-based constructions to prove their kinematic implications (e.g., Plotnick & Baumiller, 1988, Fig. 7). The digitally obtained data on the range of motion in *Eurypterus tetragonophthalmus* and *Pentecopterus decoharensis* (Bicknell, Melzer & Schmidt, 2021, **Chapter V**) as well as *Megalograptus ohioensis* and *Mixopterus kiaeri* (Schmidt et al., 2022, **Chapter VII**) added an advanced approach to those early considerations and contributed *ex vivo* data on angles as well as further ecological considerations.

Together with the comparison of extinct arthropod kinematics and the kinematics in the appendages of modern arthropod analogs (Schmidt, Melzer & Bicknell, 2022, **Chapter VI**), this field of research expands the approaches in virtual paleontology.

### 3.4 Limitations of the studies: a critical view

#### *Morphology of Chengjiang euarthropods*

Paleontological research is often hampered by biases. Fossils can contain cracks or be broken, thus yielding only limited information on the entire morphology of the animal. Fossils can be compressed or deformed, challenging the reconstruction of their true shape. But even intact fossils—suitable for  $\mu$ CT research—could be biased and need severe consideration.

Not all Chengjiang fossils, for example, can be scanned with a CT. Personal observations on Chengjiang trilobites like *Eoredlichia* showed that its biomineralized exoskeleton hampered the  $\mu$ CT output, yielding only limited information besides the gross morphology. However, studies on the Ordovician trilobite *Triarthrus* sp. (e.g., Hegna, Martin & Darroch, 2017) showed that trilobites, in general, can be scanned via  $\mu$ CT. This may be because *Triarthrus* sp. occurs in Beecher's Trilobite Bed near New York, a fossil site known for pyritization. This mode of preservation is also given in Chengjiang fossils. However, for those fossils rather soft tissues (that is, non-biomineralized organic material) are preserved.

Furthermore, the thickness of fossil slabs needs to be taken into consideration. If the stones are too thick, X-rays may not pass the material, resulting in less to no data on the morphology of the euarthropod inside the slab. Likewise, the different preserved morphological aspects of both fossil slabs might be considered.

Eventually, compaction and compression are further points to consider when interpreting appendicular structures enlightened by  $\mu$ CT. Leanchoiliids and fuxianhuiids, for example, are sometimes preserved more in lateral aspect, while nearly all described and analyzed artiopodans are only preserved in dorso-ventral aspect.

This needs to be considered when discussing their appendicular morphology, and especially when counting their appendage elements.

Speaking of leanchoiliids, also another aspect is to mention, that is, the ontogeny. A large available number of specimens makes assumptions about ontogenetic development more precise. For *Leanchoilia illecebrosa*, hundreds of specimens are available (Hou X et al., 2017), ranging in size from a few millimeters (Liu Y et al., 2016) to about three or more centimeters (Liu Y et al., 2020b, 2021, **Chapter III**). With furthermore lots of specimens being preserved both, laterally and dorso-ventrally compressed, this species also allows relatively precise morphological reconstructions and considerations about its true morphology. Ontogenetic scenarios can also be derived: Liu Y et al. (2016) could show for a 2 mm *L. illecebrosa* larva the lack of at least one posterior segment. Together with the anterior appendages being in a further developed stage than the posterior ones, for this species both, an anamorphic as well as an anterior-posterior developmental gradient could be proposed.

This kind of evidence may not be given when just considering a few specimens, which do not differ that much in size – like in *Pygmaclypeatus daziensis* (Schmidt et al., in press, 2022, **Chapter I**). For this species, only four specimens were available for  $\mu$ CT research, while out of those furthermore only two allowed severe morphological considerations. This in a certain way limits the assumptions on the true morphology – or on developmental aspects – of this species.

And whether the sub-chelate endopodites of this species indeed may have been developed for grabbing, or—if the two last elements were not articulated—rather to use them as a shovel, might only be proven if more specimens of this enigmatic and rare species will be unearthed in the future.

### *Kinematics of sea scorpion appendages*

The construction of 3D models based on two-dimensionally preserved fossils may be biased as well. As eurypterid fossils most often are preserved in dorso-ventral aspect, one needs to bear in mind that the inflation of the 3D models of the appendages can only be inferred from modern euchelicerate analogs. If the elements of an appendage would be modeled in a way too thick, this would distort the assumptions made on the kinematics of this appendage. Likewise one needs to consider that the models reflect the true morphology. Caster & Kjellesvig-Waering (1964) annotated that several anatomical details of *Megalograptus ohioensis* were not preserved or known in detail, like the distal portion of the coxa of appendage III, or even the total length of the hypertrophied spines on element 4 of this appendage. The latter, especially, is crucial, as those elongate spines turned out to have a major impact on the appendage kinematics and thus the feeding ecology in this species (Schmidt et al., 2022, Figs. 2C, G, 4A, Suppl. Fig. S2, **Chapter VII**). A further issue might be the under- or even overestimation of the angle between those two hypertrophied spines (see Suppl. Fig. S2D, F in Schmidt et al., 2022, **Chapter VII**). A smaller angle might have allowed less motion (as movement would have stopped while colliding with the respective elements). A greater angle would have allowed even more flexibility.

While in some cases, the original presence of two pairs of spines on an element might be questionable, as only one was preserved (Caster and Kjellesvig-Waering, 1964, p. 323, also plate 49, Fig. 2, Text Fig. 7 therein), a further issue to consider is the flexibility of the spines itself. Whether spines might be considered movable or not, is not easy to answer, and was already up for debate.

Caster and Kjellesvig-Waering (1964, pp. 320, 325) differed movable and fixed spines for *Megalograptus ohioensis*, while Størmer

(1934, p. 109) assumed only fixed spines in *Mixopterus kiaeri*. Ritchie (1968, p. 326) differed movable and fixed spines in *Lanarkopterus* sp. (also a mixopterid sea scorpion), and so did Selden (1981, p. 10) in his thorough analysis of the morpho-functionality of *Eurypterus tetragonophthalmus*' walking legs.

Movability of spines might have been enabled via tendons, and thus might have had further implications on the flexibility of eurypterid appendages. Selden (1981) justified the existence of movable spines in *E. tetragonophthalmus* with the fact that some fossil specimens bore spines at certain elements, while others lacked those. However, in modern analogs (like in the analyzed whip spiders in Schmidt, Melzer & Bicknell, 2022, **Chapter V**) all spines represent rather rigid cuticular outgrowths and not movable units.

In this regard it needs to be mentioned, though, that spines in eurypterids might have been also to a certain degree rather smooth than totally rigid, thus reacting to distally applied pressure. This, of course, might have also impacted the kinematic results.

Eventually, the performance of the kinematic range of motion analyses needs special attention. Schmidt et al. (2021b, **Chapter IV**) illustrated the method of constructing a kinematic marionette (also conducted in Schmidt, Hazerli and Richter, 2020), which is the first step for a further range of motion analysis in Maya. Several steps need to be conducted thoughtfully, like the correct subordination chain of the distinct appendage elements and the correct placement of the models inside the coordinate system.

Any overlooked aspects in this defiant complex process might have impact on the entire kinematic analyses—and thus on the ethological as well as ecological implications of the animals' lifestyle.

### 3.5 Conclusions and perspectives: the future of virtual paleontology research

This thesis represents different approaches of how to apply virtual paleontology techniques to uncover the secrets of the morphology and kinematics in early Paleozoic marine euarthropods.

On one hand, the publications therein answered questions on morphological innovations as well as intraspecific variation and previously undetected additional appendicular structures of arthropodan and leancholiids arthropods.

On the other hand, it answered questions on the morpho-functionality of early Paleozoic sea scorpion appendages and ecological implications on their motion ability, as well as drew conclusions about the comparability to modern analogs.

Nevertheless, there are still things hidden in the slabs. More and more fossils of the Chengjiang biota are unearthed, adding new specimens to known species and groups, and allowing more reliable information on ontogeny and infraspecific variability in certain groups. Current studies on *Chuandianella*, *Isoxys*, *Jianfengia* as well as *Retifacies* are already on the line (Zhang C et al., preprint, 2021; Zhang M et al., submitted; Zhang X et al., under review, 22).

However, also the application of kinematic studies to Chengjiang arthropods is a challenging task for the future.

#### Perspectives in virtual paleontology research of Chengjiang euarthropods

The method Schmidt et al. (2021b), **Chapter IV**, introduced, was already applied to the endopodites of the crustacean-related euarthropod *Ercaicunia multinodosa*. This approach can be further developed when considering other aspects of Chengjiang euarthropod appendages, like the terminal parts of the

endopodites. In the last head appendage as well as in all trunk appendages of *Pygmaclypeatus daziensis*, those structures are developed as subchelate elements (Schmidt et al., in press, 2022, **Chapter I**). Kinematic studies may show whether they could have been used as pincers (thus being flexible), or if they were rigid and unarticulated, intimating that they could have been used as shovels rather, like in the publication proposed. Enrollment in trilobites was already illustrated (Esteve et al., 2017, 2018), so it might be also an approach to test the flexibility of the main body segments (head, trunk, pygidium) in several arthropodans.

Haug C & Haug J (2016) demonstrated possible exopodite motion in a naraoiid, showing that it might have been used for swimming. While this approach could also be extended to the other arthropodans treated in this thesis, like *Retifacies abnormalis* (Liu Y et al., 2021, Figs. 2c, 3c, Suppl. Fig. 9a, b, **Chapter III**), it might be worth also exploring the kinematics in the exopodites of the head appendages in *Sinoburius lunaris*. The studies on the ventral morphology of this species unveiled that the structures protruding beyond the head shield are not antennae, like once considered by Luo et al. (1997, p. 10), but indeed the elongate exopodites of the first two head appendages (see Chen X et al., 2019, Figs. 1c, d, 2; Schmidt et al., 2021a, Figs. 1a, 2c, **Chapter II**). Based on in Amira generated surface reconstructions of the body and the appendages, a kinematic marionette could be constructed in Maya (like exemplified in Schmidt et al., 2021b, **Chapter IV**), and the range of motion could be calculated. This could shed light on the flexibility of those appendages and encourages to consider the evolutionary significance of those uniquely enlarged exopodites (especially in combination with the reduced adjacent endopodites). Eventually, the surface reconstruction and kinematic deflection of the short great appendages in a broader sample of megacheirans may be challenging to model, given their length and their speculative way of folding (e.g., Haug et al., 2012).



Perspectives in virtual paleontology research of sea scorpion morpho-functionality

Appendage kinematics in eurypterids can also be expanded to the chelicerae.

Pterygotid eurypterids like *Acutiramus*, *Jaekelopterus* and *Pterygotus* bore elongate chelicerae, which were already up for morpho-functional discussion (Jaekel, 1914; Kjellesvig-Waering, 1964; Lamsdell & Legg, 2010; Laub, Tollerton & Berkof, 2010; McCoy et al., 2015; Selden, 1984; Waterston, 1964).

Those hypotheses could be transferred into revisable models via the application of Maya-based range of motion analyses. For this purpose, extant species of the harvestmen genus *Ischyropsalis* would function as suitable modern analogs (Martens, 1969; Novak, Gruber & Slana, 1995; Schmidt et al., in preparation, 2022). Among harvestmen, this genus is well known for its elongate chelicerae.

While in the modern analogs, those appendages consist of three elements (a basal part, as well as a mobile and a fixed finger), the composition of the chelicerae in extinct pterygotid sea scorpions was already up for debate, with some assuming four (Clarke and Ruedemann, 1912, p. 348; Kjellesvig-Waering, 1964, p. 335), while others counting only three elements (Laub, Tollerton & Berkof, 2010; Selden, 1984). However, a chelicera being comprised of only three elements would have had limited the total range of motion (that is, the entire motion capabilities in all joints) to a great extent—as in this case a so-called “elbow joint” would be missing (Laub, Tollerton & Berkof, 2010, p. 40). This paper approach is already under development (Schmidt et al., in preparation, 2022).

The mechanisms of walking in fossil arthropods, the trace fossils leading to those assumptions, as well as proposed gait patterns based on body fossil reconstructions were already discussed (Briggs, Rolfe & Brannan, 1979; Bruton, 1981; Hanken & Størmer, 1975; Hughes, 1975; Selden, 1981; Waterston, 1979; Whittington, 1975, 1980). However, those analyses considered the aquatic locomotion of

euarthropods. Lamsdell et al. (2020) uncovered air-breathing structures in a Carboniferous *Adelophthalmus* sea scorpion. This genus is known for inhabiting mainly freshwater environments but might have also ventured on land (Lamsdell et al., 2020; Selden, 1985). It might be fruitful to model this species' capabilities for land-walking locomotion, using its swimming legs to support itself against the ground while crawling above the ground. At least, those latest eurypterids (*Adelophthalmidae* Tollerton, 1989 was the only eurypterine sea scorpion group to survive till the mid-Permian) must have had morphological adaptations making their ephemeral excursion on land easier compared to phylogenetically older (and maybe obligate aquatic) eurypterid groups.

Besides the adelophthalmid sea scorpions, the only eurypterids to survive till the mid-Permian were the stylonurines (Lamsdell, Braddy & Tetlie, 2010). This group, which split probably in the Ordovician from the rest of the eurypterids (see Lamsdell et al., 2015, Fig. 22), is recognized by retaining all appendages as walking legs (thus, not having the appendage VI pair modified as swimming legs). It might be interesting to model locomotion possibilities in this group as well, giving that all appendages increase in size posteriorly in most groups.

Eventually, the modified appendages VI, the swimming legs in eurypterine eurypterids, shall be given focus in future research. Schmidt, Hazerli & Richter (2020) analyzed kinematics in the swimming legs of extant swimming crabs (*Portunidae* Rafinesque, 1815). Those make the perfect modern analogs to compare to eurypterid swimming leg kinematics (Plotnick, 1985; Selden, 1984; Tetlie & Cuggy, 2007).

Virtual paleontology. An innovative and integrative field of research, allowing a better understanding of the life of early Paleozoic arthropods, which thrived in the ancient seas.

And there is so much more to come...

# Supplemental

## 4. Methodological approaches

Several programs and methods in the field of virtual paleontology are used in this thesis. To unravel the morphology hidden in the slabs, the fossils were scanned with a micro-computer tomograph and transferred into TIFF stacks, which were then imported into either *Drishti* (Limaye) or *Amira* (Thermo Fischer Scientific). Both are programs for the scientific visualization of volumetric datasets, which translate the two-dimensional image information (e.g., TIFFs) into a three-dimensional volume. This then can be cropped, sliced, painted, and transferred into surface models.

The modern analog models in this thesis were surface reconstructed with *Mimics* (Materialise), which is also a commercial imaging software, working similar as *Amira*. For the reconstruction of all 3D models, the free and open-source 3D graphics software *Blender* was used. The commercial 3D visualization and animation software *Maya* (Autodesk) offers similar methods to generate 3D meshes like *Blender* (The Blender Foundation). However, this program was chosen to focus on the construction of kinematic marionettes and to perform range of motion analyses.

The following sections will give a detailed overview of each of the programs and the methodological approaches.

### 4.1 The arthropod machines: application of micro-computer tomographs for understanding the morphology of euarthropods

Computed tomography (CT) has long been used for the investigation of morphology and structures and is one of the most distributed methods to study suitable fossils when it comes to virtual paleontology (Cunningham et al., 2014; Garwood, Rahman & Sutton, 2010; Sutton, Rahman & Garwood, 2014; Yin & Lu, 2019).

Computer tomographs were first introduced in the 1970s (Hounsfield, 1973) for medical purposes, and were later also used in natural sciences. For instance, scientists performed CT scans to analyze hominid skulls, or the bones of the famous *Archaeopteryx* (Haubitz et al., 1988; Wind, 1984).

By the 1980s, smaller-scale applications were desired owing to the limitations on X-ray energy and imaging time. Elliott & Dover (1982) were the first to demonstrate this new micro-computed tomography (micro-CT,  $\mu$ CT) technique. Since then, it became more and more established and is now one of the most common methods for non-invasive studies on euarthropods. A micro-computer tomograph works with X-rays. This electromagnetic radiation reaches wavelengths about 0.01-10 nm. They are emitted by a source and captured by a detector. The desired object lies in between those two and is mounted on a holder rotatable up to 360°.

Back in 2015, this technique was first applied to fossil euarthropods from the famous early Cambrian (ca. 518-million-years old) Chengjiang biota from China (Liu Y, Scholtz & Hou, 2015).

In 2022, it is a standard procedure for the investigation of the morphology of fossils from this Lagerstätte.

## 4.2 The visualization of volumetric datasets and the reconstruction of surfaces

### *Drishti*

The visualization program *Drishti* (<https://github.com/nci/drishti>; Limaye, 2012) is the main software used to unveil the ventral morphology of early Cambrian Chengjiang euarthropods (Chen X et al., 2019a; Jin et al., 2021; Liu Y et al., 2016, 2020a, b, 2021, **Chapter III**; Liu Y, Scholtz & Hou, 2015; Schmidt et al., in press, 2022, **Chapter I**; Zhai et al., 2019a, b, c, preprint, 2021; Zhang M et al., submitted; Zhang X et al., under review).

This software was developed in 2012 by Dr Ajay Limaye as a tool easily accessible for exploring volumetric data. It comes with three distinct modules. *Drishti Import* allows transferring a wide range of formats (like TIFF stacks) into *.pvl.nc* files, a format *Drishti Render* reads. In *Drishti Import*, one can furthermore resample the volumes, adjust filters or enhance contrast.

The *Drishti Render* module is the main tool for working with volumes and offers a vast range of opportunities after uploading the *.pvl.nc* files and generating the volume. *Drishti Render* allows to crop the volume, adjust clipping planes, allows measurements, or enables one to perform the so-called MOP's (morphological operations) like directly painting the volume or carving.

*Drishti Paint* is the third module (Hu Y, Limaye & Lu, 2020). This separate program also reads *.pvl.nc* files, but in contrast to the *Drishti Render* module offers to paint on distinct TIFF slices, thus to do segmentation. Those segmented areas of the volume can be exported as meshes or *.pvl.nc* files to re-import to *Drishti Render* again.

### *Amira*

The visualization program *Amira* (<https://www.thermo-fisher.com/de/de/home/electron-microscopy/products/software-em-3d-vis/amira-software.html>; FEI Visualization Sciences Group, Zuse Institut, Berlin, Germany; Ruthensteiner, 2008; Stalling, Westerhoff & Hege, 2005) was first developed in the early 1990s and has recently also been used for analyzing euarthropods of the Chengjiang biota (Liu Y, Scholtz & Hou, 2015; Schmidt et al., 2021a,b, **Chapter II, VI**). This commercial software offers similar options of scientific visualization of volumetric data as *Drishti* but comes with distinct editors in only one program. Besides pure volume rendering, the biggest advantage of this program is the segmentation editor.

*Amira* offers distinct tools (e.g., brush, magic wand, lasso, etc.) to paint onto the 2D data slices and segment areas of interest. Segmentation can be carried out slice by slice or among several slices by using the interpolation function.

The brush tool enables the viewer to paint single voxels, the magic wand allows to select all voxels containing the same grey values inside a specific and pre-defined area, thus performing region growing. The lasso tool lets the viewer draw a line around certain fields of interest and to mark them by generating a closed contour curve.

Eventually, the so-called threshold function allows to select all voxels of the same priorly specified image intensity, thus a quick segmentation can be realized.

Segmented regions then can be transferred into surface models in the label editor. Surface reconstructions can be simplified by a reduction of the number of polygons; furthermore, the models can also be smoothed.

### Post-processing steps and data formats

Surface models can be exported as *.vrm*l files from *Amira*. Depending on their further use, they may require some post-processing steps. On one hand, the *.vrm*l files could be uploaded to the open-source triangle-mesh processing tool *MeshLab*

(<https://meshlab.sourceforge.net>) and from there exported as *.obj* or *.stl* files. Both data formats are suitable for further work in mesh-based 3D programs like *Blender* or *Maya*. Another way would be to upload the *.vrm*l files to *SAP 3D Visual Enterprise Author* (<https://developers.sap.com/trials-downloads.html?search=author>), and to use the tools *Collapse Hierarchy* (to get all separated elements of the surface model individually selectable) as well as *Unify Normals* (to close regions in the points of contact between two separated elements in the surface model). Hereafter, the modified surface model can be exported from *SAP 3D Visual Enterprise Author* as an *.obj* files as well.

We used the second option for the post-processing of our *Ercaicunia multinodosa* endopod models (Schmidt et al., 2021b, **Chapter IV**).

However, there is also a third possibility: importing the *.vrm*l files from *Amira* to *MeshLab*, simply exporting them as *.obj* files and importing those directly to *Blender*. Here, one can use the Edit Mode to choose the function *Separate* → *By Loose Parts* (pressing P), which separates the selected geometry and divides the mesh into its single objects (thus replacing the *Collapse Hierarchy* function in *SAP 3D Visual Enterprise Author*). Furthermore, the *Unify Normals* function can be replaced: if two meshes of the original imported surface model exhibit open areas after separation (which means that there are gaps in the mesh), one can simply close those gaps by selecting the edges surrounding the gap and pressing F. This generates a new face, thus closes this gap. The third possibility, which is an extension of the first, is the best option, as both, *MeshLab* and *Blender* are free and open source in contrast to the commercial software *SAP 3D Visual Enterprise Author*.

## 4.3 The building of 3D computer models and the construction of kinematic marionettes

### Blender

The freely available and open-source 3D computer graphics software *Blender* (<https://blender.org>; The Blender Foundation) is widely used in virtual paleontology (Bicknell et al., 2021; Garwood & Dunlop, 2014; Haug C et al., 2014; Haug J, Briggs & Haug C, 2012; Haug J et al., 2010, 2011, 2012; Haug C & Haug J, 2016; Haug J & Haug C, 2013; Liu Y et al., 2021, **Chapter III**; Schmidt, Melzer & Bicknell, 2021, **Chapter V**; Schmidt et al., 2021a, b, 2022, in press, 2022, **Chapter I, II, IV, VII**). Besides animation and the production of high-quality figures based on priorly generated  $\mu$ CT-data, especially the creation of meshes is a useful tool for paleontologists.

The authors started with a simple cube—a “mesh primitive”, with six faces. First, we applied a *Subdivision Surface modifier*, which turned the cube into a sphere resulting in 6144 faces. We then subdivided the mesh several times using the *Multiresolution modifier*. This resulted in a dense mesh with lots of voxels, which hereafter could be deformed in the *Sculpt Mode*, mainly using the *Grab*, *Elastic Deform* or *Snake Hook* brush. The mesh was flattened and smoothed (*Flatten* brush, *Smooth* brush). If it was too dense, that is, if the rendering velocity slowed down too much, voxel density was reduced using the *Decimate modifier*, the opposite of the *Multiresolution modifier*. If required, the model was remeshed, either using the *Remesh modifier* or the *Remesh* function in the Object Data Properties section.

This way, several elements of euarthropod appendages were built and assembled. The way of deforming a mesh in the *Sculpt Mode* by using several sculpting tools was favored—rather than changing its shape in the Edit Mode by editing length, size and number of faces, vertices, and edges. The reason behind this is that each

element of an appendage was desired to be a separate structure for further kinematic analyses – similar to a priorly generated,  $\mu$ CT-based surface model of an euarthropod appendage with segmented (thus selectable) elements.

After the design process, the meshes were exported as *.obj* files and imported into *Maya* for further kinematic approaches. If only high-quality figures were desired, the models were screenshotted in solid or material mode. If meshes for embedding in 3D-PDFs were required, the *.obj* files were imported to *Maya* and exported as *.stl* files.

### Maya

The 3D modeling program *Maya* (<https://www.autodesk.com/products/maya/>; Autodesk Inc., San Rafael, CA; Wood, 2014) is a commercial program like *Blender* and offers a vast range of tools to create and animate meshes. This software, in combination with the add-on X\_ROOM tools (X-ray reconstruction of moving morphology; <https://www.xroom.org/software/>; Brainerd et al., 2010) makes it possible to get flexible appendages out of the rigid 3D meshes made in *Blender*–or surface reconstructions of  $\mu$ CT-data-based models made in *Amira* (Schmidt et al., 2021b, **Chapter IV**; Schmidt, Hazerli & Richter, 2020) or *Mimics* (Bicknell, Melzer & Schmidt, 2021, **Chapter V**; Schmidt, Melzer & Bicknell, 2022, **Chapter VI**; Schmidt et al., 2022, **Chapter VII**).

*Maya* has been widely used for kinematic research on extant (Baier & Gatesy, 2013; Dawson et al., 2011; Kambic, Roberts & Gatesy, 2015; Krings et al., 2014; Nyakatura & Fischer, 2010) and extinct (Nyakatura et al., 2015, 2019) vertebrates and invertebrates (Clark et al., 2020).

However, the precise process of constructing a kinematic euarthropod marionette portrayed below (that is, equipping the euarthropod appendages with digital joints, so-called *srjoints*), was

yet exemplified by extant brachyuran crabs (Schmidt, Hazerli & Richter, 2020) and later also explained step-by-step applied to the early Cambrian Chengjiang euarthropod *Ercaicunia multinodosa* (Schmidt et al., 2021b, **Chapter IV**). This technique furthermore was performed for extant whip spider species (Schmidt, Melzer & Bicknell, 2022, **Chapter VI**) and Ordovician and Silurian sea scorpions (Bicknell, Melzer & Schmidt, 2021; Schmidt et al., 2022, **Chapter V, VII**). The main feature in this attempt is the use of the add-on X\_ROOM tools (Brainerd et al., 2010).

This allows generating so-called *srjoints* in terms of Scientific Rotoscoping (Gatesy et al., 2010). Those sphere-like objects function as artificial joints, which can be assigned to euarthropod appendage joints. After uploading the *.obj* files of either surface-generated models or 3D models built in *Blender*, hypothetical joint axes were constructed in the most basic mathematical representation as long and thin cylinders. All kinematically analyzed euarthropod appendages in this thesis were considered as having bicondylar joints, that is, joints with two articulation points (Boxshall, 2004, 2013). As the point of rotation occurs always in the center of a mesh, the size and radius of a joint axis cylinder were simply designed for graphical purposes. After fitting the joint axes cylinders to the articulation points in each euarthropod appendage joint, the *srjoints* (created by typing in the command `joint` in the MEL line in *Maya*) were assigned to those cylinders by the commands *point constrain* and *orient constrain*. *Point constrain* made the *srjoints* adopt the translation coordinates of the joint axes cylinders, while *orient constrain* led to the adoption of the rotation coordinates. Hereafter, the subordination process was conducted: each distal joint-*srjoint*-couple (that is, for example, the ultimate element + the penultimate element + the *srjoint* combining those two + the assigned joint axis cylinder fitting the articulation points) was subordinated to the adjacent proximal couple.

Ultimately, this led to a chain of subordinated joints, the so-called kinematic marionette, where all euarthropod appendage elements were subordinated to the proximal most element.

This was—depending on the purpose of the kinematic study—either the body-appendage-element 1-joint-axis cylinder, or element 1 itself.

A detailed step-by-step description of this subordination process is shown by Schmidt et al. (2021b, Figs. 1-3, **Chapter IV**).

#### 4.4 The study of euarthropod appendage kinematics and the application of range of motion analyses

##### Euarthropod kinematics

Euarthropod kinematic research has been conducted before. Esteve et al. (2017, 2018) analyzed trilobite enrollment using 3D models designed in *Blender*. Vagts et al. (2017) investigated beetle leg joints in terms of their kinematics. However, the method applied to the swimming legs of portunid crabs (Schmidt, Hazerli & Richter, 2020), the pedipalps of whip spiders (Schmidt, Melzer & Bicknell, 2022, Schmidt et al., 2022, **Chapter VI, VII**) and the prosomal appendages of sea scorpions (Bicknell, Melzer & Schmidt, 2021; Schmidt et al., 2022, **Chapter V, VII**) presents an advanced approach in the analyses of euarthropod appendage kinematics not conducted before. For all kinematic marionettes constructed in Maya, in the same program so-called range of motion analyses were performed.

##### Range of motion analyses

The term range of motion has no general and uniform definition. It is widely used to refer to the total scope of possible movements in a joint or of an entire appendage. In this regard, also the ways and options to analyze and quantify the range of motion differ between

studies. Schmidt, Hazerli & Richter (2020) introduced the terms total range of motion (*tROM*) and single range of motion (*sROM*).

Those were created to make a difference between the range of motion measured in a single joint (for example the body-coxa-joint in a whip spider pedipalp) and the range of motion given in the whole leg. While the *sROM* is simply to understand and calculate as the maximum excursion angle or the joint angle in a single joint, the *tROM* is harder to comprehend. There is no general common way of calculation, measurement, and performance. Schmidt, Hazerli & Richter (2020) introduced a way of creating a little ball and assigning it to the distal most part of the distal element. During the process of several permutations (where the number of permutations is defined by the degrees of freedom—in bicondylar euarthropod appendage joints always two—and the number of leg elements) the elements of the entire euarthropod appendage were deflected in a Cartesian Coordinate System. Each movement (= each permutation) thus could be represented by distinct x,y,z-translation coordinates of the attached ball at the tip of the distal euarthropod appendage element (compare Schmidt, Hazerli & Richter, 2020, section 2.4.4). Those coordinates could then be plotted for several axes, given that the model prior to the *tROM* analyses was placed with its proximal most joint axis cylinder in the origin of coordinates. This method of analyzing the *tROM* will be applied also to pterygotid eurypterid chelicerae (*Acutiramus* sp.) compared to elongate harvestmen chelicerae (*Ischyropsalis* sp., Schmidt et al., in preparation, 2022), and in a broader approach furthermore to elongate harvestmen pedipalps (*Obidosus* sp., Schmidt, Melzer & Bicknell, in preparation, 2022).

However, when not calculating both, *sROM* and *tROM*, studies performing this method simply referred to range of motion for the broad description of deflecting euarthropod appendage elements, or joint angles.

In Bicknell, Melzer & Schmidt (2021, **Chapter V**) joint angles were calculated for the horse-shoe crab *Limulus polyphemus* walking and pushing leg, as well as for the prosomal appendages of the eurypterids *Eurypterus tetragonophthalmus* (prosomal appendage IV) and *Pentecopterus decoharensis* (prosomal appendages III and V).

Schmidt, Melzer & Bicknell (2022, **Chapter VI**) conducted joint angle analyses (= sROM) for the pedipalps of the two whip spider species *Damon medius* and *Heterophrynus elaphus*.

Eventually, Schmidt et al. (2022, **Chapter VII**) extended this approach to the analyses of the ferocious frontal most appendages of the two eurypterid species *Megalograptus ohioensis* and *Mixopterus kiaeri* (prosomal appendages II and III).

All three publications are included in this thesis and used the same process of measuring joint angles.

#### Measurement of joint angles

The most detailed description of how to perform joint angle measurements in euarthropod appendages is summarized in Schmidt, Hazerli & Richter (2020, section 2.4.2, Fig. 4).

The basis of the method is to separate the kinematic marionette into all the distinct joints it is composed of. Each joint (consisting of the proximal appendage element + the distal appendage element + the joint axis cylinder) was then saved as an individual *Maya* file (.mel). The kinematic chain in this joint was deleted, and the new subordination order was constructed: the distal element subordinated to the proximal

element, and the proximal element ultimately subordinated to the joint axis cylinder.

Hereafter, the entire model was placed with the joint axis cylinder inside the origin of coordinates in the vertical axis (in *Maya*, by default the vertical axis is y, but could be changed to z as well, if desired). Now, the kinematic chain was deleted again. Eventually, rotating the distal appendage element alongside the vertical axis led to a change only in one of the values (in *Maya*, by default the y-values), which was the resulting joint angle.

As no clash detection is implemented in *Maya*, the maximum joint angle (or maximum excursion angle, maximum range of motion, etc.) was given at the point of contact of the proximal and the distal element, done by eyeballing.

In summary, placing a single joint in a new Cartesian Coordinate System in the origin of coordinates with the joint axis cylinder inside the vertical axis, is the easiest way to measure the maximum angle an appendage element can have when rotating inside its joint.

## 4.5 Terminology

Different authors use different terms to sometimes describe the same morphological structure. For a broader understanding, and to avoid unfortunate coincidence with some words of the malacostracan (“Crustacea”) terminology, the term “*element*” is used throughout the main text body in this thesis (Introduction, Discussion, etc.) to refer to structures in general regarded as *articles* or *podomeres*, that is, single units an euarthropod appendage is composed of.

The supplementary table summarizes all further specific terms used in this thesis.



**Supplementary Table.** Terminology and explanation used in the publications included in this thesis.

Terminology	Explanation
<b>abduction</b>	movement away from the midline of the body
<b>adduction</b>	movement towards the midline of the body
<b>antennulae</b>	anterior most appendages, usually uniramous, deutocerebrally innervated
<b>appendage</b>	leg, in euarthropods made up of several elements
<b>article</b>	the individual unit an euarthropod appendage is made up, see element, podomere
<b>articulation point</b>	point at which the condyle of an element fits into the glenoid cavity of the adjacent element
<b>basipodite</b>	proximal most part of an appendage, giving rise to endopodite and exopodite
<b>bicondylar</b>	a joint made up of two articulation points, thus limiting movement of the adjacent element in just one plane
<b>coxa</b>	first element of an euarthropod appendage in some groups
<b>coxal process</b>	in eurypterids: elongated plate at the outer, anterior margin on the dorsal side of the coxa
<b>condyle</b>	cuticular protuberance fitting a corresponding socket
<b>depression</b>	movement in an inferior direction
<b>durophagous</b>	feeding mode on hard structures
<b>element</b>	the individual unit an euarthropod appendage is made up, see also article, podomere
<b>elevation</b>	movement in a superior direction
<b>endopodite</b>	inner branch of a biramous appendage, arising from the basipodite
<b>endite</b>	an additional, "inner" outgrowth of the basipodite (besides endo- and exopodite)
<b>exite</b>	an additional, "outer" outgrowth of the basipodite (besides endo- and exopodite)
<b>exopodite</b>	outer branch of a biramous appendage, arising from the basipodite
<b>glenoid cavity</b>	the cavity opposing a condyle
<b>femur</b>	here: the third element in Amblypygi pedipalps
<b>gnathobases</b>	structures, often at the protopodite, aiding in food manipulation
<b>head</b>	segments dorsally forming a shield, possibly a synsclerite formed by the segments of the anterior most tagma
<b>hypostome</b>	a sclerotized plate covering the mouth opening
<b>joint</b>	the flexible construction linking two adjacent elements
<b>joint angle</b>	the maximum angle an element can describe rotating inside its joint alongside its joint axis, see range of motion
<b>joint axis</b>	a hypothetical construction combining two articulation points of two adjacent elements
<b>kinematic</b>	a description of the motion of objects without considering the forces which cause them to move
<b>leg</b>	appendage, in euarthropods made up of several elements
<b>mesh</b>	an object in 3D software made up of polygons
<b>mesosoma</b>	in most Eurypterida: part of the body following the prosoma, comprises in general body segments 1-6
<b>metasoma</b>	in most Eurypterida: part of the body following the mesosoma, comprises in general body segments 7-12
<b>metastoma</b>	in most Eurypterida: ventral single plate, surrounded by the coxae of appendage VI
<b>monocondylar</b>	joint with one articulation point

<b>multi-articulated</b>	appendages consisting of several elements
<b>patella</b>	here: the fourth element in Amblypygi pedipalps
<b>podomere</b>	the individual unit an euarthropod appendage is made up, see article, element
<b>prosoma</b>	in euchelicerates: the appendage bearing anterior most body part
<b>protopodite</b>	proximal most element of an appendage
<b>pygidium</b>	posterior tagma of the trunk, recognizable by a distinct large syntergite continuous with the telson
<b>range of motion</b>	ROM, the maximum angle an element can describe rotating inside its joint alongside its joint axis, see joint angle
<b>tarsus</b>	here: the ultimate element in Amblypygi pedipalps
<b>tergite</b>	sclerotized plate on the dorsal side of the animal
<b>terminal claw</b>	the ultimate element of an euarthropod appendage in the considered species
<b>tibia</b>	here: the fifth element in Amblypygi pedipalps
<b>trochanter</b>	here: the second element in Amblypygi pedipalps
<b>trunk</b>	body region posterior to the head
<b>SGAs</b>	short great appendages, the multi-articulated frontal most appendages of megacheirans
<b>spines</b>	Thick, cuticular outgrowths we refer to as immovable
<b>srjoint</b>	artificial joint in Maya, allowing to take over the translation and rotation coordinates of an assigned object

## References

- Allwood, A. C., Walter, M. R., Kamber, B. S., Marshall, C. P., & Burch, I. W. (2006). Stromatolite reef from the Early Archaean era of Australia. *Nature*, *441*, 714–718.
- Anderson, R. P., McCoy, V. E., McNamara, M. E., & Briggs, D. E. G. (2014). What big eyes you have: the ecological role of giant pterygotid eurypterids. *Biology Letters*, *10*, 20140412.
- Andrews, H. E., Brower, J. C., Gould, S. J., & Reyment, R. A. (1974). Growth and variation in *Eurypterus remipes* DeKay. *Bulletin of the Geological Institution of the University of Uppsala*, *4*, 81–114.
- Aria, C. (2020). Macroevolutionary patterns of body plan canalization in euarthropods. *Paleobiology*, *46*, 569–593.
- Aria, C. (preprint, 2021). The origin and early evolution of arthropods. <https://doi.org/10.31233/osf.io/4zmey>
- Aria, C., Zhao, F., Zeng, H., Guo, J., & Zhu, M. (2020). Fossils from South China redefine the ancestral euarthropod body plan. *BMC Ecology and Evolution*, *20*, 4.
- Aria, C., Zhao, F., & Zhu, M. (2021). Fuxianhuids are mandibulates and share affinities with total-group Myriapoda. *Journal of the Geological Society*, *178*, jgs2020–246.
- Babcock, L. E. (2003). Trilobites in Paleozoic predator-prey systems, and their role in reorganization of early Paleozoic ecosystems. In: Kelley, P.A., Kowalewski, M., & Hansen, T.A. (eds.), *Predator-Prey Interactions in the Fossil Record*. Kluwer Academic/Plenum Publishers, New York, 55–92.
- Babcock, L. E. (2005). Interpretation of biological and environmental changes across the Neoproterozoic–Cambrian boundary: developing a refined understanding of the radiation and preservational record of early multicellular organisms. *Palaeogeography, Palaeoclimatology, Palaeoecology*, *220*, 1–226.
- Babcock, L. E., Zhang, W., & Leslie, S. A. (2001). The Chengjiang biota: record of the early Cambrian diversification of life and clues to exceptional preservation of fossils. *GSA Today*, *11*, 4–9.
- Baier, D. B., & Gatesy, S. M. (2013). Three-dimensional skeletal kinematics of the shoulder girdle and forelimb in walking alligator. *Journal of Anatomy*, *223*, 462–473.
- Barskov, I. S., Boiko, M. S., Konovalova, V. A., Leonova, T. B., Nikolaeva, S. V. (2008). Cephalopods in the marine ecosystems of the Paleozoic. *Paleontological Journal*, *42*, 1167.
- Bassett, M. (1985). Towards a “common language” in stratigraphy. *Episodes*, *8*, 87–92.
- Beasecker, J., Chamberlin, Z., Lane, N., Reynolds, K., Stack, J., Wahrer, K., Wolff, A., Devilbiss, J., Wahr, C., Durbin, D., Garneau, H., & Brandt, D. (2020). It’s Time to Defuse the Cambrian “Explosion”. *GSA Today*, *30*, 26–27.
- Bergström, J., & Hou X.-G. (1998). Chengjiang arthropods and their bearing on early arthropod evolution. In: Edgecombe, G.D. (ed.), *Arthropod Fossils and Phylogeny*. Columbia University Press, New York, 151–184.
- Bergström, J., & Hou, X.-G. (2005). Early Palaeozoic non-lamellipedian arthropods. In: Koenemann, S., & Jenner, J. A. (eds.), *Crustacea and Arthropod Relationships, Crustacean Issues*, *16*. Taylor & Francis, Boca Raton, 73–93.
- Bergström, J., Hou, X.-G., & Hålenius, U. (2007). Gut contents and feeding in the Cambrian arthropod *Naraoia*. *GFF*, *129*, 71–76.
- Berner, R. A. (2006). GEOCARBSULF: A combined model for Phanerozoic Atmospheric Oxygen and Carbon Dioxide. *Geochimica et Cosmochimica Acta*, *70*, 5653–5664.
- Bicknell, R. D. C., Holmes, J., Edgecombe, G. D., Losso, S., Ortega-Hernández, J., Wroe, S., & Paterson, J. (2021). Biomechanical analyses of Cambrian euarthropod limbs reveal their effectiveness in mastication and durophagy. *Proceedings of the Royal Society, B: Biological Sciences*, *288*, 20202075.
- Bicknell, R. D. C., Ledogar, J., Wroe, S., Gutzler, B., Watson, W., & Paterson, J. (2018a). Computational biomechanical analyses demonstrate similar shell-crushing abilities in modern and ancient arthropods. *Proceedings of the Royal Society, B: Biological Sciences*, *285*, 20181935.
- Bicknell, R. D. C., Melzer, R. R., & Schmidt, M. (2021). Three-dimensional kinematics of euchelicerate limbs uncover functional specialization in eurypterid appendages. *Biological Journal of the Linnean Society*, *135*, 174–183.

- Bicknell, R. D. C., Paterson, J. R., Caron, J. B., & Skovsted, C. B. (2018b).** The gnathobasic spine microstructure of recent and Silurian chelicerates and the Cambrian arthropodan *Sidneyia*: Functional and evolutionary implications. *Arthropod Structure & Development*, *47*, 12–24.
- Bicknell, R. D. C., Smith, P. M., & Poschmann, M. (2020).** Re-evaluating evidence of Australian eurypterids. *Gondwana Research*, *86*, 164–181.
- Bitsch, C., & Bitsch, J. (2004).** Phylogenetic relationships of basal hexapods among the mandibulate arthropods: a cladistic analysis based on comparative morphological characters. *Zoologica Scripta*, *33*, 511–550.
- Blaker, M. R., & Peel, J. S. (1997).** Lower Cambrian trilobites from North Greenland. *Meddelelser om Grønland Geoscience*, *35*, 1–145.
- Blanchard, E. (1852).** *Arachnides. L'organisation du Règne Animal, seconde édition, volume 2*, Paris. 232 pp.
- Bobrovskiy, I., Hope, J. M., Ivantsov, A., Nettersheim, B. J., Hallmann, C., & Brocks, J. J. (2018).** Ancient steroids establish the Ediacaran fossil *Dickinsonia* as one of the earliest animals. *Science*, *361*, 1246–1249.
- Bond, G. C., Nickeson, P. A., & Kominz, M. A. (1984).** Breakup of a supercontinent between 625 Ma and 555 Ma: new evidence and implications for continental histories. *Earth and Planetary Science Letters*, *70*, 325–345.
- Borradaile, L. A. (1926).** Notes upon crustacean limbs. *Annals and Magazine of Natural History, Series 9*, *17*, 193–213.
- Bottjer, D. J., Hagadorn, J. W., & Dornbos, S. Q. (2000).** The Cambrian substrate revolution. *GSA Today*, *10*, 1–7.
- Boudreaux, H. B. (1979).** *Arthropod Phylogeny—with Special Reference to Insects*. John Wiley & Sons, New York, 320 pp.
- Boxshall, G. A. (2004).** The evolution of arthropod limbs. *Biological Reviews*, *79*, 253–300.
- Boxshall, G. A. (2013).** Arthropod limbs and their development. In: Minelli, A., Boxshall, G., & Fusco, G. (eds.) *Arthropod biology and evolution*. Springer, Berlin, 241–267.
- Braddy, S. J., & Dunlop, J. A. (1997).** The functional morphology of mating in the Silurian eurypterid, *Baltoeurypterus tetragonophthalmus* (Fischer, 1839). *Zoological Journal of the Linnean Society*, *120*, 435–461.
- Braddy, S. J., Poschmann, M. & Tetlie, O. E. (2008).** Giant claw reveals the largest ever arthropod. *Biology Letters*, *4*, 106–109.
- Brainerd, E. L., Baier, D. B., Gatesy, S. M., Hedrick T. L., Metzger, K. A., Gilbert, S. L., & Crisco, J. J. (2010).** X-ray reconstruction of moving morphology (XROMM): Applications and accuracy in comparative biomechanics research. *Journal of Experimental Zoology*, *313A*, 1–18.
- Brandt, D. S., & McCoy, V. E. (2014).** Modern analogs for the study of eurypterid paleobiology. In: Hembree, D. I., Platt, B. F., & Smith, J. J. (eds.), *Experimental approaches to understanding fossil organisms*. Dordrecht, Springer, 73–88.
- Brenchley, P. J., & Newall, G. (1984).** Late Ordovician environmental changes and their effect on faunas. 65–79. In: Bruton, D. L. (ed.), *Aspects of the Ordovician system*. Palaeontological Contributions from the University of Oslo, Universitets forlaget, Oslo, 295 pp.
- Briggs, D. E. G., Bottrell, S. H., & Raiswell, R. (1991).** Pyritization of soft-bodied fossils: Beecher's Trilobite Bed, Upper Ordovician, New York State. *Geology*, *19*, 1221–1224.
- Briggs, D. E. G., Dalingwater, J. E., & Selden, P. A. (1991).** Biomechanics of locomotion in fossil arthropods. In: Rayner, J. M. V., & Wootton, R. J. (eds.), *Biomechanics in evolution*. Cambridge University Press, Cambridge, 37–56.
- Briggs, D. E. G., Erwin, D. H., & Collier, F. J. (1994).** *The Fossils of the Burgess Shale*. Smithsonian Institution Press, Washington D. C., 238 pp.
- Briggs, D. E. G., Rolfe, W. D., & Brannan, J. (1979).** A giant myriapod trail from the Namurian of Arran, Scotland. *Palaeontology*, *22*, 273–291.
- Briggs, D. E. G., Siveter, D. J., Sutton, M. D., Garwood, R. J., & Legg, D. (2012).** Silurian horseshoe crab illuminates the evolution of arthropod limbs. *PNAS*, *109*, 15702–15705.

- Brocks, J., Jarrett, A., Sirantoine, E., Hallmann, C., Hoshino, Y., & Liyanage, T. (2017). The rise of algae in Cryogenian oceans and the emergence of animals. *Nature*, *548*, 578–581.
- Bruce, H. S. (preprint, 2021). How to align arthropod leg segments. *bioRxiv*, <https://doi.org/10.1101/2021.01.20.427514>
- Bruce, H. S., & Patel, N. H. (2020). Knockout of crustacean leg patterning genes suggests that insect wings and body walls evolved from ancient leg segments. *Nature Ecology and Evolution*, *4*, 1703–1712.
- Bruton, D. L. (1981). The arthropod *Sidneyia inexpectans*, Middle Cambrian, Burgess Shale, British Columbia. *Philosophical Transactions of the Royal Society of London*, *295*, 619–656.
- Budd, G. E. (2002). A palaeontological solution to the arthropod head problem. *Nature*, *417*, 271–275.
- Budd, G. E. (2008). The earliest fossil record of the animals and its significance. *Philosophical Transactions of the Royal Society, B: Biological Sciences*, *363*, 1425–1434.
- Burmeister, H. (1843). Die Organisation der Trilobiten, aus ihren lebenden Verwandten entwickelt; nebst einer systematischen Uebersicht aller zeither beschriebenen Arten. xii + 147 S, VI Tafeln. G. Reimer. Berlin.
- Butterfield, N. J. (1990). Organic preservation of non-mineralizing organisms and the taphonomy of the Burgess Shale. *Paleobiology*, *16*, 272–286.
- Butterfield, N. J. (2003). Exceptional fossil preservation and the Cambrian explosion. *Integrative and Comparative Biology*, *43*, 166–177.
- Butterfield, N. J., Balthasar, U., & Wilson, L. A. (2007). Fossil diagenesis in the Burgess Shale. *Palaeontology*, *50*, 537–543.
- Caron, J.-B., & Jackson, D. A. (2008). Paleocology of the Greater Phyllopod Bed community, Burgess Shale. *Palaeogeography, Palaeoclimatology, Palaeoecology*, *258*, 222–256.
- Caster, K. E., & Kjellesvig-Waering, E. N. (1955). Untitled contribution. p. P36 in Størmer, L. Chelicerata. Treatise on Invertebrate Paleontology. Geological Society of America and University of Kansas Press, Lawrence, Kansas, U.S.A.
- Caster, K. E., & Kjellesvig-Waering, E. N. (1964). Upper Ordovician eurypterids of Ohio. *Palaeontographica Americana*, *4*, 297–358.
- Chen, J. (2009). The sudden appearance of diverse animal body plans during the Cambrian explosion. *The International Journal of Developmental Biology*, *53*, 733–751.
- Chen, J., Edgecombe, G. D., & Ramsköld, L. (1997). Morphological and ecological disparity in naraoiids (Arthropoda) from the Early Cambrian Chengjiang Fauna, China. *Records of the Australian Museum*, *49*, 1–24.
- Chen, J., Hou, X.-G., & Lu, H. (1989). Early Cambrian netted scale-bearing worm-like sea animal. *Acta Palaeontologica Sinica*, *28*, 1–16, [in Chinese, with English summary].
- Chen, J., Waloszek, D., & Maas, A. (2004). A new ‘great-appendage’ arthropod from the Lower Cambrian of China and homology of chelicerate chelicerae and raptorial antero-ventral appendages. *Lethaia*, *37*, 3–20.
- Chen, J., Zhou, G., Zhu, M., & Yeh, K. (1996). *The Chengjiang biota. A unique window of the Cambrian explosion*. National Museum of Natural Science, Taichung, Taiwan, 222 pp. [in Chinese].
- Chen, X., Ortega-Hernández, J., Wolfe, J. M., Zhai, D., Hou, X.-G., Chen, A., Mai, H., & Liu, Y. (2019a). The appendicular morphology of *Sinoburius lunaris* and the evolution of the artiopodan clade Xandarelida (Euarthropoda, early Cambrian) from South China. *BMC Evolutionary Biology*, *19*, 165.
- Chen, J., & Zhou, G. (1997). Biology of the Chengjiang fauna. *Bulletin of the National Museum of Natural Science*, *10*, 11–106.
- Chen, L., Luo, H., Hu, S., Yin, J., Jiang, Z., Wu, Z., Li, F., & Chen, A. (2002). Early Cambrian Chengjiang fauna in eastern Yunnan, China. Yunnan Science and Technology Press, Kunming, China [in Chinese].
- Chen, Z., Zhou, C., Yuan, X., & Xiao, S. (2019b). Death march of a segmented and trilobate bilaterian elucidates early animal evolution. *Nature*, *573*, 412–415.
- Clark, E. G., Hutchinson, J. R., Bishop, P. J., & Briggs, D. E. G. (2020). Arm waving in stylophoran echinoderms: Three-dimensional mobility analysis illuminates cornute locomotion. *Royal Society Open Science*, *7*, 200191.
- Clarke, J. N., & Ruedemann, R. (1912). *The Eurypterida of New York*. New York State Museum, Memoir, 14, New York, 439 pp.

- Cocks, L. R. M., & Torsvik, T. (2013). The dynamic evolution of the Palaeozoic geography of eastern Asia. *Earth Science Reviews*, 117, 40–79.
- Cotton, T. J., & Braddy, S. J. (2003). The phylogeny of arachnomorph arthropods and the origin of the chelicerata. *Transactions of the Royal Society of Edinburgh: Earth Sciences*, 94, 169–193.
- Cunningham, J. A., Rahman, I. A., Lautenschlager, S., Rayfield, E. J., & Donoghue, P. C. J. (2014). A virtual world of paleontology. *Trends Ecology and Evolution*, 29, 347–357.
- Dalingwater, J. E. (1975). Further observations on eurypterid cuticles. *Fossils and Strata*, 4, 271–279.
- Dalingwater, J. E. (1985). Biomechanical approaches to eurypterid cuticles and chelicerate exoskeletons. *Transactions of the Royal Society of Edinburgh: Earth Sciences*, 76, 359–364.
- Dawson, M. M., Metzger, K. A., Baier, D. B., & Brainerd, E. L. (2011). Kinematics of the quadrate bone during feeding in Mallard ducks. *Journal of Experimental Biology*, 214, 2036–2046.
- Daley, A., Antcliffe, J., Drage, H., & Pates, S. (2018). Early fossil record of Euarthropoda and the Cambrian Explosion. *PNAS*, 115, 5323–5331.
- Daley, A., & Edgecombe, G. D. (2014). Morphology of *Anomalocaris canadensis* from the Burgess Shale. *Journal of Paleontology*, 88, 68–91.
- Davies, N. S., Garwood, R. J., McMahon, W. J., Schneider, J. W., & Shillito, A. P. (2021). The largest arthropod in Earth history: insights from newly discovered Arthropleura remains (Serpukhovian Stainmore Formation, Northumberland, England). *Journal of the Geological Society*, gs2021-115.
- De Kay, E. (1825). Observations on a fossil crustacean animal of the Order Branchiopoda. *Annals of the Lyceum of Natural History New-York*, 1, 375–377.
- De Vivo, G., Lautenschlager, S., & Vinther, J. (2021). Three-dimensional modelling, disparity and ecology of the first Cambrian apex predators. *Proceedings of the Royal Society, B: Biological Sciences*, 288, 1955.
- Diener, C. (1924). Eurypterida. In Diener, C. (ed.), *Fossilium Catalogus I: Animalia*, 25. W. Junk, Berlin, 1–26.
- Dohle, W. (2001). Are the insects terrestrial crustaceans? A discussion of some new facts and arguments and the proposal of the proper name ‘Tetraconata’ for the monophyletic unit Crustacea + Hexapoda. In: Deuve, T. (ed.), *Origin of the Hexapoda*. Annales De La Societe Entomologique De France (N.S.), 37, 85–103.
- Duan, Y., Han, J., Fu, D.; Zhang, X., Yang, X., Komiya, T., & Shu, D. (2014). Reproductive strategy of the bradoriid arthropod *Kunmingella douvillei* from the Lower Cambrian Chengjiang Lagerstätte, South China. *Gondwana Research*, 25, 983–990.
- Dunlop, J. A. (2006). New ideas about the euchelicerate stemlineage. *Acta Zoologica Bulgaria* (Supplement 1), 9–23.
- Dunn, F., Liu, A., Grazhdankin, D., Vixseboxse, P., Flannery, J. F., Green, E., Harris, S., Wilby, P., & Donoghue, P. (2021). The developmental biology of *Charnia* and the eumetazoan affinity of the Ediacaran rangeomorphs. *Science Advances*, 7, 1–30.
- Dunlop, J. A., Penney, D. & Jekel, D. (2020). A summary list of fossil spiders and their relatives. In: World Spider Catalog, Natural History Museum Bern, <https://wsc.nmbe.ch> version 20.5
- Dunlop, J. A., Penney, D., Tetlie, O. E., & Anderson, L. I. (2008). How many species of fossil arachnids are there? *Journal of Arachnology*, 36, 267–272.
- Dunlop, J. A., & Selden, P. A. (1998). The early history and phylogeny of the chelicerates. In: Fortey, R. A., & Thomas, R. H. (eds.), *Arthropod Relationships*, Systematics Association Special Volume, Series 55. Chapman & Hall, London, 221–235.
- Edgecombe, G. D., & Legg, D. A. (2014). Origins and early evolution of arthropods. *Palaeontology*, 57, 457–468.
- Edgecombe, G. D., & Ramsköld, L. (1999). Relationships of Cambrian Arachnata and the systematic position of Trilobita. *Journal of Paleontology*, 73, 263–287.
- Elliott, J.C., & Dover, S. D. (1982). X-ray microtomography. *Journal of Microscopy*, 126, 211–213.
- Ellis, C. H. (1944). The mechanism of extension in the legs of spiders. *Biological Bulletin*, 86, 41–50.
- Erwin, D. H., & Valentine, J. W. (2013). *The Cambrian explosion: The Construction of Animal Biodiversity*. Roberts & Company, Greenwood Village, Colorado, USA, 416 pp.
- Esteve, J., Gutiérrez-Marco, J. C., Rubio, P., & Rábano, I. (2018). Evolution of trilobite enrolment during the Great Ordovician Biodiversification Event: insights from kinematic modelling. *Lethaia*, 51, 207–217.

- Esteve, J., Rubio, P., Zamora, S., & Rahman, I. A. (2017). Modelling enrolment in Cambrian trilobites. *Palaeontology*, *60*, 423–432.
- Evans, S. D., Hughes, I. V., Gehling, J. G., & Droser, M. L. (2020). Discovery of the Oldest Bilaterian from the Ediacaran of South Australia. *PNAS*, *117*, 7845–7850.
- Falkingham, P. L., & Gatesy, S. M. (2014). The birth of a dinosaur footprint: subsurface 3D motion reconstruction and discrete element simulation reveal track ontogeny. *PNAS*, *111*, 18279–18284.
- Fahrbach, S. E. (2004). What arthropod brains say about arthropod phylogeny. *PNAS*, *101*, 3723–3724.
- Fanenbruck, M., Harzsch, S., & Wägele, J. W. (2004). The brain of the Remipedia (Crustacea) and an alternative hypothesis on their phylogenetic relationships. *PNAS*, *101*, 3868–3873.
- Fischer de Waldheim, G. (1839). Notes sur un crustacé fossile du genre Eurypterus de Podolie. *Bulletin de la Societe Imperiale des Naturalistes de Moscou*, *11*, 125–128.
- Foelix, R. (2010). *Biology of spiders*. Oxford University Press, New York, 432 pp.
- Friedrich, M., & Tautz, D. (1995). Ribosomal DNA phylogeny of the major extant arthropod classes and the evolution of myriapods. *Nature*, *376*, 165–167.
- Fu, D., Tong, G., Dai, T., Liu, W., Yang, Y., Zhang, Y., Cui, L., Li, L., Yun, H., Wu, Y., Sun, A., Liu, C., Pei, W., Gaines, R., & Zhang, X. (2019). The Qingjiang biota—A Burgess Shale-type fossil Lagerstätte from the early Cambrian of South China. *Science*, *363*, 1338–1342.
- Fu, D., Zhang, X., Budd, G. E., Liu, W., & Pan, X. (2014). Ontogeny and dimorphism of *Isoxys auritus* (Arthropoda) from the Early Cambrian Chengjiang biota, South China. *Gondwana Research*, *25*, 975–982.
- Gabbott, S. E., Hou, X.-G., Norry, M., & Siveter, D. J. (2004). Preservation of early Cambrian animals of the Chengjiang biota. *Geology*, *32*, 901–904.
- Gaines, R. R. (2014). Burgess Shale-type preservation and its distribution in space and time. In: Laflamme, M., Schiffbauer, J. D., & Darroch, S. (eds), *Reading and Writing of the Fossil Record: Preservational Pathways to Exceptional Fossilization*. The Paleontological Society Papers, *20*, 123–146.
- Gaines, R. R., Briggs, D. E. G., & Zhao Y. (2008). Cambrian Burgess Shale-type deposits share a common mode of fossilization. *Geology*, *36*, 755–758.
- Gaines, R. R., Hammarlund, E. U., Hou, X.-G., Qi, C., Gabbott, S. E., Zhao, Y., Peng, J., & Canfield, D. E. (2012). Mechanism for Burgess Shale-type preservation. *PNAS*, *109*, 5180–5184.
- García-Bellido, D. C., & Collins, D. (2007). Reassessment of the genus *Leancoilia* (Arthropoda, Arachnomorpha) from the Middle Cambrian Burgess Shale, British Columbia, Canada. *Palaeontology*, *50*, 693–709.
- Garwood, R. J., & Dunlop, J. A. (2014). The walking dead: Blender as a tool for paleontologists with a case study on extinct arachnids. *Journal of Paleontology*, *88*, 735–746.
- Garwood, R. J., Rahman, I. A., & Sutton, M. D. (2010). From clergymen to computers—the advent of virtual palaeontology. *Geology Today*, *26*, 96–100.
- Gatesy, S. M., Baier, D. B., Jenkins, F. A., & Dial, K. P. (2010). Scientific rotoscoping: A morphology-based method of 3-D motion analysis and visualization. *Journal of Experimental Zoology*, *313A*, 244–261.
- Gehling, J. G., Jago, J. B., Paterson, J. R., García-Bellido, D. C., & Edgecombe, G. D. (2011). The geological context of the Lower Cambrian (Series 2) Emu Bay Shale Lagerstätte and adjacent stratigraphic units, Kangaroo Island, South Australia. *Australian Journal of Earth Science*, *58*, 243–257.
- Gibson, B., Rahman, I. A., Maloney, K., Racicot, R., Mocke, H., Laflamme, M., & Darroch, S. (2019). Gregarious suspension feeding in a modular Ediacaran organism. *Science Advances*, *5*, eaaw0260.
- Gill, B. C., Lyons, T. W., Young, S. A., Kump, L. R., Knoll, A. H., & Saltzman, M. R. (2011). Geochemical evidence for widespread euxinia in the Later Cambrian ocean. *Nature*, *469*, 80–83.
- Giribet, G., Edgecombe, G. D., & Wheeler, W. C. (2001). Arthropod phylogeny based on eight molecular loci and morphology. *Nature*, *413*, 157–161.
- Gould, S. J. (1989). *Wonderful Life: The Burgess Shale and the Nature of History*. W. W. Norton & Company, New York, 352 pp.
- Hallam, A., & Wignall, P. B. (1997). Mass extinctions and their aftermath. Oxford University Press, New York, 320 pp.
- Hanken, N.-M., & Størmer, L. (1975). The trail of a large Silurian eurypterid. *Fossils and Strata*, *4*, 255–270.
- Hansen, H. J. (1925). *Studies on Arthropoda II. On the comparative morphology of the appendages in the Arthropoda. A. Crustacea*. Gyldendalske Boghandel, Copenhagen, Denmark, 158 pp.

- Haq, B. U., & Schutter, S. R. (2008).** A chronology of Paleozoic sealevel changes. *Science*, 322, 64–68.
- Harper, D. A. T., Hammerlund, E. U., & Rasmussen, C. M. Ø. (2014).** End Ordovician extinctions: a coincidence of causes. *Gondwana Research*, 25, 1294–1307.
- Haubitz, B., Prokop, M., Doehring, W., Ostrom, J. H., & Wellnhofer, P. (1988).** Computed tomography of *Archaeopteryx*. *Palaeobiology*, 14, 206–213.
- Haug, C. (2020).** The evolution of feeding within Eichelicerata: data from the fossil groups Eurypterida and Trigonotarbitida illustrate possible evolutionary pathways. *PeerJ*, 8, e9696.
- Haug, C., Briggs, D. E. G., Mikulic, D. G., Kluessendorf, J., & Haug, J. T. (2014).** The implications of a Silurian and other thylacocephalan crustaceans for the functional morphology and systematic affinities of the group. *BMC Evolutionary Biology*, 14, 159.
- Haug, C., & Haug, J. T. (2016).** New insights into the appendage morphology of the Cambrian trilobite-like arthropod *Naraoia compacta*. *Bulletin of Geosciences*, 91, 221–227.
- Haug, J. T., Briggs, D. E. G., & Haug, C. (2012).** Morphology and function in the Cambrian Burgess Shale megacheiran arthropod *Leanchoilia superlata* and the application of a descriptive matrix. *BMC Evolutionary Biology*, 12, 162.
- Haug, J. T., & Haug, C. (2013).** An unusual fossil larva, the ontogeny of achelatan lobsters, and the evolution of metamorphosis. *Bulletin of Geosciences*, 88, 195–206.
- Haug, J. T., Maas, A., Haug, C., & Waloszek, D. (2011).** *Sarotrocercus oblitus*—small arthropod with great impact on the understanding of arthropod evolution? *Bulletin of Geosciences*, 86, 725–736.
- Haug, J. T., Waloszek, D., Haug, C., & Maas, A. (2010).** High-level phylogenetic analysis using developmental sequences: The Cambrian *Martinsonnia elongata*, *Muscacaris gerdgeyeri* gen. et sp. nov. and their positions in early crustacean evolution. *Arthropod Structure & Development*, 39, 154–173.
- Haug, J. T., Waloszek, D., Maas, A., Liu, Y., & Haug, C. (2012).** Functional morphology, ontogeny and evolution of mantis shrimp-like predators in the Cambrian. *Palaeontology*, 55, 369–399.
- He, Y., Cong, P., Liu, Y., Edgecombe, G. D., & Hou, X.-G. (2017).** Telson morphology of Leanchoiliidae (Arthropoda: Megacheira) highlighted by a new *Leanchoilia* from the Cambrian Chengjiang biota. *Alcheringa: An Australasian Journal of Palaeontology*, 41, 581–589.
- Hegna, T., Martin, M., & Darroch, S. (2017).** Pyritized in situ trilobite eggs from the Ordovician of New York (Lorraine Group): Implications for trilobite reproductive biology. *Geology*, 45, 199–202.
- Heymons, R. (1901).** Die Entwicklungsgeschichte der Scolopender. *Zoologica*, 33, 1–244.
- Holm, G. (1898).** Über die Organisation des *Eurypterus fischeri* Eichw. *Mémoires de l'Académie impériale des sciences de St.-Petersbourg, Serie VIII*, vol. VIII, № 2.
- Hou, J., Hughes, N. C., & Hopkins, M. J. (2021).** The trilobite upper limb branch is a well-developed gill. *Science Advances*, 7, eabe7377.
- Hou, X.-G. (1987a).** Two new arthropods from Lower Cambrian, Chengjiang, eastern Yunnan. *Acta Palaeontologica Sinica*, 26, 236–256, [in Chinese, with English summary].
- Hou, X.-G. (1987b).** Three new large arthropods from Lower Cambrian, Chengjiang, eastern Yunnan. *Acta Palaeontologica Sinica*, 26, 272–285, [in Chinese, with English summary].
- Hou, X.-G. (1987c).** Early Cambrian large bivalved arthropods from Chengjiang, eastern Yunnan. *Acta Palaeontologica Sinica*, 26, 286–298, [in Chinese, with English summary].
- Hou, X.-G. (1999).** New rare bivalved arthropods from the Lower Cambrian Chengjiang fauna, Yunnan, China. *Journal of Paleontology*, 73, 102–116.
- Hou, X.-G., & Bergström, J. (1991).** The arthropods of the Lower Cambrian Chengjiang fauna, with relationships and evolutionary significance. In: Simonetta, A. M. & Morris, S. C. (eds), *The Early Evolution of Metazoa and the Significance of Problematic Taxa*. Cambridge University Press, Cambridge, 179–187.
- Hou, X.-G., & Bergström, J. (1995).** Cambrian lobopodians – ancestors of extant onychophorans? *Zoological Journal of the Linnean Society*, 114, 3–19.
- Hou, X.-G., & Bergström, J. (1997).** Arthropods of the Lower Cambrian Chengjiang fauna, southwest China. *Fossils and Strata* 45, 1–113.
- Hou, X.-G., & Bergström, J. (1998).** Three additional arthropods from the Early Cambrian Chengjiang fauna, Yunnan, southwest China. *Acta Palaeontologica Sinica*, 37, 395–401.



- Hou, X.-G., Bergström, J., & Ahlberg, P. (1995). *Anomalocaris* and Other Large Animals in the Lower Cambrian Chengjiang Fauna of Southwest China. *GFF*, 117, 163–183.
- Hou, X.-G., Bergström, J., Wang, H., Feng, X., & Chen A. (1999). *The Chengjiang Fauna. Exceptionally Well-Preserved Animals from 530 Million Years Ago*. Yunnan Science and Technology Press, Kunming, China [in Chinese, with English summary].
- Hou, X.-G., Chen, J., & Lu, H. (1989). Early Cambrian new arthropods from Chengjiang, Yunnan. *Acta Palaeontologica Sinica*, 28, 42–57, [in Chinese, with English summary].
- Hou, X.-G., Ramsköld, L., & Bergström, J. (1991). Composition and preservation of the Chengjiang fauna – a Lower Cambrian soft-bodied biota. *Zoologica Scripta*, 20, 395–411.
- Hou, X., Siveter, D. J., Aldridge, R. J., & Siveter, D. J. (2009). A new arthropod in chain-like associations from the Chengjiang Lagerstätten (Lower Cambrian), Yunnan, China. *Palaeontology*, 52, 951–961.
- Hou, X.-G., Siveter, D. J., Siveter, D. J., Aldridge, R., Cong, P., Gabbott, S. E., Ma, X., Purnell, M., & Williams, M. (2017). *The Cambrian Fossils of Chengjiang, China: The Flowering of Early Animal Life*. John Wiley & Sons, London, 327 pp.
- Hou, X., Siveter, D. J., Williams, M., & Feng X. (2002). A monograph of bradoriid arthropods from the Lower Cambrian of southwest China. *Transactions of the Royal Society of Edinburgh: Earth Sciences*, 92, 347–409.
- Hou, X., Siveter, D. J., Williams, M., Waloszek, D., & Bergström, J. (1996). Appendages of the arthropod *Kunmingella* from the early Cambrian of China: its bearing on the systematic position of the Bradoriida and the fossil record of the Ostracoda. *Philosophical Transactions of the Royal Society, B: Biological Sciences*, 351, 1131–1145.
- Hou, X.-G., & Sun, W. (1988). Discovery of Chengjiang fauna at Meishucun, Jinning, Yunnan. *Acta Palaeontologica Sinica*, 27, 1–12, [in Chinese, with English summary].
- Hou, X., Williams, M., Siveter, D. J., Aldridge, R. J., & Sansom, R. S. (2010). Soft-part anatomy of the Early Cambrian bivalved arthropods *Kunyangella* and *Kunmingella*: significance for the phylogenetic relationships of Bradoriida. *Proceedings of the Royal Society, B: Biological Sciences*, 277, 1835–1841.
- Hounsfield, G. N. (1973). Computerized transverse axial scanning (tomography): part I. Description of system. *British Journal of Radiology*, 46, 1016–1022.
- Hu, S. (2005). Taphonomy and palaeoecology of the Early Cambrian Chengjiang Biota from Eastern Yunnan, China. *Berliner Paläobiologische Abhandlungen*, 7, 1–197.
- Hu, S., Zhu, M., Luo, H., Steiner, M.; Zhao, F., Li, G., Liu, Q., & Zhang, Z. (2013). *The Guanshan Biota*. Yunnan Science and Technology Press, Kunming, China.
- Hu, Y., Limaye, A., & Lu, J. (2020). Three-dimensional segmentation of computed tomography data using Drishti Paint: new tools and developments. *Royal Society Open Science*, 7, 201033.
- Hughes, C. P. (1975). Redescription of *Burgessia bella* from the Middle Cambrian Burgess Shale, British Columbia. *Fossils and Strata*, 4, 415–435.
- Huo, S. (1965). Additional notes on Lower Cambrian Archaeostraca from Shensi and Yunnan. *Acta Palaeontologica Sinica*, 13, 291–307, [in Chinese, with English summary].
- ICS (2021). International Commission on Stratigraphy. Chart / Time Scale. [www.stratigraphy.org](http://www.stratigraphy.org)
- IUCN (2012). International Union for Conservation of Nature evaluations of nominations of natural and mixed properties to the World Heritage List, 2012. Report for the World Heritage Committee, 36th Session, Saint Petersburg, Russian Federation.
- Jaekel, O. (1914). Ein grosser Pterygotus aus dem rheinischen Unterdevon. *Paläontologische Zeitschrift*, 1, 379–382.
- Javaux, E. J. (2019). Challenges in evidencing the earliest traces of life. *Nature*, 572, 451–460.
- Jell, P.A. (2003). Phylogeny of Early Cambrian trilobites. *Special Papers in Palaeontology*, 70, 45–57.
- Jiang, Z. (1982). Small shelly fossils. In: Luo, H., Jiang Z., Wu, X., Song, X. & Ouyang, L. (eds.), *The Sinian-Cambrian Boundary in Eastern Yunnan, China*. People's Publishing House of Yunnan, China, 163–199 [in Chinese].
- Jin, C., Mai, H., Chen, H., Liu, Y., Hou, X.-G., Wen, R., & Zhai, D. (2021). A new species of the Cambrian bivalved euarthropod *Pectocaris* with axially differentiated enditic armatures. *Papers in Palaeontology*, 7, 1781–1792.

- Jockusch, E. L. (2017). Developmental and Evolutionary Perspectives on the Origin and Diversification of Arthropod Appendages. *Integrative Comparative Biology*, 57, 533–545.
- Kambic, R. E., Roberts, T. J., & Gatesy, S. M. (2015). Guineafowl with a twist: Asymmetric limb control in steady bipedal locomotion. *Journal of Experimental Biology*, 18, 3836–3844.
- Kjellesvig-Waering, E. N. (1955). A new phyllocarid and eurypterid from the Silurian of Florida. *Journal of Paleontology*, 29, 295–297.
- Kjellesvig-Waering, E. N. (1958). The genera, species and subspecies of the family Eurypteridae Burmeister, 1845. *Journal of Paleontology*, 32, 1107–1148.
- Kjellesvig-Waering, E.N. (1964). A Synopsis of the Family Pterygotidae Clarke and Ruedemann, 1912 373 (Eurypterida). *Journal of Paleontology*, 38, 331–361.
- Knoll, A. H., Walter, M. R., Narbonne, G. M., & Christie-Blick, N. (2004). A New Period for the Geologic Time Scale. *Science*, 305, 621–622.
- Knoll, A. H., Walter, M. R., Narbonne, G. M., & Christie-Blick, N. (2006). The Ediacaran Period: a new addition to the geologic time scale. *Lethaia*, 39,13–30.
- Koenemann, S., Jenner, R. A., Hoenemann, M., Stemme, T., & von Reumont, B. M. (2010). Arthropod phylogeny revisited, with a focus on crustacean relationships. *Arthropod Structure & Development*, 39, 88–110.
- Kravchinsky, V. A. (2012). Paleozoic large igneous provinces of Northern Eurasia: Correlation with mass extinction events. *Global and Planetary Change*, 86, 31–36.
- Krings, M., Nyakatura, J. A., Fischer, M. S., & Wagner, H. (2014). The cervical spine of the American Barn Owl (*Tyto furcata pratincola*): I. Anatomy of the vertebrae and regionalization in their S-shaped arrangement. *PLoS One*, 9, e91653.
- Kühl, G., Briggs, D. E. G., & Rust, J. (2009). A Great-Appendage Arthropod with a Radial Mouth from the Lower Devonian Hunsrück Slate, Germany. *Science*, 323, 771–773.
- Lamsdell, J. C., & Braddy, S. J. (2009). Cope's rule and Romer's theory: patterns of diversity and gigantism in eurypterids and Palaeozoic vertebrates. *Biology Letters*, 6, 265–269.
- Lamsdell, J. C., Braddy, S. J., & Tetlie, O. E. (2010). The systematics and phylogeny of the Stylonurina (Arthropoda: Chelicerata: Eurypterida). *Journal of Systematic Palaeontology*, 8, 49–61.
- Lamsdell, J. C., Briggs, D. E. G., Liu, H. P., Witzke, B. J., & McKay, R. M. (2015). The oldest described eurypterid: a giant Middle Ordovician (Darriwilian) megalograptid from the Winneshiek Lagerstätte of Iowa. *BMC Evolutionary Biology*, 15, 169.
- Lamsdell, J., Gunderson, G., & Meyer, R. (2019). A common arthropod from the Late Ordovician Big Hill Lagerstätte (Michigan) reveals an unexpected ecological diversity within Chasmataspida. *BMC Evolutionary Biology*, 19, 8.
- Lamsdell, J. C., & Legg, D. A. (2010). An isolated pterygotid ramus (Chelicerata: Eurypterida) from the Devonian Beartooth Butte Formation, Wyoming. *Journal of Paleontology*, 84, 1206–1208.
- Lamsdell, J. C., Marshall, D. J., & Briggs, D. E. G. (2018). Hit and Miss: (A Comment on Persons and Acorn, “A Sea Scorpion's Strike: New Evidence of Extreme Lateral Flexibility in the Opisthosoma of Eurypterids”). *The American Naturalist*, 191, 352–354.
- Lamsdell, J. C., McCoy, V. E., Perron-Feller, O. A., & Hopkins, M. J. (2020). Air breathing in an exceptionally preserved 340-million-year-old sea scorpion. *Current Biology*, 30, 4316–4321.
- Lamsdell, J. C., & Selden, P. A. (2017). From success to persistence: identifying an evolutionary regime shift in the diverse Paleozoic aquatic arthropod group Eurypterida, driven by the Devonian biotic crisis. *Evolution*, 71, 95–110.
- Lan, T., Zhao, J., Zhao, F., He, Y., Martinez, P., & Strausfeld, N. J. (2021). Leancoiliidae reveals the ancestral organization of the stem euarthropod brain. *Current Biology*, 31, 4397–4404.e2
- Lang, W. H., & Cookson, I. C. (1935). On a flora, including vascular land plants, associated with *Monograptus*, in rocks of Silurian age, from Victoria, Australia. *Philosophical Transactions of the Royal Society of London, B: Biological Sciences*, 224, 421–449.
- Lankester, E. R. (1904). The structure and classification of Arthropoda. *Quarterly Journal Microscopical Science*, 47, 523–582.

- Lapworth, C. (1879).** On the tripartite classification of the Lower Paleozoic rocks. *Geological Magazine*, 6, 1–15.
- Laub, R. S., Tollerton, V. P., Berkof, R. S. (2010).** The cheliceral claw of *Acutiramus* (Arthropoda: Eurypterida): functional analysis based on morphology and engineering principles. *Bulletin of the Buffalo Society of Natural Sciences*, 39, 29–42.
- Lee, Y. (1975).** On the Cambrian ostracodes with new material from Sichuan, Yunnan and Shaanxi, China. *Professional Papers on Stratigraphy and Palaeontology*, 2, 37–72, [in Chinese].
- Legg, D. A., Sutton, M. D., Edgecombe, G. D., & Caron, J.-B. (2012).** Cambrian bivalved arthropod reveals origin of arthropodization. *Proceedings of the Royal Society, B: Biological Sciences*, 279, 4699–4704.
- Legg, D. A., Sutton, M. D., & Edgecombe, G. D. (2013).** Arthropod fossil data increase congruence of morphological and molecular phylogenies. *Nature Communications*, 4, 2485.
- Lichtenstein, A. A. H., & Herbst, J. F. W. (1797).** *Naturgeschichte der ungeflügelten Insekten. 1. Heft. Naturgeschichte der Insekten-Gattungen Solpuga und Phalangium*. Gottlieb August Lange, Berlin.
- Limaye, A. (2012).** Drishti: a volume exploration and presentation tool. *Proc. SPIE*, 8506. Developments in X-Ray Tomography VIII, 85060X.
- Linnaeus, C. (1758).** *Systema Naturae per Regna Tria Naturae Secundum Classes, Ordines, Genera, Species, cum Characteribus, Differentiis, Synonymis, Locis*, Vol. 1, 10<sup>th</sup> ed. Reformata. Holmiae, Laurentii Salvii, 824 pp.
- Liu, H., McKay, R. M., Witzke, B. J., & Briggs, D. E. G. (2009).** The Winneshiek Lagerstätte and its depositional environments. *Geological Journal of China Universities*, 15, 285–295, [in Chinese with English summary].
- Liu, H., & Shu D. (2004).** New information on *Chuandianella* from the Lower Cambrian Chengjiang Fauna, Yunnan, China. *Journal of Northwest University*, 34, 453–456 [in Chinese, with English summary].
- Liu, H., & Shu D. (2008).** *Chuandianella ovata* from Lower Cambrian Chengjiang biota. *Acta Palaeontologica Sinica*, 47, 352–361.
- Liu, Y., Edgecombe, G. D., Schmidt, M., Bond, A. D., Melzer, R. R., Zhai, D., Mai, H., Zhang, M., & Hou, X.-G. (2021).** Exites in Cambrian arthropods and homology of arthropod limb branches. *Nature Communications*, 12, 4619.
- Liu, Y., Haug, J. T., Haug, C., Briggs, D. E. G., & Hou X.-G. (2014).** A 520 million-year-old chelicerate larva. *Nature Communications*, 5, 4440.
- Liu Y., Hou, X.-G., & Bergström, J. (2007).** Chengjiang arthropod *Leancoilia illecebrosa* (Hou, 1987) reconsidered. *GFF*, 129, 263–272.
- Liu, Y., Melzer, R. R., Haug, J. T., Haug, C., Briggs, D. E. G., Hörnig, M. K., He, Y., & Hou, X.-G. (2016).** Three-dimensionally preserved minute larva of a great appendage arthropod from the early Cambrian Chengjiang biota. *PNAS*, 113, 5542–5546.
- Liu, Y., Ortega-Hernández, J., Chen, H., Mai, H., Zhai, D., Hou, X.-G. (2020a).** Computed tomography sheds new light on the affinities of the enigmatic euarthropod *Jianshaniania furcatus* from the early Cambrian Chengjiang biota. *BMC Evolutionary Biology*, 20, 2.
- Liu, Y., Ortega-Hernández, J., Zhai, D., & Hou, X.-G. (2020b).** A reduced labrum in a Cambrian great-appendage euarthropod. *Current Biology*, 30, 3057–3061.e2
- Liu, Y., Scholtz, G., & Hou, X.-G. (2015).** When a 520-million-year old Chengjiang fossil meets a modern micro-CT – a case study. *Scientific Reports*, 5.
- Lu, Y. (1940).** On the ontogeny and phylogeny of *Redlichia intermedia* Lu (sp. nov.). *Bulletin of the Geological Society of China*, 20, 333–342, [in Chinese].
- Luo, H., Hu, S., Chen, L., Zhang, S., & Tao, Y. (1999).** *Early Cambrian Chengjiang fauna from Kunming region China*. Yunnan Science and Technology Press, Kunming, China [in Chinese].
- Luo, H., Hu, S., Zhang, S., & Tao, Y. (1997).** New occurrence of the Early Cambrian Chengjiang fauna in Haikou, Yunnan Province, and study on Trilobitoidea. *Acta Geologica Sinica*, 71, 122–132.
- Ma, X., Hou, X.-G., Edgecombe, G. D., & Strausfeld, N. J. (2012).** Complex brain and optic lobes in an early Cambrian arthropod. *Nature*, 490, 258–262.

- Maas, A., Braun, A., Dong, X., Donoghue, P. C. J., Müller, K. J., Olempska, E., Repetski, J. E., Siveter, D. J., Stein, M., & Waloszek, D. (2006). The ‘Orsten’ – more than a Cambrian Konservat-Lagerstätte yielding exceptional preservation. *Palaeoworld*, 15, 266–282.
- Maas, A., Waloszek, D., Chen, J., Braun, A., Wang, X., & Huang, D. (2004). Phylogeny and life habits of early arthropods—predation in the Early Cambrian sea. *Progress in Natural Science*, 14, 158–166.
- MacGabhann, B. A. (2014). There is no such thing as the ‘Ediacara Biota’. *Geoscience Frontiers*, 5, 53–62.
- Mallatt, J. M., Garey, J. R., & Shultz, J. W. (2004). Ecdysozoan phylogeny and Bayesian inference: first use of nearly complete 28S and 18S rRNA gene sequences to classify the arthropods and their kin. *Molecular Phylogenetics and Evolution*, 31, 178–191.
- Marshall, C. R. (2006). Explaining the Cambrian “explosion” of animals. *Annual Review of Earth and Planetary Sciences*, 34, 355–384.
- Martens, J. (1969). Die Abgrenzung von Biospezies auf biologisch-ethologischer und morphologischer Grundlage am Beispiel der Gattung *Ischyropsalis* C. L. Koch 1839 (Opiliones, Ischyropsalididae). *Zoologische Jahrbücher Systematik*, 96, 133–264.
- McMahon, S., Matthews, J., Brasier, A., & Still, J. (2021). Late Ediacaran life on land: desiccated microbial mats and large biofilm streamers. *Proceedings of the Royal Society, B: Biological Sciences*, 288, 1–10.
- Manning, P.L., & Dunlop, J.A. (1995). The respiratory organs of eurypterids. *Palaeontology*, 38, 287–297.
- Mansuy, H. (1912). Pt. 2, Paléontologie. In: Deprat, J. & Mansuy, H. (eds.), *Etude géologique du Yun-Nan oriental*. Mémoires du service géologique de l’Indochine 1, 146 pp.
- Manton, S. M. (1973). Arthropod phylogeny—a modern synthesis. *Journal of Zoology*, 171, 111–130.
- Manton, S. M. (1977). *The Arthropoda: Habits, Functional Morphology and Evolution*. Oxford University Press, Oxford.
- McCoy, V. E., Lamsdell, J. C., Poschmann, M., Anderson, R. P., & Briggs, D. E. G. (2015). All the better to see you with: eyes and claws reveal the evolution of divergent ecological roles in giant pterygotid eurypterids. *Biology Letters*, 11, 20150564.
- Mckerrow, W. S., Scotese, C. R., Brasier, M. D. (1992). Early Cambrian continental reconstructions. *Journal of the Geological Society*, 149, 599–606.
- McLean, C. J., Garwood, R. J., & Brassey, C. (2020). The kinematics of amblypygid (Arachnida) pedipalps during predation: Extreme elongation in raptorial appendages does not result in a proportionate increase in prey capture performance. In: McLean, C. J. (ed.), *Biomechanics and Functional Morphology of Amblypygid Predation* (PhD thesis). Manchester Metropolitan University, Manchester, UK.
- McMenamin, M. A. S. (1996). Ediacaran biota from Sonora, Mexico. *PNAS*, 93, 4990–4993.
- Melzer, R. R., Diersch, R., Nicastro, D., & Smola, U. (1997). Compound eye evolution: highly conserved retinula and cone cell patterns indicate a common origin of the insect and crustacean ommatidium. *Naturwissenschaften*, 84, 542–544.
- Melzer, R. R., Michalke, C., & Smola, U. (2000). Walking on insect paths? Early ommatidial development in the compound eye of the ancestral crustacean, *Triops cancriformis*. *Naturwissenschaften*, 87, 308–311.
- Miller, S. A. (1874). Notes and description of Cincinnatian group fossils. *Cincinnati Quarterly Journal of Science*, Vol. 1, 343–351 ii.
- Minelli, A. (2003). The origin and evolution of appendages. *International Journal of Developmental Biology*, 47, 573–581.
- Mironenko, A. A (2018). Endocerids: suspension feeding nautiloids? *Historical Biology* 32, 281–289.
- Moore, R. C., Teichert, C., & Robinson, R. A. (1953). *Treatise on invertebrate paleontology*, Vol. 1. Geological Society of America.
- Morris, S. C. (1998). *The Crucible of Creation: The Burgess Shale and the Rise of Animals*. Oxford University Press, New York, 276 pp.
- Morris, S. C. (2000). The Cambrian “explosion”: Slow-fuse or megatonnage? *PNAS*, 97, 4426–4429.
- Morris, S. C. (2003). The Cambrian “explosion” of metazoans and molecular biology: would Darwin be satisfied? *International Journal of Developmental Biology*, 47, 505–515.
- Morris, S. C. (2006). Darwin’s dilemma: the realities of the Cambrian ‘explosion’. *Philosophical Transactions of the Royal Society, B: Biological Sciences*, 361, 1069–1083.

- Morris, S. C., & Whittington, H. B. (1985).** Fossils of the Burgess Shale, a national treasure in Yoho National Park, British Columbia. *Geological Survey of Canada, Miscellaneous Report*, 43.
- Murchison, R. I. (1839).** *The Silurian System, Founded on Geological Researches in the Counties of Salop, Hereford, Radnor, Montgomery, Caermarthen, Brecon, Pembroke, Monmouth, Gloucester, Worcester, and Stafford: With Descriptions of the Coal-fields and Overlying Formations*. John Murray, London, vol. 1, 576 pp.
- Müller, K. J. (1979).** Phosphatocopine ostracodes with preserved appendages from the Upper Cambrian of Sweden. *Lethaia*, 12, 1–27.
- Müller, K. J. (1985).** Exceptional preservation in calcareous nodules. *Philosophical Transactions of the Royal Society of London, B: Biological Sciences*, 311, 67–73.
- Müller, K. J. & Waloszek, D. (1985).** A remarkable arthropod fauna from the Upper Cambrian “Orsten” of Sweden. *Transactions of the Royal Society of Edinburgh Earth Sciences*, 76, 161–172.
- Narbonne, G., Myrow, P., Landing, E., & Anderson, M. (1987).** A candidate stratotype for the Precambrian-Cambrian boundary, Fortune Head, Burin Peninsula, Southeastern Newfoundland. *Canadian Journal of Earth Sciences*, 24, 1277–1293.
- Nedin, C. (1999).** *Anomalocaris* predation on nonmineralized and mineralized trilobites. *Geology*, 27, 987–990.
- Nieszkowski, X. (1858).** *D. Eurypterus remipes* aus den obersilurischen Schichten der Insel Oesel. Archiv für Naturkunde Liv-, Est- und Kurlands. Ser. I, Bd. 2.
- Novak, T., Gruber, J., & Slana, L. (1995).** A contribution to the knowledge of the harvestmen (Opiliones) from the submediterranean region of Slovenia. *Annales*, 7/95, 181–192.
- Nyakatura, J. A., Allen, V. R., Lauströer, J., Andikfar, A., Danczak, M., Ullrich, H. J., Hufenbach, W., Martens, T., & Fischer, M. S. (2015).** A three-dimensional skeletal reconstruction of the stem amniote *Orobates pabsti* (Diadectidae): Analyses of body mass, centre of mass position, and joint mobility. *PLoS One*, 10, e0137284.
- Nyakatura, J. A., & Fischer, M. S. (2010).** Functional morphology and three-dimensional kinematics of the thoraco-lumbar region of the spine of the two-toed sloth. *Journal of Experimental Biology*, 213, 4278–4290.
- Nyakatura, J. A., Melo, K., Horvat, T., Karakasiliotis, K., Allen, V. R., Andikfar, A., Andrada, E., Arnold, P., Lauströer, J., Hutchinson, J. R., Fischer, M. S., & Ijspeert, A. J. (2019).** Reverse-engineering the locomotion of a stem amniote. *Nature*, 565, 351–355.
- Olesen, J., Richter, S., & Scholtz, G. (2001).** The evolutionary transformation from phyllopodous to stenopodous limbs in the Branchiopoda (Crustacea)—is there a common mechanism for early limb development in arthropods? *International Journal of Developmental Biology*, 45, 869–876.
- Orr, P. J., Benton, M. J., & Briggs, D. E. G. (2003).** Post-Cambrian closure of the deep-water slope-basin taphonomic window. *Geology*, 31, 769–772.
- Ortega-Hernández, J. (2016).** Making sense of ‘lower’ and ‘upper’ stem-group Euarthropoda, with comments on the strict use of the name Arthropoda von Siebold, 1848. *Biological reviews of the Cambridge Philosophical Society*, 91, 255–273.
- Ortega-Hernández, J., Legg, D. A., & Braddy, S. J. (2013).** The phylogeny of aglaspidid arthropods and the internal relationships within Artiopoda. *Cladistics*, 29, 15–45.
- Page, A., Gabbott, S. E., Wilby, P. R., & Zalasiewicz, J. A. (2008).** Ubiquitous Burgess Shale-style “clay templates” in lowgrade metamorphic mudrocks. *Geology*, 36, 855–858.
- Palmer, A. R. (1973).** Cambrian trilobites. In: Hallam, A. (ed.), *Atlas of Palaeobiogeography*. Elsevier, New York, 3–18.
- Palmer, A. R. (1984).** The biomere problem; evolution of an idea. *Journal of Paleontology*, 58, 599–611.
- Paterson, J. R., Edgecombe, G. D., García-Bellido, C. D., Jago, J. B., & Gehling, J. B. (2010).** Nektaspid arthropods from the Early Cambrian Emu Bay Shale Lagerstätte, South Australia, with a reassessment of lamellipedian relations. *Palaeontology*, 53, 377–402.
- Paterson, J. R., García-Bellido, D. C., & Edgecombe, D. C. (2012).** New artiopodan arthropods from the Early Cambrian Emu Bay Shale Konservat-lagerstätte of South Australia. *Journal of Paleontology*, 86, 340–357.

- Paterson, J. R., García-Bellido, D., Lee, M. S. Y., Brock, G., Jago, J., & Edgecombe, G. D. (2011). Acute vision in the giant Cambrian predator *Anomalocaris* and the origin of compound eyes. *Nature*, *480*, 237–240.
- Paterson, J. R., García-Bellido, C. D., Jago, J. B., Gehling, J. B., Lee, M. S. Y., & Edgecombe, G. D. (2015). The Emu Bay Shale Konservat-Lagerstätte: a view of Cambrian life from East Gondwana. *Journal of the Geological Society*, *173*, 1–11.
- Peel, J. S., & Ineson, J. R. (2011). The extent of the Sirius Passet Lagerstätte (early Cambrian) of North Greenland. *Bulletin of Geosciences*, *86*, 535–543.
- Pehr, K., Love, G. D., Kuznetsov, A., Podkovyrov, V., Junium, C. K., Shumlyansky, L., Sokur T., & Bekker, A. (2018). Ediacara biota flourished in oligotrophic and bacterially dominated marine environments across Baltica. *Nature Communications*, *9*, 1807.
- Persons, W. S. (2018). Additional Specimens and a Critical Consideration of Eurypterid Opisthosoma Flexibility: (A Reply to Lamsdell et al.). *The American Naturalist*, *191*, 355–358.
- Persons, W. S., & Acorn, J. (2017). A Sea Scorpion's Strike: New Evidence of Extreme Lateral Flexibility in the Opisthosoma of Eurypterids. *The American Naturalist*, *190*, 152–156.
- Petrunkevitch, A. (1909). Contributions to our knowledge of the anatomy and relationships of spiders. *Annals of the Entomological Society of America*, *2*, 1–21.
- Pisani, D., Poling, L. L., Lyons-Weiler, M., & Hedges, S. B. (2004). The colonization of land by animals: molecular phylogeny and divergence times among arthropods. *BMC Biology*, *2*, 1.
- Plotnick, R. E. (1985). Lift based mechanisms for swimming in eurypterids and portunid crabs. *Transactions of the Royal Society of Edinburgh: Earth Sciences*, *76*, 325–337.
- Plotnick, R. E., & Baumiller, T. K. (1988). The pterygotid telson as a biological rudder. *Lethaia*, *21*, 13–27.
- Pocock, R. I. (1903). Descriptions of four new Arachnida of the orders Pedipalpi, Solifugae, and Araneae. *Annals and Magazine of Natural History, Including Zoology, Botany and Geology, Series 7*, 220–226.
- Poschmann, M. J., & Rozefelds, A. (2021). The last eurypterid – a southern high-latitude record of sweep-feeding sea scorpion from Australia constrains the timing of their extinction. *Historical Biology*. <https://doi.org/10.1080/08912963.2021.1998033>
- Poschmann, M., Schoenemann, B., & McCoy, V. E. (2016). Telltale eyes: the lateral visual systems of Rhenish Lower Devonian eurypterids (Arthropoda, Chelicerata) and their palaeobiological implications. *Palaeontology*, *59*, 295–304.
- Poschmann, M., & Tetlie, O.E. (2004). On the Emsian (Early Devonian) arthropods of the Rhenish Slate Mountains: 4. The eurypterids *Alkenopterus* and *Vinetopterus* n. gen. (Arthropoda: Chelicerata). *Senckenbergiana lethaea*, *84*, 173–193.
- Powell, W. G. (2003). Greenschist-facies metamorphism of the Burgess Shale and its implications for models of fossil formation and preservation. *Canadian Journal of Earth Sciences*, *40*, 13–25.
- Rafinesque, C. S. (1815). *Analyse de la Nature ou tableau de l'univers et des corps organisés*. Palermo, 223 pp.
- Ramsköld, L., & Chen, J. (1998). Cambrian lobopodians: Morphology and phylogeny. In: Edgecombe, G. D. (ed.), *Arthropod Fossils and Phylogeny*. Columbia University Press, New York, 107–150.
- Ramsköld, L., Chen, J., Edgecombe, G. D., & Zhou, G. (1996). Preservational folds simulating tergite junctions in tegopeltid and naraoid arthropods. *Lethaia*, *29*, 15–20.
- Ramsköld, L., Chen, J., Edgecombe, G. D., & Zhou, G. (1997). *Cindarella* and the arachnate clade Xandarellida (Arthropoda, Early Cambrian) from China. *Transactions of the Royal Society of Edinburgh: Earth Sciences*, *88*, 19–38.
- Rayfield, E. J. (2007). Finite element analysis and understanding the biomechanics and evolution of living and fossil organisms. *Annual Reviews in Earth and Planetary Sciences*, *35*, 541–576.
- Regier, J., Shultz, J., Zwick, A., Hussey, A., Ball, B., Wetzer, R., Martin, J. W., & Cunningham, C. W. (2010). Arthropod relationships revealed by phylogenomic analysis of nuclear protein-coding sequences. *Nature*, *463*, 1079–1083.
- Retallack, G. (2012). Ediacaran life on land. *Nature*, *493*, 89–92.
- Richter, S. (2002). The Tetraconata concept: hexapod-crustacean relationships and the phylogeny of Crustacea. *Organisms Diversity & Evolution*, *2*, 217–237.

- Ritchie, A. (1968). *Lanarkopterus dolichoshelus* (Størmer) gen. nov., a mixopterid eurypterid from the Upper Silurian of the Lesmahagow and Hagshaw Hills inliers, Scotland. *Scottish Journal of Geology*, 4, 317–338.
- Rota-Stabelli, O., Campbell, L., Brinkmann, H., Edgecombe, G. D., Longhorn, S. J., Peterson, K. J., Pisani, D., Philippe, H., & Telford, M. J. (2011). A congruent solution to arthropod phylogeny: phylogenomics, microRNAs and morphology support monophyletic Mandibulata. *Proceedings of the Royal Society, B: Biological Sciences*, 278, 298–306.
- Royer, D. L., Berner, R. A., Montañez, I. P., Tabor, N. J., & Beerling, D. J. (2004). CO<sub>2</sub> as a primary driver of Phanerozoic climate. *GSA Today*, 14, 4–10.
- Ruedemann, R. (1921). A recurrent Pittsford (Salina) fauna. *New York State Museum Bulletin*, 219–220, 205–215.
- Runnegar, B. (2021). Following the logic behind biological interpretations of the Ediacaran biotas. *Geological Magazine*. <https://doi.org/10.1017/S0016756821000443>
- Ruthensteiner, B. (2008). Soft Part 3D visualization by serial sectioning and computer reconstruction. *Zoosymposia*, 1, 63–100.
- Santer, R. D., & Hebets, E. A. (2009). Prey capture by the whip spider *Phrynos marginemaculatus* C. L. Koch. *Journal of Arachnology*, 37, 109–112.
- Schmidt, M., Hazerli, D., & Richter, S. (2020). Kinematics and morphology: A comparison of 3D patterns in the 5th pereopod of swimming and non-swimming crab species (Malacostraca, Decapoda, Brachyura). *Journal of Morphology*, 281, 1547–1566.
- Schmidt, M., Hou, X.-G., Zhai, D., Mai, H., Belojević, J., Chen, X., Melzer, R. R., Ortega-Hernández, J., & Liu, Y. (in press, 2022). Before trilobite legs: *Pygmaclypeatus daziensis* reconsidered and the ancestral appendicular organization of Cambrian arthropods. *Philosophical Transactions of the Royal Society, B: Biological Sciences*. <https://doi.org/10.1098/rstb.2021.0030>
- Schmidt, M., Liu, Y., Hou, X.-G., Haug, J. T., Haug, C., Mai, H., & Melzer, R. R. (2021a). Intraspecific variation in the Cambrian: new observations on the morphology of the Chengjiang euarthropod *Sinoburius lunaris*. *BMC Ecology and Evolution*, 21, 127.
- Schmidt, M., Liu, Y., Zhai, D., Hou, X.-G., & Melzer, R. R. (2021b). Moving legs: A workflow on how to generate a flexible endopod of the 518 million-year-old Chengjiang arthropod *Ercaicunia multinodosa* using 3D-kinematics (Cambrian, China). *Microscopy Research and Technique*, 84, 695–704.
- Schmidt, M., Melzer, R. R., & Bicknell, R. D. C. (2021). Kinematics of whip spider pedipalps: a 3D comparative morpho-functional approach. *Integrative Zoology*, 17, 156–167.
- Schmidt, M., Melzer, R. R., Plotnick, R. E., Bicknell, R. D. C. (2022). Spines and baskets of apex predatory sea scorpions uncovers unique feeding strategies using 3D-kinematic modeling. *iScience*, 25, 103662.
- Schmidt, M., Melzer, R. R., & Bicknell, R. D. C. (in preparation, 2022). Range of motion analyses of Laniatores harvestmen elongate pedipalps: a conceptualized approach.
- Schmidt, M., Melzer, R. R., Plotnick, R. E., & Bicknell, R. D. C. (in preparation, 2022). Bend and bow: 3D morpho-functional kinematics of elongate eurypterid and harvestmen chelicerae.
- Schoenemann, B. (2012). The eyes of a tiny ‘Orsten’ crustacean—A compound eye at receptor level? *Vision research*, 76, 89–93.
- Schoenemann, B., Poschmann, M., & Clarkson, E. N. K. (2019). Insights into the 400 million-year-old eyes of giant sea scorpions (Eurypterida) suggest the structure of Palaeozoic compound eyes. *Scientific Reports*, 9, 17797.
- Scholtz, G., Staude, A., & Dunlop, J. (2019). Trilobite compound eyes with crystalline cones and rhabdoms show mandibulate affinities. *Nature Communications*, 10, 2503.
- Scotese, C. R., Song, H., Mills, J. W. B., & van der Meer, D. G. (2021). Phanerozoic paleotemperatures: the earth’s changing climate during the last 540 million years. *Earth Science Reviews*, 215, 1–48.
- Seilacher, A., & Pflüger, F. (1994). From biomats to benthic agriculture: A biohistoric revolution. In: Krumbein, W. E., Peterson, D. M., & Stal, L. J. (eds.), *Bio stabilization of Sediments*. Bibliotheks- und Informations system der Carl von Ossietzky Universität Oldenburg, Oldenburg, 97–105.
- Seiter, M., Lemell, P., Gredler, R., & Wollf, J. O. (2019). Strike kinematics in the whip spider *Charon* sp. (Amblypygi: Charontidae). *Journal of Arachnology*, 47, 260–265.

- Sedgwick, A., & Murchison, R. I. (1835). On the Silurian and Cambrian Systems, exhibiting the order in which the older sedimentary strata succeed each other in England and Wales. *The London and Edinburgh Philosophical Magazine and Journal of Science*, 7, 483e535.
- Selden, P. A. (1981). Functional morphology of the prosoma of *Baltoerypteris tetragonophthalmus* (Fischer) (Chelicerata: Eurypterida). *Transactions of the Royal Society of Edinburgh: Earth Sciences*, 72, 9–48.
- Selden, P. A. (1984). Autecology of Silurian eurypterids. *Special Papers in Palaeontology*, 32, 39–54.
- Selden, P.A. (1985). Eurypterid respiration. *Philosophical Transactions of the Royal Society of London, B: Biological Sciences*, 309, 219–226.
- Selden, P. A., Lamsdell, J. C., Qi, L. (2015). An unusual euchelicerate linking horseshoe crabs and eurypterids, from the Lower Devonian (Lochkovian) of Yunnan, China. *Zoologica Scripta*, 44, 645–652.
- Sepkoski, J. J. Jr, & Sheehan, P. M. (1983). Diversification, faunal change, and community replacement during the Ordovician radiation. In: Tevesz, M. J. S., & McCall, P.M. (eds), *Biotic Interactions in Recent Fossil Benthic Communities*. Plenum, New York, 673–718.
- Servais, T., & Harper, D. A. T. (2018). The Great Ordovician Biodiversification Event (GOBE): definition, concept and duration. *Lethaia*, 51, 151–164.
- Servais, T., Harper, D. A. T., Li, J., Munnecke, A., Owen, A. W. & Sheehan, P. M. (2009). Understanding the Great Ordovician Biodiversification Event (GOBE): influences of paleogeography, paleoclimate, or paleoecology? *GSA Today*, 19, 4–10.
- Servais, T., Owen, A. W., Harper, D. A. T., Kröger, B. & Munnecke, A. (2010). The Great Ordovician Biodiversification Event (GOBE): the palaeoecological dimension. *Palaeogeography, Palaeoclimatology, Palaeoecology*, 294, 99–119.
- Seton, M., Müller, R. D., Zahirovic, S., Gaina, C., Torsvik, T., Shephard, G., Talsma, A., Gurnis, M., Maus, S., & Chandler, M. (2012). Global continental and ocean basin reconstructions since 200Ma. *Earth-Science Reviews*, 113, 212–270.
- Shu, D., Vannier, J., Luo, H., Chen, L., Zhang, X., & Hu, S. (1999). Anatomy and lifestyle of *Kunmingella* (Arthropoda, Bradoriida) from the Chengjiang fossil Lagerstätte (Lower Cambrian, Southwest China). *Lethaia*, 32, 279–298.
- Shu, D., Zhang, X., & Geyer, G. (1995). Anatomy and systematic affinities of the Lower Cambrian bivalved arthropod *Isoxys auritus*. *Alcheringia*, 19, 333–342.
- Shultz, J. W. (1989). Morphology of locomotor appendages in Arachnida: Evolutionary trends and phylogenetic implications. *Zoological Journal of the Linnean Society*, 97, 1–56.
- Simon, M. E. (1892). Arachnides. Etude sur les Arthropodes cavernicoles de île Luzon, Voyage de M. E. Simon aux îles Philippines (Mars et avril 1890). *Annales de la Société Entomologique de France*, vol. 61, 35–52.
- Snodgrass, R. E. (1938). The evolution of Annelida, Onychophora, and Arthropoda. *Smithsonian Miscellaneous Collections*, 97, 1–159.
- Snodgrass, R. E. (1958). Evolution of arthropod mechanisms. *Smithsonian Miscellaneous Collections*, 138, 1–77.
- Sombke, A., Lipke, E., Kenning, M., Müller, C. H. G., Hansson, B. S., & Harzsch, S. (2012). Comparative analysis of deutocerebral neuropils in Chilopoda (Myriapoda): implications for the evolution of the arthropod olfactory system and support for the Mandibulata concept. *BMC Neuroscience*, 13, 1.
- Song, H., Song, H., Rahman, I. A., & Chu, D. (2021). Computational fluid dynamics confirms drag reduction associated with trilobite queuing behaviour. *Palaeontology*, 64, 597–608.
- Sperling, E. A., Frieder, C. A., Raman, A. V., Girguis, P. R., Levin, L. A., & Knoll, A. H. (2013). Oxygen, ecology, and the Cambrian radiation of animals. *PNAS*, 110, 13446–13451.
- Sperling, E. A., & Vinther, J. (2010). A placozoan affinity for *Dickinsonia* and the evolution of late Proterozoic metazoan feeding modes. *Evolution & Development*, 12, 201–209.
- Sprigg, R. C. (1947). Early Cambrian (?) jellyfishes from the Flinders Ranges, South Australia. *Transactions of the Royal Society of South Australia*, 71, 212–224.
- Stalling, D., Westerhoff, M., & Hege, H.-C. (2005). Amira: A highly interactive system for visual data analysis. In: Hansen, C. D., & Johnson, C. R. (eds.), *The visualization handbook*. Elsevier, Amsterdam, the Netherlands, 749–767.



- Stigall, A. (2017).** Ordovician oxygen and biodiversity. *Nature Geoscience*, *10*, 887–888.
- Størmer, L. (1934).** Merostomata from the Downtonian Sandstones of Ringerike, Norway. Skrifter utgitt av Det Norske Videnskaps-Akademi I Oslo, I. Matem.-Naturvid. Klasse, 1–125.
- Størmer, L. (1955).** Merostomata. Treatise on Invertebrate Paleontology, Part P Arthropoda 2, Chelicerata, P36. as Stylonuracea.
- Strang, K. M., Armstrong, H. A., Harper, D. A. T., & Trabucho-Alexandre, J. P. (2016).** The Sirius Passet Lagerstätte: Silica death masking opens the window on the earliest matground community of the Cambrian explosion. *Lethaia*, *49*, 631–643.
- Sutton, M. D., Briggs, D. E. G., Siveter, D. J., Siveter, D. J. & Orr, P. J. (2002).** The arthropod *Offacolus kingi* (Chelicerata) from the Silurian of Herefordshire, England: computer based morphological reconstructions and phylogenetic affinities. *Proceedings of the Royal Society, B: Biological Sciences*, *269*, 1195–1203.
- Sutton, M. D., Rahman, I. A., & Garwood, R. J. (2014).** *Techniques for virtual palaeontology*. John Wiley & Sons, London, 200 pp.
- Suzuki, Y., & Bergström, J. (2008).** Respiration in trilobites: a reevaluation. *GFF*, *130*, 211–229.
- Tanaka, G., Hou, X.-G., Ma, X., Edgecombe, G. D., & Strausfeld, N. J. (2013).** Chelicerate neural ground pattern in a Cambrian great appendage arthropod. *Nature*, *502*, 364–368.
- Teichert, C., & Kummel, B. (1960).** Size of endoceroid cephalopods. *Breviora Museum of Comparative Zoology*, *128*, 1–7.
- Telford, M., & Thomas, R. (1995).** Demise of the Atelocerata? *Nature*, *376*, 123–124.
- Tetlie, O. E. (2007).** Distribution and dispersal history of Eurypterida (Chelicerata). *Palaeogeography, Palaeoclimatology, Palaeoecology*, *252*, 557–574.
- Tetlie, O. E., & Cuggy, M. B. (2007).** Phylogeny of the basal swimming eurypterids (Chelicerata; Eurypterida; Eurypterina). *Journal of Systematic Palaeontology*, *5*, 345–356.
- Tetlie, O. E., & Poschmann, M. (2008).** Phylogeny and palaeoecology of the Adelophthalmoidea (Arthropoda; Chelicerata; Eurypterida). *Journal of Systematic Palaeontology*, *6*, 237–249.
- Tetlie, O. E., & Rábano, I. (2007).** Specimens of Eurypterus (Chelicerata, Eurypterida) in the collections of Museo Geominero (Geological Survey of Spain), Madrid. *Boletín Geológico y Minero*, *118*, 117–126.
- Thiele, J. (1905).** Betrachtungen über die Phylogenie der Crustaceenbeine. *Zeitschrift für wissenschaftliche Zoologie*, *82*, 445–471.
- Tiegs, O. W., & Manton, S. M. (1958).** The evolution of the Arthropoda. *Biological Review*, *33*, 255–337.
- Tollerton, V. P. (1989).** Morphology, taxonomy, and classification of the order Eurypterida Burmeister, 1843. *Journal of Palaeontology*, *63*, 642–657.
- Torsvik, T. H., & Cocks, L. R. M. (2004).** Earth geography from 400 to 250 Ma: a palaeomagnetic, faunal and facies review. *Journal of the Geological Society*, *161*, 555–572.
- Turner, M. L., Falkingham, P. L., & Gatesy, S. M. (2020).** It's in the loop: shared sub-surface foot kinematics in birds and other dinosaurs shed light on a new dimension of fossil track diversity. *Biology Letters*, *16*, 20200309.
- Vagts, S., Schlattmann, J., Busshardt, P., Kleinteich, T., & Gorb, S. N. (2017).** The application of multi-body simulation approach in the kinematic analysis of beetle leg joints. *Artificial Life and Robotics*, *22*, 412–420.
- Vannier, J. (2007).** Early Cambrian origin of complex marine ecosystems. In: Williams, M., Haywood, A. M., Gregory, F. J., & Schmidt, D. N. (eds), *Deep-Time Perspectives on Climate Change: Marrying the Signal from Computer Models and Biological Proxies*. Micropaleontological Society Special Publications. Geological Society, London, 81–100.
- Vannier, J. (2009).** The Cambrian explosion and the emergence of modern ecosystems. *Comptes Rendus Palevol*, *8*, 133–154.
- Vannier, J., & Chen, J. (2002).** Digestive system and feeding mode in Cambrian naraoiid arthropods. *Lethaia*, *35*, 107–120.
- Wacey, D., Kilburn, M. R., Saunders, M., Cliff, J., & Brasier, M. D. (2011).** Microfossils of sulphur-metabolizing cells in 3.4-billion-year-old rocks of Western Australia. *Nature Geoscience*, *4*, 698–702.
- Walcott, C. D. (1882).** Description of a New Genus of the Order Eurypterida from the Utica Slate. *The American Journal of Science*. Third series, Vol. XXIII, 213–216.

- Walcott, C. D. (1890).** The fauna of the Lower Cambrian or *Olenellus* Zone. In: *Tenth Annual Report of the Director, 1888–1889. Part 1.* United States Geological Survey, 509–774.
- Walcott, C. D. (1911).** Cambrian geology and paleontology II: No. 2. Middle Cambrian Merostomata. *Smithsonian Miscellaneous Collections*, 57, 18–41.
- Walcott, C. D. (1912).** Cambrian geology and paleontology II: Middle Cambrian Branchiopoda, Malacostraca, Trilobita, and Merostomata. *Smithsonian Miscellaneous Collections*, 57, 453–456.
- Waloszek, D. (2003a).** Cambrian ‘Orsten’-type preserved arthropods and the phylogeny of Crustacea. In: Legakis, A., Sfenthourakis, S., Polymeni, R., & Thessalou-Legaki, M. (eds), *The New Panorama of Animal Evolution*. Pensoft Publishers, Sofia-Moscow, 69–87.
- Waloszek, D. (2003b).** The ‘Orsten’ Window – Three-dimensionally preserved Upper Cambrian Meiofauna and its Contribution to our Understanding of the Evolution of Arthropoda. *Paleontological Research*, 7, 71–88.
- Waloszek, D., Hinz, I., Shergold, J. H., & Müller, K. J. (1993).** Three-dimensional preservation of arthropod soft integument from the Middle Cambrian of Australia. *Lethaia*, 26, 7–15.
- Waloszek, D., Maas, A., Olesen, J., Haug, C., & Haug, J. (2014).** A eucrustacean from the Cambrian ‘Orsten’ of Sweden with epipods and a maxillary excretory opening. *Palaeontology*, 57, 909–930.
- Waloszek, D., & Müller, K. J. (1997).** Cambrian ‘Orsten’-type arthropods and the phylogeny of Crustacea. In: Fortey, R. A., & Thomas, R. H. (eds.), *Arthropod relationships*. The Systematics Association Special Volume Series book series, 55, 139–153.
- Waloszek, D., Repetski, J. E., & Müller, K. J. (1994).** An exceptionally preserved parasitic arthropod, *Heymonsicambria taylori* n. sp. (Arthropoda incertae sedis: Pentastomida), from Cambrian-Ordovician boundary beds of Newfoundland, Canada. *Canadian Journal of Earth Sciences*, 31, 1664–1671.
- Waloszek, D., & Szaniawski, H. (1991).** *Cambrocaris baltica* n. gen. n. sp., a possible stem-lineage crustacean from the Upper Cambrian of Poland. *Lethaia*, 24, 363–378.
- Waterston, C. D. (1964).** II. Observations on Pterygotid Eurypterids. *Transactions of the Royal Society of Edinburgh*, 66, 9–33.
- Waterston, C. D. (1979).** Problems of functional morphology and classification in stylonuroid eurypterids (Chelicerata, Merostomata), with observations on the Scottish Silurian Stylonuroidea. *Transactions of the Royal Society of Edinburgh*, 70, 251–322.
- Watson, T. (2020).** The bizarre species that are rewriting animal evolution. *Nature*, 586, 662–665.
- Wägele, J. W. (1993).** Rejection of the “Uniramia” Hypothesis and Implications of the Mandibulata Concept. *Zoologische Jahrbücher Systematik*, 120, 253–288.
- Wheeler, H. E. (1947).** Base of the Cambrian System. *Journal of Geology*, 55, 153–159.
- Whiteaves, J. F. (1892).** Description of a new genus and species of phyllocarid Crustacea from the Middle Cambrian of Mount Stephen, B. C. *The Canadian Record of Science*, 5, 205–208.
- Whittington, H. B. (1975).** Trilobites with appendages from the Burgess Shale, Middle Cambrian, British Columbia. *Fossils and Strata*, 4, 97–136.
- Whittington, H. B. (1980).** Exoskeleton, moult stage, appendage morphology, and habits of the Middle Cambrian trilobite *Olenoides serratus*. *Palaeontology*, 23, 171–204.
- Wind, J. (1984).** Computerized X-ray tomography of fossil hominid skulls. *American Journal of Physical Anthropology*, 63, 265–282.
- Whyte, M. A. (2005).** A gigantic fossil arthropod trackway. *Nature*, 438, 576.
- Wolff, J. O., Martens, J., Schönhofer, A. L., & Gorb, S. N. (2016).** Evolution of hyperflexible joints in sticky prey capture appendages of harvestmen (Arachnida, Opiliones). *Organisms Diversity & Evolution*, 16, 549–557.
- Wolff, C., & Scholtz, G. (2008).** The clonal composition of biramous and uniramous arthropod limbs. *Proceedings of the Royal Society, B: Biological Sciences*, 275, 1023–1028.
- Wood, A. (2014).** Behind the Scenes: A Study of Autodesk Maya. *Animation*, 9, 317.
- Woodward, H. (1865).** On a new genus of Eurypterida from the Lower Ludlow rock of Leintwardine, Shropshire. *Quarterly Journal of the Geological Society of London*, 21, 490–492.
- Xiao, S., & Knauth, L. (2013).** Fossils come in to land. *Nature*, 493, 28–29.

- Xu, G. (2004). New specimens of rare arthropods from the early Cambrian Chengjiang fauna, Yunnan, China. *Acta Palaeontologica Sinica*, 43, 325–331.
- Yang, J., Ortega-Hernández, J., Butterfield, N. J., & Zhang, X. (2013). Specialized appendages in fuxianhuiids and the head organization of early arthropods. *Nature*, 494, 468–471.
- Yang, J., Ortega-Hernández, J., Legg, D. A., Lan, T., Hou, J., & Zhang, X. (2018). Early Cambrian fuxianhuiids from China reveal origin of the gnathobasic protopodite in euarthropods. *Nature Communications*, 9, 470.
- Yin, Z., & Lu, J. (2019). Virtual Palaeontology: when fossils illuminated by X-ray. *Palaeoworld*, 28, 425–428.
- Yochelson, E. L. (1996). Discovery, Collection, and Description of the Middle Cambrian Burgess Shale Biota by Charles Doolittle Walcott. *Proceedings of the American Philosophical Society*, 140, 469–545.
- Zeng, H., Zhao, F., Niu, K., Zhu, M., & Huang, D. (2020). An early Cambrian euarthropod with radiodont-like raptorial appendages. *Nature*, 588, 101–105.
- Zeng, H., Zhao, F., Yin, Z., & Zhu, M. (2017). Appendages of an early Cambrian metadoxidid trilobite from Yunnan, SW China support mandibulate affinities of trilobites and artiopods. *Geological Magazine*, 154, 1306–1328.
- Zhai, D., Edgecombe, G. D., Bond, A. D., Mai, H., Hou, X.-G., & Liu, Y. (2019a). Fine-scale appendage structure of the Cambrian trilobitormorph *Naraoia spinosa* and its ontogenetic and ecological implications. *Proceedings of the Royal Society, B: Biological Sciences*, 286, 2019–2371.
- Zhai, D., Ortega-Hernández, J., Wolfe, J. M., Hou, X.-G., Cao, C., & Liu, Y. (2019b). Three-Dimensionally Preserved Appendages in an Early Cambrian Stem-Group Pancrustacean. *Current Biology*, 29, 171–177.
- Zhai, D., Williams, M., Siveter, D. J., Harvey, T. H. P., Sansom, R. S., Gabbott, S. E., Siveter, D. J., Ma, X., Zhou, R., Liu, Y., & Hou, X.-G. (2019c). Variation in appendages in early Cambrian bradoriids reveals a wide range of body plans in stem-euarthropods. *Communications Biology*, 2, 329.
- Zhai, D., Williams, M., Siveter, D. J., Siveter, D. J., Harvey, T. H. P., Sansom, R. S., Mai, H., Zhou, R., & Hou, X.-G. (preprint, 2021). An exceptionally preserved euarthropod with unique feather-like appendages from the Chengjiang biota. <https://doi.org/10.1101/2021.01.22.427827>
- Zhang, C., Liu, Y., Ortega-Hernández, J., Wolfe, J. M., Jin, C., Mai, H., Hou, X.-G., Guo, J., & Zhai, D. (preprint, 2021). Differentiated appendages in *Isoxys* illuminate origin of arthropodization. <https://doi.org/10.21203/rs.3.rs-861892/v1>
- Zhang, M., Liu, Y., Hou, X.-G., Ortega-Hernández, J., Mai, H., Schmidt, M., Melzer, R. R., & Guo, J. (submitted). Ventral morphology of the early Cambrian artiopod *Retifacies abnormalis*. *PeerJ*.
- Zhang, W., Chen, P., & Palmer, A. R. (2003). Biostratigraphy of China. Science Press, Beijing, China.
- Zhang, W., & Hou, X.-G. (1985). Preliminary notes on the occurrence of the unusual trilobite *Naraoia* in Asia. *Acta Palaeontologica Sinica*, 24, 591–595, [in Chinese, with English summary].
- Zhang, X., & Cui, L. (2016). Oxygen requirements for the Cambrian explosion. *Journal of Earth Sciences*, 27, 187–195.
- Zhang, X., Han, J., & Shu, D. (2000). A new arthropod, *Pygmaclypeatus daziensis*, from the Early Cambrian Chengjiang Lagerstätte, South China. *Journal of Paleontology*, 74, 800–803.
- Zhang, X., Han, J., Zhang Z., Liu, H., & Shu, D. (2004). Redescription of the Chengjiang arthropod *Squamacula clypeata* Hou & Bergström from the Lower Cambrian of China. *Palaeontology*, 47, 605–617.
- Zhang, X., Liu, Y., O'Flynn, R. J., Schmidt, M., Melzer, R. R., Hou, X.-G., Mai, H., Guo, J., & Ortega-Hernández J. (under review). Ventral organisation in the megacheiran *Jianfengia multisegmentalis* Hou, 1987, and its implications for the euarthropod head problem. *Palaeontology*.
- Zhang, X., Liu, W., & Zhao, Y. (2008). Cambrian Burgess Shale-type Lagerstätten in South China: distribution and significance. *Gondwana Research*, 14, 255–262.
- Zhang, X., & Shu, D. (2021). Current understanding on the Cambrian Explosion: questions and answers. *Paläontologische Zeitschrift*, 95, 641–660.

- Zhang, X., Shu, D., & Erwin, D. H. (2007). Cambrian naraoiids (Arthropoda): morphology, ontogeny, systematics, and evolutionary relationships. *Journal of Palaeontology*, 81(S86) *Paleontological Society Memoir*, 1–52.
- Zhang, X., Shu, D., Li, Y., & Han, J. (2001). New sites of Chengjiang fossils: crucial windows on the Cambrian Explosion. *Journal of the Geological Society*, 158, 211–218.
- Zhao, F., Bottjer, D. J., Hu S., Yin, Z., & Zhu, M. (2013). Complexity and diversity of eyes in Early Cambrian ecosystems. *Scientific Reports*, 3, 2751.
- Zhao F., Caron, J.-B., Bottjer, D. J., Hu S., Yin, Z., & Zhu M. (2014). Diversity and species abundance patterns of the early Cambrian (Series 2, Stage 3) Chengjiang Biota from China. *Paleobiology*, 40, 50–69.
- Zhao, F., Caron, J.-B., Hu, S., & Zhu, M. (2009). Quantitative analysis of taphofacies and paleocommunities in the Early Cambrian Chengjiang Lagerstätte. *Palaios*, 24, 826–839.
- Zhao, F., Hu, S., Caron, J.-B., Zhu, M., Yin, Z., & Lu, M. (2012). Spatial variation in the diversity and composition of the Lower Cambrian (Series 2, Stage 3) Chengjiang Biota, Southwest China. *Palaeogeography, Palaeoclimatology, Palaeoecology*, 346-347, 54–65.
- Zhao, T., Hou, X.-G., Zhai, D., Wu, D., Chen, H., Zhang, S., & Liu, Y. (2017). Application of the micro-CT technique in the studies of arthropods from the Chengjiang biota: a case of *Misszhouia longicaudata*. *Acta Palaeontologica Sinica*, 56, 476–482.
- Zhao, Y., Yuan, J., Zhu, M., Yang, R., Guo, Q., Qian, Y., Huang, Y., & Pan, Y. (1999). A progress report on research on the early Middle Cambrian Kaili biota, Guizhou, P.R.C. *Acta Palaeontologica Sinica*, 38 (supplement 1), 1–14, [in Chinese, with English summary].
- Zhu, M., Zhang, J., & Li, G. (2001). Sedimentary environments of the early Cambrian Chengjiang biota: sedimentology of the Yu'an-shan Formation in Chengjiang County, eastern Yunnan. In: Zhu, M., Van Iren, H., Peng, S., & Li, G. (eds.), *The Cambrian of South China*. *Acta Palaeontologica Sinica*, 40 (supplement), 80–105.
- Zrzavý, J., & Štys, P. (1997). The basic body plan of arthropods: insights from evolutionary morphology and developmental biology. *Journal of Evolutionary Biology*, 10, 353–367.

## Acknowledgements

First and foremost, I thank my supervisor, Prof. Dr. Roland R. Melzer (Bavarian State Collection of Zoology, Bavarian Natural History Collections, Munich, Germany). He was the one I addressed all the questions over the last three years, and who showed me the way to this thesis. I also thank Prof. Dr. Joachim T. Haug as well as Prof. Dr. Martin Heß, (Ludwig-Maximilians-University, Munich, Germany) for their fruitful and helpful comments during the TAC meetings, and regarding some manuscript ideas. Furthermore, I thank Prof. Dr. Yu Liu (Yunnan Key Laboratory for Palaeobiology, Kunming, China) for the opportunity to work on early Cambrian Chengjiang euarthropods and for having me several times in China. Moreover, I thank Dr. Russel D. C. Bicknell (University of New England, Armidale, Australia) for the interest in my work and for the chance to collaborate on sea scorpion appendage kinematics. Finally, I thank my mother. She always guided me the right way.

*Academic Education*

Doctoral studies	May 2019-April 2022	Ludwig-Maximilians-University, Munich Bavarian State Collection of Zoology, Munich Topic of the thesis: <b>Virtual paleontology in early Paleozoic marine euarthropods</b>
Master Studies	WS16/17 – SS18	M.Sc. ' <b>Marine Biology</b> ' University of Rostock Final grade: <b>very good</b> (1.3) ECTS grade: <b>A</b> Grade Master Thesis: <b>very good</b> (1.0)
	WS14/15 – SS16	M.Sc. ' <b>Organismic Biology and Evolution</b> ' Humboldt University Berlin Final grade: <b>very good</b> (1.4) ECTS grade: <b>A</b> Grade Master Thesis: <b>very good</b> (1.0)
Bachelor Studies	WS11/12 – SS14	B.Sc. ' <b>Biology</b> ' Martin-Luther-University Halle-Wittenberg Final grade: <b>good</b> (1.8) ECTS grade: <b>B</b> Grade Master Thesis: <b>very good</b> (1.0)
	WS10/11 – SS11	B.A. ' <b>Greek and Latin Philology</b> ' University of Leipzig
A level	2006 – 2008	Geschwister Scholl Gymnasium Zeitz

*Awards*

11/10/18	' <b>Institutspreis Biowissenschaften 2018</b> ', price for the best Master Thesis in Biological Sciences, University of Rostock
----------	---

*Practical Courses*

<u>University of Rostock</u>	01/08/18 – 02/02/18	' <b>German Oceanographic Museum</b> ' Stralsund, Germany
	08/06/17 – 08/20/17	' <b>Klubbans Biologiska Station</b> ' Uppsala Universitet, Fiskebäckskil, Sweden
	06/25/17 – 07/09/17	' <b>Biological Station Helgoland</b> ' (AWI) Helgoland, Germany
<u>Humboldt University Berlin</u>	05/07/16 – 05/19/16	' <b>Ecological Field Station Fabrikschleichach</b> ' Steigerwald, Institute for Animal Ecology & Tropical Biology, Julius-Maximilians-University Würzburg
	09/13/15 – 09/27/15	' <b>Wadden Sea Station Sylt</b> ' (AWI) Sylt, Germany
	06/06/15 – 06/20/15	' <b>Ecological Field Course in Trafoi</b> ' Trafoi, South Tyrol, Italy

*Work*

- 
- |  |  |
|--|--|
| 05/01/19 – 31/04/22                        | <b>Research associate at the Bavarian State Collection of Zoology</b> , Bavarian Natural History Collections (SNSB), section Arthropoda varia, Munich, Germany |
| 06/15/19 – 07/21/19<br>11/16/19 – 12/13/19 | <b>Yunnan Key Laboratory for Palaeobiology</b> , Kunming, Yunnan Province, People's Republic of China  |

*Engagement*

- 
- |                     |  |
|---------------------|--|
| 07/11/17 – 08/04/17 | Volunteer at the <i>Society for the Protection of Turtles, S.P.O.T</i> – project, run by the Exceter University, UK, North Cyprus, Season 2017 |
| 06/22/15 – 08/14/15 | Volunteer at the <i>Sea Turtle Conservation Project North Cyprus</i> , Rhizokarpaso, North Cyprus, Season 2015                                 |

*Further Information*

- 
- |                   |  |
|-------------------|--|
| Languages         | German (native), English (fluently)  |
| Program knowledge | Amira, Autodesk AutoCAD, Autodesk Maya, Blender, Drishti, Microsoft Office, PAST, SPSS |

## Publication history

1. Bicknell, R. D. C., Melzer, R. R., & **Schmidt, M.** (2021). Three-dimensional kinematics of euchelicerate limbs uncover functional specialization in eurypterid appendages. *Biological Journal of the Linnean Society*, 135, 174–183.  
<https://doi.org/10.1093/biolinnea/blab108>
2. Bicknell, R. D. C., **Schmidt, M.**, Rahman, I. A., Edgecombe, G. D., Daley, A. C., Melzer, R. R., Wroe, S., & Paterson J. R. (in preparation, 2022). Exploring *Anomalocaris* raptorial appendages using 3D kinematics, computational fluid dynamics and finite element analysis.
3. Liu, Y., Edgecombe, G. D., **Schmidt, M.**, Bond, A. D., Melzer, R. R., Zhai, D., Mai, H., Zhang, M., & Hou, X.-G. (2021). Exites in Cambrian arthropods and homology of arthropod limb branches. *Nature Communications*, 12, 4619.  
<https://doi.org/10.1083/s41467-021-24918-8>
4. Plotnick, R. E., **Schmidt, M.**, Melzer, R. R., & Bicknell, R. D. C. (in preparation, 2022). Reconsideration of the appendicular morphology of pterygotid sea scorpions.
5. **Schmidt, M.**, Hazerli, D., & Richter, S. (2020). Kinematics and morphology: A comparison of 3D-patterns in the fifth pereopod of swimming and non-swimming crab species (Malacostraca, Decapoda, Brachyura). *Journal of Morphology*, 281, 1547–1566.  
<https://doi.org/10.1002/jmor.21268>
6. **Schmidt, M.**, Haug, J. T., Haug, C., & Melzer, R. R. (in preparation, 2022). Ontogeny and appendicular morphology in the Burgess Shale arthropod *Marella splendens*.
7. **Schmidt, M.**, Hou, X.-G., Zhai, D., Mai, H., Belojević, J., Chen, X., Melzer, R. R., Ortega-Hernández, J., & Liu, Y. (in press, 2022). Before trilobite legs: *Pygmaclypeatus daziensis* reconsidered and the ancestral appendicular organization of Cambrian arthropods. *Philosophical Transactions of the Royal Society, B: Biological Sciences*, 20210030.  
<https://doi.org/10.1098/rstb.2021.0030>
8. **Schmidt, M.**, & Korn, D. (2021). Conch geometry, ontogeny and dimorphism in the Early Bajocian ammonoid *Stephanoceras* from Normandy, France. *Lethaia*.  
<https://doi.org/10.1111/let.12439>
9. **Schmidt, M.**, Liu, Y., Hou, X.-G., Haug, J. T., Haug, C., Mai, H., & Melzer, R. R. (2021). Intraspecific variation in the Cambrian: New observations on the morphology of the Chengjiang euarthropod *Sinoburius lunaris*. *BMC Ecology and Evolution*, 21, 127.  
<https://doi.org/10.1186/s12862-021-01854-1>



10. **Schmidt, M.**, Liu, Y., Melzer, R. R., & Hou, X.-G. (in preparation). Drishti, Amira and the visualization of early Cambrian Chengjiang euarthropods from China.
  
11. **Schmidt, M.**, Liu, Y., Zhai, D., Hou, X.-G., & Melzer, R. R. (2021). Moving legs: A workflow on how to generate a flexible endopod of the 518 million-year-old Chengjiang arthropod *Ercaicunia multinodosa* using 3D-kinematics (Cambrian, China). *Microscopy Research and Technique*, 84, 695–704.  
<https://doi.org/10.1002/jemt.23628>
  
12. **Schmidt, M.**, Melzer, R. R., & Bicknell, R. D. C. (2021). Kinematics of whip spider pedipalps: a 3D comparative morpho-functional approach. *Integrative Zoology*, 17, 156–167.  
<https://doi.org/10.1111/1749-4877.12591>
  
13. **Schmidt, M.**, Melzer, R. R., Plotnick, R. E., & Bicknell, R. D. C. (2022). Spines and baskets in apex predatory sea scorpions uncover unique feeding strategies using 3D-kinematics. *iScience*, 25, 103662. <https://doi.org/10.1016/j.isci.2021.103662>
  
14. **Schmidt, M.**, Melzer, R. R., & Bicknell, R. D. C. (in preparation, 2022). Range of motion analyses of Laniatores harvestmen elongate pedipalps: a conceptualized approach.
  
15. **Schmidt, M.**, Melzer, R. R., Plotnick, R. E., & Bicknell, R. D. C. (in preparation, 2022). Bend and bow: 3D morpho-functional kinematics of elongate eurypterid and harvestmen chelicerae.
  
16. Zhang, M., Liu, Y., Hou, X.-G., Ortega-Hernández, J., Mai, H., **Schmidt, M.**, Melzer, R. R., & Guo, J. (submitted). Ventral morphology of the early Cambrian artiopod *Retifacies abnormalis*. *PeerJ*.
  
17. Zhang, X., Liu, Y., O'Flynn, R. J., **Schmidt, M.**, Melzer, R. R., Hou, X.-G., Mai, H., Guo, J., & Ortega-Hernández J. (under review). Ventral organisation in the megacheiran *Jianfengia multisegmentalis* Hou, 1987, and its implications for the euarthropod head problem. *Palaeontology*.

